



**HAL**  
open science

## Air pollution, mobility and health in the Grenoble area

Marie-Laure Aix

► **To cite this version:**

Marie-Laure Aix. Air pollution, mobility and health in the Grenoble area. Human health and pathology. Université Grenoble Alpes [2020-..], 2023. English. NNT : 2023GRALS050 . tel-04825385

**HAL Id: tel-04825385**

**<https://theses.hal.science/tel-04825385v1>**

Submitted on 8 Dec 2024

**HAL** is a multi-disciplinary open access archive for the deposit and dissemination of scientific research documents, whether they are published or not. The documents may come from teaching and research institutions in France or abroad, or from public or private research centers.

L'archive ouverte pluridisciplinaire **HAL**, est destinée au dépôt et à la diffusion de documents scientifiques de niveau recherche, publiés ou non, émanant des établissements d'enseignement et de recherche français ou étrangers, des laboratoires publics ou privés.

THÈSE

Pour obtenir le grade de

**DOCTEUR DE L'UNIVERSITÉ GRENOBLE ALPES**

École doctorale : ISCE - Ingénierie pour la Santé la Cognition et l'Environnement

Spécialité : MBS - Modèles, méthodes et algorithmes en biologie, santé et environnement

Unité de recherche : Translational Innovation in Medicine and Complexity

**Pollution atmosphérique, mobilités et santé dans l'agglomération grenobloise**

**Air pollution, mobility and health in the Grenoble area**

Présentée par :

**Marie-Laure AIX**

Direction de thèse :

**Dominique J. BICOUT**  
DOCTEUR EN SCIENCES HDR, UNIVERSITE GRENOBLE ALPES

Directeur de thèse

Rapporteurs :

**PIETRO SALIZZONI**  
PROFESSEUR DES UNIVERSITES, ECOLE CENTRALE LYON  
**ISABELLA ANNESI-MAESANO**  
DIRECTRICE DE RECHERCHE, INSERM OCCITANIE MEDITERRANEE

Thèse soutenue publiquement le **7 décembre 2023**, devant le jury composé de :

<b>DOMINIQUE BICOUT</b> DOCTEUR EN SCIENCES HDR, UNIVERSITE GRENOBLE ALPES	Directeur de thèse
<b>PIETRO SALIZZONI</b> PROFESSEUR DES UNIVERSITES, ECOLE CENTRALE LYON	Rapporteur
<b>ISABELLA ANNESI-MAESANO</b> DIRECTRICE DE RECHERCHE, INSERM OCCITANIE MEDITERRANEE	Rapporteuse
<b>BRUNO DEGANO</b> PROFESSEUR DES UNIVERSITES - PRATICIEN HOSPITALIER, UNIVERSITE GRENOBLE ALPES	Président
<b>NATHALIE REDON</b> MAITRESSE DE CONFERENCES, IMT NORD EUROPE	Examinatrice
<b>LAURENT SPINELLE</b> INGENIEUR DE RECHERCHE, INERIS	Examinateur

Invités :

**CLAIRE CHAPPAZ**  
INGENIEURE, ATMO AUVERGNE-RHONE-ALPES





## REMERCIEMENTS

Je me mets à rédiger ce manuscrit en pensant tout d'abord à mon directeur de thèse, le Dr Dominique Bicout, qui a su me laisser la liberté dont j'avais besoin, tout en me formant au métier de chercheur. Le goût que j'avais de faire de la recherche est resté intact, ce qui montre à quel point il a su m'accompagner dans cette démarche. Je remercie ensuite les membres du jury pour l'intérêt qu'ils portent à mon travail : le Pr Isabella Annesi-Maesano, le Pr Pietro Salizzoni, mes rapporteurs, le Dr Nathalie Redon et le Dr Laurent Spinelle, mes examinateurs. Le Pr Bruno Degano, qui m'accompagne depuis le début, et dont les conseils bienveillants m'ont guidée. Merci également au Dr Sonia Chardonnel pour son implication tout au long de cette thèse.

Je souhaite aussi remercier mes professeurs du Master ESTE (Environnement Santé Toxicologie Écotoxicologie) dont les cours étaient absolument passionnants. Je dois beaucoup au Pr Anne Maître qui a eu l'ouverture d'esprit de s'intéresser aux trajectoires non rectilignes. Merci également au Pr Christine Demeilliers qui dirige mon équipe de recherche et m'a fourni un excellent environnement de travail. Les collègues d'EPSP (Environnement et Prévention en Santé des Populations) ont su m'offrir une ambiance si agréable pendant mon stage, que j'ai souhaité rester en leur compagnie pour trois années supplémentaires. Franck Balducci, notre intervalle de confiance, notre numérateur, avec sa finesse d'esprit et d'humour. Pascal Petit, avec qui j'ai eu beaucoup de plaisir à collaborer. Merci encore pour ta gentillesse infinie à mon arrivée dans l'équipe. Sylvette Liaudy, pour la formation aux outils bibliographiques et les conseils de lecture. Olivier Pedano pour sa présence bienveillante, les connaissances qu'il sait si bien faire partager, et le matériel informatique toujours au top qu'il m'a fourni. Grâce à toi, j'ai tout de suite aimé ce milieu de la recherche et de l'ouverture d'esprit. Jamais je n'avais connu de pauses café aussi intéressantes. Il y a aussi le Dr Valérie Guieu, qui vient d'arriver dans l'équipe et qui a toujours un mot sympa pour m'encourager. Enfin j'embrasse très fort Joanna et Maguy, mes deux collègues doctorantes.

Vous l'aurez compris, j'ai passé d'excellentes années dans le laboratoire TIMC (Translational Innovation in Medicine and Complexity), dont je remercie la Direction. Une pensée toute particulière au Dr Sandrine Voros qui m'a fourni une aide très importante pour le déploiement des capteurs fixes. Et aussi aux sept hébergeurs de capteurs, qui se reconnaîtront, sans lesquels mon chapitre 4 n'aurait jamais existé. Je dois aussi beaucoup à Nicolas Dalleau et Frédéric Bard qui m'ont appris presque tout sur les microcapteurs, au sein de l'association Enairgie Commune. Je suis par ailleurs extrêmement reconnaissante envers Atmo Auvergne-Rhône-Alpes pour l'ensemble des données ouvertes mises à disposition. C'est une chance pour nous de pouvoir accéder à toutes ces mesures. Je souhaite remercier très vivement Claire Chappaz et Prisca Ray pour leur implication dans notre projet. D'autre part, je tiens à souligner l'implication considérable du Pr Didier Donsez dans ce travail de thèse. Grâce à une collaboration avec ses étudiants, Gilles Mertens et Bertrand Baudeur, nous avons pu avancer, et surtout aboutir, sur le projet de capteurs LoRA.

Enfin, je dois beaucoup au Dr Françoise Leriche (VetAgro Sup), que j'aurais dû écouter lorsqu'en 2005, elle me recommandait de faire une thèse. Effectivement, 15 ans après, le naturel est revenu au galop ! C'est aussi à VetAgro Sup, que j'ai rencontré le Dr Lucie Pauron, devenue depuis ma meilleure amie, qui m'a également encouragée à poursuivre dans la recherche. Je t'en suis très reconnaissante. J'adresse maintenant une pensée très forte à Bernardo, qui est présent dans mon quotidien et dans toutes mes aventures. Tu m'as apporté une aide incommensurable au cours de ma thèse. Merci pour l'intérêt fascinant que tu as porté à mon travail. Même si tu ne l'as peut-être pas remarqué, nos discussions m'ont toujours permis d'avancer. Je pense également à mon frère, à sa copine Marilou, et à ma sœur qui poursuivent eux aussi de belles aventures. Et il y a enfin et surtout mes parents, sans lesquels je ne serais pas qui je suis. Je leur dédie ce travail, car c'est grâce à eux que j'ai pu développer toutes ces compétences. Vous m'avez tout donné pour que je puisse faire des études et je vous en remercie. Mais vous m'avez surtout transmis deux qualités fondamentales pour faire de la recherche : le courage et la curiosité.

*À mes parents,*

## RÉSUMÉ

La pollution de l'air représente le principal danger environnemental pour la santé humaine, causant une part significative de la mortalité mondiale, ainsi que diverses maladies chroniques. Ses conséquences sanitaires risquent de s'accroître avec le changement climatique, l'urbanisation et le vieillissement de la population. Cela souligne l'importance de surveiller les polluants atmosphériques, en particulier les particules fines (PM), qui sont les plus associées à la mortalité. Les objectifs de cette thèse sont 1) identifier les risques sanitaires liés aux polluants atmosphériques à Grenoble, 2) mesurer de la manière la plus fine possible l'exposition aux PM pour calculer au mieux les risques associés.

Ce travail débute par l'étude de 4 polluants de l'air pendant la pandémie de COVID-19 : les PM<sub>2.5</sub> (PM < 2.5 µm), les PM<sub>10</sub> (PM < 10 µm), le dioxyde d'azote (NO<sub>2</sub>) et l'ozone (O<sub>3</sub>). Elle a montré des variations de niveaux en NO<sub>2</sub> (- 32%), PM<sub>2.5</sub> (- 22%), PM<sub>10</sub> (- 15%) et O<sub>3</sub> (+ 11%) par rapport à 2015-2019 aux stations de référence d'Atmo Auvergne-Rhône-Alpes. Ces changements de concentrations étaient associés à des baisses de risques sanitaires à court-terme liés aux PM<sub>2.5</sub> (- 3% de visites aux urgences pour asthme infantile) et au NO<sub>2</sub> (- 2% d'hospitalisations pour maladies respiratoires). Les baisses de risques santé à long-terme concernaient surtout les PM<sub>2.5</sub> (- 3% de mortalité toutes causes, - 2% de cancers du poumon, - 8% de petits poids de naissance) et le NO<sub>2</sub> (- 1% de mortalité non-accidentelle). Les variations des concentrations en PM<sub>10</sub> et O<sub>3</sub> n'avaient quant à elles presque pas d'effet sur les risques. La majorité des conséquences sanitaires étant liées aux PM<sub>2.5</sub>, la suite de cette thèse s'est consacrée à leur mesure, ainsi qu'à celle des PM<sub>1</sub> (PM < 1 µm).

Afin de mieux comprendre la variabilité spatiale ou temporelle des niveaux de PM, des stations de mesures, constituées de capteurs low-cost (LCS), ont été assemblées pour compléter les stations de référence et augmenter le nombre de points de mesure. Les LCS présentaient l'avantage de pouvoir être déployés en grand nombre, du fait de leur faible coût. Afin de garantir la précision de leurs mesures, plusieurs méthodes de calibration ont été testées. Pour calibrer les PM<sub>1</sub>, la technique de régression linéaire était la plus efficace. Le random-forest, méthode de type machine-learning, donnait les meilleurs résultats pour les PM<sub>2.5</sub>. Il était par ailleurs essentiel d'exclure les jours de dusts sahariens car ils altéraient la mesure des PM<sub>2.5</sub>. Les LCS utilisés étant peu performants pour mesurer les PM<sub>10</sub>, l'étude a été poursuivie sans les inclure.

Une fois calibrés, 8 LCS ont été déployés à Grenoble, révélant des variations temporelles et spatiales, un capteur situé en centre-ville montrant des niveaux en  $PM_{10}$  ainsi que des ratios à la référence ( $PM_{10 \text{ ratio}} = PM_{10} / PM_{10 \text{ Ref}}$ ) plus élevés. Cette étude a montré que la calibration devrait se dérouler avec des niveaux en PM similaires à ceux du déploiement. De plus, une expérience en mobilité avec les LCS a montré l'importance de considérer le mode de transport, l'heure de déplacement et les sites traversés, ceux-ci étant influencés par le trafic et/ou la configuration de la rue. Le mode de transport le plus exposé ( $PM_{10 \text{ ratios}}$  élevés) était le vélo, suivi de la marche (- 2% par rapport au vélo), du bus (- 9% par rapport au vélo) et du tramway (- 14%). Cependant, lorsque l'on calculait les doses inhalées, l'ordre s'inversait avec la marche en tête, suivie du vélo (- 2% par rapport à la marche), du bus (- 26%) et du tramway (- 32%).

Cette thèse montre l'importance de considérer les variations temporelles et spatiales dans l'analyse de l'exposition aux polluants, les LCS permettant de mieux appréhender la variabilité des PM. En conclusion, des recommandations sont fournies concernant le montage, la calibration et le déploiement des LCS, qui pourraient être de plus en plus utilisés par les scientifiques et par les citoyens dans un contexte de science participative ou de prévention.

# CONTENTS

<b>1</b>	<b>Introduction and literature review</b>	<b>1</b>
1.1	Background.....	1
1.1.1	Air pollution is a proven public health concern.....	1
1.1.2	Future challenges associated with air pollution.....	2
1.2	Air pollutants.....	3
1.2.1	Particulate matter.....	3
1.2.1.1	The importance of PM size.....	3
1.2.1.2	PM sources and composition.....	4
1.2.1.3	Health impacts of PM.....	5
1.2.2	Nitrogen dioxide.....	5
1.2.2.1	Sources.....	5
1.2.2.2	Health effects of NO <sub>2</sub> .....	6
1.2.2.3	The future of NO <sub>2</sub> emissions in Europe.....	6
1.2.3	Ground level ozone.....	6
1.2.3.1	Ozone formation and depletion.....	7
1.2.3.2	Health effects of O <sub>3</sub> .....	8
1.3	Health risks assessment of air pollution.....	8
1.3.1	The importance of exposure duration.....	8
1.3.2	Relation between concentration and risk.....	8
1.3.3	Health risk calculations.....	10
1.4	Air pollution measurement.....	12
1.4.1	Central monitoring with reference stations.....	13
1.4.2	Fixed Low-cost sensors network.....	13
1.4.2.1	Focus on PM measurement.....	13
1.4.2.2	Working principle of PM LCS.....	14
1.4.3	Mobile measurements with low-cost sensors.....	15
1.5	The situation in Grenoble.....	16
1.5.1	The study area.....	16
1.5.2	Local air pollution context in Grenoble.....	17
1.5.2.1	Pollutants sources and health impact.....	17
1.5.2.2	The problem of PM <sub>2.5</sub> .....	19

1.6	Thesis objectives .....	20
1.6.1	What are health risks related to air pollutants in Grenoble?.....	20
1.6.2	How to accurately measure exposure to PM in Grenoble? .....	21
1.6.2.1	Fixed measurements with a LCS network .....	22
1.6.2.2	Mobile measurements .....	22
1.7	Thesis structure .....	23
1.7.1	Originality.....	23
1.7.2	Why did we focus on PM?.....	23
1.7.3	Thesis outline.....	24
<b>2</b>	<b>Health risks associated with air pollution</b>	<b>26</b>
2.1	Introduction.....	26
2.1.1	Research gap and objectives .....	26
2.1.2	Method.....	27
2.1.2.1	Dose – response functions.....	27
2.1.2.2	Pollutant’s concentrations .....	27
2.1.2.3	Health risks calculations .....	29
2.2	Article n°1 .....	30
2.3	Conclusion .....	42
2.3.1	Main results .....	42
2.3.1.1	Concentrations changes .....	42
2.3.1.2	Health effects changes .....	43
2.3.2	Perspectives.....	43
<b>3</b>	<b>Low-cost sensors for PM measurement: calibration method</b>	<b>45</b>
3.1	Introduction.....	45
3.2	Article n°2.....	47
3.3	Article n°3.....	52
3.4	Conclusion .....	80
<b>4</b>	<b>An experimental network of low-cost PM sensors in Grenoble</b>	<b>84</b>
4.1	Introduction.....	84
4.2	Materials and methods .....	86
4.2.1	Measuring instruments .....	86
4.2.2	Sampling locations and time period .....	86
4.2.3	Data cleaning .....	88

4.2.4	Calibration and time period selection .....	91
4.2.5	Exposure calculations.....	94
4.3	Results.....	95
4.3.1	Descriptive statistics .....	95
4.3.2	PM concentrations .....	95
4.3.3	PM ratios .....	97
4.4	Discussion.....	100
4.4.1	Main findings .....	100
4.4.2	Study limitations.....	102
4.5	Conclusion .....	103
4.6	Acknowledgements.....	104
4.7	Appendix.....	104
<b>5</b>	<b>Exposure to PM when commuting in the urban area of Grenoble</b>	<b>107</b>
5.1	Introduction.....	107
5.2	Article n°4.....	107
5.3	Conclusion .....	164
<b>6</b>	<b>Conclusions and perspectives</b>	<b>165</b>
6.1	Main results of the thesis .....	165
6.1.1	What are health risks related to air pollutants in Grenoble?... 165	
6.1.2	How to accurately measure exposure to PM in Grenoble? .... 166	
6.1.2.1	LCS calibration.....	166
6.1.2.2	Fixed measurements.....	166
6.1.2.3	Mobile measurements .....	166
6.2	Limitations of the study .....	167
6.2.1	The importance of LCS electronic components .....	167
6.2.1.1	Humidity sensors .....	167
6.2.1.2	PM sensors.....	168
6.2.2	The significance of an extensive calibration.....	168
6.3	Recommendations for future use of LCS .....	168
6.4	Future research perspectives .....	171
6.4.1	Autonomy and connectivity .....	171
6.4.2	Holistic air pollution monitoring.....	171
6.4.3	Growing importance of wildfires monitoring.....	173



6.4.4	Proposals for future research on calibration.....	173
6.4.5	Simplify PM measurement.....	174
6.5	Last words on air pollution and health.....	174
<b>7</b>	<b>References</b>	<b>175</b>
<b>8</b>	<b>Appendix</b>	<b>205</b>
	Appendix A - Publications and communications .....	205
	Appendix B - LCS study measuring exposure to PM in mobility .....	208
	Appendix C - LCS for PM measurement.....	219
	Appendix D - Designing LCS for high-quality PM monitoring .....	220
	Appendix E - Video on PM, mobility and health .....	221
	Appendix F - Scientific Game Jam.....	222

## ILLUSTRATIONS

Figure 1. Major chemical components composition of PM <sub>2.5</sub> .....	4
Figure 2. Formation of ground-level ozone.....	7
Figure 3. Number of publications per year since 1990 related to air pollution & health..	9
Figure 4. Summary of main air pollution health effects & notable related studies.....	10
Figure 5. Health risk calculation .....	11
Figure 6. Working principle of the Plantower PMS7003.....	14
Figure 7. Picture of an AirBeam2 device.....	16
Figure 8. Geographical location of Grenoble within a distinctive Y-shaped valley.....	17
Figure 9. Pollutant sources and annual concentrations in Grenoble .....	18
Figure 10. Time-series data of monthly average temperatures and PM <sub>2.5</sub> concentrations	19
Figure 11. Structure of the thesis manuscript.....	25
Figure 12. Map of the stations from Atmo AuRA used for exposure study. ....	28
Figure 13. O <sub>3</sub> mean calculation for $\Delta$ RR determination .....	28
Figure 14. Short-term and long-term health risks calculations. ....	29
Figure 15. Main results regarding concentrations and health risks changes.....	42
Figure 16. Steps to low-cost sensors deployment. ....	46
Figure 17. Scatterplot of the raw PM <sub>2.5</sub> <sub>LCS</sub> levels against the official PM <sub>2.5</sub> <sub>Ref</sub> data .....	53
Figure 18. Layout of a PM monitoring station.....	86
Figure 19. Map of the network of LCS showing sensors locations and the reference ...	88
Figure 20. Flowchart of the data cleaning and selection procedure.....	89
Figure 21. Dust identification steps .....	90
Figure 22. Scatterplots showing calibrated PM <sub>1</sub> levels versus PM <sub>1</sub> <sub>Ref</sub> .....	91
Figure 23. Scatterplots showing raw PM <sub>1</sub> levels versus PM <sub>1</sub> <sub>Ref</sub> for winter and autumn..	92
Figure 24. Scatterplot of hourly LCS average PM <sub>1</sub> concentrations versus PM <sub>1</sub> <sub>Ref</sub> .....	93
Figure 25. Simplified representation of urban structure and pollution levels.....	94
Figure 26. Distances in meters, PM <sub>2.5</sub> and PM <sub>1</sub> correlation matrixes.....	96
Figure 27. Scatterplot of correlation coefficient between sensors versus distances. ....	97
Figure 28. Average hourly PM <sub>2.5</sub> ratios across all deployment locations .....	98
Figure 29. Sensors clustering using k-means on PM ratios. ....	98
Figure 30. PM <sub>2.5</sub> <sub>ratio</sub> landscape by IDW interpolation.....	99
Figure 31. PM <sub>1</sub> <sub>ratio</sub> landscape by IDW interpolation.....	100
Figure 32. Framework proposal for individuals interested in PM LCS .....	170

## TABLES

Table 1. Example of dose-response functions showing association strengths.....	12
Table 2. Calibration formulas for $PM_1$ , $PM_{2.5}$ , and $PM_{10}$ with their uncertainties.	81
Table 3. Sampling sites description and deployment time period .....	87
Table 4. Dust events time periods discarded from the dataset.....	90
Table 5. Descriptive statistics for calibrated LCS and reference. ....	95
Table 6. Main pollutants changes & health outcomes during the COVID-19 ....	165

## ABBREVIATIONS

**AQS:** Air Quality Station

**Atmo AuRA:** Atmo Auvergne-Rhône-Alpes

**CO:** Carbon Monoxide

**COPD:** Chronic Obstructive Pulmonary Disease

**EEA:** European Environment Agency

**EU:** European Union

**GBD:** Global Burden of Disease

**INSEE:** Institut National de la Statistique et des Études Économiques

**LCS:** Low-Cost Sensors

**LCSQA:** Laboratoire Central de Surveillance de la Qualité de l'Air

**NO:** Nitric Oxide

**NO<sub>2</sub>:** Nitrogen Dioxide

**NO<sub>x</sub>:** Nitrogen Oxides

**O<sub>3</sub>:** Ground-level Ozone

**PAHs:** Polycyclic Aromatic Hydrocarbons

**PM:** Particulate Matter

**PM LCS:** PM measuring Low-Cost Sensors

**PM<sub>10</sub>:** PM with an aerodynamic diameter equal to or less than 10  $\mu\text{m}$

**PM<sub>2.5</sub>:** PM with an aerodynamic diameter equal to or less than 2.5  $\mu\text{m}$

**PM<sub>2.5-10</sub>:** PM with an aerodynamic diameter between 2.5 and 10  $\mu\text{m}$

**RH:** Relative Humidity

**ROMMA:** Réseau d'Observation Météo du Massif Alpin

**RR:** Relative Risk

**SO<sub>2</sub>:** Sulfur dioxide

**US EPA:** United States Environmental Protection Agency

**VOCs:** Volatile Organic Compounds

**WHO:** World Health Organization

# 1 INTRODUCTION AND LITERATURE REVIEW

## 1.1 BACKGROUND

Despite widespread media coverage, air pollution remains a complex problem for the general public due to its intangible nature. Chronic pollution is not visible even though it is the most hazardous form of air pollutant exposure (Botero, 2021). Because numerous air pollutants are invisible, people struggle to grasp the associated risks. Individual reactions to air pollution vary, and health effects often manifest later in life, making it challenging for citizens to take ownership of the issue. People who are sensitive, such as the elderly or children, tend to experience the most adverse effects of pollutants. It is crucial to better understand this invisible threat but also the associated risks and strategies to mitigate its effects (Palupi & Abeng, 2023).

### 1.1.1 Air pollution is a proven public health concern

In recent years, Europe has witnessed notable progress in air quality. Starting in 2005, the emissions of all key air pollutants continued to decrease, despite a rise in gross domestic production over the same period (European Environment Agency [EEA], 2023). Nonetheless, scientists keep warning that pollution can impact health, even at very low concentrations below common air quality standards (Al-Kindi et al., 2020; Belz et al., 2022; Danesh Yazdi et al., 2021; de Nazelle, 2021; Di et al., 2017). In Europe, almost all urban populations are exposed to air pollutants exceeding the World Health Organization (WHO) recommended levels (EEA, 2020). Air pollution is now acknowledged as the biggest environmental threat to human health, leading to approximately seven million deaths globally in 2016 (World Health Organization [WHO], 2018).

Almost 12% of global deaths could be attributed to air pollution (GBD 2019 Risk Factors Collaborators, 2020; Ritchie & Roser, 2020). Extensive research conducted across various regions leaves no room for doubt regarding the health effects of air pollutants. Moreover, the list of potential health effects attributable to air pollution continues to grow with recent studies on diabetes, reproduction, and neurocognitive issues (WHO, 2021b). A growing body of research also focusses on understanding the mechanisms through which air pollutants exert their toxicity, as evidenced by two recent studies on lung cancer (Hill et al., 2023; Sipos et al., 2023). Numerous case studies also revealed that decreases in air pollutants levels would generate immediate health benefits. A US-wide research highlighted a correlation between decreases in PM<sub>2.5</sub> (PM with an aerodynamic diameter equal to or less than 2.5  $\mu\text{m}$ ) levels from 1980 to 2000 and improvements in life expectancy (Pope et al., 2009). Recently, the closure of a coal coking plant in Pittsburgh resulted in a 42% immediate drop in cardiovascular emergency department visits (Yu & Thurston, 2023). Air pollution also has a significant impact on health care facilities. For instance, Mebrahtu et al. (2023) studied the impact of particulate matter (PM) and nitrogen dioxide (NO<sub>2</sub>) on respiratory health service attendance. Air pollution levels exceeding WHO's 24-hour thresholds increased healthcare demand for up to 100 days post-exposure.

### 1.1.2 Future challenges associated with air pollution

The European Green Deal, whose aim is to promote ecological transition, stated that by 2030, the European Union (EU) should reduce by more than 55% the health impacts of air pollution, specifically premature deaths (European Commission, 2021). However, the future poses many challenges with population aging, urbanization, and climate warming. By 2050, 68% of the world's population should live in urban areas, reflecting a 13% increase from the current figures (United Nations Department of Economic and Social Affairs, 2018). Furthermore, the number of people aged 65 or older is expected to more than double, reaching 1.6 billion by 2050 (United Nations Department of Economic and Social Affairs, 2023). Climate change may increase ground-level ozone (O<sub>3</sub>) formation and exacerbate wildfires or dust events, which elevate PM levels (United States Environmental Protection Agency [US EPA], 2022; Aguilera et al., 2021). An increasing number of scientific papers also deal with synergistic effects of air pollution and temperature. Rai et al. (2023) found that heat was associated with increased cardiorespiratory mortality, air pollutants amplifying these effects. Xu, Huang, et al. (2023) found that up to 2.8% of myocardial infarction

deaths could be attributed to the combination of extreme temperatures and PM<sub>2.5</sub>. The risk of a fatal heart attack doubled during 4-day heat waves with high PM<sub>2.5</sub> levels. In this context, providing strategies to minimize personal exposure to air pollutants seems important and urgent.

## 1.2 AIR POLLUTANTS

Air pollution refers to the presence of gases or particles harmful to human health or the environment (Pearson & Derwent, 2022). PM, NO<sub>2</sub> and O<sub>3</sub> are the most concerning air pollutants for public health in Europe (EEA, 2020; Tiwary et al., 2018). Therefore, significant focus has recently been placed on these pollutants, particularly from a regulatory perspective.

### 1.2.1 Particulate matter

PM is a mixture of solid and liquid particles small enough not to settle on the Earth's surface under the influence of gravity (WHO, 2021b). PM is omnipresent in the environment. A recent study using machine learning and ground-based data from 65 countries revealed that only 0,001% of the world population was exposed to PM<sub>2.5</sub> concentrations under the safe limit set by the WHO (Yu et al., 2023).

#### 1.2.1.1 The importance of PM size

PM is generally classified by aerodynamic diameter, usually called particle size. The aerodynamic diameter of a particle refers to the diameter of a hypothetical sphere with a 1g.cm<sup>-3</sup> density, behaving aerodynamically the same as the particle itself (same settling velocity) assuming laminar flow conditions. Common PM naming conventions include: PM<sub>10</sub>, with an aerodynamic diameter less than 10 μm, PM<sub>2.5</sub> (< 2.5 μm), and PM<sub>1</sub> (< 1 μm). The size of PM determines how long it remains in the air, and where it is going to be deposited within the respiratory system. Larger PM like PM<sub>10</sub> tends to settle primarily in the upper airways, whereas smaller PM travels to the bronchi or pulmonary alveoli and can enter the bloodstream. Larger PM also deposits more rapidly in the atmosphere than smaller PM, such as PM<sub>1</sub>, which can linger in the air for several days.

### 1.2.1.2 PM sources and composition

PM originates from human activities and natural sources (such as Saharan dust or wildfires). In Europe, PM<sub>2.5</sub> mainly comes from energy consumption in the residential, commercial, and institutional sectors (58% of emissions), followed by industry (14%), road transport (9%), waste and agriculture (EEA, 2022). Unfortunately, PM composition remains not fully known (van Donkelaar et al., 2019) and is highly complex (National Research Council, 2010). PM contains organic and inorganic components, but, as shown in Figure 1, its composition and mass vary over time and space (Bell et al., 2007). PM is mainly made of organic matter, sulphate, nitrate, ammonium, black carbon, sea salt, and mineral dust (Philip et al., 2014; van Donkelaar et al., 2019; Weagle et al., 2018).

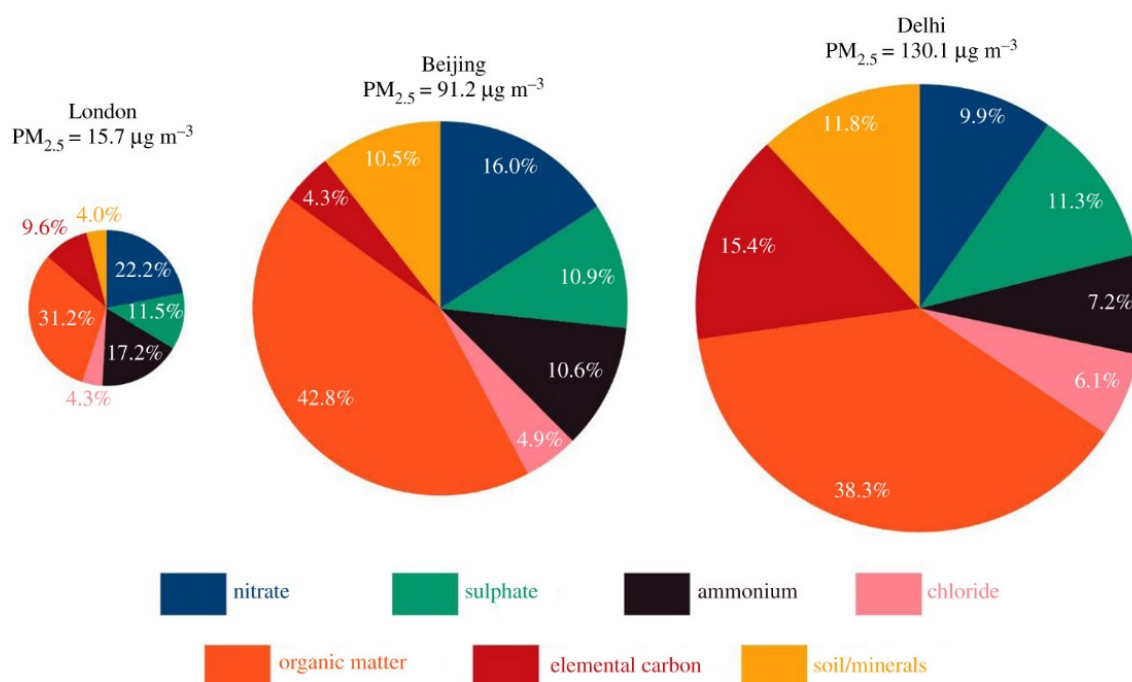


**Figure 1. Major chemical components composition of PM<sub>2.5</sub> collected during winter campaigns in London (North Kensington), Beijing and Delhi.** Source : Harrison (2020)

The organic components of PM include polycyclic aromatic hydrocarbons (PAHs) and volatile organic compounds (VOCs). Furthermore, PM can incorporate inorganic elements such as metals contributing to its toxicity. An emerging field of study involves investigating the oxidative potential of PM as a toxicity metric (Bates et al., 2019; Daellenbach et al., 2020).



### 1.2.1.3 Health impacts of PM

During the last 10 years, there has been a dramatic increase in the number of scientific papers on PM and health impacts (Lee et al., 2021). PM primarily leads to cardiovascular, respiratory effects, and premature mortality. Exposure to PM<sub>2.5</sub> would be associated with 7,6% of total global deaths (Cohen et al., 2017). Over the past three decades, the global stroke burden linked to ambient PM<sub>2.5</sub> has surged (Yacong et al., 2023). According to the International Agency for Research on Cancer, PM<sub>2.5</sub> is also classified as a causal agent (group 1 carcinogen) for lung cancer (Hamra et al., 2014). Furthermore, emerging studies indicate possible health effects of PM on reproduction or metabolic diseases such as diabetes, although these are less documented. A growing body of research also suggests that PM<sub>1</sub> could have higher health effects than larger PM because of its smaller size, and ability to carry toxic components such as heavy metals (Yang et al., 2022). Chen et al. (2017) showed that PM<sub>1</sub> and PM<sub>2.5</sub> were both associated with significantly increased daily emergency hospital visits, with comparable relative risk (RR). However, PM<sub>1-2.5</sub> (PM between 1 and 2.5 µm in size) showed no relation with emergency hospital visits, indicating that hospital visits associated with PM<sub>2.5</sub> likely came from its PM<sub>1</sub> fraction. Lin et al. (2016) stated that PM<sub>1</sub> could be the main contributor to cardiovascular effects of PM, especially for cardiovascular deaths. A meta-analysis also found strong impacts of PM<sub>1</sub> on cardiovascular and respiratory mortalities (Mei et al., 2022). However, regarding PM<sub>1</sub> and respiratory morbidity, the only identified association was that of asthma. Further epidemiological and toxicological studies on PM<sub>1</sub> are needed. They are still relatively scarce, likely due to the lack of official stations measuring PM<sub>1</sub> levels.

## 1.2.2 Nitrogen dioxide

### 1.2.2.1 Sources

Commonly known as NO<sub>x</sub>, nitrogen oxides are mostly produced during high-temperature fossil-fuel combustion when nitrogen reacts with oxygen (O<sub>2</sub>), particularly in engines and industrial processes (Tiwari & Mishra, 2019). NO<sub>2</sub> is one of the most closely monitored NO<sub>x</sub> affecting human health. Originating as a primary pollutant, it is an odourless brown gas, and the only gaseous air

pollutant with visible light absorption (Koenig, 2012). NO<sub>2</sub> is generally considered to be traffic-related, road transport being the main source of NO<sub>x</sub> (EEA, 2022).

### 1.2.2.2 Health effects of NO<sub>2</sub>

NO<sub>2</sub> mainly affects the respiratory system. High NO<sub>2</sub> levels can worsen asthma or other respiratory diseases, and long-term exposure to NO<sub>2</sub> can lead to these illnesses (Mallik, 2019). This is clearly demonstrated by the respiratory diseases observed among individuals living close to busy roads. Proximity to streets with high NO<sub>2</sub> levels increases the risk of respiratory issues, including asthma and decreased lung function (Bowatte et al., 2017). Individuals with respiratory disorders, heart diseases, asthma, and young children are particularly susceptible. The inhalation of NO<sub>2</sub> by children increases the severity of respiratory infections (Chauhan et al., 2003) and may lead to poorer lung function (Frischer et al., 1993). Elevated NO<sub>2</sub> levels also correlate with higher mortality rates (Faustini et al., 2014) and hospital admissions for respiratory diseases (Fusco et al., 2001).

### 1.2.2.3 The future of NO<sub>2</sub> emissions in Europe

The new Euro7/VII vehicle emission standards aimed to reduce NO<sub>x</sub> emissions by 35% for cars and vans compared to Euro 6 (European Commission, 2022). However, car manufacturers and eight countries, including France and Italy, opposed these new norms, arguing that they could divert the investments needed to phase out internal combustion engine vehicles (Automotive News Europe, 2023; Reuters, 2023). Increasing the electrification of vehicles could further reduce NO<sub>x</sub> (Mulholland et al., 2022). It is also worth noting that NO<sub>x</sub> influences ground-level O<sub>3</sub> photochemistry (Ravina et al., 2022), as explained in the next section.

## 1.2.3 Ground level ozone

While O<sub>3</sub> in the stratosphere protects against ultraviolet radiation, it is harmful when present in high concentrations at ground-level (Manisalidis et al., 2020).

### 1.2.3.1 Ozone formation and depletion

Unlike  $\text{NO}_2$  and PM, ozone does not originate directly from emissions (EEA, 2011). It is a secondary pollutant generated through a sequence of photochemical reactions occurring when sunlight interacts with precursor pollutants, such as  $\text{NO}_x$  and VOCs (Figure 2). As a result,  $\text{O}_3$  becomes especially problematic in summer.

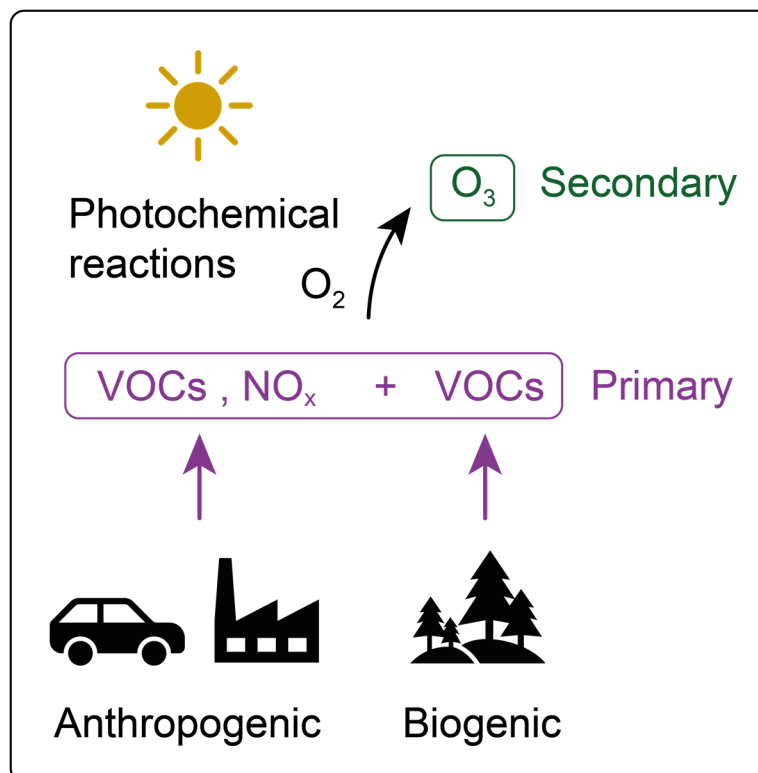


Figure 2. Formation of ground-level ozone.

$\text{NO}$  can also react with  $\text{O}_3$  to produce secondary  $\text{NO}_2$ , increasing its health concerns (Tiwary et al., 2018).  $\text{NO}_2$  also combines with  $\text{O}_3$  to form  $\text{NO}$  and  $\text{O}_2$ , removing  $\text{O}_3$  from the atmosphere (Crutzen, 1979). Therefore, reductions in  $\text{NO}_x$  can lead to increases in  $\text{O}_3$  concentrations (Jhun et al., 2015). This explains why  $\text{O}_3$  is generally more important in rural areas, where there is less  $\text{NO}_x$  due to reduced traffic.

### 1.2.3.2 Health effects of O<sub>3</sub>

O<sub>3</sub> exposure can cause shortness of breath, airway inflammation, worsened lung conditions, and chronic obstructive pulmonary disease (US EPA, 2023; Mallik, 2019). Overall, health effects associated with O<sub>3</sub> seem to be less significant than those related to PM and NO<sub>2</sub>. However, evidence suggests a link between O<sub>3</sub> and mortality (Jerrett et al., 2009; Vicedo-Cabrera et al., 2020), but further research is needed to fully understand this relationship.

## 1.3 HEALTH RISKS ASSESSMENT OF AIR POLLUTION

### 1.3.1 The importance of exposure duration

Air pollution can have both short-term (acute) and long-term (chronic) impacts on health. Acute or immediate symptoms include eye, nose or throat irritations, wheezing, coughing, headaches and even bronchitis or pneumonia. These effects can lead to hospitalizations or general practitioner consultations. Long-term effects include development of heart disease, chronic obstructive pulmonary disease (COPD), cancer, and asthma (Tiway et al., 2018). Long-term health effects, originating from prolonged exposure to air pollutants, are generally more substantial, as they lead to chronic diseases, which in worst cases, can lead to death.

### 1.3.2 Relation between concentration and risk

Since 2014, there has been an almost exponential increase in the number of systematic reviews and meta-analyses concerning the effects of air pollution on health, most of them being related to PM and NO<sub>2</sub> (Dominski et al., 2021). A search in PubMed with “air pollution” and “health” as MeSH words confirms that the number of papers published in this area is increasing since 1990 (Figure 3).

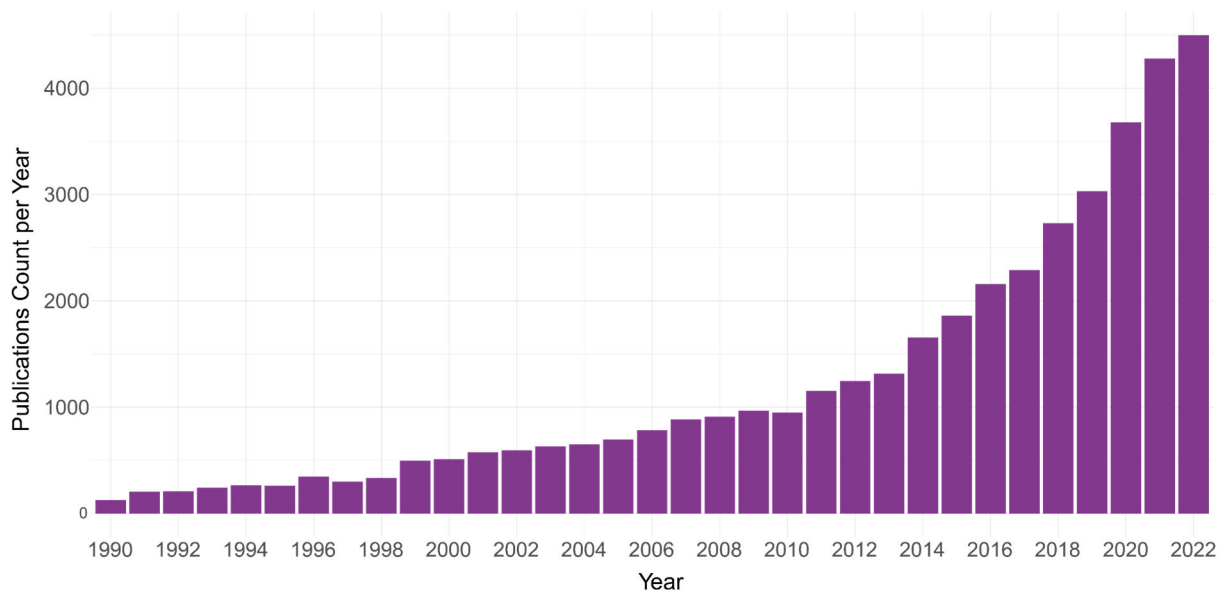


**Figure 3. Number of publications per year since 1990 related to “air pollution” and “health” in PubMed.**

The field of diseases attributed to air pollution is very broad, but some associations are more robust than others, especially because they have been studied for a longer time (Figure 4). A recent paper reported for the first time a link between PM and antibiotic resistance (Zhou et al., 2023). However, for the association to be validated, a substantial body of research, with numerous papers pointing in the same direction, is required, and this takes time. For instance, the link between PM and mortality is now widely established because of the significant number of studies on the subject. The first work showing a relation between PM and death was the Six Cities Study by Dockery et al. (1993). They compared pollutant levels and mortality in six American cities, revealing a clear link between PM and reduced life expectancy. A more extensive epidemiological work led by the American Cancer Society (Pope et al., 1995), followed and validated the conclusions of the Six Cities Study. They associated PM with cardiopulmonary and lung cancer mortality. Since then, many articles confirmed these associations. Robust correlations were found between air pollution and cardiovascular health in addition to respiratory effects. New studies also suggest that air pollution could have harmful effects on the central nervous system, reproduction, development, metabolic outcomes, and cancer (Thurston et al., 2017). However, more research is needed on those topics (Chandra et al., 2022; Tan et al., 2017). Figure 4 outlines the main health impacts of air pollutants along with notable associated studies.

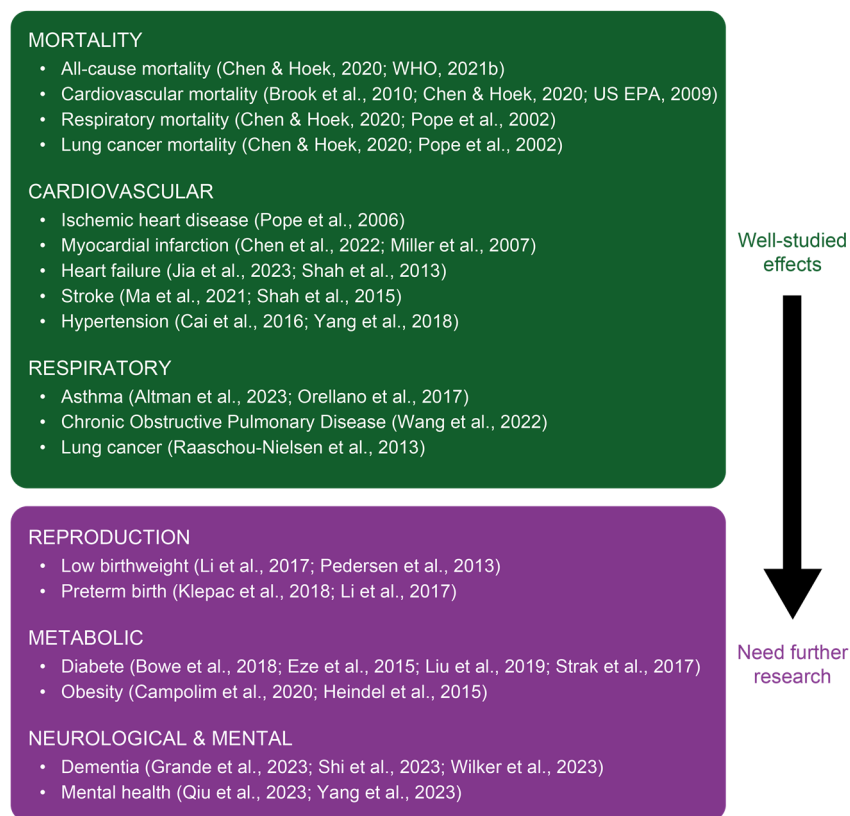


**Figure 4. Summary of main air pollution health effects & notable related studies.** References in Chapter 7.

Epidemiological studies quantify the relationship between pollutant concentrations and health outcomes (dose-response relationship), crucial for subsequent health risk assessments. These connections between pollutant levels and health outcomes form the basis to assess burdens such as mortality and diseases. These connections are expressed as “dose-response relationship” or “relative risk” (RR). The RRs associated with short-term impacts are generally derived from time-series analyses, and RRs for long-term effects typically come from cohorts involving people over years (Corso et al., 2019). Risk estimates of long-term exposure studies are usually higher than those of short-term studies (WHO, 2021a).

### 1.3.3 Health risk calculations

The health risk related to air pollutants increases with exposure (Tiwarly et al., 2018). Hence, the initial step in a health risk assessment involves precisely determining pollutant concentrations through measurement or modelling. Subsequently, we compute the health risk function measuring the probability of developing a health outcome like a disease (morbidity) or mortality (Figure 5).

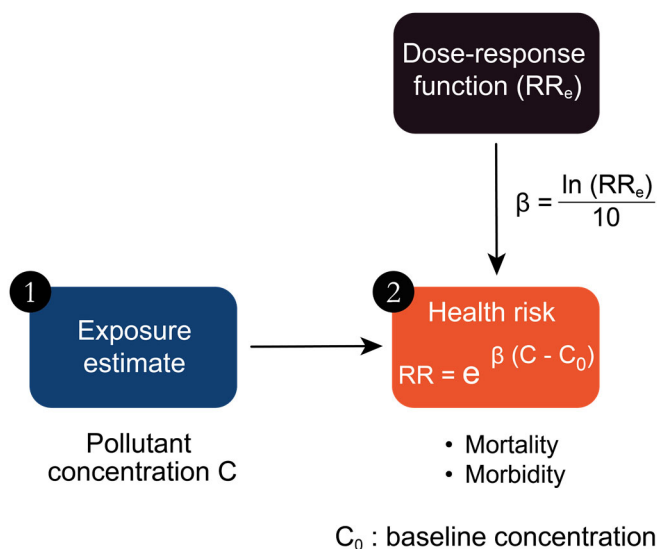


**Figure 5. Health risk calculation**

In Western Europe, a health risk related to air pollution is typically assessed using a log-linear dose-response function (Ostro & WHO, 2004; Soares et al., 2022; WHO, 2013):

$$RR = e^{\beta * (C - C_0)} \quad (1)$$

Where the RR illustrates the probability of a specific outcome in people exposed to a pollutant, compared to those not exposed. A RR of 1 indicates no difference in risk among the two groups.  $C$  denotes the pollutant concentration to which the population is exposed.  $C_0$  (baseline concentration) can either be the threshold concentration below which there is no additional health risk, the pollutant background concentration, or a counterfactual concentration. These counterfactual concentrations are generally used:  $5 \mu\text{g}/\text{m}^3$  for  $\text{PM}_{2.5}$  and  $10 \mu\text{g}/\text{m}^3$  for  $\text{NO}_2$  (WHO, 2021b).  $\beta$  is computed as follows:

$$\beta = \frac{\ln(RR_e)}{\delta}$$

where  $RR_e$  is the RR from epidemiological studies (usually meta-analyses) for the corresponding pollutant - health outcome association, and  $\delta$  the associated pollutant concentration increment, usually  $10 \mu\text{g}/\text{m}^3$ . Examples of  $RR_e$  (also called dose-response functions), can be found in Table 1. For example, regarding  $\text{PM}_{2.5}$  and long-term mortality, a  $RR_e$  of 1.15 indicates that a  $10 \mu\text{g}/\text{m}^3$  increase in  $\text{PM}_{2.5}$  would be associated with a 15% mortality rise.

**Table 1. Example of dose-response functions ( $RR_e$ ) showing association strengths between  $PM_{2.5}$  concentrations (per  $10 \mu\text{g}/\text{m}^3$  increment) and mortality or morbidities, with their 95% confidence interval.**  
 Extracted from Aix et al. (2022).

Pollutant	Exposure time	Age group	Health outcome	$RR_e$ [CI 95%] per $10 \mu\text{g}/\text{m}^3$	Reference
$PM_{2.5}$	Short-term /daily mean	all	Non-accidental mortality	1.0063 [1.0025– 1.0101]	C. Liu et al. (2019)
			Hospitalizations for respiratory causes	1.0190 [0.9982– 1.0402]	WHO (2013)
			Hospitalizations for cardiovascular causes (including strokes)	1.0091 [1.0017– 1.0166]	WHO (2013)
	Long-term /annual	$\leq 17$	Emergency room visits for asthma	1.0980 [1.0120– 1.1900]	Host et al. (2018)
		$\geq 30$	Mortality, all causes	1.1500 [1.0500– 1.2500]	Pascal et al. (2016)
		Adults	Lung cancer incidence	1.0900 [1.0400– 1.1400]	Hamra et al. (2014)
	Infants	Low birthweight at full term	1.3900 [1.1200– 1.7700]	Pedersen et al. (2013)	

In light of the health risk calculation formula, it becomes evident that a risk assessment cannot be carried out without precisely measuring pollutant concentrations.

## 1.4 AIR POLLUTION MEASUREMENT

In Western Europe, authorities typically use costly stationary instruments to measure air pollutants. PM concentrations are often measured with gravimetric methods, considered as gold standard, and based on PM weighting. Other techniques have been developed and are now considered equivalent to the gravimetry. This includes monitors based on light diffusion, considered as equivalent to the reference, like the Fidas 200 (Palas GmbH, 2020). All these expensive reference stations offer highly accurate measurements, but are not always fully representative of what the individuals are actually breathing, as they can be far from populated areas. Two ways recently emerged in order to improve exposure assessments: the development of fixed sensors networks and the use of mobile sensors. These approaches have been facilitated by



the rise of the Internet of Things (IoT) and the use of low-cost sensors (LCS). In this thesis, these two novel approaches were used, as well as the traditional, central monitoring method involving reference stations.

### 1.4.1 Central monitoring with reference stations

We first started by using reference measurements made locally by Atmo Auvergne Rhône-Alpes (Atmo AuRA), the regulatory instance measuring air pollutants in Grenoble. The city has a significant network of official stations providing hourly measurements. Those data have the advantage of being easy to retrieve through an Application Programming Interface (Atmo AuRA, 2023a). Various types of reference stations can be found like traffic stations, located near a major road, or background stations, far from traffic, and more representative of the average population exposure. The main background reference station from Atmo AuRA is located in “Les Frênes” within a park in the south of Grenoble. However, these reference stations are not sufficient to get a good overview on what people breathe locally, studies showing a high spatiotemporal variability of pollutants in cities (Dias & Tchepel, 2018; Nikolova et al., 2011). Various papers indicated that central monitoring was inadequate to describe people’s exposure to air pollutants (Han et al., 2021; Peters et al., 2013). Therefore, other ways of getting finer measurements, both temporally and spatially, can be explored. Using affordable calibrated sensors, in both static and mobile scenarios, emerges as an optimal solution to capture population’s exposure variability.

### 1.4.2 Fixed Low-cost sensors network

#### 1.4.2.1 Focus on PM measurement

In recent years, low-cost sensors appeared as a novel trend in air quality measurement (Giordano et al., 2021; Raysoni et al., 2023). Heavily used by citizens, scientists and authorities measuring air pollution, they are good supplements to standard monitoring sites for high-resolution spatial-temporal PM mapping (Li & Biswas, 2022). Most studies focus on LCS measuring PM, as it is still challenging to quantify gases with LCS for a number of reasons. Results can be affected by long response times, instability or interference from other gases (Gerboles et al., 2017). Lewis

et al. (2016) studied NO<sub>2</sub> electrochemical sensors and emphasized that artefact signals from pollutants like CO<sub>2</sub> could surpass NO<sub>2</sub> signals (Hagan et al., 2018). LCS measuring O<sub>3</sub> also tend to be affected by NO<sub>2</sub> interference. They can show good agreement with reference at rural sites where O<sub>3</sub> is higher than NO<sub>2</sub> but struggle to provide good results at urban and traffic sites (Spinelle et al., 2015). Many studies show good results of gas LCS in laboratory chambers but once in the field, larger discrepancies can be seen (Castell et al., 2017; Hagan et al., 2018). Variability between identical sensors is also an issue and longer response time makes them unsuitable for mobile measurements (Hagan et al., 2018). Additionally, they tend to degrade faster compared to PM sensors (Mueller et al., 2017; Papaconstantinou et al., 2023). Low-cost PM sensors (PM LCS) show superior reliability and ease of use in the field (Hassani et al., 2023).

#### 1.4.2.2 Working principle of PM LCS

PM LCS can measure the intensity of light scattered by PM on a detector and convert this signal to a concentration in  $\mu\text{g}/\text{m}^3$ . The working principle of a common PM sensor PMS7003 (Plantower, 2016) is shown in Figure 6. This sensor is one of the most widely used PM LCS, providing good performances despite its cheap price (around 24€) (Alfano et al., 2020).

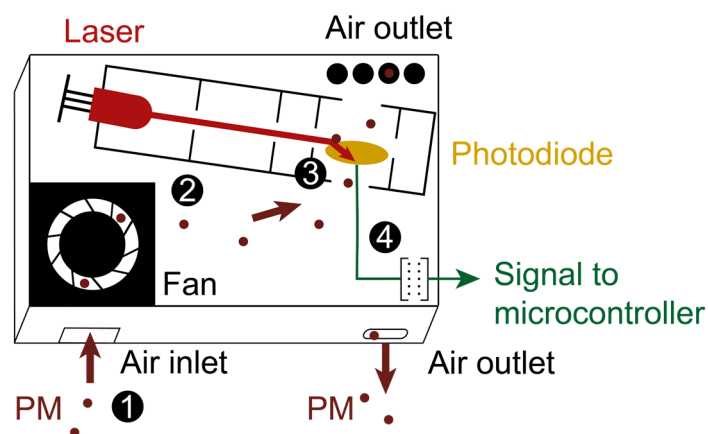


Figure 6. Working principle of the Plantower PMS7003

Within the sensor, air is drawn (1) and propelled by a fan (2) towards air holes at the top right. The air sample containing PM crosses a laser beam, which gets diffracted (3) by PM and impacts the photodiode detector at various angles based on PM sizes. This signal gets converted by the

photodiode into an electric signal (4) sent to the microcontroller, where a proprietary algorithm further computes PM concentration in  $\mu\text{g}/\text{m}^3$ . This optical sensor can effectively measure  $\text{PM}_{10}$  and  $\text{PM}_{2.5}$  but shows unsatisfactory performance for coarse PM, recent studies advising against using it to measure  $\text{PM}_{10}$  (Aix et al., 2023; Molina Rueda et al., 2023). LCS offer a cost effective and flexible solution, but they have limitations. The main concern arises from the calibration performed by the manufacturer, generally occurring in environments with different aerosols than the ones at the operating sites. Therefore, initial calibration algorithms tend to become inaccurate for new environments and often remain inaccessible for confidentiality reasons. This calibration issue contributes to the fact that PMS7003 tends to overestimate PM (Aix et al., 2023; Báthory et al., 2021; Bulot et al., 2019; HabitatMap, 2022b). It is also crucial to acknowledge that relative humidity causes hygroscopic PM growth and can therefore significantly affect PM LCS optical measurements (Bulot et al., 2019; Won et al., 2021). This emphasizes the need to apply corrections to raw PM concentrations given by LCS. A calibration process is therefore recommended, where LCS are placed near a reference instrument in a collocation study.

### 1.4.3 Mobile measurements with low-cost sensors

Various studies highlight the inadequacy of fixed ambient monitoring to represent personal pollutant exposure, particularly in transit microenvironments (Apte et al., 2011; Kaur et al., 2007; Park & Kwan, 2017). Research suggested that people living in the same neighbourhood may have different exposures to pollutants due to different mobility patterns (Dons et al., 2011; Ma et al., 2019). Hence, it is also important to conduct measurements in mobility to get a comprehensive understanding of individual exposure. Transportation is likely to result in peak air pollution exposures in everyday life (Dons et al., 2019), and when compared to other daily activities, exposure generally reaches its highest levels during travel (Singh et al., 2021). To measure exposure while in mobility, the same optical sensor as previously described (PMS7003) can be used. However, adding a GPS is essential to capture locations accurately. AirBeam2 (HabitatMap, 2022a) is a portable PM measuring device (Figure 7) entailing a PMS7003 and a GPS device. AirBeam2 costs 249\$, has a 10-hours autonomy and showed good performances in mobility (Lim et al., 2019; Ma et al., 2020), while also measuring temperature and humidity. AirBeam2 can be paired to a smartphone and attached to a backpack, providing measurements at a fine temporal scale, with data recorded every

second. An online visualization interface (HabitatMap, 2023) allows to retrieve recorded data for subsequent analysis.



**Figure 7. Picture of an AirBeam2 device**

It is important to calibrate AirBeam2 sensors by comparing them to a reference, especially because their calibration equation does not account for humidity (HabitatMap, 2022b). Once properly calibrated, mobile and fixed LCS can be combined with reference stations to offer a holistic approach to assess population's exposure. This strategy allows to identify local PM variations which are not seen at the reference station.

## 1.5 THE SITUATION IN GRENOBLE

### 1.5.1 The study area

Grenoble is located in the French Alps, within an alpine valley surrounded by three substantial mountain ranges over 2000 meters high. With a population of 448,457 inhabitants (INSEE, 2023), Grenoble ranks among the 20 largest French metropolitan areas. Located at the confluence of two rivers, the Drac and the Isère, Grenoble lies within a Y-shaped valley (Figure 8).

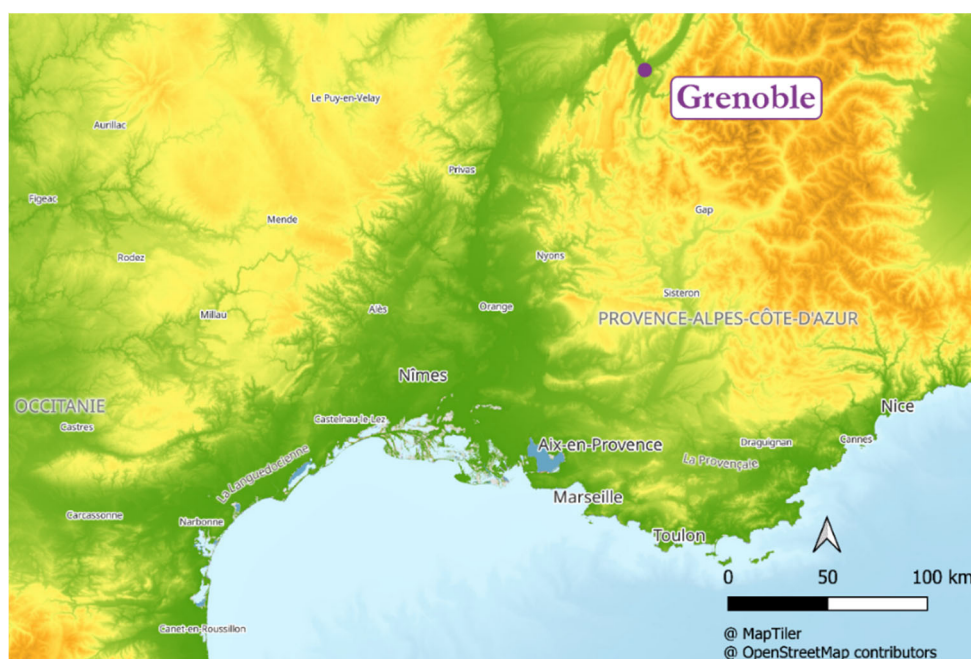


**Figure 8. Geographical location of Grenoble within a distinctive Y-shaped alpine valley**

The topography around Grenoble makes the city prone to long winter pollution events, particularly due to thermal inversions. Largeron and Staquet (2016) stated that lasting inversions occurred between November and February, under high-pressure regimes, covering 35% of winter time. In their study, most  $PM_{10}$  pollution spikes were related to inversions. These winter events, linked to the stagnation of air masses, are generally associated with residential wood heating.

## 1.5.2 Local air pollution context in Grenoble

### 1.5.2.1 Pollutants sources and health impact

Between 2008 and 2015, Grenoble ranked second among the most polluted French cities in terms of  $PM_{2.5}$  (Amrani et al., 2019). Locally, residential heating is the primary contributor to PM (70.2% for  $PM_{2.5}$  and 61% for  $PM_{10}$ ), followed by transportation and industry (Figure 9). Road traffic is the main  $NO_x$  emitter (47.4%), followed by industry and energy sectors. Regarding  $O_3$  formation in Grenoble, climate warming brings more favourable conditions causing average levels to rise in recent years ( $+0.5 \mu\text{g}/\text{m}^3/\text{year}$ ) (Atmo AuRA, 2023c). This trend is projected to continue, as southeastern France is anticipated to be significantly impacted by climate warming (Météo-

France, 2021). Grenoble may also see more intense but less frequent Saharan dust episodes due to climate change, according to Clifford et al. (2019). Dusts events significantly increase local PM<sub>10</sub> and PM<sub>2.5</sub> concentrations, the rise in PM<sub>10</sub> being mainly linked to an increase of the coarse fraction between 2.5 and 10µm (Perez et al., 2008; Quénel et al., 2021). Grenoble experienced numerous Saharan dust episodes in 2021, notably on February 6<sup>th</sup> and from February 22<sup>nd</sup> to 26<sup>th</sup> (Atmo AuRA, 2022c). While dusts can explain some PM<sub>10</sub> alerts, the PM<sub>2.5</sub> issue in Grenoble is generally linked to residential wood heating.

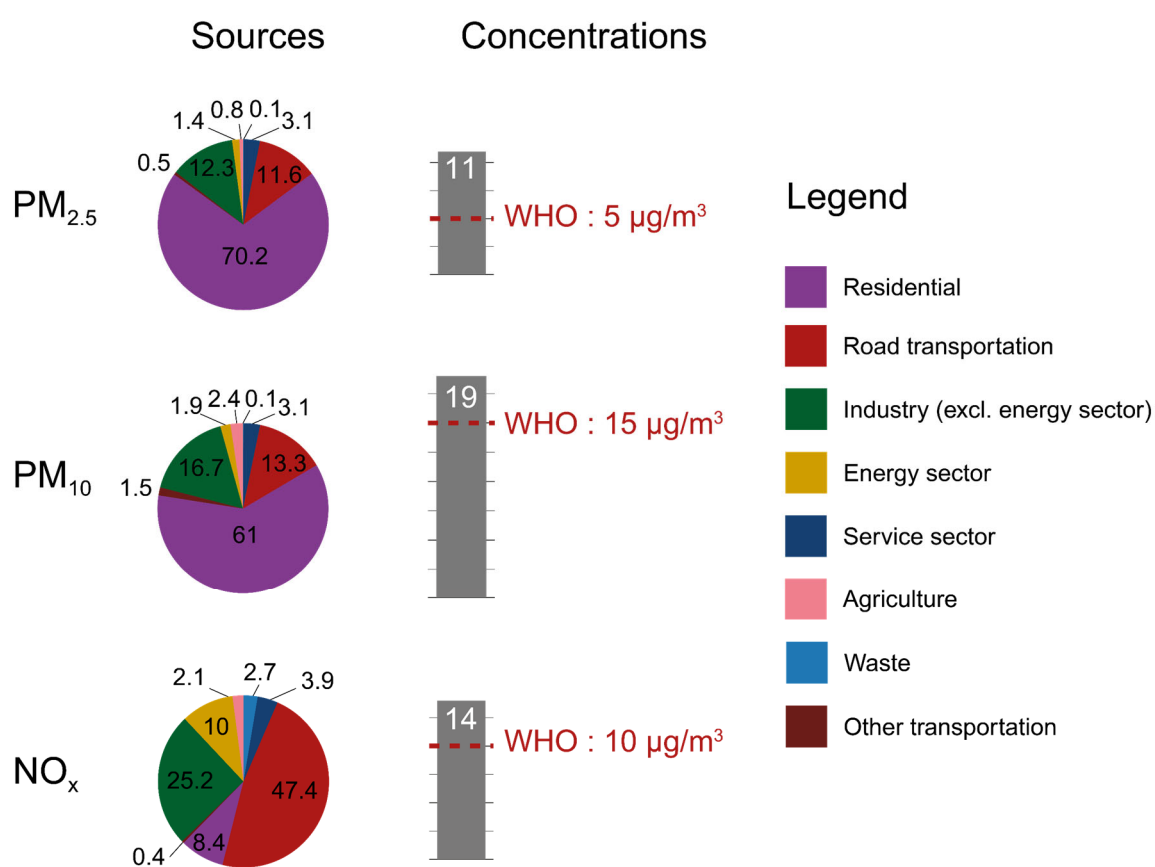


**Figure 9. Pollutant sources and annual concentrations in Grenoble-Alpes Metropole (Les Frênes background station), with WHO's recommended levels (in red).** Data sources : Atmo AuRA (2022a) and World Health Organization (2021b)

In Grenoble, PM<sub>2.5</sub> annual concentrations exceed WHO's recommended levels by 120% (Figure 9), PM<sub>10</sub> by 27%, and NO<sub>x</sub> by 40%. According to Atmo AuRA (2022b), 100% of the residents would be exposed to exceedances of the WHO guidelines for PM<sub>2.5</sub>, 67% for PM<sub>10</sub>, and 94% for NO<sub>2</sub>. Moreover, 11% of the population would exceed the health target value for O<sub>3</sub>, the only regulated pollutant showing no decrease in Grenoble (Préfet de l'Isère, 2022). PM levels are

probably the main lever to significantly improve the health of populations in urban areas like Grenoble (Institute for Advanced Biosciences, 2016). Each year, PM<sub>2.5</sub> is responsible for the premature death of 145 people in Grenoble (Morelli et al., 2019). NO<sub>2</sub> emissions are projected to decrease with the new EURO7 regulations and the rise of electric vehicles. Therefore, it is likely that PM will remain the main issue in Grenoble, another concern also arising from more toxic PM generated by brakes and tires (Tan et al., 2023). Grenoble is a proactive city regarding environmental matters, especially through Atmo AuRA, equipping citizens with mobile or fixed sensors measuring PM (Atmo AuRA, 2023d). To protect public health, it is crucial to communicate risks related to air pollution and to involve the population (Pfleger et al., 2023).

### 1.5.2.2 The problem of PM<sub>2.5</sub>

In Grenoble, highest PM levels are generally recorded in autumn and winter because of higher emission rates, and air stagnation episodes related to temperature inversions (Atmo AuRA, 2023b). On Figure 10, we can see a correlation between temperature and PM<sub>2.5</sub> levels. Maximum PM<sub>2.5</sub> concentrations (in blue) are generally seen during winters.

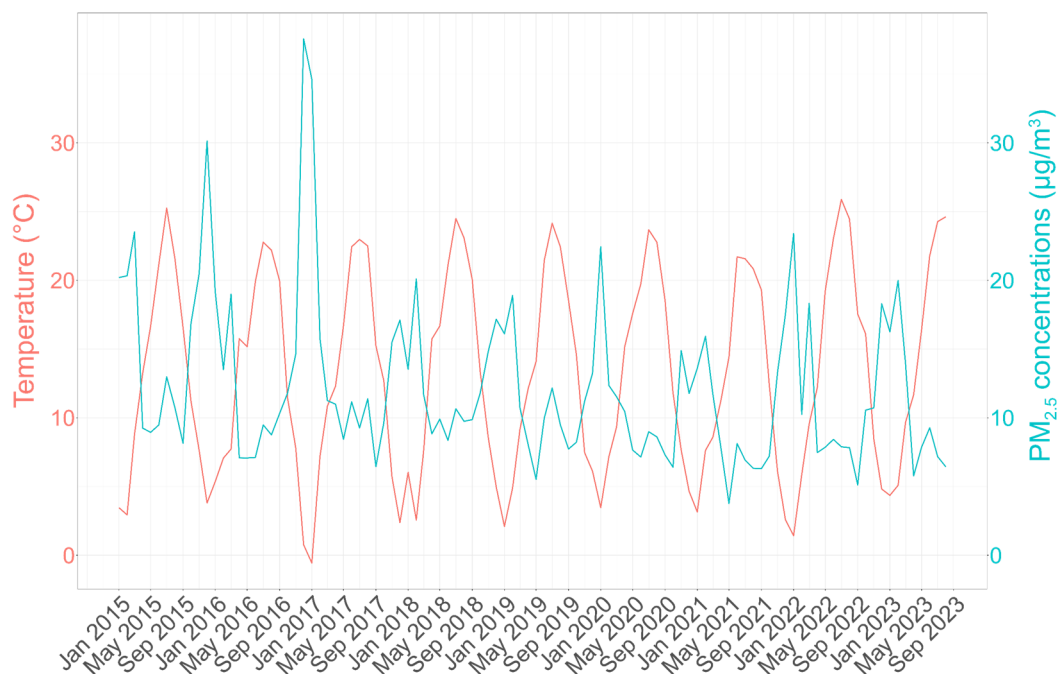


**Figure 10.** Time-series data of monthly average temperatures and PM<sub>2.5</sub> concentrations from January 2015 to July 2023. PM<sub>2.5</sub> concentrations (in blue) are measured in Grenoble (Les Frênes) and provided by Atmo AuRA. Temperatures (in pink) are measured in Saint-Martin d'Hères (3km from Les Frênes) by ROMMA (Réseau d'Observation Météo du Massif Alpin, 2022).

According to Atmo AuRA (2023c), the decline in PM<sub>2.5</sub> levels, observed since 2007 (around -1 µg/m<sup>3</sup> per year) slowed down in 2022 with average concentrations rising. This shift is noteworthy, given the mild winter temperatures normally reducing heating needs. The increase in fossil fuel prices may have encouraged a shift towards cheaper wood heating alternatives.

## 1.6 THESIS OBJECTIVES

In summary, after a thorough exploration of the literature, we observed that:

- Air pollution is a public health concern, as proven by numerous epidemiological and toxicological studies
  - WHO's air quality guidelines are unmet in Grenoble, exposing the population to various health risks
  - Population aging and climate warming will impact Grenoble, intensifying health effects associated with pollution
- ➔ Addressing air pollution and associated health risks is key, and the main objectives of this work were:

### 1.6.1 What are health risks related to air pollutants in Grenoble?

Gaining a deeper understanding of the connection between air pollutants and health is crucial. With a substantial part of the thesis taking place during the pandemic, we started by investigating health risks associated with air pollutants in Grenoble during the COVID-19 crisis (Chapter 2, refer Figure 11 below). When searching the literature on health risks, it appeared that little work had been done on long-term and short-term risks during the pandemic. Often, researchers focused on studying the influence of a single pollutant on mortality or a specific disease, with a primary focus on short-term effects. The impacts of multiple pollutants on diverse health outcomes had rarely been explored. Frequently, researchers focus on a pollutant's effect on mortality or a specific disease, with limited exploration of multiple pollutants' impact on various health outcomes.



Dwivedi et al. (2022) also acknowledged that studies synthesizing evidence for the associations between various air pollutants and cardiovascular outcomes were missing. They conducted such synthesis, exploring the strength of associations among various pollutants and various health outcomes related to cardiovascular issues and mortality. Their study was performed on both short-term and long-term outcomes. Our intention was to follow a similar approach, but for all pathologies. Following a methodology defined by Corso et al. (2019), we listed all short-term or long-term associations between air pollutants (PM, NO<sub>2</sub> and O<sub>3</sub>) and health outcomes, supported by extensive studies. To estimate risks, we used pollutants concentrations measured by reference stations from Atmo AuRA in Grenoble. This method using reference stations, also called “central monitoring technique”, provided accurate and officially validated pollutants concentrations in order to calculate relative risks using the previously explained formula (Equation 1, section 1.3.3). As seen in this RR formula, health risks heavily depend on concentrations estimates. Therefore, it is important to use finely measured concentrations. To mitigate health risks related to air pollution, two approaches are feasible (or a combination of both):

1. Reduce the overall population exposure through policies (Xing & Wong, 2022).
2. Teach individuals prevention strategies to minimize their exposure (Hoang et al., 2022; Y. Zhang et al., 2019).

In the following chapters, novel techniques using sensors were explored to better measure people’s exposure. Various research papers consider central monitoring as inadequate to describe individual exposure to air pollutants (Han et al., 2021; Peters et al., 2013). In this thesis, optical sensors were used to measure exposure at a finer scale, both temporally and spatially. Using LCS appeared to be the most suitable strategy due to their cost-effectiveness, enabling the deployment of an important number of devices.

## 1.6.2 How to accurately measure exposure to PM in Grenoble?

Koenig (2012) stressed the importance of high-quality exposure assessment due to its crucial role in air pollution epidemiology. In this thesis, a significant amount of effort was dedicated to

improve the granularity of pollutants measurements. The objectives were 1) to refine health risk evaluations and 2) to provide people with strategies to lessen their exposure, by modifying their behaviour, particularly their travel habits. Slama et al. (2008) emphasized the need to work on better methods for gauging individuals' exposure duration and intensity, and account for residential mobility. They advocated for exposure models to target finer temporal precision and include time-activity patterns, arguing that spatial and temporal confounding factors should be considered in exposure calculations. Jo et al. (2021) also highlighted the necessity of considering personal factors in health risk management. They admitted that using fixed official stations was a limitation, as exposure relied on variables like time spent outdoors, workplace, and distance to the monitoring station from home. They highlighted that significant differences in average exposure estimate could occur if the station-home distance was important. Improving spatial granularity was one of the reasons why we decided to install a sensors network in Grenoble.

#### 1.6.2.1 Fixed measurements with a LCS network

To improve personal exposure assessment, we started to deploy a stationary LCS network enabling continuous PM monitoring. Various research articles suggest that measuring PM in mobility is more difficult than with fixed monitors (Alas et al., 2019). Quantifying PM with a mobile device can be more challenging, as they are sensitive to unintentional variations and bias (Peters et al., 2013). Mui et al. (2021) also found that the velocity of measurement could impact LCS performance. Consequently, we initiated our study by using stationary devices prior to start a mobile measurement campaign.

#### 1.6.2.2 Mobile measurements

However, various studies underscore the inadequacy of fixed monitoring to represent personal pollutant exposure, particularly in transit environments (Apte et al., 2011; Kaur et al., 2007; Park & Kwan, 2017). Gulliver and Briggs (2004) showed that PM<sub>10</sub> concentrations displayed stronger correlation between various transport modes than with measurements from the fixed-site monitor. Beckx et al. (2009) compared dynamic exposure estimates with traditional static measurements. Results indicated significant differences, especially during the day, as the dynamic approach

accounted for individual mobility patterns. Both approaches exhibited a relative difference of more than 20% in term of hours spent at PM<sub>2.5</sub> concentrations exceeding 20 µg/m<sup>3</sup>. The static method showed significantly lower exposure estimates than the dynamic approach. Research also suggested that people living in the same neighbourhood may have different exposures to pollutants due to different mobility patterns (Dons et al., 2011; Ma et al., 2019). A disadvantage of fixed sensors or monitors is that they are far from individuals' breathing zones. Hence, we also performed measurements in mobility to get a more comprehensive view of individual exposure.

## 1.7 THESIS STRUCTURE

### 1.7.1 Originality

The originality of this thesis lies in this holistic approach to air pollution. First, by examining a set of air pollutants along with their various health effects (Chapter 2), and subsequently, by studying exposure through a method involving both fixed and mobile tools in a complementary approach (Chapters 3, 4 and 5). First, we investigated how to calculate the relative risks of various diseases caused by different pollutants in Grenoble (Chapter 2). Through this research, we acknowledged the significance of accurately estimate individual exposure, a topic we addressed in the later chapters.

### 1.7.2 Why did we focus on PM?

Numerous studies demonstrate that PM are the main contributors to the majority of adverse effects related to air pollution (Araujo, 2010). Among the key atmospheric pollutants, PM displays the strongest causal association with mortality (WHO, 2021b; Pond et al., 2022). Lefler et al. (2019) demonstrated that PM<sub>2.5</sub> exhibited the strongest mortality associations compared to other pollutants (PM<sub>2.5-10</sub>, SO<sub>2</sub>, NO<sub>2</sub>, O<sub>3</sub>, CO). PM doesn't have a concentration threshold below which no health effect would occur. Chapter 2 confirmed that PM carried the greatest health risk, as PM exhibited the most significant associations with the highest RR, particularly for mortality. Studying

PM has a promising future, because PM is ubiquitous in the environment and emerges as the pollutant with the most pronounced negative health impacts (Karagulian, 2023).

Furthermore, due to LCS limitations in measuring gases, we focussed on PM measurements, particularly small PM that could be effectively seen by LCS. Given the significant health impacts of small PM, our focus was mainly directed towards measuring small PM. As calibration methods continue to advance, both mobile and stationary LCS can be efficiently combined with official monitoring stations. In this thesis, we used three approaches to assess individual exposure to air pollutants: central monitoring, LCS networks and mobile LCS. This aligned well with calls from scientists advocating for adopting various complementary approaches to estimate individuals' exposure (Chambliss et al., 2020).

### 1.7.3 Thesis outline

The manuscript is organized into 6 chapters

- **Chapter 1:** General introduction.
- **Chapter 2:** One of the few multipollutant studies covering short-term and long-term risks related to various air pollutants during the COVID-19 crisis.
- **Chapter 3:** A new calibration methodology for PM LCS calibration.
- **Chapter 4:** Deployment and use of a PM LCS network in Grenoble.
- **Chapter 5:** A mobility study to measure PM in commuting microenvironments.
- **Chapter 6:** General conclusion.

The structure of the manuscript is schematically represented on the next page (Figure 11).

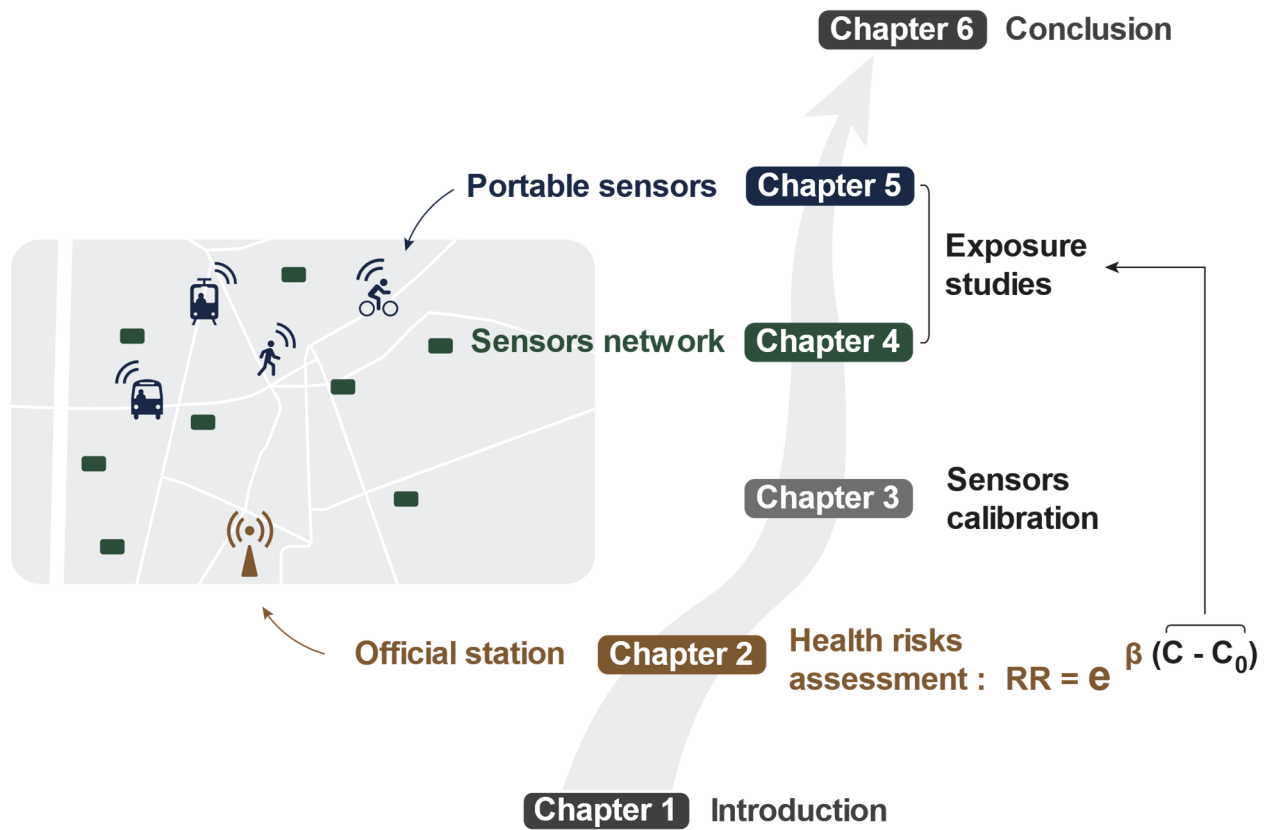


Figure 11. Structure of the thesis manuscript

# 2 HEALTH RISKS ASSOCIATED WITH AIR POLLUTION

## Summary - Introduction Chapter 2

- Problem: Limited research focus on studying short-term and long-term health risks resulting from variations in various air pollutants levels during the COVID-19 crisis
- Objectives:
  1. Compare pollutants levels in Grenoble during COVID-19 versus 2015-2019
  2. Assess health risks associated with these concentration changes

## 2.1 INTRODUCTION

### 2.1.1 Research gap and objectives

This chapter aims to conduct a health risk assessment in Grenoble in the midst of the COVID-19 crisis. While many research papers focused on quantifying variations in air pollutant concentrations, fewer studied the resulting health risks changes. Our research aimed to fill this gap and contribute to a more comprehensive understanding of these relationships. The objective of this study could be summarized in two main questions:

- 1) What were the levels of pollutants concentrations in 2020 compared to 2015-2019 period?
- 2) What were the consequences of those concentration shifts for health risks?

## 2.1.2 Method

We followed guidelines established by Santé Publique France, the French National Public Health Agency (Corso et al., 2019), as they offered a comprehensive and practical approach to conduct a quantitative health impact assessment. The methodology aligned with the framework recommended by the WHO and had been used in European research projects like APHEIS (Ballester et al., 2008) or Aphekom (Pascal et al., 2013), but also for a local study in the Arve Valley (Pascal et al., 2020).

### 2.1.2.1 Dose – response functions

In this method, health risks were classified within two categories: group A and B. Group A referred to pollutant–outcome pairs for which enough data was available to enable reliable quantification of effects. Group B denoted pairs for which there was more uncertainty about the precision of the data used for effects quantification. In this study, we focused on group A health risks to compile dose-response functions ( $RR_e$ ). Also included were the  $RR_e$  from an extensive study on  $O_3$  and mortality involving 406 cities in 20 countries between 1985 and 2015 (Vicedo-Cabrera et al., 2020).

### 2.1.2.2 Pollutant's concentrations

To perform the health impact assessment, all four background stations from Atmo AuRA were used (see Figure 12, in blue). The traffic stations were only employed to analyze concentrations changes (see Figure 12, in red), because these stations are usually considered less representative of the pollutants levels to which the population is regularly exposed.



Figure 12. Map of the 7 stations from Atmo AuRA used for 2015-2020 exposure study. Filled circles represent locations of urban background (in blue) and traffic stations (in red).

To calculate short-term health risks related to O<sub>3</sub>, a specific method was employed to determine O<sub>3</sub> concentrations (Figure 13).

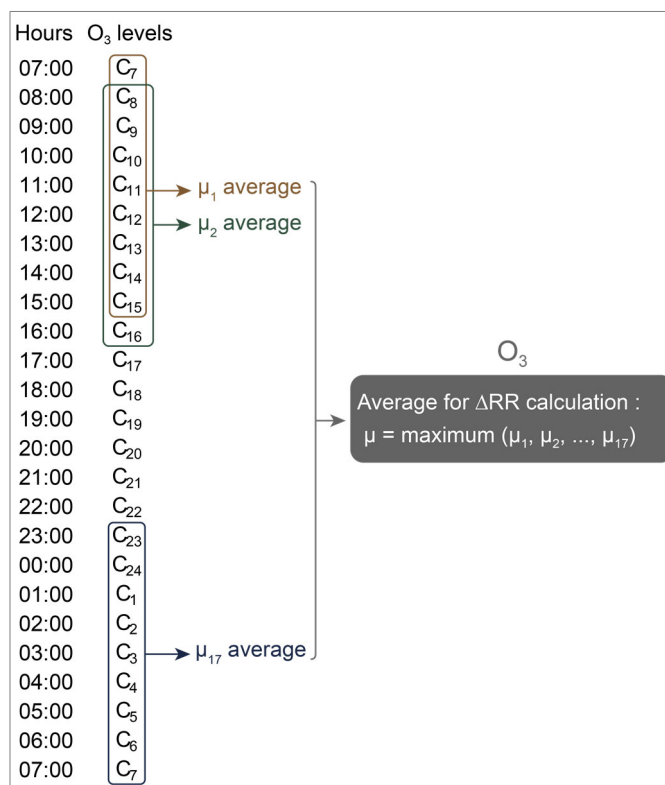
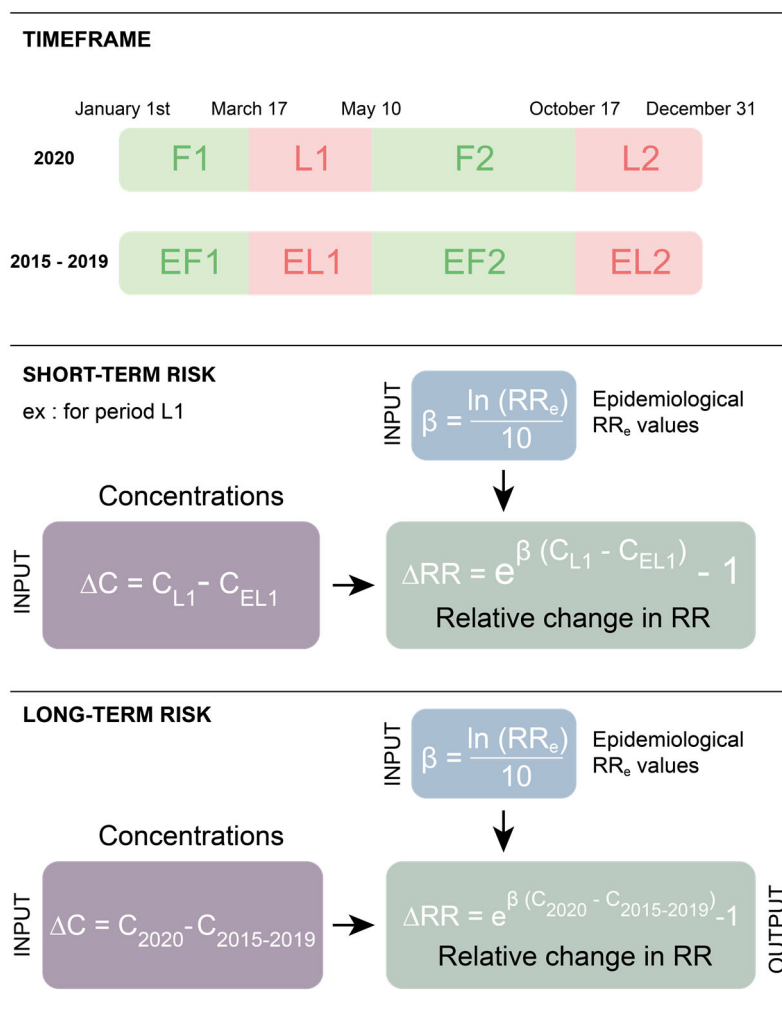


Figure 13. O<sub>3</sub> mean calculation for ΔRR determination



### 2.1.2.3 Health risks calculations

Health risks were assessed using different timeframes and formulas based on whether they were short-term or long-term (Figure 14). For short-term risks, different periods in 2020 were studied with varying restrictions levels. L1 was the period of the first strict lockdown. F2 followed with relaxed measures and L2 was a milder lockdown. An example of rate of short-term (ST) risk change calculation ( $\Delta RR$ ) can be seen in Figure 14 for L1. All time periods beginning with "E" (for "equivalent") correspond to the same timeframes as those in 2020, but they occur within the years 2015-2019. The formula used for long-term (LT) risks calculation is also illustrated in Figure 14.



**Figure 14. Short-term and long-term health risks calculations.**  $C_{L1}$ : daily mean pollutant average concentrations during the 1<sup>st</sup> lockdown.  $C_{EL1}$ : daily mean pollutant average concentrations during the corresponding 2015-2019 period.  $C_{2020}$ : annual pollutant concentration in 2020.  $C_{2015-2019}$ : average of the annual concentrations between 2015 and 2019

## 2.2 ARTICLE N°1

The following paper can be found at: <https://doi.org/10.1016/j.envpol.2022.119134>.



Contents lists available at ScienceDirect

## Environmental Pollution

journal homepage: [www.elsevier.com/locate/envpol](http://www.elsevier.com/locate/envpol)Air pollution and health impacts during the COVID-19 lockdowns in Grenoble, France<sup>☆</sup>Marie-Laure Aix, Pascal Petit, Dominique J. Bicot<sup>\*</sup>

Univ. Grenoble Alpes, CNRS, UMR 5525, VetAgro Sup, Grenoble INP, TIMC, 38000, Grenoble, France

## ARTICLE INFO

**Keywords:**  
 COVID-19  
 Lockdowns  
 Air pollutants  
 Health risks  
 Grenoble

## ABSTRACT

It is undeniable that exposure to outdoor air pollution impacts the health of populations and therefore constitutes a public health problem. Any actions or events causing variations in air quality have repercussions on populations' health. Faced with the worldwide COVID-19 health crisis that began at the end of 2019, the governments of several countries were forced, in the beginning of 2020, to put in place very strict containment measures that could have led to changes in air quality. While many works in the literature have studied the issue of changes in the levels of air pollutants during the confinements in different countries, very few have focused on the impact of these changes on health risks. In this work, we compare the 2020 period, which includes two lockdowns (March 16 - May 10 and a partial shutdown Oct. 30 - Dec. 15) to a reference period 2015–2019 to determine how these government-mandated lockdowns affected concentrations of NO<sub>2</sub>, O<sub>3</sub>, PM<sub>2.5</sub>, and PM<sub>10</sub>, and how that affected human health factors, including low birth weight, lung cancer, mortality, asthma, non-accidental mortality, respiratory, and cardiovascular illnesses. To this end, we structured 2020 into four periods, alternating phases of freedom and lockdowns characterized by a stringency index. For each period, we calculated (1) the differences in pollutant levels between 2020 and a reference period (2015–2019) at both background and traffic stations; and (2) the resulting variations in the epidemiological based relative risks of health outcomes. As a result, we found that relative changes in pollutant levels during the 2020 restriction period were as follows: NO<sub>2</sub> (–32%), PM<sub>2.5</sub> (–22%), PM<sub>10</sub> (–15%), and O<sub>3</sub> (+10.6%). The pollutants associated with the highest health risk reductions in 2020 were PM<sub>2.5</sub> and NO<sub>2</sub>, while PM<sub>10</sub> and O<sub>3</sub> changes had almost no effect on health outcomes. Reductions in short-term risks were related to reductions in PM<sub>2.5</sub> (–3.2% in child emergency room visits for asthma during the second lockdown) and NO<sub>2</sub> (–1.5% in hospitalizations for respiratory causes). Long-term risk reductions related to PM<sub>2.5</sub> were low birth weight (–8%), mortality (–3.3%), and lung cancer (–2%), and to NO<sub>2</sub> for mortality (–0.96%). Overall, our findings indicate that the confinement period in 2020 resulted in a substantial improvement in air quality in the Grenoble area.

## 1. Introduction

Outdoor air pollution has a major influence on the health of populations, and has been of utmost concern for many years. Air pollution is classified as carcinogenic to humans by the International Agency for Research on Cancer (IARC) and is estimated to be responsible for approximately 3.1 million premature deaths worldwide every year and 3.2% of the global burden of disease (Babatola, 2018; Loomis et al., 2013, 2014). In addition to the associated mortality, the inhalation of such air pollution leads to a series of problems for human health: while short-term exposures can trigger or aggravate existing respiratory

and/or cardiovascular problems and increase cases associated hospitalizations, long-term exposures are linked in particular to lung cancer and a greater susceptibility to respiratory tract infections. Anthropogenic sources, such as road traffic, fossil-fuel combustion and households, are the main sources of outdoor air pollution. However, the COVID-19 pandemic has caused a significant reduction in anthropogenic activities (prominent sources of air pollution) at certain times. Indeed, the global spread of SARS-COV-2 (COVID-19) has led governments to implement unprecedented restrictive and preventive measures to slow down COVID-19 outbreaks. Some of these actions (e.g., stay-at-home or national lockdown, curfew) which restricted vehicle

<sup>☆</sup> This paper has been recommended for acceptance by Da Chen.

<sup>\*</sup> Corresponding author.

E-mail address: [dominique.bicot@univ-grenoble-alpes.fr](mailto:dominique.bicot@univ-grenoble-alpes.fr) (D.J. Bicot).

<https://doi.org/10.1016/j.envpol.2022.119134>

Received 24 November 2021; Received in revised form 5 March 2022; Accepted 9 March 2022

Available online 10 March 2022

0269-7491/© 2022 Elsevier Ltd. All rights reserved.

traffic and other activities, had a direct impact on air quality and therefore on public health.

### 1.1. Changes in air pollution during lockdowns

Shortly after the start of the COVID-19 pandemic, a few studies reported that there was a significant drop in air pollutants during the lockdown period (Dutheil et al., 2020; Venter et al., 2020). Although there were still high air pollution events like in northern China (Wang et al., 2020), most publications found decreased background concentrations of pollutants (Bhat et al., 2021; Singh et al., 2020) and improved air quality indices (Bao and Zhang, 2020; He et al., 2020; Mahato et al., 2020; Naqvi et al., 2021; Sahraei et al., 2021) during lockdowns. The decrease in pollutant concentrations at background stations was also confirmed by satellite measurements, especially for nitrogen dioxide (Dutheil et al., 2020; Naqvi et al., 2021; Shehzad et al., 2020; Venter et al., 2020). Currently, more than 200 studies worldwide have assessed the effects of lockdown measures on air quality. Most of them go in the same direction and agree in concluding that the levels of fine particulate matter (PM) and nitrogen dioxide (NO<sub>2</sub>) generally decreased, whereas ozone (O<sub>3</sub>) concentrations increased during lockdowns (Gkatzelis et al., 2021). O<sub>3</sub> levels remained a challenge in some parts of the world as they showed dramatic increases (Grange et al., 2021; Huang et al., 2021). In this context, some works attempted to understand the role of meteorological conditions in the recorded pollution levels and observed reduction (He et al., 2020; Petetin et al., 2020; Ropkins and Tate, 2021). To study the associations between restrictive measures and air pollution, Gkatzelis et al. (2021) and Schneider et al. (2022) used the stringency index (Hale et al., 2021), an indicator to characterize the strictness of government measures. They found significant negative correlations between the stringency index and pollutant concentration changes, especially for NO<sub>2</sub>.

### 1.2. Health impacts related to changes in air pollution during lockdowns

One of the main consequences of the changes in air quality is to be sought on the health of populations. Although epidemiological studies have highlighted the relationship between mortality records or hospital admissions and changes in air quality during COVID-19 restrictions (Bozack et al., 2021; Hameed et al., 2021; Naqvi et al., 2021), little work has been done on the health impacts resulting from these changes in air pollutant levels compared to the number of studies on air quality during lockdowns. Table 1 summarizes the result of the comprehensive literature review on health risks related to changes in air pollution during lockdowns. Most of these studies focus only on short-term health effects and mortality risks. It appears from these works that the occurrence of all these health effects has declined during the lockdowns due to

decreasing levels of air pollutant

Regarding other health impacts, several studies found that outdoor air pollution had an impact on the incidence, prevalence or mortality of COVID-19, as exposure to pollutants can impair immune responses and affect the host's immunity from respiratory virus infections (Katoto et al., 2021). For instance, Zhu et al. (2020), using a generalized additive model, found associations between PM<sub>2.5</sub>, PM<sub>10</sub>, CO, NO<sub>2</sub>, and O<sub>3</sub> levels and COVID-19 cases. Similarly, using artificial neural networks, Magazzino et al. (2020) identified PM thresholds related to COVID-19 deaths. And according to a meta-analysis by Katoto et al. (2021), it appears that COVID-19 cases are most consistently associated with PM<sub>2.5</sub> and NO<sub>2</sub> exposures. Other work has investigated mechanistic aspects of COVID-19 virus infection. Frontera et al. (2020), established a relationship between pollutant exposure and overexpression of the pulmonary ACE-2 receptor associated with severe COVID-19 infections. Frontera et al. (2020), established a relationship between pollutant exposure and overexpression of the pulmonary ACE-2 receptor associated with severe COVID-19 infections. A large cohort study associated NO<sub>2</sub> and PM<sub>2.5</sub> with high titres of anti-COVID-19 IgG antibodies (Kogevinas et al., 2021), likely reflecting high viral exposure. However, pollutant levels were not implicated in the prevalence of COVID-19 which led Hansell and Villeneuve, 2021 to state that reducing air pollution during the pandemic could not be considered a COVID-19 mitigation measure.

In this context, we can legitimately ask whether the restrictive measures implemented to counter COVID-19 outbreaks could have been beneficial not only for air quality, but also for the health of populations regularly exposed to these pollutants, or is there rather a double penalty, i.e., poor air quality plus the COVID-19 health crisis. Concomitant with COVID-19, several surveillance systems observed a decline in infectious diseases such as influenza or gastroenteritis (Kuo et al., 2020; Hatoun et al., 2020; Soo et al., 2020), suggesting that social distancing or other measures taken during the pandemic could have helped to prevent some contagious diseases. From the French Public Health Agency (Santé Publique France (Geodes), 2020), in the Isère department, where the city of Grenoble is located, the number of home emergency acts for influenza and gastroenteritis, and the rate of emergency room visits for gastroenteritis, declined in 2020 compared to 2010–2019.

### 1.3. Study objectives

In this study, we therefore propose taking stock of whether 2020, due to the health crisis, was less heavy in terms of exposure to air pollutants compared to past years. We do not intend to explain the mechanisms and factors that could lead to the changes and drop in air pollution levels, but rather to obtain an idea of the magnitude of variation in exposure levels, regardless of the origin during 2020 in the city of Grenoble, France.

**Table 1**  
Studies associating air pollution with health risks during lockdowns.

Pollutant	Health outcome	Effect <sup>a</sup>	Reference
NO <sub>2</sub> , O <sub>3</sub>	Non-accidental mortality	ST	Achebak et al. (2020)
PM <sub>2.5</sub> , NO <sub>2</sub>	Non-accidental & cardiovascular mortality, mortality for hypertensive disease, coronary heart disease, stroke & chronic obstructive pulmonary disease	ST	Chen et al., 2020
PM <sub>2.5</sub> , O <sub>3</sub>	Mortality all causes, cardiovascular & respiratory	ST	Chen et al., 2021
NO <sub>2</sub>	Mortality	ST, LT	Cole et al. (2020)
PM <sub>2.5</sub>	Mortality	ST, LT	Giani et al. (2020)
PM <sub>2.5</sub>	Mortality	ST	Han and Hong (2020)
PM <sub>2.5</sub>	Mortality	LT	Hao et al. (2021)
PM <sub>10</sub> , NO <sub>2</sub> , O <sub>3</sub> , SO <sub>2</sub>	Hospital admission for respiratory & cardiovascular diseases	ST	Hossain et al. (2021)
PM <sub>2.5</sub> , O <sub>3</sub>	Mortality	ST	Maji et al. (2021)
PM <sub>2.5</sub> , PM <sub>10</sub> , NO <sub>2</sub>	Mortality	ST, LT	Medina et al. (2021)
PM <sub>2.5</sub> , PM <sub>10</sub> , NO <sub>2</sub> , O <sub>3</sub> , SO <sub>2</sub> , CO	Mortality	ST	Nie et al. (2021)
PM <sub>2.5</sub> , PM <sub>10</sub> , NO <sub>2</sub> , O <sub>3</sub>	Mortality	ST	Schneider et al. (2022)
PM <sub>2.5</sub> , NO <sub>2</sub> , O <sub>3</sub>	Mortality, paediatric asthma emergency room visits	ST	Venter et al. (2021)
NO <sub>2</sub> , O <sub>3</sub> , CO	Mortality	ST	Xu et al. (2021)

<sup>a</sup> Abbreviations: ST = short-term, LT = long-term.



Subsequently, we will determine whether these reductions in pollution levels were sufficient to induce a reduction in risks to human health. Concretely, we aim to answer the following two questions:

- To what extent did outdoor air pollution decrease in Grenoble during the lockdown period in 2020 compared to previous years?
- What would have been the impact of such a reduction in air pollution on the short- and long-term risks to human health?

## 2. Methods

### 2.1. Study area

This study focuses on Grenoble, the largest city in the French Alps. This metropolis has approximately 450,000 inhabitants, spread over an area of 545 km<sup>2</sup>. Located in a flat, Y-shaped valley at an altitude of approximately 215 m, Grenoble is surrounded by three large mountain ranges reaching almost 3000 m in height. The local weather is temperate with a continental influence and an effect of the mountainous region. Hot summers and cold winters generate an important thermal amplitude between day and night. Rainfall is relatively high. The surrounding mountains make the city prone to episodes of heavy air pollution. The topography makes it difficult for pollutants to be evacuated horizontally, and the temperature inversion (a meteorological phenomenon in which a layer of hot air overhangs the cold air in a given layer of the atmosphere) often worsens the situation by creating an obstacle to vertical dispersion. The major part of the urbanization is located in the valley.

### 2.2. Study period

In December 2019, a coronavirus disease epidemic started in Wuhan, China. In March 2020, the World Health Organization (WHO) qualified this outbreak as a pandemic. On March 16th, the President of France announced a full lockdown starting the day after. People were ordered to stay at home unless they needed to satisfy essential needs (e.g., buying food, medical appointments, etc.). This mandatory lockdown ended on May 10th. After a relaxed summer, France launched another series of measures starting on October 17th. A curfew was imposed in Grenoble, followed by a second nationwide lockdown, which started on October 30th and ended on December 15th. This lockdown was much softer than the first one, schools remained open, and many people were still working, although many did so remotely.

To structure the comparison of air pollution before, during and after government pandemic measures, we divided 2020 into four periods, and computed a mean daily stringency index for each period (Table 2). The stringency index, ranging from 0 (free and no restrictions at all) to 100 (strictest), allows for the quantification of the severity of measures taken by governments to mitigate the effects of COVID-19 (Hale et al., 2021). This composite index uses nine governmental response indicators, including school, workplace and transport closures, as well as restrictions on gathering. Fig. 1 displays the stringency index trajectory of France in 2020. Clearly, mean stringencies were very high for lockdowns L1 and L2, moderate during the free period F2, and low but different from zero in F1 as the measures gradually settled in at the beginning of the health crisis. By definition, all the years before 2020 were

characterized by a zero-stringency index.

### 2.3. Air pollution data

We considered four airborne pollutants: NO<sub>2</sub>, O<sub>3</sub>, and PM of sizes less than 2.5 μm (PM<sub>2.5</sub>) and 10 μm (PM<sub>10</sub>), respectively. We obtained pollutant concentrations from four background and three traffic monitoring stations, all managed by Atmo Auvergne Rhône-Alpes (the regional non-profit organization accredited by the French authorities to measure and assess air quality). We collected hourly concentration data from January 1st 2015 to December 31st 2020 thanks to an Application Programming Interface (<https://api.atmo-aura.fr/>). The use of hourly values over a 6-year reference period made the analysis more representative and smoothed interannual weather-induced fluctuations. There was a total of 3447 slightly negative values out of 839,493 pollutant levels (0.4%). For NO<sub>2</sub> and O<sub>3</sub>, negative values (0.5%) were replaced by half of the instrumental limit of detection (LOD) values equal to 1 ppb (1 ppb corresponding to 1.88 μg/m<sup>3</sup> for NO<sub>2</sub> and 2 μg/m<sup>3</sup> for O<sub>3</sub>). For PM, negative concentrations (0.3%) were replaced by zero as no LOD were available.

We compared pollutant levels monitored in 2020 to measurements made between 2015 and 2019 (hereafter referred to as the “historical” or “reference period”). The quantity of interest is the relative change in the daily mean pollutant levels, calculated as follows:

$$\Delta P = \frac{P_{2020} - P_{2015-2019}}{P_{2015-2019}} \quad (1)$$

where  $P_{2020}$  and  $P_{2015-2019}$  correspond to daily mean pollutant concentrations in 2020 and during the historical 2015–2019 period, respectively. As daily mean concentrations were distributions for the reference 2015–2019 period, we reported descriptive statistics for. We computed the  $\Delta P$  values for all pollutants considered: NO<sub>2</sub>, O<sub>3</sub>, PM<sub>2.5</sub>, and PM<sub>10</sub>. We performed all statistical analyses using R software 4.0.5 (R Core Team, 2018) for Windows 10©.

### 2.4. Health risk assessment

To assess the health impacts of lockdowns, we followed guidelines from a quantitative health impact assessment tool developed by Santé Publique France together with the WHO (Blanchard et al., 2019). For such an assessment, we used the pollutant concentrations measured at background stations because they are more representative of population exposure than traffic stations (Corso et al., 2019). The health effect caused by exposure to a pollutant for a given period is determined using the relative risk formula, as follows:

$$RR = e^{\beta(C-C_0)} \quad (2)$$

where  $C$  is the pollutant concentration,  $C_0$  is the low concentration threshold below which there is no risk of health effects, and the coefficient  $\beta$  is obtained as follows:

$$\beta = \frac{\ln(RR_e)}{\delta} \quad (3)$$

where  $RR_e$  is the relative risk of health effects obtained from epidemiological studies, and  $\delta$  is the associated concentration increment (see

**Table 2**  
Restriction schemes and the average stringency index.

Timeframe	Period	Description	Average stringency index
01.01.20 (01:00) – 17.03.20 (11:00)	F1	No measures	15
17.03.20 (12:00) – 10.05.20 (00:00)	L1	Strict lockdown	88
11.05.20 (01:00) – 17.10.20 (00:00)	F2	Relaxation of measures	55
18.10.20 (01:00) – 31.12.20 (00:00)	L2	Soft lockdown	70

Note: L1 and L2 represent the 1st and 2nd lockdowns, and F1 and F2 represent the 1st and 2nd “free” periods.

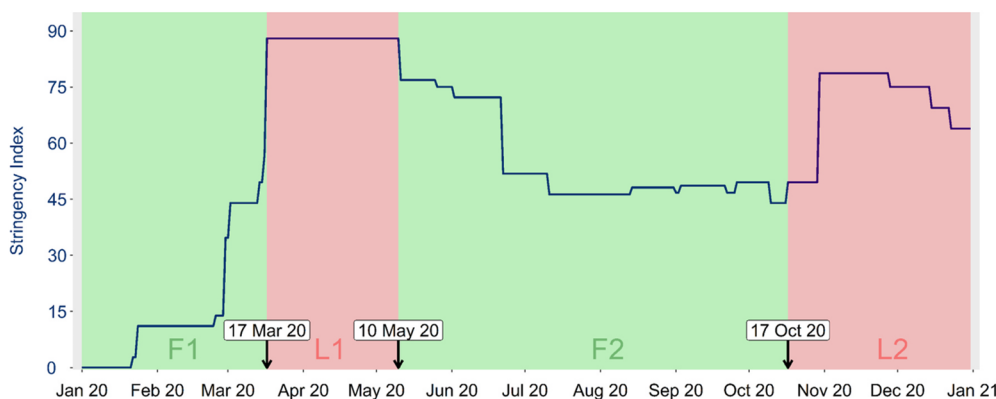


Fig. 1. Evolution of the COVID-19 stringency index in France in 2020.

Table 3). The quantity of interest is the relative change in relative risks:

$$\Delta RR = \frac{RR_{2020} - RR_{2015-2019}}{RR_{2015-2019}} = e^{\beta (C_{2020} - C_{2015-2019})} \quad (4)$$

where  $C_{2020}$  and  $C_{2015-2019}$  are the pollutant concentrations in 2020 and during the 2015–2019 period, respectively, averaged over the appropriate timeframe, and “daily” and “yearly” are the bases for short- and long-term risks, respectively. Since both daily and yearly means were distributions for the reference period of 2015–2019, we reported descriptive statistics (median [95% CI]) for  $\Delta R$ . We computed the  $\Delta RR$  for all pairs of pollutant-health outcomes listed in Table 3. As above, all statistical analyses were performed using R software 4.0.5.

Two parameters control the magnitude of the relative risk index in Eq. (4): the coefficient  $\beta$  (related to the relative risk of health effects ( $RR_e$  in Table 3)) in Eq. (3) and the change of in the pollutant concentration. Therefore, for a given pollutant, the most important health effects are those associated with higher  $\beta$  while for the same given health effects, the most important pollutants are those associated with higher values of both  $\beta$  and variations in concentrations.

To obtain the  $\beta$ , the WHO guidelines use relative risks  $RR_e$  from well-supported epidemiological studies to calculate health benefits from a change in air pollution. In this study, we focused on pollutant–outcome pairs for which data were available to allow for reliable effect quantification (Table 3). We used all  $RR_e$ , accounting for an increase of  $\delta = 10 \mu\text{g}/\text{m}^3$  of pollutant exposure, and coming from Western studies with pollution levels comparable to those observed in Grenoble. We included

a recent  $RR_e$  relating daily mortality to  $\text{O}_3$  calculated for France in the assessment (Vicedo-Cabrera et al., 2020). However, no long-term effects associated with  $\text{O}_3$  were included in our analysis due to large uncertainties in the data (WHO, 2013) and because the impact on all-cause mortality would be minor or non-existent (Hvidtfeldt et al., 2019).

### 3. Results

#### 3.1. Air pollutant concentrations

Fig. 2 shows 7-day moving averages of pollutant ( $\text{NO}_2$ ,  $\text{O}_3$ ,  $\text{PM}_{2.5}$ ,  $\text{PM}_{10}$ ) concentrations during 2020 (purple lines) and the five previous years (2015–2019) (blue lines). Seasonal norms (shaded areas) are represented by the 95% confidence interval (CI) of the 2015–2019 reference period. Of the four pollutants, we observed the largest reduction in 2020 compared to 2015–2019 for  $\text{NO}_2$  levels.

$\text{NO}_2$  levels in 2020 steeply declined during the first ten days after the L1 announcement, especially at traffic stations. During L1,  $\text{NO}_2$  levels lay well below the seasonal norms, even at background stations.  $\text{NO}_2$  concentrations slowly returned to normal after L1 ended. Changes were more important at traffic stations than at background stations, especially during summer holidays and in September 2020. During L2, the levels of  $\text{NO}_2$  at the traffic stations were still below seasonal norms, but to a lesser extent than during L1.

We noted a positive anomaly (above seasonal norms) in 2020 for  $\text{O}_3$  during L1, and two periods with lower levels stood out in September.

Table 3  
Pollutant associated health outcomes and relative risks.

Pollutant	Exposure/timeframe	Age group	Health outcome	$RR_e$ [CI 95%] per 10 $\mu\text{g}/\text{m}^3$	Reference
$\text{O}_3$	Short-term/8h-maximum daily mean	all	Mortality, all causes	1.0019 [1.0006–1.0031]	Vicedo-Cabrera et al. (2020)
		$\geq 65$	Hospitalizations for respiratory causes	1.0044 [1.0007–1.0083]	WHO (2013)
			Hospitalizations for cardiovascular causes (excluding strokes)	1.0089 [1.0050–1.0127]	WHO (2013)
$\text{NO}_2$	Short-term/daily mean	all	Non-accidental mortality	1.0075 [1.0040–1.0110]	Corso et al. (2019)
			Hospitalizations for respiratory causes	1.0180 [1.0115–1.0245]	WHO (2013)
		$\leq 17$	Emergency room visits for asthma	1.0101 [0.9900–1.0200]	Host et al. (2018)
$\text{PM}_{10}$	Short-term/daily mean	all	Non-accidental mortality	1.0030 [1.0013–1.0047]	Liu et al. (2019)
			Non-accidental mortality	1.0063 [1.0025–1.0101]	Liu et al. (2019)
$\text{PM}_{2.5}$	Short-term/daily mean	all	Hospitalizations for respiratory causes	1.0190 [0.9982–1.0402]	WHO (2013)
		$\leq 17$	Emergency room visits for asthma	1.0980 [1.0120–1.1900]	Host et al. (2018)
		all	Hospitalizations for cardiovascular causes (including strokes)	1.0091 [1.0017–1.0166]	WHO (2013)
$\text{NO}_2$	Long-term/annual mean	$\geq 30$	Mortality, all causes	1.1500 [1.0500–1.2500]	Pascal et al. (2016)
		Adults	Lung cancer incidence	1.0900 [1.0400–1.1400]	Hamra et al. (2014)
		Infants	Low birthweight at full term	1.3900 [1.1200–1.7700]	Pedersen et al. (2013)
$\text{NO}_2$	Long-term/annual mean	$\geq 30$	Mortality, all causes	1.0230 [1.0080–1.0370]	Committee on the Medical Effects of Air Pollutants, 2018

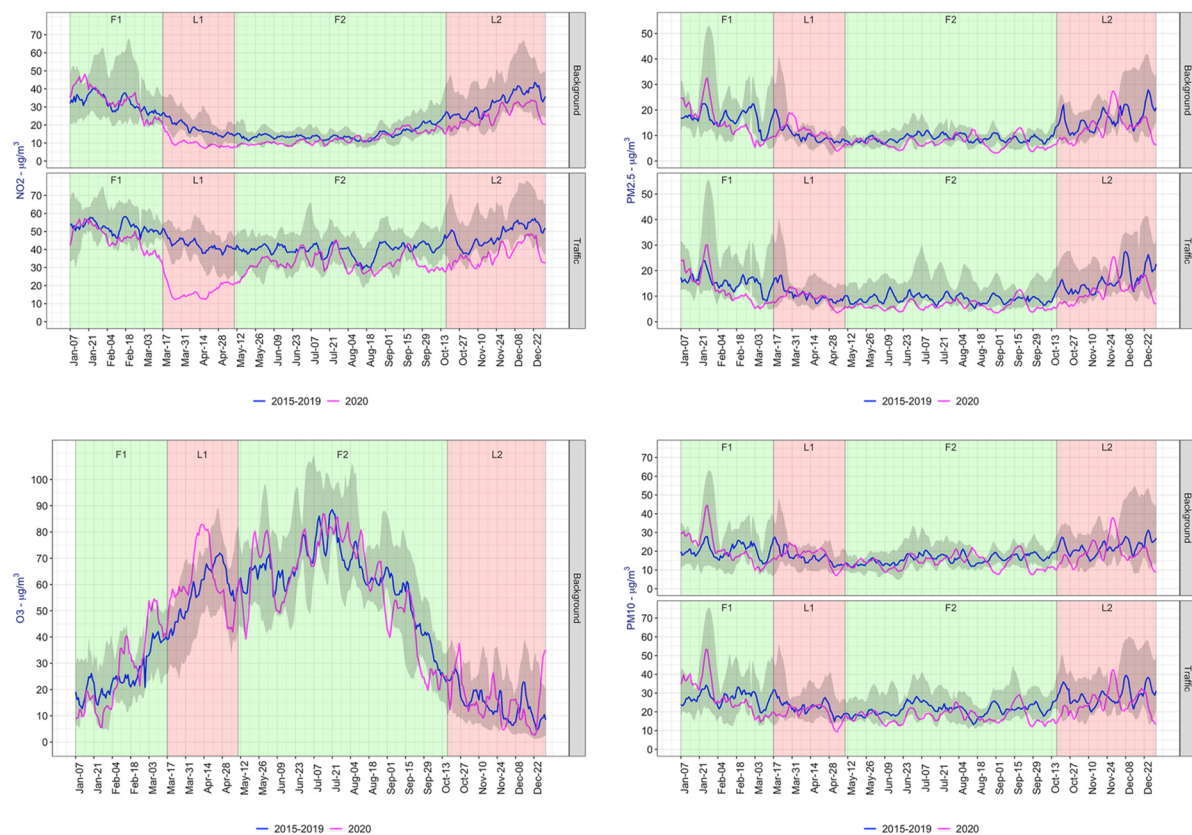


**Fig. 2.** Seven-day rolling averages of pollutant ( $\text{NO}_2$ ,  $\text{O}_3$ ,  $\text{PM}_{2.5}$ ,  $\text{PM}_{10}$ ) concentrations during 2020 (purple lines) and averaged over the five previous years (2015–2019) (blue lines). Solid lines are medians and the shaded areas represent the 95% CI for the 2015–2019 reference period. (For interpretation of the references to colour in this figure legend, the reader is referred to the Web version of this article.)

There was no clear trend during L2, but we observed two peaks above the seasonal norms.

We witnessed a large 2020 PM increase at the beginning of L1 at background stations, with levels above the seasonal norms. Another positive anomaly was recorded at the end of November 2020.  $\text{PM}_{2.5}$  concentration changes (compared to seasonal norms) appeared more important during winter than during summer. Traffic values tended to be lower in 2020 than in 2015–2019, and slightly lower than background values. Time series profiles of  $\text{PM}_{2.5}$  concentrations were similar at the background and traffic stations. The peak seen in 2020 at the beginning of L1 in background stations was less pronounced at traffic stations.

In 2020, the general trend of  $\text{PM}_{10}$  levels was very similar to that of  $\text{PM}_{2.5}$ , except that  $\text{PM}_{10}$  levels were more frequently within the seasonal norms, even during L1. However, similar anomalies were noted for both PMs.

### 3.2. Changes in air pollutant levels

To quantify differences in concentration between 2020 and the period of 2015–2019, we used the descriptive statistics of the relative change in pollutant concentrations,  $\Delta P$ , defined in Eq. (1), as summarized in Figs. 3 and 4. First, Fig. 3 shows that with high Pearson and Spearman correlation coefficients ( $r$ ,  $\rho \geq 0.8$ ), the general trend is a decrease (increase) in  $\text{NO}_2$  ( $\text{O}_3$  and  $\text{PM}_{2.5}$ ) as a function of the average stringency index and no changes ( $r$ ,  $\rho < 0.35$ ) for  $\text{PM}_{10}$ . We found significant ( $p < 0.05$ ) negative correlations between the 2020

concentrations of  $\text{NO}_2$  and the average stringency index of the F1, L1, F2, and L2 periods, but no such correlations for  $\text{O}_3$  and PM (see Fig. 3). That is, high stringency indices were associated with low concentrations of  $\text{NO}_2$  and vice versa.

Next, in Fig. 4, at background stations, there was a substantial decrease (–48%) in daily mean  $\text{NO}_2$  levels during L1 when compared to 2015–2019. The release of the measures in F2 showed an increase in  $\text{NO}_2$  levels (see Fig. 2), but daily mean  $\text{NO}_2$  levels were still lower than that in 2015–2019 (–19% and –18% at background and traffic stations, respectively). During L2,  $\text{NO}_2$  levels declined by about –25%. The  $\text{NO}_2$  level decrease was 25% higher at traffic stations than for background stations during L1, but almost the same during F2 and L2.

For  $\text{O}_3$  at background stations ( $\text{O}_3$  not measured at traffic stations), concentration levels increased during L1 and L2 in 2020, and the situation returned to normal during F2.

During L1 in 2020, daily mean  $\text{PM}_{10}$  concentrations increased (+3%) at background stations, but the maximum level was reduced by 46% and the 97.5th percentile by 14% thus indicating a change in the profile of the distribution. There was no clear trend for  $\text{PM}_{10}$  during L1. After L1, the daily mean  $\text{PM}_{10}$  levels at background stations stayed well below the historical values until the end of the year (–15% in F2 and –22% in L2). The general pattern for  $\text{PM}_{2.5}$  was similar to that of  $\text{PM}_{10}$ . Overall, positive or negative concentration changes appeared more pronounced for  $\text{PM}_{2.5}$  than for  $\text{PM}_{10}$  during L1, F2, and L2. In contrast to background stations, PM concentrations were reduced (e.g., a mean of –19% and –17% for  $\text{PM}_{2.5}$  and  $\text{PM}_{10}$ , respectively) during L1 at traffic stations.



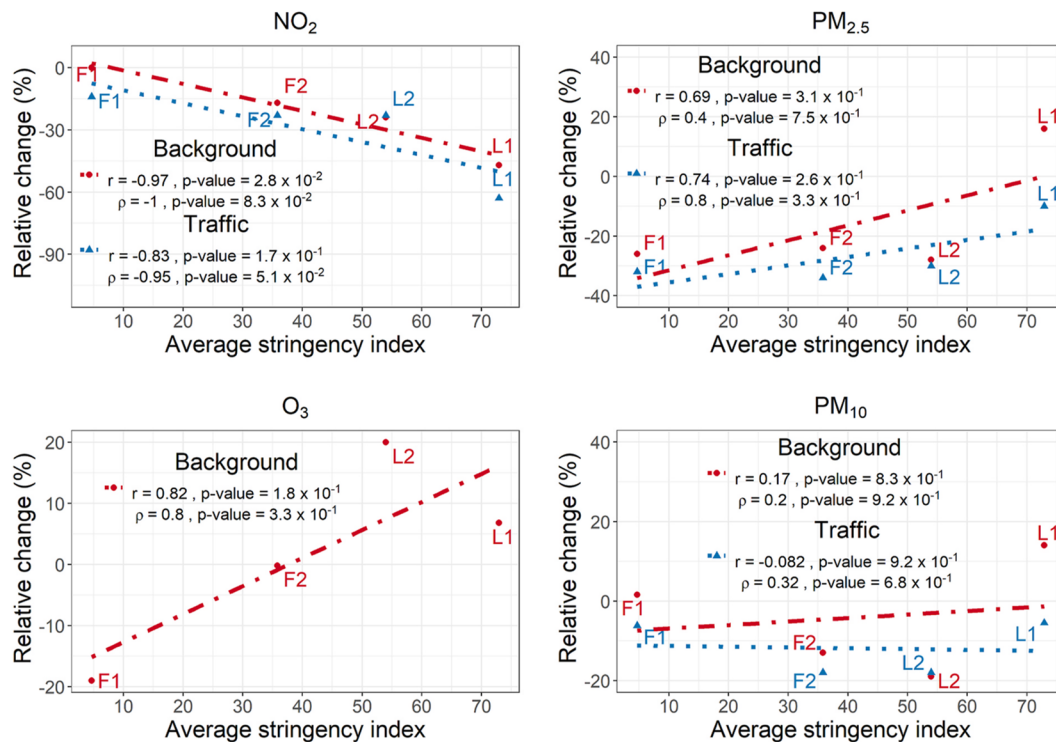


Fig. 3. Pollutant relative changes (median) between 2020 and 2015–2019 as a function of the average stringency index in 2020. Symbols represent data and straight lines represent linear regressions of data for trends. Pearson and Spearman correlation coefficients are given by  $r$  and  $\rho$ , respectively.

### 3.3. Changes in health risks

We assessed the impact of air pollution changes in 2020 on health outcomes using the relative change in relative risks,  $\Delta RR$ , defined in Eq. (4), as reported in Fig. 5. The long-term (average of the entire year) impacts of air pollution changes turned out to be larger than short-term impacts.

Long-term decreases in PM<sub>2.5</sub> levels would result in 2%, 3%, and 8% reductions in the risk of lung cancer, mortality, and low birth weight, respectively. Likewise, the decline in NO<sub>2</sub> levels could result in a 0.95% reduction in the associated long-term mortality risk.

Regarding short-term outcomes, the most important reductions occurred after the health crisis began (in L1, F2, and L2), except for the PM<sub>2.5</sub>-related child emergency room visits for asthma (−1% in F1). During L1, the drop in NO<sub>2</sub> levels would result in 0.63%, 0.86%, and 1.5% reductions in non-accidental mortality, emergency admissions for asthma, and hospitalizations for respiratory causes, respectively. During F2, the most important risk reduction was related to PM<sub>2.5</sub> for emergency room visits for asthma (−1.8%). The decline in O<sub>3</sub> concentrations during F2 would lead to a 0.6% reduction in hospitalizations for cardiovascular causes. During L2, the decrease in NO<sub>2</sub> concentrations reduced the risk of emergency room visits for asthma by 0.8%, non-accidental mortality by 0.6%, and hospitalizations for respiratory causes by 1.5%.

## 4. Discussion

Our main objectives were to assess the magnitude of changes in outdoor air pollution levels in Grenoble during 2020 (structured in stringency periods) compared to previous years (of zero stringency), and to examine the associated potential impacts on short- and long-term

human health risks.

Over the entire restriction period of 2020 (i.e., from March 17th to the end of December), the overall level (average of the mean values in Fig. 4 over the periods L1, F2 and L2 on the two stations) decreased compared to previous years for NO<sub>2</sub> (−32%), PM<sub>2.5</sub>, (−22%), and PM<sub>10</sub> (−15%) at both background and traffic monitoring stations, but there was an increase of O<sub>3</sub> (+10.6%) at background stations. Unexpectedly, PM levels rose at background stations during L1. Similar observations have been noted in several studies (Le et al., 2020; Seo et al., 2020; Ropkins and Tate, 2021). Seo et al. (2020) reported PM<sub>2.5</sub> concentration decreases of 36% and 31% in Seoul and Daegu, respectively. In the UK, Ropkins and Tate (2021) revealed a rise at both traffic and background stations in contrast to Grenoble, where traffic PM levels fell. In Beijing, Le et al. (2020) stated that PM<sub>2.5</sub> levels rose significantly, as did O<sub>3</sub>. In our study, we witnessed an important O<sub>3</sub> increase during lockdowns, as in other European studies (Collivignarelli et al., 2020; Sicard et al., 2020). In Barcelona, for example, Tobías et al. (2020) also observed a significant increase in O<sub>3</sub> (about +50%) during the lockdown from March 14 to 30 which they attribute to the chemical mechanisms of the decrease in NO<sub>x</sub> causing an increase in O<sub>3</sub> and a decrease in NO reducing O<sub>3</sub> titration. At background stations, they found large relative changes for NO<sub>2</sub> (−47%), PM<sub>10</sub> (−27.8%) and O<sub>3</sub> (+28.5%) between pre-lockdown (from February 16 to March 13) and during confinement (March 14 to 30). We also observed the most critical concentration reduction in Grenoble for NO<sub>2</sub>, with levels significantly ( $p < 0.01$ ) and negatively correlated with the average Oxford stringency index ( $r^2 = 0.9$ ). Likewise, Gkatzelis et al. (2021) stated in a worldwide analysis that NO<sub>2</sub> level decreases were due to the stringency of lockdown measures. Reductions in traffic-related NO<sub>2</sub> levels were also reported in the UK (Brown et al., 2021).

Recall that we are looking here at the differences in the monitored



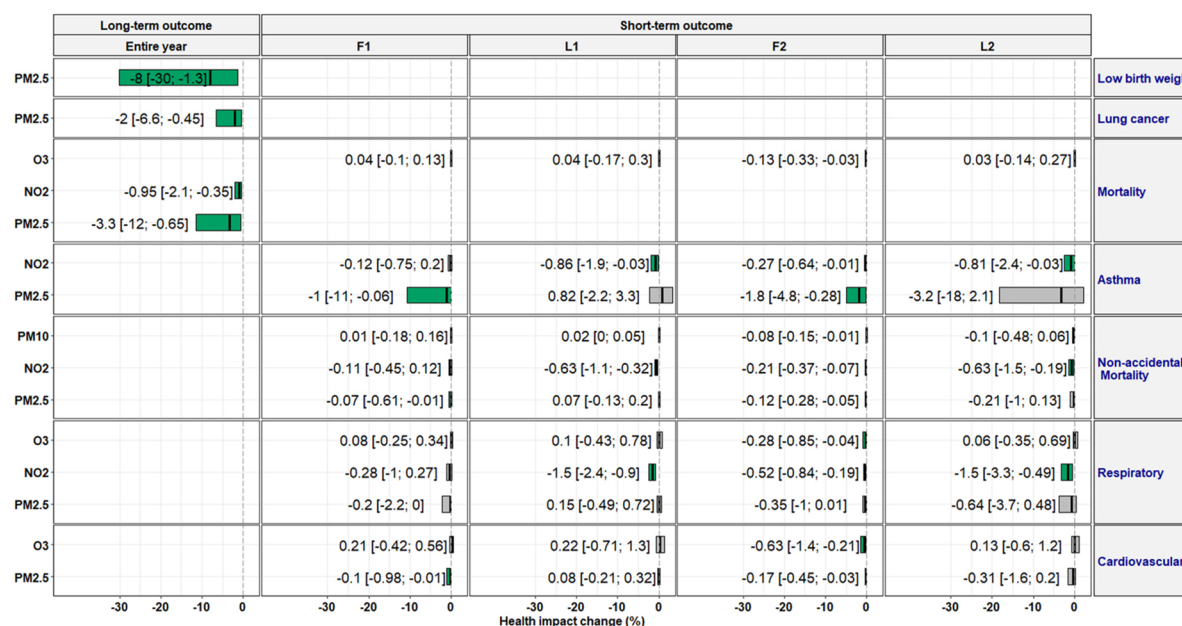


Fig. 4. Relative changes and descriptive statistics of daily mean pollutant levels at background (top) and traffic (bottom) stations. Horizontal bars with quoted percentages represent the relative changes between 2020 (Lockd) and 2015–2019 (Hist), and values are daily mean concentrations in  $\mu\text{g}/\text{m}^3$ .

pollutant concentrations (i.e., outdoor exposure) over several years without investigating the mechanisms and/or factors (e.g., meteorological conditions, changes in the behavior of population displacement, pollutant transportation, etc.) that could have contributed to these changes in pollutant levels in 2020. For instance, according to Airparif (2021), meteorology accounted for one-third of the NO<sub>2</sub> concentration decrease in 2020.

Currently, it is well known that exposure to air pollution may result in a variety of acute or chronic health effects. Short-term outcomes occur

within a few days after acute exposure. Thus, air pollution peaks increase the risks of emergency room visits for asthma, mortality, and hospitalizations for cardiovascular or respiratory causes and mortality. Such acute effects impact vulnerable people including children, the elderly, and patients with respiratory or cardiovascular diseases. Long-term health effects, originating from persistent exposure to air pollutants, are much greater because they lead to the development of chronic pathologies. In this study, we found that the most important health risk reductions in 2020 were related to PM<sub>2.5</sub> and NO<sub>2</sub>, while PM<sub>10</sub> and O<sub>3</sub>



**Fig. 5.** Percentage change in health risks in 2020 from baseline 2015–2019, associated with air pollution changes during the examined periods. Horizontal bars represent the 2.5th, 50th (median), and 97.5th percentiles as given by the quoted numbers. Health impacts at the 97.5th percentile  $< 0$  are highlighted in green. See Table 2 for the description of health outcomes. (For interpretation of the references to colour in this figure legend, the reader is referred to the Web version of this article.)

changes had almost no effect on health outcomes.

For long-term health outcomes, the reduction of  $PM_{2.5}$  levels in 2020 could lower the risk of low birthweight (from  $-1.3\%$  up to  $-30\%$ ), mortality ( $-3.3\%$ ), and lung cancer ( $-2\%$ ). In an Irish study, Philip et al. (2020) indicated a  $-73\%$  reduction in very low birthweight between January and April 2020 compared with the preceding 20 years. Kim et al. (2021) observed that during the COVID-19 period in South Korea, the low birthweight rate was 2.2 times lower than that during the pre-COVID-19 period (2011–2019). For France, in a study by Medina et al. (2021), the long-term mortality decrease was estimated to be approximately  $-0.4\%$  for metropolitan France, which was lower than that in Grenoble. Likewise, we found a risk reduction of  $-0.95\%$  in mortality associated with a decrease in long-term  $NO_2$  levels in Grenoble, whereas Medina et al.'s (2021) estimation showed a  $-0.2\%$  decline for all of France. Although going in the same direction, differences in values between the findings of Medina et al. (2021) and those of our research mainly reflect the heterogeneity of exposure to air pollutants across France. Like most urban cities, Grenoble is very connected to major intercity transport networks and therefore very prone to  $NO_2$  pollution. The drop in pollutants would have been more pronounced in Grenoble than the average across the whole country.

Among all short-term effects, those concerning  $PM_{2.5}$  and childhood asthma would be the most impacted, with  $-1\%$ ,  $-1.8\%$ , and  $-3.22\%$  risk reductions during F1, F2 and L2, respectively. Other European studies reported larger decreases. In Slovenia, Krivec et al. (2020) indicated a  $-71\%$  to  $-78\%$  decline in paediatric asthma admissions from March 16th to April 20th, 2020 compared to 2017–2019. Shah et al. (2021) found a statistically significant change in the level ( $-0.196$ ;  $p = 0.008$ ) of the asthma exacerbation rate in England after March 23rd 2020. According to Davies et al. (2021), the lockdown in Scotland and Wales was associated with a  $-36\%$  pooled reduction in emergency admissions for asthma.

For short-term effects on non-accidental mortality,  $NO_2$  turned out to be more critical than  $PM_{2.5}$  in contrast to what was seen for long-term

effects. We found a short-term risk reduction of  $-0.6\%$  in mortality related to  $NO_2$  levels in Grenoble during L1, consistent with Medina et al.'s (2021) estimation of  $-0.3\%$  for the entire country. Because of the high  $NO_2$  concentration decreases, hospitalizations for respiratory causes could have been reduced by  $-1.5\%$  during L1 and L2 in Grenoble. In a cohort study in Greece, Kyriakopoulos et al. (2021) reported that the incidence rate for respiratory diseases between March and April 2020 was 21.4 admissions per day, compared to 40.8 in 2018 or 39.9 in 2019 (i.e., an approximately 47% reduction). The risk reduction ( $-0.63\%$ ) of hospitalizations for cardiovascular causes was mainly associated with  $O_3$  levels during F2 in Grenoble. Bhatt et al. (2020) observed a significant daily decline in ( $-5.9\%$ ) hospitalizations for primary acute cardiovascular reasons in March 2020 across a large American tertiary care health system.

Beyond the differences in values that can be attributed to differences in methods, epidemiological and environmental contexts, there is a concordance between all these observations and ours in the reduction of the health risks associated with air quality during the entire lockdown period. Other things to consider include hospital avoidance behavior during the COVID-19 crisis and indoor air. Indeed, many patients may have delayed treatment for fear of catching the COVID-19 virus in hospitals. Czeisler et al. (2020) estimated that 41% of American adults delayed or avoided health care during the pandemic because of concerns about COVID-19. In addition, the quality of indoor air would certainly have had an impact on health (perhaps contrasted with outdoor air) during lockdowns, particularly during L1, when a large proportion of the population was housebound. All estimates presented in this study are based only on outdoor air pollutant exposure.

In sum, pollutants with major health impacts in 2020 were  $NO_2$  and  $PM_{2.5}$  for both short- and long-term risks. Although  $O_3$  was the only pollutant that underwent an increase during that period, those changes were not sufficient to induce major health risk increases. The most impacted short-term outcomes during lockdowns were asthma and hospitalizations for respiratory ailments. This is consistent with several

studies showing greater decreases during lockdowns for respiratory illnesses than for cardiovascular diseases. Impacted long-term outcomes include low birthweight, mortality, and lung cancer. The mortality in question here would be the delta of deaths to be subtracted from the large number of deaths caused by COVID-19.

As mentioned above, the experience of lockdowns in 2020 has shown that the main health impacts were related to NO<sub>2</sub> and PM<sub>2.5</sub>. In Grenoble area, 56% of NO<sub>x</sub> emissions can be attributed to transport while 63% of PM<sub>2.5</sub> emissions originate from wood heating (Atmo, 2020). This therefore indicates that both emission sectors need to be considered when designing effective policies to reduce pollution levels. Interestingly, Bouscasse et al. (2022) have recently developed an inverse approach for the Grenoble urban area, starting from public health objectives to define urban policies compatible with these objectives. They report that replacing all inefficient wood-burning appliances with pellet stoves and reducing private vehicle traffic by 36% would result in a two-thirds reduction in fine particulate mortality by 2030.

## 5. Conclusion

As expected, the lockdowns in Grenoble resulted in a substantial drop in PM and NO<sub>2</sub> levels. While the NO<sub>2</sub> concentration decrease could be significantly statistically associated with the stringency of governmental mitigation measures, no such clear trend could be drawn for PM concentration changes, especially during the first lockdown (L1). The most pronounced health effects were found to be associated with PM<sub>2.5</sub> with long-term outcomes such as low birthweight, mortality, or lung cancer, but also with short-term effects such as childhood asthma. A decrease in NO<sub>2</sub> levels was associated, to a lesser extent than a decrease in PM<sub>2.5</sub>, with a drop in long-term mortality risk and a short-term decline in hospitalizations for respiratory causes. During the restrictions, levels of O<sub>3</sub> or PM<sub>10</sub> did not induce an important change in health risk compared to the other pollutants. Now that all kinds of activities are on the rise, it would be instructive to redo this analysis with data from 2021 and years to come to learn more about how the trends outlined in this study will evolve.

## Funding

We did not receive any specific grant from agencies in the public, commercial, or not-for-profit sectors. This work has been partially supported by MIAI@Grenoble Alpes (ANR-19-P3IA-0003).

## Author contributions

**Marie-Laure Aix:** data curation, formal analysis, investigation, software, visualization, writing (original draft and reviewing). **Pascal Petit:** formal analysis, investigation, visualization, writing (review and editing). **Dominique J Bicout:** conceptualization, formal analysis, funding acquisition, investigation, methodology, project administration, software, supervision, validation, visualization, writing (review and editing).

## Declaration of competing interest

The authors declare that they have no known competing financial interests or personal relationships that could have appeared to influence the work reported in this paper.

## Acknowledgments

M-LA is a PhD student supported by a grant from the Ministry of Education and Research of France through the Ecole Doctorale Ingénierie pour la Santé, la Cognition et l'Environnement (ED-ISCE) of Grenoble Alpes University. We would also like to thank Atmo Auvergne Rhône-Alpes for providing air pollution data and the MIAI Grenoble

Alpes chair "Detection, classification and localisation of pollutants in air and liquids".

## References

- Achebak, H., Petetin, H., Quijal-Zamorano, M., Bowdalo, D., García-Pando, C.P., Ballester, J., 2020. Reduction in air pollution and attributable mortality due to COVID-19 lockdown. *Lancet. Planet. Health.* 4 (7), e269. [https://doi.org/10.1016/S2542-5196\(20\)30148-0](https://doi.org/10.1016/S2542-5196(20)30148-0).
- Airparif, 2021. COVID-19 et qualité de l'air. Airparif dossier, p. 16. Edition Mai 2021. <https://www.airparif.asso.fr/sites/default/files/pdf/Airparif-Dossier-3-4-COVID19.pdf>.
- Atmo, AuRA., 2020. Bilan Qualité de l'Air 2019 – Isère/Métropole de Grenoble/Pays Viennois, p. 33. <https://www.atmo-auvergnepaysviennois.fr/sites/ra/files/atoms/files/bilanqa2019-zoom38-isere.pdf>. (Accessed 2 February 2022).
- Bao, R., Zhang, A., 2020. Does lockdown reduce air pollution? Evidence from 44 cities in northern China. *Sci. Total Environ.* 731, 139052. <https://doi.org/10.1016/j.scitotenv.2020.139052>.
- Babatola, S.S., 2018. Global burden of diseases attributable to air pollution. *J. Publ. Health Afr.* 9 (3), 813. <https://doi.org/10.4081/jphia.2018.813>.
- Bhat, S.A., Bashir, O., Bilal, M., Ishaq, A., Din Dar, M.U., Kumar, R., Bhat, R.A., Sher, F., 2021. Impact of COVID-related lockdowns on environmental and climate change scenarios. *Environ. Res.* 195, 110839. <https://doi.org/10.1016/j.envres.2021.110839>.
- Bhatt, A.S., Moscone, A., McElrath, E.E., Varshney, A.S., Claggett, B.L., Bhatt, D.L., Butler, J., Adler, D.S., Solomon, S.D., Vaduganathan, M., 2020. Fewer hospitalizations for acute cardiovascular conditions during the COVID-19 pandemic. *J. Am. Coll. Cardiol.* 76 (3), 280–288. <https://doi.org/10.1016/j.jacc.2020.05.038>.
- Blanchard, M., Host, S., Medina, S., 2019. Pollution atmosphérique. Guide pour la réalisation d'une évaluation quantitative des impacts sur la santé (EQIS). EQIS d'une intervention. Santé publique France, p. 104. <https://www.santepubliquefrance.fr/determinants-de-sante/pollution-et-sante/air/documents/guide/pollution-atmospherique-guide-pour-la-realisation-d-une-evaluation-quantitative-des-impacts-sur-la-sante-eqis-eqis-d-une-intervention>.
- Bouscasse, H., Gabet, S., Kerneis, G., Provent, A., Rieux, C., Ben Salem, N., Dupont, H., Troude, F., Mathy, S., Slama, R., 2022. Designing local air pollution policies focusing on mobility and heating to avoid a targeted number of pollution-related deaths: forward and backward approaches combining air pollution modeling, health impact assessment and cost-benefit analysis. *Environ. Int.* 159, 107030. <https://doi.org/10.1016/j.envint.2021.107030>.
- Bozack, A., Pierre, S., DeFelice, N., Colicino, E., Jack, D., Chillrud, S.N., Rundle, A., Astua, A., Quinn, J.W., McGuinn, L., Yang, Q., Johnson, K., Masci, J., Lukban, L., Maru, D., Lee, A.G., 2021. Long-term air pollution exposure and COVID-19 mortality: a patient-level analysis from New York city. *Am. J. Respir. Crit. Care Med.* <https://doi.org/10.1164/rccm.202104-0845OC>.
- Brown, L., Barnes, J., Hayes, E., 2021. Traffic-related air pollution reduction at UK schools during the Covid-19 lockdown. *Sci. Total Environ.* 780, 146651. <https://doi.org/10.1016/j.scitotenv.2021.146651>.
- Chen, K., Wang, M., Huang, C., Kinney, P.L., Anastas, P.T., 2020. Air pollution reduction and mortality benefit during the COVID-19 outbreak in China. *Lancet Planet. Health* 4 (6), e210–e212. [https://doi.org/10.1016/S2542-5196\(20\)30107-8](https://doi.org/10.1016/S2542-5196(20)30107-8).
- Chen, G., Tao, J., Wang, J., Dong, M., Li, X., Sun, X., Cheng, S., Fan, J., Ye, Y., Xiao, J., Hu, J., He, G., Sun, J., Lu, J., Guo, L., Li, X., Rong, Z., Zeng, W., Zhou, H., Chen, D., Li, J., Yuan, L., Bi, P., Du, Q., Ma, W., Liu, T., 2021. Reduction of air pollutants and associated mortality during and after the COVID-19 lockdown in China: impacts and implications. *Environ. Res.* 200, 111457. <https://doi.org/10.1016/j.envres.2021.111457>.
- Cole, M.A., Elliott, R.J.R., Liu, B., 2020. The impact of the wuhan covid-19 lockdown on air pollution and health: a machine learning and augmented synthetic control approach. *Environ. Resour. Econ.* 76, 553–580. <https://doi.org/10.1007/s10640-020-00483-4>.
- Collivignarelli, M.C., Abbà, A., Bertanza, G., Pedrazzani, R., Ricciardi, P., Carnevale Miino, M., 2020. Lockdown for CoViD-2019 in Milan: what are the effects on air quality? *Sci. Total Environ.* 732, 139280. <https://doi.org/10.1016/j.scitotenv.2020.139280>.
- Committee on the Medical Effects of Air Pollutants (COMEAP), 2018. Associations of Long-Term Average Concentrations of Nitrogen Dioxide with Mortality, p. 152. [https://assets.publishing.service.gov.uk/government/uploads/system/uploads/attachment\\_data/file/734799/COMEAP\\_NO2\\_Report.pdf](https://assets.publishing.service.gov.uk/government/uploads/system/uploads/attachment_data/file/734799/COMEAP_NO2_Report.pdf). (Accessed 10 February 2022).
- Corso, M., Lagarrigue, R., Medina, S., 2019. Pollution atmosphérique. Guide pour la réalisation d'une évaluation quantitative des impacts sur la santé (EQIS). EQIS avec une exposition mesurée. Santé publique France, p. 92. <https://www.santepubliquefrance.fr/determinants-de-sante/pollution-et-sante/air/documents/guide/pollution-atmospherique-guide-pour-la-realisation-d-une-evaluation-quantitative-des-impacts-sur-la-sante-eqis-eqis-avec-une-exposition-mesuree>.
- Czeisler, M.E., Marynak, K., Clarke, K.E.N., Salah, Z., Shykya, I., Thierry, J.M., Ali, N., McMillan, H., Wiley, J.F., Weaver, M.D., Czeisler, C.A., Rajaratnam, S.M.W., Howard, M.E., 2020. Delay or avoidance of medical care because of COVID-19-related concerns - United States, June 2020. *MMWR Morb. Mortal. Wkly. Rep.* 69 (36), 1250–1257. <https://doi.org/10.15585/mmwr.mm6936a4>.
- Davies, G.A., Alsallakh, M.A., Sivakumaran, S., Vasileiou, E., Lyons, R.A., Robertson, C., Sheikh, A., EAVE II Collaborators, 2021. Impact of COVID-19 lockdown on emergency asthma admissions and deaths: national interrupted time series analyses for Scotland and Wales. *Thorax* 76 (9), 867–873. <https://doi.org/10.1136/thoraxjnl-2020-216380>.



- Dutheil, F., Baker, J.S., Navel, V., 2020. COVID-19 as a factor influencing air pollution? *Environ. Pollut.* 263, 114466. <https://doi.org/10.1016/j.envpol.2020.114466>.
- Frontera, A., Cianfanelli, L., Vlachos, K., Landoni, G., Cremona, G., 2020. Severe air pollution links to higher mortality in COVID-19 patients: the "double-hit" hypothesis. *J. Infect.* 81, 255–259. <https://doi.org/10.1016/j.jinf.2020.05.031>.
- Giani, P., Castruccio, S., Anav, A., Howard, D., Hu, W., Crippa, P., 2020. Short-term and long-term health impacts of air pollution reductions from COVID-19 lockdowns in China and Europe: a modelling study. *Lancet Planet. Health* 4 (10), e474–e482. [https://doi.org/10.1016/S2542-5196\(20\)30224-2](https://doi.org/10.1016/S2542-5196(20)30224-2).
- Gkatzelis, G.I., Gilman, J.B., Brown, S.S., Eskes, H., Gomes, A.R., Lange, A.C., McDonald, B.C., Peischl, J., Petzold, A., Thompson, C.R., Kiendler-Scharr, A., 2021. The global impacts of COVID-19 lockdowns on urban air pollution: a critical review and recommendations. *Elem. Sci. Anth.* 9 (1), 1–46. <https://doi.org/10.1525/elementa.2021.00176>.
- Grange, S.K., Lee, J.D., Drysdale, W.S., Lewis, A.C., Hueglin, C., Emmenegger, L., Carslaw, D.C., 2021. COVID-19 lockdowns highlight a risk of increasing ozone pollution in European urban areas. *Atmos. Chem. Phys.* 21, 4169–4185. <https://doi.org/10.5194/acp-21-4169-2021>.
- Hale, T., Angrist, N., Goldszmidt, R., Kira, B., Petherick, A., Phillips, T., Webster, S., Cameron-Blake, E., Hallas, L., Majumdar, S., Tatlow, H., 2021. A global panel database of pandemic policies (Oxford COVID-19 Government Response Tracker). *Nat. Hum. Behav.* 5 (4), 529–538. <https://doi.org/10.1038/s41562-021-01079-8>.
- Hameed, S., Khan, M., Fatmi, Z., Wasay, M., 2021. Exploring the relationship between air quality and ischemic stroke admissions during the COVID-19 pandemic. *J. Stroke Cerebrovasc. Dis.* 30 (8), 105860. <https://doi.org/10.1016/j.jstrokecerebrovasdis.2021.105860>.
- Hama, G.B., Guha, N., Cohen, A., Laden, F., Raaschou-Nielsen, O., Samet, J.M., Vineis, P., Forastiere, F., Saldiva, P., Yorifuji, T., Loomis, D., 2014. Outdoor particulate matter exposure and lung cancer: a systematic review and meta-analysis. *Environ. Health Perspect.* 122 (9), 906–911. <https://doi.org/10.1289/ehp.1408092>.
- Han, C., Hong, Y.C., 2020. Decrease in ambient fine particulate matter during COVID-19 crisis and corresponding health benefits in Seoul, Korea. *Int. J. Environ. Res. Publ. Health* 17 (15), 5279. <https://doi.org/10.3390/ijerph17155279>.
- Hansell, A.L., Villeneuve, P.J., 2021. Invited perspective: ambient air pollution and SARS-CoV-2: research challenges and public health implications. *Environ. Health Perspect.* 129 (11) <https://doi.org/10.1289/EHP10540>.
- Hao, X., Li, J., Wang, H., Liao, H., Yin, Z., Hu, J., Wei, Y., Dang, R., 2021. Long-term health impact of PM<sub>2.5</sub> under whole-year COVID-19 lockdown in China. *Environ. Pollut.* 290, 118118. <https://doi.org/10.1016/j.envpol.2021.118118>.
- Hatoun, J., Correa, E.T., Donahue, S.M.A., Vernacchio, L., 2020. Social distancing for COVID-19 and diagnoses of other infectious diseases in children. *Pediatrics* 146 (4), e2020006460. <https://doi.org/10.1542/peds.2020-006460>.
- He, G., Pan, Y., Tanaka, T., 2020. The short-term impacts of COVID-19 lockdown on urban air pollution in China. *Nat. Sustain.* 3, 1005–1011. <https://doi.org/10.1038/s41893-020-0581-y>.
- Hossain, M.S., Frey, H.C., Louie, P.K.K., Lau, A.K.H., 2021. Combined effects of increased O<sub>3</sub> and reduced NO<sub>2</sub> concentrations on short-term air pollution health risks in Hong Kong. *Environ. Pollut.* 270, 116280. <https://doi.org/10.1016/j.envpol.2020.116280>.
- Host, S., Saunai, A., Honoré, C., Joly, F., Le Tertre, A., Medina, S., 2018. Bénéfices sanitaires attendus d'une zone à faibles émissions : évaluation quantitative d'impact sanitaire prospective pour l'agglomération parisienne. *Observatoire régional de santé Ile-de-France*, p. 106. [https://www.ors-idf.org/fileadmin/DataStorageKit/ORS/Etudes/2018/Etude2018\\_8/ORS\\_benefices\\_sanitaires\\_attendus\\_ZFE\\_vd.pdf](https://www.ors-idf.org/fileadmin/DataStorageKit/ORS/Etudes/2018/Etude2018_8/ORS_benefices_sanitaires_attendus_ZFE_vd.pdf).
- Huang, X., Ding, A., Gao, J., Zheng, B., Zhou, D., Qi, X., Tang, R., Wang, J., Ren, C., Nie, W., Chi, X., Xu, Z., Chen, L., Li, Y., Che, F., Pang, N., Wang, H., Tong, D., Qin, W., Cheng, W., Liu, W., Fu, Q., Liu, B., Chai, F., Davis, S.J., Zhang, Q., He, K., 2021. Enhanced secondary pollution offset reduction of primary emissions during COVID-19 lockdown in China. *Natl. Sci. Rev.* 8, nwa137. <https://doi.org/10.1093/nsr/nwaa137>.
- Hvidtfeldt, U.A., Sorensen, M., Geels, C., Ketzel, M., Khan, J., Tjønneland, A., Overvad, K., Brandt, J., Raaschou-Nielsen, O., 2019. Long-term residential exposure to PM<sub>2.5</sub>, PM<sub>10</sub>, black carbon, NO<sub>2</sub>, and ozone and mortality in a Danish cohort. *Environ. Int.* 123, 265–272. <https://doi.org/10.1016/j.envint.2018.12.010>.
- Katoto, P.D.M.C., Brand, A.S., Bakan, B., Obadia, P.M., Kuhangana, C., Kayembe-Kitenge, T., Kitenge, J.P., Nkulu, C., Vanoirbeek, J., Nawrot, T.S., Hoet, P., Nemery, B., 2021. Acute and chronic exposure to air pollution in relation with incidence, prevalence, severity and mortality of COVID-19: a rapid systematic review. *Environ. Health.* 20 (1), 41. <https://doi.org/10.1186/s12940-021-00714-1>.
- Kim, S.Y., Kim, S.Y., Kil, K., Lee, Y., 2021. Impact of COVID-19 mitigation policy in South Korea on the reduction of preterm or low birth weight birth rate: a single center experience. *Children* 8 (5), 332. <https://doi.org/10.3390/children8050332>.
- Kogevinas, M., Castaño-Vinyals, G., Karachaliou, M., Espinosa, A., de Gid, R., Garcia-Aymerich, J., Carreras, A., Cortés, B., Pleguezuelos, V., Jiménez, A., Vidal, M., O'Callaghan-Gordo, C., Cirach, M., Santano, R., Barrios, D., Puyol, L., Rubio, R., Izquierdo, L., Nieuwenhuijsen, M., Dadvand, P., Aguilar, R., Moncunill, G., Dobano, C., Tonne, C., 2021. Ambient air pollution in relation to SARS-CoV-2 infection, antibody response, and COVID-19 disease: a cohort study in Catalonia, Spain (COVICAT study). *Environ. Health Perspect.* 129 (11) <https://doi.org/10.1289/EHP9726>.
- Krivec, U., Kofol Seliger, A., Tursic, J., 2020. COVID-19 lockdown dropped the rate of paediatric asthma admissions. *Arch. Dis. Child.* 105 (8), 809–810. <https://doi.org/10.1136/archdischild-2020-319522>.
- Kuo, S.-C., Shih, S.-M., Chien, L.-H., Hsiung, C.A., 2020. Collateral benefit of COVID-19 control measures on influenza activity, Taiwan. *Emerg. Infect. Dis.* 26 (8), 1928–1930. <https://doi.org/10.3201/eid2608.201192>.
- Kyriakopoulos, C., Gogali, A., Exarchos, K., Potonos, D., Tatsis, K., Apollonatu, V., Loukides, S., Papiris, S., Sigala, I., Katsaounou, P., Aggelidis, M., Fouka, E., Porpodis, K., Kontakiotis, T., Sampsonas, F., Karampitsakos, T., Tzouveleki, A., Bibaki, E., Karagiannis, K., Antoniou, K., Tzanakis, N., Dimeas, I., Daniil, Z., Gourgoulialis, K., Kouratzi, M., Steiropoulos, P., Antonakis, E., Papanikolaou, I.C., Ntrisos, G., Kostikas, K., 2021. Reduction in hospitalizations for respiratory diseases during the first COVID-19 wave in Greece. *Respiration* 100 (7), 588–593. <https://doi.org/10.1159/000515323>.
- Le, T., Wang, Y., Liu, L., Yang, J., Yung, Y.L., Li, G., Seinfeld, J.H., 2020. Unexpected air pollution with marked emission reductions during the COVID-19 outbreak in China. *Science* 369 (6504), 702–706. <https://doi.org/10.1126/science.abb7431>.
- Liu, C., Chen, R., Sera, F., Vicedo-Cabrera, A.M., Guo, Y., Tong, S., Coelho, M.S.Z.S., Saldiva, P.H.N., Lavigne, E., Matus, P., Valdes Ortega, N., Osorio Garcia, S., Pascal, M., Stafoggia, M., Scortichini, M., Hashizume, M., Honda, Y., Hurtado-Díaz, M., Cruz, J., Nunes, B., Teixeira, J.P., Kim, H., Tobias, A., Iñiguez, C., Forsberg, B., Åström, C., Ragetti, M.S., Guo, Y.L., Chen, B.Y., Bell, M.L., Wright, C. Y., Scovronick, N., Garland, R.M., Milojevic, A., Kysely, J., Urban, A., Orru, H., Indermitte, E., Jaakkola, J.J.K., Rytö, N.R.I., Katsuyanni, K., Analitis, A., Zanobetti, A., Schwartz, J., Chen, J., Wu, T., Cohen, A., Gasparri, A., Kan, H., 2019. Ambient particulate air pollution and daily mortality in 652 cities. *N. Engl. J. Med.* 381 (8), 705–715. <https://doi.org/10.1056/NEJMoa1817364>.
- Loomis, D., Grosse, Y., Lauby-Secretan, B., El Ghissassi, F., Bouvard, V., Benbrahim-Talaa, L., Guha, N., Baan, R., Mattock, H., Straif, K., International Agency for Research on Cancer Monograph Working Group IARC, 2013. The carcinogenicity of outdoor air pollution. *Lancet Oncol.* 14 (13), 1262–1263. [https://doi.org/10.1016/S1470-2045\(13\)70487-x](https://doi.org/10.1016/S1470-2045(13)70487-x).
- Loomis, D., Hunag, W., Chen, G., 2014. The International Agency for Research on Cancer (IARC) evaluation of the carcinogenicity of outdoor air pollution: focus on China. *Chin. J. Cancer* 33 (4), 189–196. <https://doi.org/10.5732/cjc.014.10028>.
- Mahato, S., Pal, S., Ghosh, K.G., 2020. Effect of lockdown amid COVID-19 pandemic on air quality of the megacity Delhi, India. *Sci. Total Environ.* 730, 139086. <https://doi.org/10.1016/j.scitotenv.2020.139086>.
- Magazzino, C., Mele, M., Schneider, N., 2020. The relationship between air pollution and COVID-19-related deaths: an application to three French cities. *Appl. Energy* 279, 115835. <https://doi.org/10.1016/j.apenergy.2020.115835>.
- Maji, K.J., Namdeo, A., Bell, M., Goodman, P., Nagendra, S.M.S., Barnes, J.H., De Vito, L., Hayes, E., Longhurst, J.W., Kumar, R., Sharma, N., Kuppli, S.K., Alshetty, D., 2021. Unprecedented reduction in air pollution and corresponding short-term premature mortality associated with COVID-19 lockdown in Delhi, India. *J. Air Waste Manag. Assoc.* 71 (9), 1085–1101. <https://doi.org/10.1080/10962247.2021.1905104>.
- Medina, S., Adélaïde, L., Wagner, V., de Crouy Chanel, P., Real, E., Colette, A., Couvidat, F., Bessagnet, B., Durou, A., Host, S., Hulín, M., Corso, M., Pascal, M., 2021. Impact de pollution de l'air ambiant sur la mortalité en France métropolitaine. Réduction en lien avec le confinement du printemps 2020 et nouvelles données sur le poids total pour la période 2016-2019. *Santé publique France*, p. 63. <https://www.santepubliquefrance.fr/determinants-de-sante/pollution-et-sante-air/documents/en-quetes-etudes/impact-de-pollution-de-l-air-ambiant-sur-la-mortalite-en-france-metropolitaine-reduction-en-lien-avec-le-confinement-du-printemps-2020-et-nou-vet>.
- Naqvi, H.R., Datta, M., Mutreja, G., Siddiqui, M.A., Naqvi, D.F., Naqvi, A.R., 2021. Improved air quality and associated mortalities in India under COVID-19 lockdown. *Environ. Pollut.* 268, 115691. <https://doi.org/10.1016/j.envpol.2020.115691>.
- Nie, D., Shen, F., Wang, J., Ma, X., Li, Z., Ge, P., Ou, Y., Jiang, Y., Chen, M., Chen, M., Wang, T., Ge, X., 2021. Changes of air quality and its associated health and economic burden in 31 provincial capital cities in China during COVID-19 pandemic. *Atmos. Res.* 249, 105328. <https://doi.org/10.1016/j.atmosres.2020.105328>.
- Pascal, M., de Crouy Chanel, P., Wagner, V., Corso, M., Tillier, C., Bentayeb, M., Blanchard, M., Cochet, A., Pascal, L., Host, S., Gorla, S., Le Tertre, A., Chatignoux, E., Ung, A., Beaudou, P., Medina, S., 2016. The mortality impacts of fine particles in France. *Sci. Total Environ.* 571, 416–425. <https://doi.org/10.1016/j.scitotenv.2016.06.213>.
- Pedersen, M., Giorgis-Allemand, L., Bernard, C., Aguilera, I., Andersen, A.M., Ballester, F., Beelen, R.M.J., Chatzi, L., Cirach, M., Danilovicute, A., Dedele, A., van Eijsden, M., Estarlich, M., Fernández-Somoano, A., Fernández, M.F., Forastiere, F., Gehring, U., Grazuleviciene, R., Gruziova, O., Heude, B., Hoek, G., de Hoogh, K., van den Hooven, E.H., Häberg, S.E., Jaddoe, V.W.V., Klümper, C., Korek, M., Krämer, U., Lerchundi, A., Lepeule, J., Nafstad, P., Nystad, W., Patelarou, E., Porta, D., Postma, D., Raaschou-Nielsen, O., Rudnai, P., Sunyer, J., Stephanou, E., Sorensen, M., Thiering, E., Tuffnell, D., Varró, M.J., Vrijkotte, T.G.M., Wijga, A., Wilhelm, M., Wright, J., Nieuwenhuijsen, M.J., Pershagen, G., Brunekreef, B., Kogevinas, M., Slama, R., 2013. Ambient air pollution and low birthweight: a European cohort study (ESCAPE). *Lancet Respir. Med.* 1 (9), 695–704. [https://doi.org/10.1016/S2213-2600\(13\)70192-9](https://doi.org/10.1016/S2213-2600(13)70192-9).
- Petin, H., Bowdalo, D., Soret, A., Guevara, M., Jorba, O., Serradell, K., Pérez García-Pando, C., 2020. Meteorology-normalized impact of the COVID-19 lockdown upon NO<sub>2</sub> pollution in Spain. *Atmos. Chem. Phys.* 20, 11119–11141. <https://doi.org/10.5194/acp-20-11119-2020>.
- Phillip, R.K., Purtill, H., Reidy, E., Daly, M., Imcha, M., McGrath, D., O'Connell, N.H., Dunne, C.P., 2020. Unprecedented reduction in births of very low birthweight (VLBW) and extremely low birthweight (ELBW) infants during the COVID-19 lockdown in Ireland: a 'natural experiment' allowing analysis of data from the prior two decades. *BMJ Glob. Health* 5, e003075. <https://doi.org/10.1136/bmjgh-2020-003075>.

- Ropkins, K., Tate, J.E., 2021. Early observations on the impact of the COVID-19 lockdown on air quality trends across the UK. *Sci. Total Environ.* 754, 142374. <https://doi.org/10.1016/j.scitotenv.2020.142374>.
- Sahraei, M.A., Kuşkan, E., Çodur, M.Y., 2021. Public transit usage and air quality index during the COVID-19 lockdown. *J. Environ. Manag.* 286, 112166. <https://doi.org/10.1016/j.jenvman.2021.112166>.
- Santé Publique France (Geodes), 2020. Indicateurs : cartes, données et graphiques. Taux de passages aux urgences et taux d'actes médicaux SOS Médecins pour gastro-entérite aiguë ou pour grippe 2010-2020 [Indicators : maps, data and graphs. Rate of emergency room visits and rate of home emergency acts for acute gastroenteritis or influenza 2010-2020]. <https://geodes.santepubliquefrance.fr>. (Accessed 27 May 2021).
- Schneider, R., Masselot, P., Vicedo-Cabrera, A.M., Sera, F., Blangiardo, M., Forlani, C., Douros, J., Jorba, O., Adani, M., Kouznetsov, R., Couvidat, F., Arteta, J., Raux, B., Guevara, M., Colette, A., Barré, J., Peuch, V.-H., Gasparrini, A., 2022. Differential impact of government lockdown policies on reducing air pollution levels and related mortality in Europe. *Sci. Rep.* 12, 726. <https://doi.org/10.1038/s41598-021-04277-6>.
- Seo, J.H., Jeon, H.W., Sung, U.J., Sohn, J.-R., 2020. Impact of the COVID-19 outbreak on air quality in Korea. *Atmosphere* 11 (10), 1137. <https://doi.org/10.3390/atmos11101137>.
- Shah, S.A., Quint, J.K., Nwaru, B.I., Sheikh, A., 2021. Impact of COVID-19 national lockdown on asthma exacerbations: interrupted time-series analysis of English primary care data. *Thorax* 76 (9), 860–866. <https://doi.org/10.1136/thoraxjnl-2020-216512>.
- Shehzad, K., Sarfraz, M., Shah, S.G.M., 2020. The impact of COVID-19 as a necessary evil on air pollution in India during the lockdown. *Environ. Pollut.* 266, 115080. <https://doi.org/10.1016/j.envpol.2020.115080>.
- Sicard, P., De Marco, A., Agathokleous, E., Feng, Z., Xu, X., Paoletti, E., Rodriguez, J.J.D., Calatayud, V., 2020. Amplified ozone pollution in cities during the COVID-19 lockdown. *Sci. Total Environ.* 735, 139542. <https://doi.org/10.1016/j.scitotenv.2020.139542>.
- Singh, V., Singh, S., Biswal, A., Kesarkar, A.P., Mor, S., Ravindra, K., 2020. Diurnal and temporal changes in air pollution during COVID-19 strict lockdown over different regions of India. *Environ. Pollut.* 266, 115368. <https://doi.org/10.1016/j.envpol.2020.115368>.
- Soo, R.J.J., Chiew, C.J., Ma, S., Pung, R., Lee, V., 2020. Decreased influenza incidence under COVID-19 control measures, Singapore. *Emerg. Infect. Dis.* 26 (8), 1933–1935. <https://doi.org/10.3201/eid2608.201229>.
- Tobías, A., Carnerero, C., Reche, C., Massagué, J., Via, M., Minguillón, M.C., Alastuey, A., Querol, X., 2020. Changes in air quality during the lockdown in Barcelona (Spain) one month into the SARS-CoV-2 epidemic. *Sci. Total Environ.* 726, 138540. <https://doi.org/10.1016/j.scitotenv.2020.138540>.
- Venter, Z.S., Aunan, K., Chowdhury, S., Lelieveld, J., 2020. COVID-19 lockdowns cause global air pollution declines. *Proc. Natl. Acad. Sci. U. S. A.* 117 (32), 18984–18990. <https://doi.org/10.1073/pnas.2006853117>.
- Venter, Z.S., Aunan, K., Chowdhury, S., Lelieveld, J., 2021. Air pollution declines during COVID-19 lockdowns mitigate the global health burden. *Environ. Res.* 192, 110403. <https://doi.org/10.1016/j.envres.2020.110403>.
- Vicedo-Cabrera, A.M., Sera, F., Liu, C., Armstrong, B., Milojevic, A., Guo, Y., Tong, S., Lavigne, E., Kyselý, J., Urban, A., 2020. Short term association between ozone and mortality: global two stage time series study in 406 locations in 20 countries. *BMJ* 368, m108. <https://doi.org/10.1136/bmj.m108>.
- Wang, P., Chen, K., Zhu, S., Wang, P., Zhang, H., 2020. Severe air pollution events not avoided by reduced anthropogenic activities during COVID-19 outbreak. *Resour. Conserv. Recycl.* 158, 104814. <https://doi.org/10.1016/j.resconrec.2020.104814>.
- WHO, 2013. Health Risks of Air Pollution in Europe - Hrapie Project - Recommendations for Concentration-Response Functions for Cost-Benefits Analysis of Particulate Matter, Ozone and Nitrogen Dioxide, p. 60. [https://www.euro.who.int/\\_data/assets/pdf\\_file/0006/238956/Health\\_risks\\_air\\_pollution\\_HRAPIE\\_project.pdf](https://www.euro.who.int/_data/assets/pdf_file/0006/238956/Health_risks_air_pollution_HRAPIE_project.pdf).
- Xu, Z., Cao, R., Hu, X., Han, W., Wang, Y., Huang, J., Li, G., 2021. The improvement of air quality and associated mortality during the COVID-19 lockdown in one megacity of China: an empirical strategy. *Int. J. Environ. Res. Publ. Health* 18 (16), 8702. <https://doi.org/10.3390/ijerph18168702>.
- Zhu, Y., Xie, J., Huang, F., Cao, L., 2020. Association between short-term exposure to air pollution and COVID-19 infection: evidence from China. *Sci. Total Environ.* 727, 138704. <https://doi.org/10.1016/j.scitotenv.2020.138704>.

## 2.3 CONCLUSION

### 2.3.1 Main results

#### 2.3.1.1 Concentrations changes

Figure 15 provides a summary of the concentrations and health effects changes outlined in the Article n°1. When comparing pollutants concentrations during the 2020 restrictions with the same timeframes in 2015-2019, the largest concentration reductions were seen for NO<sub>2</sub> (- 32% average) and PM<sub>2.5</sub> (- 22% average). O<sub>3</sub> had increased (+ 11%), contrary to the other pollutants.

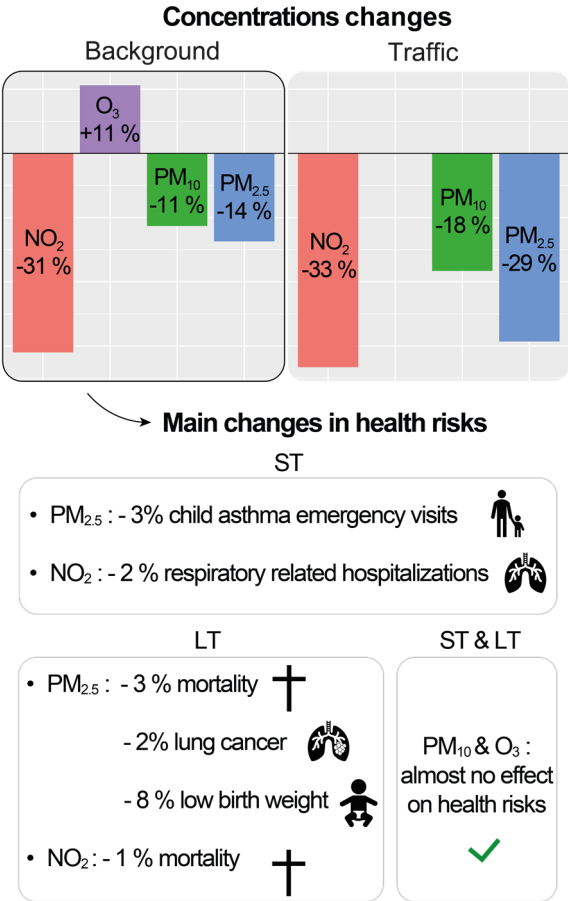


Figure 15. Main results regarding concentrations and health risks changes between 2020 (L1, F1, L2) and 2015-2019. ST: short-term, LT: long-term. Concentrations changes refer to all stations (background and traffic) whereas health risks were calculated using background stations only.

An important finding was the correlation between NO<sub>2</sub> levels and the stringency index. This implies that this index could be used to forecast changes in NO<sub>2</sub> concentrations based on levels of imposed restrictions. For instance, it seems feasible to establish a list of restrictions, quantify their severity using the Oxford stringency index, and subsequently predict the NO<sub>2</sub> trends accordingly.

### 2.3.1.2 Health effects changes

It appears from Figure 15 that the consequences of long-term (LT) effects are greater than that of short-term (ST) effects. In summary, we found that the most significant health improvements in 2020 were related to reductions in PM<sub>2.5</sub> and NO<sub>2</sub>, while changes in PM<sub>10</sub> and O<sub>3</sub> had little impact on health outcomes. Now that this health risk assessment has been done, it would be instructive to supplement these results with an epidemiological study evaluating hospitalizations for respiratory issues or child visits for asthma during the pandemic. However, such a study is rather challenging and need to consider several biases like for example the population's tendency to avoid hospitals in 2020. Similarly, validating mortality data is challenging as well due to its overlap with the significant deaths attributed to COVID-19. An interesting outcome of this study was the limited impact on cardiovascular diseases. Cross-checking this with hospital admission figures would have also been valuable.

### 2.3.2 Perspectives

This study could be applied to different times of the year, different years, or over longer periods. For instance, we could use this health risk assessment approach to compare higher PM<sub>2.5</sub> values from the winter of 2022 (in the context of energy crisis) with those of previous winters. Benefiting from freely accessible pollutants concentrations data provided by Atmo AuRA is a clear advantage. Nevertheless, the centralized monitoring approach has its limitations. Reference stations do not fully reflect actual human exposure, as they are generally far from areas where people live, travel, or work. Indeed, for populations residing near road traffic or spending a significant amount of time in places with high or low concentrations of pollutants, the use of data coming only from background stations in health risk calculations clearly becomes insufficient, or even erroneous. Figure 15 illustrates the difference in concentrations between two types of stations.

According to the expressions in Figure 14, a variation in the concentration of  $\Delta C = \ln(1 + x)/\beta$  would result in a variation of  $x$  % in the risk of the effect associated with  $\beta$ . For example, a concentration difference of  $6.82 \mu\text{g}/\text{m}^3$  on  $\text{PM}_{2.5}$  can lead to a 10% variation on the risk of long-term mortality. These differences will therefore be more or less significant depending on the pollutant and associated effect considered. All of this therefore requires a detailed estimate of the exposure of individuals locally and along travel routes. We therefore opted to deploy a sensors network to get measurements at a finer spatial scale. Furthermore, this study also revealed that  $\text{PM}_{2.5}$  had more pronounced health effects than  $\text{NO}_2$ , particularly for LT impacts, often resulting in chronic diseases or mortality. As a result, we chose to prioritize PM analysis in upcoming chapters, focusing on  $\text{PM}_1$  or  $\text{PM}_{2.5}$ . This was in phase with the limitations of LCS in measuring gases and coarse particles like  $\text{PM}_{10}$  (Hassani et al., 2023).

### Summary - Results Chapter 2

#### During COVID-19 restrictions:

- - 32%  $\text{NO}_2$ , - 22%  $\text{PM}_{2.5}$ , - 15%  $\text{PM}_{10}$ , + 11%  $\text{O}_3$ .
- Short-term risks of child asthma (- 3%) & hospitalization for respiratory diseases (- 2%).
- Long-term risks of low birth weight (- 8%), mortality (- 4%), and lung cancer (- 2%).
- Most pronounced health effects of  $\text{PM}_{2.5}$ , particularly for long-term risks.

#### Health risks calculations:

- Small pollutants concentrations differences can lead to important risks variations.



# 3

## LOW-COST SENSORS FOR PARTICLE MATTER MEASUREMENT: CALIBRATION METHOD

### Summary - Introduction Chapter 3

- Background: Low-cost sensors (LCS) offer the possibility for finer spatial and temporal measurements of air pollutant levels but raise questions about the quality of raw data. The use of LCS therefore requires calibration before any deployment.
- Objectives:
  1. Develop a standardized approach for calibration of LCS;
  2. Apply the calibration method to our LCS and assess the performance in Grenoble.

### 3.1 INTRODUCTION

Low-cost sensors (LCS) networks are becoming increasingly popular in air quality monitoring. They can provide pollutants concentrations data near places where individual live, addressing the spatial and temporal variability of air quality (Williams, 2019). Another advantage of LCS is their affordability, allowing for deployment of various devices within a city. However, one of their main limitations is the low accuracy of their raw data, which may be attributed to inappropriate

correction algorithms developed by manufacturers for some contexts, and to the influence of meteorological factors such as relative humidity or dusts. Consequently, substantial time must be allocated to recalibrate LCS before usage in monitoring. Calibration involves locating the sensors near a reference instrument to compare sensor values with the reference and, when needed, adjust sensor outputs using various correction methods, such as multi linear regression or machine learning. Figure 16 summarizes the various steps required before LCS deployment. First, LCS are assembled with an optical PM sensor, a microcontroller (central processing unit), and a sensor measuring temperature and humidity. Then, to ensure the quality of PM measurements made by the LCS, we compare them with a reference monitor (colocation study). A calibration equation is then constructed to correct raw LCS data. Finally, the sensors can be deployed in similar conditions to those of the colocation. This Chapter 3 is devoted to the description of the calibration method, while the following Chapter 4 will address sensors deployment and the analysis of network-generated results.

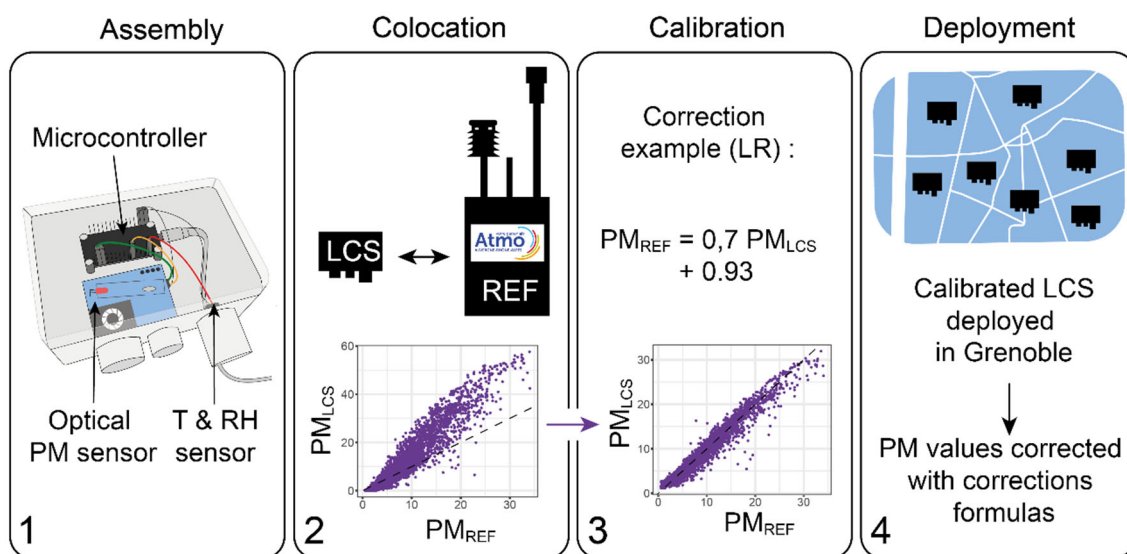


**Figure 16. Steps to low-cost sensors (LCS) deployment.** REF: Reference station from Atmo AuRA in “Les Frênes”. T: temperature, RH: relative humidity, LR: Linear regression. Step 4 is addressed in Chapter 4.

As standardized methods are not yet available, calibrating LCS is a complicated process (Giordano et al., 2021). The US EPA implemented guidelines that provide metrics to be achieved to ensure effective PM LCS calibration. However, there is a lack of directives concerning the calibration techniques to be employed to reach these metrics. Three main techniques can be used to calibrate PM LCS: 1) Linear and non-linear regressions, 2) mechanistic models involving

humidity, and 3) sophisticated machine learning (ML) methods (Liang, 2021). A combination of all three methods is also possible. These three techniques were evaluated to identify the most suitable for our local environment. In this chapter, we present two papers dealing with calibration. The first article (article n°2, in French) will present linear and mechanistic methods. The second article (article n°3) will show how machine learning can help improving PM LCS performance metrics. The approaches described in both papers can be adapted and applied to similar devices.

## 3.2 ARTICLE N°2

This paper introduces two distinct calibration methods using regressions. First, a simple linear regression technique corrects the sensor's measured value using an equation of the form “ $y = ax + b$ ”. Second, a mechanistic non-linear method accounting for humidity is used. Most studies have pointed out the importance of humidity in the calibration equation for PM LCS, as humidity impacts PM sizes and directly affects optical measurements.

The following paper can be found at: <https://doi.org/10.25576/ASFERA-CFA2023-32891>.

Pour citer cet article : Auteurs (2023), Titre, Congrès Français sur les Aérosols 2023, Paris

## PROTOCOLE D'ÉVALUATION ET D'UTILISATION D'UNE STATION LOW-COST DE MESURE DES PARTICULES FINES

M.-L. Aix\*<sup>1</sup>, D J. Bicout<sup>1</sup>

<sup>1</sup>Univ. Grenoble Alpes, CNRS, UMR 5525, VetAgro Sup, Grenoble INP, TIMC, 38000 Grenoble, France

\* marie-laure.aix@univ-grenoble-alpes.fr

### TITLE

Protocole for evaluation and use of a low-cost particulate matter monitoring station

### RÉSUMÉ

Les capteurs « low-cost » pourraient révolutionner la mesure des particules fines (PM) mais il paraît nécessaire d'évaluer leurs performances. Ce travail propose un protocole de montage, d'évaluation et d'utilisation d'une station comportant un capteur PMS7003. Les performances de mesure des PM<sub>2.5</sub> (PM de taille <2,5µm) sont comparées aux directives de l'Environmental Protection Agency américaine (EPA). Il apparaît que certaines métriques (pente et NRMSE) sont non conformes en l'absence de calibration. Une calibration linéaire les ramène dans les limites de l'EPA et une calibration mécanistique améliore encore la précision. Les RMSEs sont alors de 0.90 µg/m<sup>3</sup> (échelle horaire) et 0.48 µg/m<sup>3</sup> (journée).

### ABSTRACT

The use of low-cost sensors could revolutionize the measurement of fine particles (PM). Therefore, we must evaluate their performance. Here we report the assembly, evaluation and use of a station using a PMS7003 sensor. Its performance to measure PM<sub>2.5</sub> (PM<2.5µm) is compared to the recommendations of the US Environmental Protection Agency (EPA). Some metrics (slope, NRMSE) are not compliant. A linear calibration brings them within EPA limits and a mechanistic calibration further improves accuracy. We can achieve RMSEs of 0.90 µg/m<sup>3</sup> (hourly scale) and 0.48 µg/m<sup>3</sup> (daily scale).

**MOTS-CLÉS:** capteurs low-cost, PM<sub>2.5</sub>, calibration / **KEYWORDS:** low-cost sensors, PM<sub>2.5</sub>, calibration

## 1. INTRODUCTION

Ces dernières années, nous assistons à une croissance de l'intérêt pour les microcapteurs optiques "low-cost". Parmi ceux-ci, le PMS7003 est l'un des plus utilisés pour la mesure des particules fines (PM). Il est plébiscité à la fois par les citoyens, les organismes officiels de mesure de qualité de l'air et la communauté scientifique. Il paraît donc important de mieux connaître ses performances et d'évaluer l'incertitude associée à ses mesures. S'appuyant sur une méthodologie développée par l'EPA (Duvall et al., 2021) et déjà utilisée récemment dans une étude (Zimmerman, 2022), notre travail vise à donner un aperçu des performances et des limites d'un concept de station de qualité de l'air utilisant le PMS7003. Notre objectif est de fournir un mode d'emploi couvrant le montage, l'évaluation des performances et le déploiement de ce type de dispositif. Nous nous focalisons ici sur la mesure des particules fines de taille inférieure à 2,5µm (PM<sub>2.5</sub>). L'approche décrite ci-dessus peut s'adapter et s'appliquer à d'autres dispositifs similaires.

## 2. MONTAGE

Le dispositif de mesure des PM que nous avons mis en œuvre comporte deux capteurs low-cost : le PMS 7003 (Plantower), capteur optique de PM, ainsi que le DHT22 (MaxDetect), capteur d'humidité relative et de température. Ils sont connectés à un microcontrôleur Wi-Fi ESP8266 qui collecte les informations et les transforme selon un algorithme. Des fils de couleur sont utilisés pour connecter les composants entre eux et un boîtier en polycarbonate IP66 les protège des intempéries. Fin 2020, le coût total d'une telle station avoisinait les 65€. Pour la réalisation des objectifs de ce travail, nous avons construit 9 stations en partenariat avec Atmo Auvergne-Rhône-Alpes (Atmo AuRA).

## 3. PERFORMANCES

Pour évaluer les performances des stations, nous avons réalisé une expérience de colocation sur la station des Frênes (Grenoble) en collaboration avec Atmo AuRA. Il s'était agi alors de comparer les valeurs des

Pour citer cet article : Auteurs (2023), Titre, Congrès Français sur les Aérosols 2023, Paris

capteurs à celles remontées par le Fidas ® 200 (Palas GmbH) d'Atmo. Ce processus de colocation s'est étalé sur 8 mois, du 28 janvier 2021 au 29 septembre 2021.

### 3.1. Critères de l'EPA (Duvall et al., 2021)

L'EPA est l'agence qui implémente les lois fédérales de protection de l'environnement aux États-Unis. C'est le cas par exemple du Clean Air Act, qui règlemente l'ensemble des émissions atmosphériques. Dès 1998, le Congrès a demandé à l'EPA d'élargir ses recherches sur les effets sanitaires des PM. Depuis, l'EPA soutient activement la recherche sur les PM. Particulièrement active dans le domaine des capteurs low-cost, elle a défini 5 critères permettant de comparer les valeurs des capteurs à celles d'une référence : le coefficient de détermination ( $R^2$ ), la pente, l'ordonnée à l'origine, la racine de l'erreur quadratique moyenne (RMSE) et la racine de l'erreur quadratique moyenne normalisée (NRMSE). Le  $R^2$  rend compte de la relation linéaire entre le capteur et la référence, tandis que le RMSE reflète l'écart entre les mesures des stations low-cost et celles de la référence ; il indique donc la précision du capteur. Enfin, l'EPA utilise d'autres indicateurs, obtenus en comparant les valeurs des différents capteurs low-cost entre elles, indépendamment de la référence. C'est par exemple le cas du coefficient de variation (CV) et de l'écart-type (SD). Les standards de l'EPA pour les capteurs (repris en gris sur la Figure 2) sont les suivants :  $R^2 \geq 0.7$ ,  $RMSE \leq 7 \mu\text{g}/\text{m}^3$  ou  $NRMSE \leq 30\%$ ,  $SD \leq 5 \mu\text{g}/\text{m}^3$  ou  $CV \leq 30\%$ , pente =  $1 \pm 0.35$  et  $-5 \leq \text{intercept} \leq 5 \mu\text{g}/\text{m}^3$  (Duvall et al., 2021).

### 3.2. Avant calibration

Nous avons retiré du jeu de données les périodes de dust sahariens et celles où l'humidité relative (HR) dépassait 98%. Lorsque l'on étudie les données des stations à la fréquence horaire, les métriques telles que la pente et le NRMSE sortent des standards de l'EPA (Figure 2, partie "Avant calibration") ; les autres métriques restant conformes. Lorsque l'on passe à une fréquence journalière, on constate que le NRMSE s'améliore, mais reste non conforme. La pente évolue peu. Il est donc nécessaire de procéder à une calibration des stations. Par ailleurs, le passage à une fréquence journalière permet une amélioration de l'ensemble des autres métriques, sauf l'ordonnée à l'origine (intercept) qui est légèrement dégradée.

### 3.3. Calibration

Dans un souci de simplicité et de transparence, nous avons utilisé deux modèles empiriques : (1) un modèle linéaire, (2) un modèle mécanistique prenant en compte l'HR et la température mesurées par le capteur. Ces modèles ont été ajustés sur 75% du jeu de données et testés sur les 25% restants (Figure 1).



Figure 1. Découpage de la période de colocation

Les formules des modèles (Tableau 1 ci-dessous), dont les coefficients sont issus du meilleur ajustement, ont été obtenues avec le logiciel « RStudio Server 2021.09.1 ».

Tableau 1. Formules de calibration ( $PM_{2.5 \text{ adj}}$  = concentration en  $PM_{2.5}$  ajustée (corrigée) du capteur,  $RH_{\text{int}}$  = humidité relative interne mesurée par le capteur DHT22,  $T_{\text{int}}$  = température interne mesurée par le DHT22).

Échelle	Modèle linéaire	Modèle mécanistique
Horaire	$PM_{2.5 \text{ adj}} = 0.49 PM_{2.5} + 2.49$ (Aix et al., 2023)	$PM_{2.5 \text{ adj}} = 0.50 + 0.65 \frac{PM_{2.5}}{\left(1 + 0.25 \frac{RH_{\text{int}}}{100 - RH_{\text{int}}}\right)^{\frac{1}{3}}} + 0.08 T_{\text{int}}$ (Aix et al., 2023)
Journalière	$PM_{2.5 \text{ adj}} = 0.54 PM_{2.5} + 1.92$	$PM_{2.5 \text{ adj}} = 0.27 + 0.67 \frac{PM_{2.5}}{\left(1 + 0.38 \frac{RH_{\text{int}}}{100 - RH_{\text{int}}}\right)^{\frac{1}{3}}} + 0.07 T_{\text{int}}$

Pour citer cet article : Auteurs (2023), Titre, Congrès Français sur les Aérosols 2023, Paris

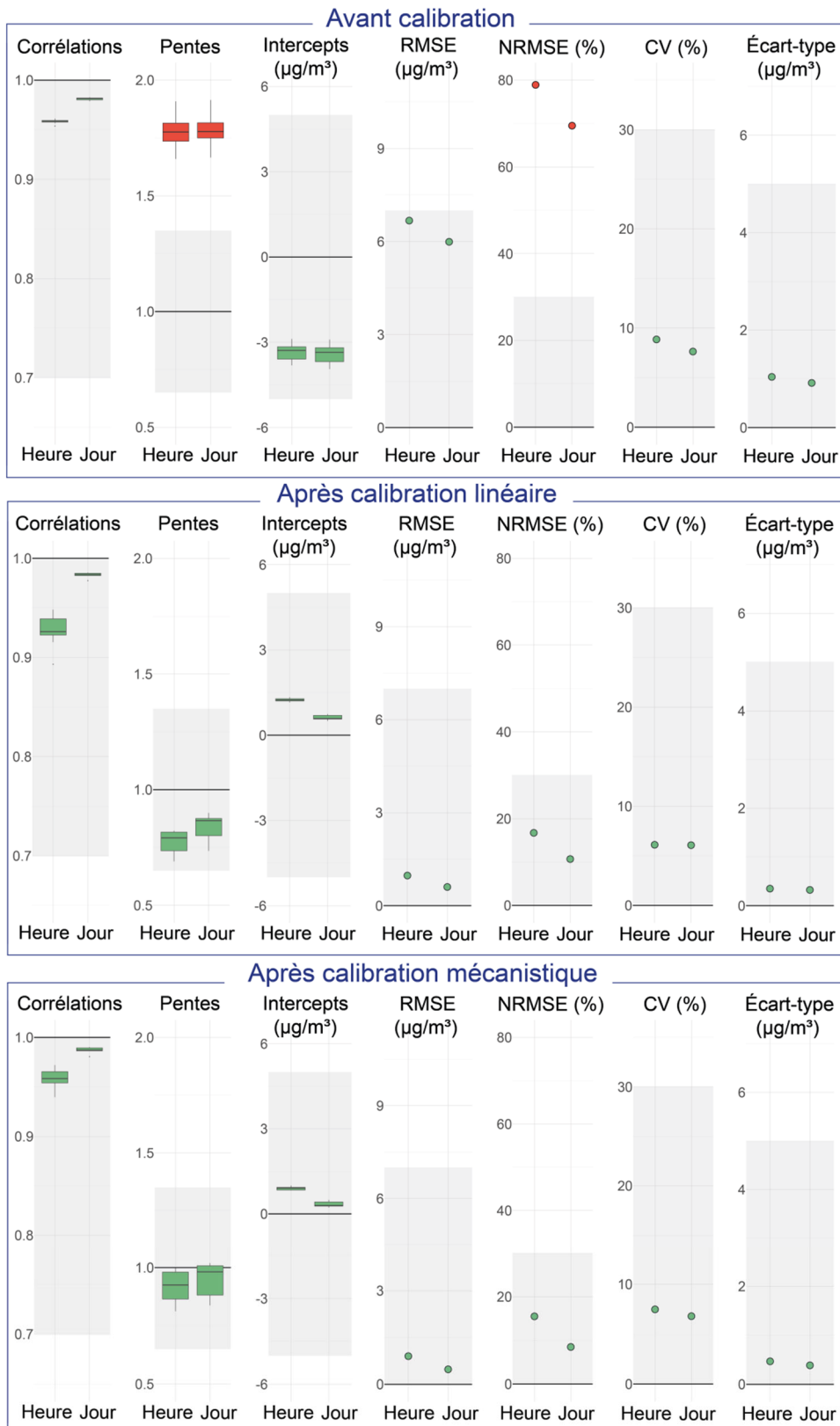


Figure 2. Indicateurs de performance des stations low-cost (zones grisées : standards EPA, lignes en gras : valeurs cibles, "Heure" = fréquences horaires, "Jour" = fréquences journalières). Le rouge est utilisé lorsque les métriques sortent des limites recommandées par l'EPA, le vert correspondant à une conformité.



Pour citer cet article : Auteurs (2023), Titre, Congrès Français sur les Aérosols 2023, Paris

### 3.4. Après calibration

La régression linéaire permet de corriger efficacement les concentrations remontées par les capteurs. L'ensemble des métriques devient conforme aux exigences de l'EPA (Figure 2, partie "Après calibration linéaire"). Au niveau horaire, on observe une légère baisse de 3.4% du  $R^2$  médian. L'utilisation de fréquences journalières offre des métriques plus performantes sans dégradation du  $R^2$  et avec une amélioration de 40% du RMSE. La calibration mécanistique au niveau horaire permet quant à elle, par rapport à la régression linéaire, une amélioration de 7,4% du RMSE et de 3,5% du  $R^2$ . On observe en revanche une légère dégradation des indicateurs suivants : CV et écart-type. Au niveau journalier, on observe une hausse de 0,4% du  $R^2$  médian et une amélioration de 20,7% du RMSE par rapport à la régression linéaire.

## 4. DÉPLOIEMENT

Une fois calibrées, les stations low-cost peuvent être déployées pour l'expérimentation. De manière générale, les conditions environnementales dans lesquelles sont installées les stations doivent être aussi proches que possible de celles de la colocation :

- Le lieu de l'installation doit être situé près d'une alimentation et à portée d'un réseau Wi-Fi.
- Les dispositifs doivent être éloignés de zones fumeurs ou de chantiers.
- La hauteur d'accroche doit être similaire à celle du site d'accueil.
- Aucun obstacle, autre que le support, ne doit se trouver dans un périmètre de 1m.
- Il est recommandé de ne pas orienter les capteurs plein sud et de les abriter (exposition au soleil).

Enfin, nous avons constaté une baisse des performances de mesure de certains capteurs d'humidité relative (DHT22) après 7 mois, une partie des capteurs donnant continuellement des valeurs égales à 100%. Nous recommandons donc l'utilisation de capteurs d'humidité et de température plus robustes (Bosch BME280, Sensirion SHT85...).

## 5. CONCLUSION

Il ressort de cette expérience qu'une simple calibration linéaire suffit à rendre les métriques de nos stations low-cost conformes aux recommandations de l'EPA en termes de performances. Une calibration mécanistique améliore significativement la précision des capteurs mais entraîne une très légère dégradation du CV et de l'écart-type, restants néanmoins dans les plages de l'EPA. À l'échelle horaire, la calibration mécanistique permet d'atteindre un RMSE de  $0.90 \mu\text{g}/\text{m}^3$  et un  $R^2$  médian de 0.96, ce qui est très satisfaisant. À l'échelle journalière, il est même possible d'obtenir un RMSE de  $0.48 \mu\text{g}/\text{m}^3$  et un  $R^2$  de 0.99 par correction mécanistique. De manière générale, nous constatons qu'il est plus facile de satisfaire les critères de performance EPA lorsque l'on transpose les concentrations à une échelle journalière, plutôt qu'à une échelle horaire.

## RÉFÉRENCES

Aix, M.-L., Schmitz, S., Bicout, D. J. (2023). Open-source calibration of low-cost sensors for high-quality monitoring of fine particulate matter [Document soumis pour publication]

Duvall, R., A. Clements, G. Hagler, A. Kamal, Vasu Kilaru, L. Goodman, S. Frederick, K. Johnson Barkjohn, I. VonWald, D. Greene, T. Dye. (2021). Performance Testing Protocols, Metrics, and Target Values for Fine Particulate Matter Air Sensors: Use in Ambient, Outdoor, Fixed Site, Non-Regulatory Supplemental and Informational Monitoring Applications. U.S. EPA Office of Research and Development, Washington, DC, EPA/600/R-20/280. [https://cfpub.epa.gov/si/si\\_public\\_record\\_report.cfm?dirEntryId=350785&Lab=CEMM](https://cfpub.epa.gov/si/si_public_record_report.cfm?dirEntryId=350785&Lab=CEMM)

Zimmerman, N. (2022). Tutorial: Guidelines for implementing low-cost sensor networks for aerosol monitoring. *Journal of Aerosol Science*, 159, 105872. <https://doi.org/10.1016/j.jaerosci.2021.105872>

## REMERCIEMENTS

Marie-Laure Aix est soutenue par une bourse du Ministère de l'Éducation Nationale de l'Enseignement Supérieur, de la Recherche et de l'Innovation. Elle réalise sa thèse au sein de l'École Doctorale Ingénierie pour la Santé, la Cognition et l'Environnement (ED ISCE) de l'Université Grenoble Alpes. Nous tenons à remercier chaleureusement Atmo Auvergne-Rhône-Alpes pour l'assistance au montage et à la colocation des stations dans le cadre de notre partenariat.

**Summary – Conclusion Article n°2**

The key findings of this paper were the following:

- A linear regression formula may be sufficient to align LCS metrics with EPA performance recommendations.
- Mechanistic calibration improves sensor accuracy by reducing hourly and daily RMSEs by 7% and 21%, respectively.

Based on these findings, we used the mechanistic calibration in our first study on mobility (Appendix B). However, we subsequently highlighted that, although linear and mechanistic regression had the advantage of simplicity, they did not appear to deliver the best performance when compared to more sophisticated methods like machine-learning (Liang, 2021). Therefore, we experimented machine learning techniques in the following article and compared them to traditional linear or mechanistic regression methods.

### 3.3 ARTICLE N°3

In our literature review on LCS calibration, we found a study that took an initial step towards methods harmonization. Schmitz et al. (2021) presented a seven-step technique using machine-learning to calibrate gas sensors together with an open-access code (Schmitz et al., 2020). Inspired by that approach, we adapted the method to calibrate our PM LCS. Since the method was initially designed to calibrate LCS measuring gases such as NO<sub>2</sub> or O<sub>3</sub>, and not specifically for PM LCS, we tailored it to fit our PM sensors study. The adaptation process included specific steps, such as excluding extreme relative humidity values or days when Saharan dusts events occurred. Dusts episodes led to elevated levels of PM<sub>2.5</sub> and PM<sub>10</sub>, which the LCS struggled to accurately measure, unlike the reference instruments. Figure 17 highlights these dust periods, when high PM<sub>2.5</sub> or PM<sub>10</sub>



levels are recorded by the reference but not by the LCS, and the Copernicus Sentinel-5P satellite shows the presence of a dust. This suggests the difficulty of the LCS to capture those coarse PM.

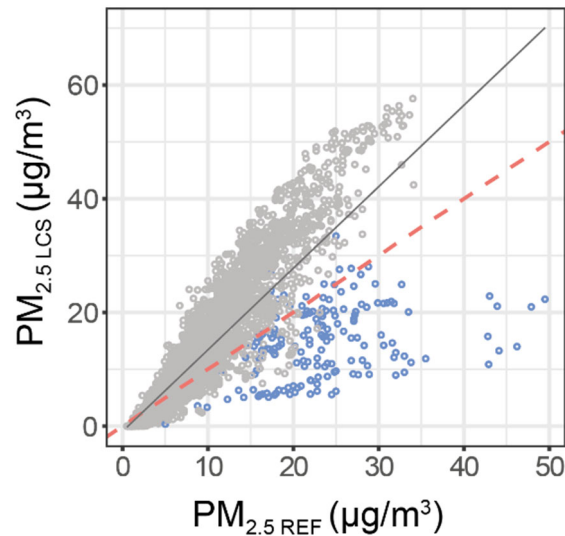


**Figure 17. Scatterplot of the raw  $PM_{2.5\text{ LCS}}$  levels against the official  $PM_{2.5\text{ REF}}$  data from Atmo AuRA. Dust episodes observed during the colocation . Grey points denote normal days when no dust was identified. Blue points refer to dust events identified with our technique. The dashed red line shows the parity line, and the black line is the best linear fit.**

To detect and discard dusts events, we adopted a hybrid approach combining field observations and dust data from the Copernicus Sentinel-5P satellite (Météo-France, 2020). This extension to the method by Schmitz et al. was published and will be detailed in the next section. The aim of the paper was to present the LCS calibration method along with the associated performance.

The paper can be found at: <https://doi.org/10.1016/j.scitotenv.2023.164063>.



Contents lists available at ScienceDirect

Science of the Total Environment

journal homepage: [www.elsevier.com/locate/scitotenv](http://www.elsevier.com/locate/scitotenv)

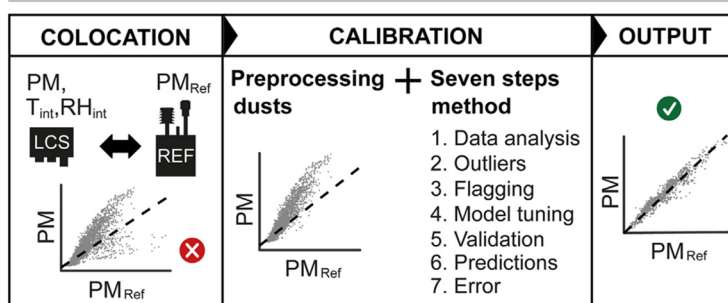
## Calibration methodology of low-cost sensors for high-quality monitoring of fine particulate matter

Marie-Laure Aix<sup>a</sup>, Seán Schmitz<sup>b</sup>, Dominique J. Bicot<sup>c,\*</sup><sup>a</sup> Univ. Grenoble Alpes, CNRS, UMR 5525, VetAgro Sup, Grenoble INP, TIMC, 38000 Grenoble, France<sup>b</sup> Research Institute for Sustainability, Helmholtz Centre Potsdam, Berliner Strasse 130, 14467 Potsdam, Germany<sup>c</sup> Univ. Grenoble Alpes, CNRS, UMR 5525, VetAgro Sup, Grenoble INP, TIMC, 38000 Grenoble, France

### HIGHLIGHTS

- Low-cost calibrated sensors can be an effective tool in PM exposure assessment.
- A 7-step protocol and guidelines are designed to calibrate low-cost sensors.
- RFR & MLR methods performed better than traditional ones for all PM sizes.
- For PM<sub>1</sub>: R<sup>2</sup> = 0.94, NRMSE = 12 % and for PM<sub>2.5</sub>: R<sup>2</sup> = 0.92, NRMSE = 12 %
- Calibration of PM<sub>10</sub> turned out to be less good (R<sup>2</sup> = 0.54, NRMSE = 27 %).

### GRAPHICAL ABSTRACT



### ARTICLE INFO

Editor: Pavlos Kassomenos

#### Keywords:

Air pollution  
PM<sub>1</sub>  
PM<sub>2.5</sub>  
PM<sub>10</sub>  
Dust events  
Sensors calibration  
Machine learning

### ABSTRACT

Low concentrations of pollutants may already be associated with significant health effects. An accurate assessment of individual exposure to pollutants therefore requires measuring pollutant concentrations at the finest possible spatial and temporal scales. Low-cost sensors (LCS) of particulate matter (PM) meet this need so well that their use is constantly growing worldwide. However, everyone agrees that LCS must be calibrated before use. Several calibration studies have already been published, but there is not yet a standardized and well-established methodology for PM sensors. In this work, we develop a method combining an adaptation of an approach developed for gas-phase pollutants with a dust event preprocessing to calibrate PM LCS (PMS7003) commonly used in urban environments. From the selection of outliers to model tuning and error estimation, the developed protocol allows to analyze, process and calibrate LCS data using multilinear (MLR) and random forest (RFR) regressions for comparison with a reference instrument. We demonstrate that the calibration performance was very good for PM<sub>1</sub> and PM<sub>2.5</sub> but turns out less good for PM<sub>10</sub> (R<sup>2</sup> = 0.94, RMSE = 0.55 μg/m<sup>3</sup>, NRMSE = 12 % for PM<sub>1</sub> with MLR, R<sup>2</sup> = 0.92, RMSE = 0.70 μg/m<sup>3</sup>, NRMSE = 12 % for PM<sub>2.5</sub> with RFR and R<sup>2</sup> = 0.54, RMSE = 2.98 μg/m<sup>3</sup>, NRMSE = 27 % for PM<sub>10</sub> with RFR). Dust events removal significantly improved LCS accuracy for PM<sub>2.5</sub> (11 % increase of R<sup>2</sup> and 49 % decrease of RMSE) but no significant changes for PM<sub>1</sub>. Best calibration models included internal relative humidity and temperature for PM<sub>2.5</sub> and only internal relative humidity for PM<sub>1</sub>. It turns out that PM<sub>10</sub> cannot be properly measured and calibrated because of technical limitations of the PMS7003 sensor. This work therefore provides guidelines for PM LCS calibration. This represents a first step toward standardizing calibration protocols and facilitating collaborative research.

\* Corresponding author at: Laboratoire TIMC, Domaine de la Merci, 38706 La Tronche, France.

E-mail addresses: [marie-laure.aix@univ-grenoble-alpes.fr](mailto:marie-laure.aix@univ-grenoble-alpes.fr) (M.-L. Aix), [sean.schmitz@rifs-potsdam.de](mailto:sean.schmitz@rifs-potsdam.de) (S. Schmitz), [dominique.bicot@univ-grenoble-alpes.fr](mailto:dominique.bicot@univ-grenoble-alpes.fr) (D.J. Bicot).

<http://dx.doi.org/10.1016/j.scitotenv.2023.164063>

Received 2 February 2023; Received in revised form 15 April 2023; Accepted 7 May 2023

Available online 17 May 2023

0048-9697/© 2023 Elsevier B.V. All rights reserved.

## 1. Introduction

Air pollution is a leading environmental risk factor, causing around 7 million deaths each year (Fuller et al., 2022). In 2021, new World Health Organization guidelines were established and most of the limits per pollutant were lowered as a result of new evidence from epidemiological studies (World Health Organization, 2021). It was found that even small rises (of  $1 \mu\text{g}/\text{m}^3$ ) in pollutants could trigger mortality increases (Danesh Yazdi et al., 2021). Particulate matter (PM) is a complex mixture of solid and liquid particles suspended in air (Adams et al., 2015). In Europe, it is mainly emitted from anthropogenic sources like residential heating, industry, traffic or agriculture (European Environment Agency, 2020). PM represents a threat to the environment and human health (Rai, 2016). Classified as carcinogenic (Loomis et al., 2013), PM induces public health effects depending on its size (Valavanidis et al., 2008). A growing body of research shows that  $\text{PM}_{10}$  may be more toxic than  $\text{PM}_{2.5}$  (Wu et al., 2022b; Zhang et al., 2020a, 2020b). A considerable amount of damage is also caused to plants where PM can inhibit photosynthesis and protein synthesis (Rai, 2016). For all these reasons, it is important to effectively measure PM.

Regulatory-grade stations, also called reference monitors, are highly reliable. However, they are expensive (10,000 to 100,000€) and few are implemented, especially in developing countries (deSouza et al., 2020). Moreover, they cannot be easily moved close to people's breathing zone and are not always well located to properly capture population exposure (Duyzer et al., 2015).

Low-cost sensors (LCS) are small portable systems measuring PM at a fine scale, both temporally and spatially. They provide almost real-time data and are affordable, generally less than €300 per unit. LCS use is increasing worldwide and studies are emerging in developing countries (McFarlane et al., 2021a; Raheja et al., 2022), where official measurement stations are rare. It is expected that LCS will not achieve the same accuracy as reference-grade instruments (Zimmerman, 2022), so it is imperative that LCS undergo a calibration before being used. Once calibrated and quality checked, they compare well with traditional reference instruments and can supplement regulatory-grade networks (Malings et al., 2020).

Various methods are used to calibrate LCS including linear regression (Barkjohn et al., 2021; Hua et al., 2021; Kosmopoulos et al., 2020), multiple linear regression (Barkjohn et al., 2021; Malings et al., 2020; Puttaswamy et al., 2022), mechanistic models based on hygroscopic growth correction (Barkjohn et al., 2021; Crilley et al., 2020; Malings et al., 2020) and machine learning (Kumar and Sahu, 2021; Nowack et al., 2021; Patra et al., 2021). Spatial calibration using regulatory and satellite data also proved to be efficient to calibrate  $\text{PM}_{2.5}$  (Lu et al., 2021; Mousavi and Wu, 2021). Linear regression (LR) generally lacks accuracy compared to multiple linear regression (MLR) considering several factors (Badura et al., 2019). Mechanistic models accounting for PM aerosol hygroscopic growth can further improve precision. The performance of traditional linear methods is generally limited compared to mechanistic approaches or machine learning. They struggle to capture cross-sensitivities between variables (Jiang et al., 2021; McFarlane et al., 2021a), but their simplicity and transparency are key advantages compared to machine learning.

Although various methodologies have been developed to evaluate LCS performance (Duvall et al., 2021; Fishbain et al., 2017; Languille et al., 2020), there is currently no harmonized protocol to calibrate LCS, which makes calibration studies difficult to start and compare. Calibrating LCS is a complex topic that can involve several questions (Giordano et al., 2021). For example, LCS users typically wonder how to detect outliers, which calibration model to select, and how long the calibration is valid. In 2019, researchers stated that there was no methodology indicating how to calibrate sensor networks and no ready-to-use open-source code (Barcelo-Ordinas et al., 2019). Since then, scientists developed process workflows (Bi et al., 2020; Chojer et al., 2022; Hong et al., 2021) but none of these studies offered an open-source code or went through a pre-processing step removing dust events. However, it is critical to check the presence of dust events in a dataset (Giordano et al., 2021), especially

when using a LCS which can be blind to dust events like PMS7003. Molina Rueda et al. (2023) recently acknowledged that other popular LCS like Sensirion SPS30 and Piersa IPS-7100 were also affected by this issue.

Schmitz et al. (2021) tackled complexity and transparency issues by developing a transparent approach to select the best calibration model. Their 7-step method and open-access code were made available for easy implementation (Schmitz et al., 2020). In this study, we employ and adapt this open-source protocol, initially developed for gas-phase pollutants, to calibrate a LCS measuring PM. In addition, we integrate critical measures such as dust events pre-processing and degradation checks to ensure accuracy and reliability. The originality of our approach lies in this holistic methodology which makes a valuable contribution to the field of low-cost PM sensors. Our objective was not to provide calibration formulas for various environments but to develop a complete protocol applicable to different settings. Our objective is not to provide a calibration formula that could be used in various environments but rather to develop a complete protocol applicable to different settings demonstrating hence how it is possible to construct a formula by using the same protocol for different settings. This new framework will be illustrated on a LCS collocation case study conducted in Grenoble.

## 2. Materials and methods

### 2.1. Field evaluation in Grenoble

#### 2.1.1. Low-cost sensors

Nine low-cost air quality stations measuring  $\text{PM}_{10}$ ,  $\text{PM}_{2.5}$ ,  $\text{PM}_{10}$ , temperature, and relative humidity (RH) were assembled. Each air quality station (AQS) had an optical PM sensor (Plantower PMS7003) and a MaxDetect DHT22 sensor measuring internal RH ( $\text{RH}_{\text{int}}$ ) and temperature ( $T_{\text{int}}$ ). PMS7003 usually shows a high correlation with reference instrument (Bauerová et al., 2020; Kang et al., 2021), stability over at least 15 months (Báthory et al., 2021), and good reproducibility (Badura et al., 2019). The AQS operates by drawing PM-carrying air through a pipe (Figs. S1 and S2). The air then passes through a laser (wavelength  $\approx 650 \text{ nm}$ ), which gets scattered by PM and impacts a photodiode detector (Kelly et al., 2017). The resulting signal is converted into an electrical signal and transmitted to the microcontroller (ESP8266), which uses a proprietary algorithm to calculate PM concentrations in  $\mu\text{g}/\text{m}^3$ .

#### 2.1.2. Collocation site, timeframe, and reference device

The study was conducted in Grenoble (France), the largest city in the Alps with 450,000 inhabitants. The local climate is semi-continental with cold winters and hot summers. Before deploying our AQSs, we had to calibrate them through comparison with reference-grade instruments certified for regulatory use. Therefore, we conducted a collocation study with Atmo Auvergne-Rhône-Alpes, the local regulatory instance measuring air quality. We hung our AQSs close to the inlet of their reference monitor (approximately 3 m) for 8 months from January 28, 2021 to September 29, 2021. The reference station, called "Les Frênes", was located close to a park in a low-traffic zone of Grenoble (GPS coordinates: latitude =  $45.162^\circ$ , longitude =  $5.735^\circ$ ). Considered as an urban background station, it uses a Fidas Palas GmbH 200, a certified optical aerosol spectrometer for regulatory air pollution monitoring. Contrary to the LCS, it is equipped with a sampler drawing air at a constant flow rate and an aerosol drying system removing water vapor. The gold standard method to determine PM mass is based on a gravimetric analysis (Giordano et al., 2021; Noble et al., 2001). It involves collecting PM on a pre-weighed filter and subsequently weighing it after sampling and conditioning to eliminate particle-bound water (Wallace and Hopke, 2022). Fidas 200 does not weight particles but uses the light scattered to determine particles sizes and count them. It assumes the particles have a spherical shape and a specific density to calculate their mass concentration using a proprietary algorithm. Fidas 200 is considered equivalent to the gravimetric EN12341 method for urban background environments by the Central Laboratory for Air quality Monitoring (LCSQA, 2017).



### 2.1.3. Meteorological data

We sourced weather data from ROMMA (Réseau d'Observation Météo du Massif Alpin, 2022), an association maintaining automatic semi-professional stations. The nearest station to our collocation site was located 3 km away (GPS coordinates: latitude = 45.169°, longitude = 5.768°). A Davis Vantage Pro2 instrument registered all parameters and rainfall (in mm) was measured using an Ultrimeter gauge. The following ambient variables were used: temperature ( $T_{amb}$ , in °C), relative humidity ( $RH_{amb}$ , in %), and average wind speed (WS, in km/h). WS was measured as a 10-min average, with a measurement frequency of 2.5–3 s. All other data had a 10-min time resolution. A binary time-of-day factor (ToD) from the NOAA Solar Calculator (<https://gml.noaa.gov/grad/solcalc/>) was extracted to account for diurnal changes. Hourly measurements made during the night were assigned a value of zero, while daytime measurements were given a value of one. All data analyses were performed with RStudio Server 2021.09.1 (Build 372) for Ubuntu Bionic and R statistical software (R Core Team, 2022).

### 2.1.4. Data cleaning

After collocation, the next crucial step is to prepare data for the first analyses. This involves checking sensors working ranges, performing time alignments to match LCS and reference data, and determining whether to fuse sensor data for comparison. The PMS7003 technical datasheet (Plantower, 2016) specifies a working humidity of 0 to 99 %, to which we added a 1 % safety margin. Consequently, LCS measurements were filtered out if the internal LCS RH was <1 % or >98 %. Between 0 % and 14 % of the dataset was removed depending on the AQS. Approximately 78 % of RH values exceeding 98 % were recorded after 6 months of service. PM concentrations,  $RH_{int}$  and  $T_{int}$  recorded every 150 s by the LCS but also weather data reported every 10 min, had to be rescaled to hourly values and converted to UTC (Universal Time Coordinated). The value of the current hour represented the average of measurements during the previous hour. As all LCS stations were giving highly correlated results within units over the whole study period (Pearson's correlation coefficient,  $r > 0.99$  for  $PM_1$ ,  $PM_{2.5}$ ,  $PM_{10}$ ,  $T_{int}$ , and  $r > 0.97$  for  $RH_{int}$ ), we used the “sensor fusion” method by calculating medians of the nine LCS outputs to ease data processing. Such a clustering method is considered more robust because it reduces calibration errors and inter-sensor variability effects (Barcelo-Ordinas et al., 2019; Smith et al., 2017; Smith et al., 2019).

### 2.2. Target accuracy metrics for PM sensors

Upon completion of the initial data cleaning process, it still remains to check LCS data quality. Checking raw sensor performances to see if calibration is needed should always be the first step. This entails assessing the closeness of the data to the reference values. The US EPA (United States Environmental Protection Agency) developed guidelines for assessing PM sensors (Duvall et al., 2021), including 5 accuracy metrics: Root Mean Square Error (RMSE), Normalized Root Mean Square Error (NRMSE), coefficient of determination ( $R^2$ ), slope and intercept. A scatter plot is drawn to compare LCS outputs to reference data, and a fitted regression line is used to calculate slope and intercept. If all points align with the bisector, LCS calibration is unnecessary. The US EPA recommends that the intercept be within  $-5$  and  $+5 \mu\text{g}/\text{m}^3$  with a target slope of  $1.0 \pm 0.35$ .  $R^2$  should exceed 0,70 for linearity reasons. RMSE is calculated as follows:

$$RMSE = \sqrt{\frac{\sum_{i=1}^n (y_i - x_i)^2}{n}} \quad (1)$$

where  $y_i$  and  $x_i$  are PM concentrations measured with the reference and LCS, respectively.  $R^2$  reflects the accuracy as the closeness between LCS and reference values. For  $PM_{2.5}$ , the EPA recommends a RMSE target below  $7 \mu\text{g}/\text{m}^3$  and  $NRMSE \leq 30 \%$ , calculated as:

$$NRMSE = \frac{RMSE}{\bar{y}} \times 100 \quad (2)$$

where  $\bar{y}$  is the average reference value.

The EPA recommends checking either the RMSE or NRMSE metrics to assess LCS performance. Although the EPA metrics were originally designed for  $PM_{2.5}$  performance testing, we also applied them to  $PM_1$  and  $PM_{10}$ . In France, the Central Laboratory for Air quality Monitoring (LCSQA) established uniform calibration criteria for  $PM_{2.5}$  and  $PM_{10}$ , using a relative extended uncertainty (REU) metric rather than RMSE (LCSQA, 2020). The  $7 \mu\text{g}/\text{m}^3$  EPA limit for RMSE may not be suitable for  $PM_1$  or  $PM_{10}$  due to their varying magnitudes. As a result, we mostly used NRMSE when assessing compliance with EPA criteria for  $PM_1$  and  $PM_{10}$ , which also enables easy comparison across studies. We followed the EPA guidelines to analyze our dataset and during the regression analysis of LCS values against the reference as per the US EPA requirement, we observed a distortion of the point cloud (Fig. 1A). There were two distinct patterns for  $PM_{2.5}$  and  $PM_{10}$  that were associated with two different slopes. Further investigation revealed that the lower slope outliers corresponded to dust events from Sahara Desert.

### 2.3. Pre-processing technique for the detection and removal of dust events

In the European Alps, a significant proportion of dust events comes from the Sahara (Di Mauro et al., 2019). We confirmed that PM measurement was impacted by those events by checking the daily Pearson correlation coefficient ( $r$ ) between LCS and reference hourly values (Fig. 2A). Each time a dust event occurred,  $r$  was negative because LCS from Plantower (PMS) can be “blind” to coarse particles like desert dust (Kosmopoulos et al., 2020; Kuula et al., 2020; Vogt et al., 2021). The following two steps method, shown in Fig. 2, was used on  $PM_{2.5}$  to remove dust events on all datasets: (1) select all times with negative  $r$ , (2) validate the presence of a dust event with CAMS (Copernicus Atmosphere Monitoring Service) satellite data (retrieved  $0.1^\circ \times 0.1^\circ$  resolution dust values from ENSEMBLE dataset (Météo-France et al., 2020) ('analysis' type)) (Fig. 2B). These satellite data were recovered via a free CAMS Web Application Programming Interface (API). The code we developed for extracting dust events from Copernicus API is available in the open-source repository Zenodo (see DOI below). It turned out that all events with negative  $r$  corresponded to dust events seen by CAMS. All those events (5 % of the full period) were removed from the complete datasets for  $PM_1$ ,  $PM_{2.5}$ , and  $PM_{10}$  (Fig. 2C). Next, using analysis of EPA accuracy criteria revealed some metrics did not meet standards, indicating calibration was necessary.

### 2.4. Calibration

After having pre-processed the dataset and checked EPA metrics, we were ready to apply the Schmitz 7-step calibration method. We also intended to compare this method to more traditional approaches that do not use artificial intelligence. Following the same approach as Schmitz et al., we split the dataset into training and testing sets using a 75/25 ratio for both Schmitz and traditional approaches (Fig. 3). The first 183 days of the collocation were used to identify the best models, which were then evaluated using the final 60 days.

#### 2.4.1. Traditional approaches

Linear regression aims at finding a linear relationship between reference measurements (dependent variable) and LCS data (predictor variables). As an example, the equation for  $PM_{2.5}$  is:

$$PM_{2.5 \text{ ref}} = \alpha_0 + \alpha_1 PM_{2.5} \quad (3)$$

where  $PM_{2.5 \text{ Ref}}$  represents reference concentrations,  $PM_{2.5}$  the LCS concentrations,  $\alpha_1$  the slope of linear regression and  $\alpha_0$  the intercept. In the mechanistic approach, temperature and RH are included in the calibration formula. When moisture is high, there is more condensed water on PM surface which scatters more light. This can affect the LCS which tends to give higher values than it should (Wang et al., 2015). As such, numerous studies recommend including RH in calibration equations (Badura et al., 2019; Crilly et al., 2020; Hua et al., 2021). Although with a relatively small

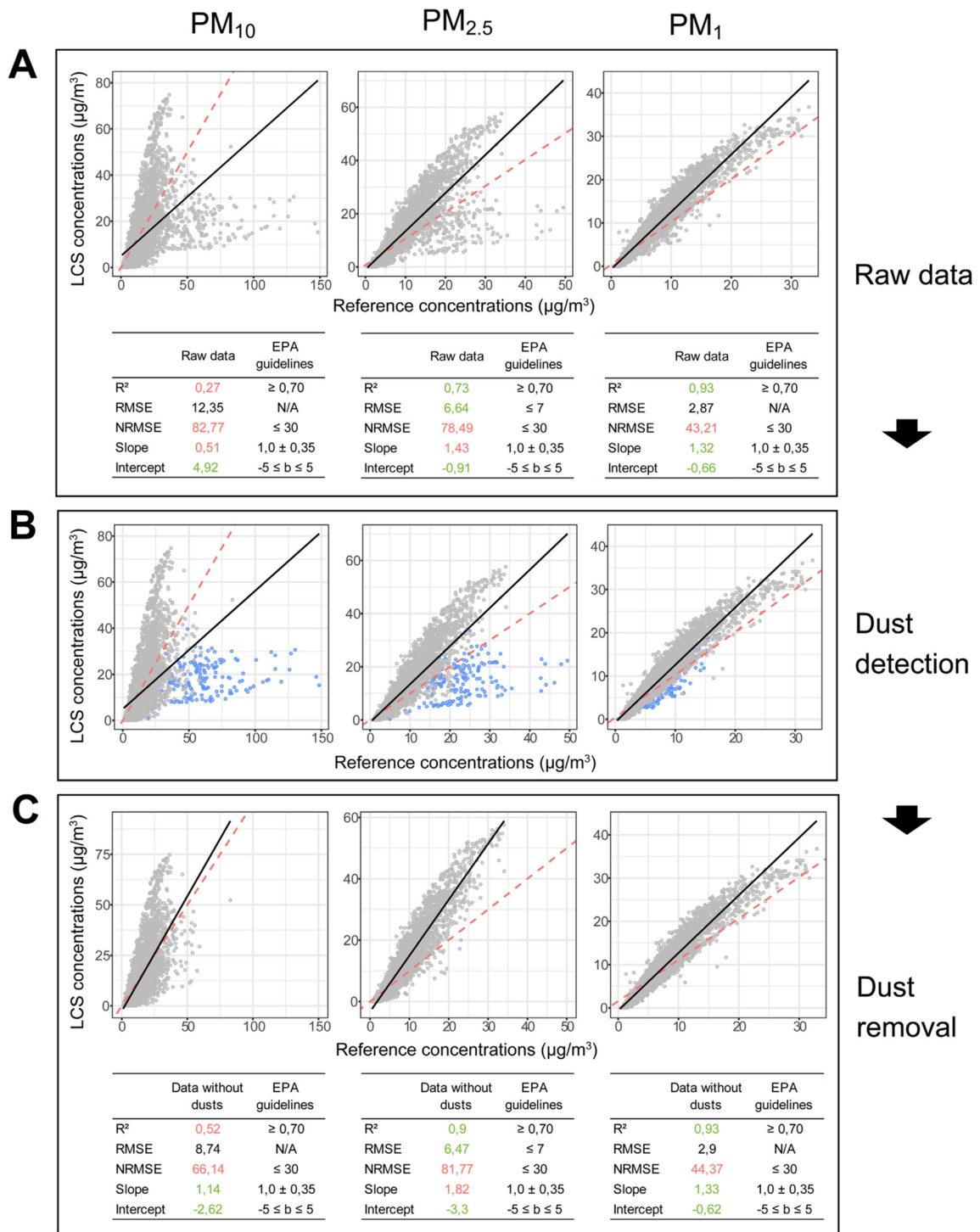


**Fig. 1.** Effect of dust pre-processing on regressions of LCS versus reference concentrations (hourly values) and accuracy metrics. The dashed red lines indicate the parity ( $y = x$ ), and the black lines are the best linear fit. The raw dataset is shown in (A), while (B) displays the dusts identified with our method (in blue), (C) shows the dataset after dust removal. Accuracy metrics such as  $R^2$ , RMSE ( $\mu\text{g}/\text{m}^3$ ), NRMSE (%), intercept ( $\mu\text{g}/\text{m}^3$ ) and slope are included (see Section 2.2 for metrics definitions). The use of green color indicates EPA compliant metrics, while red color denotes non-compliant metrics with EPA standards.

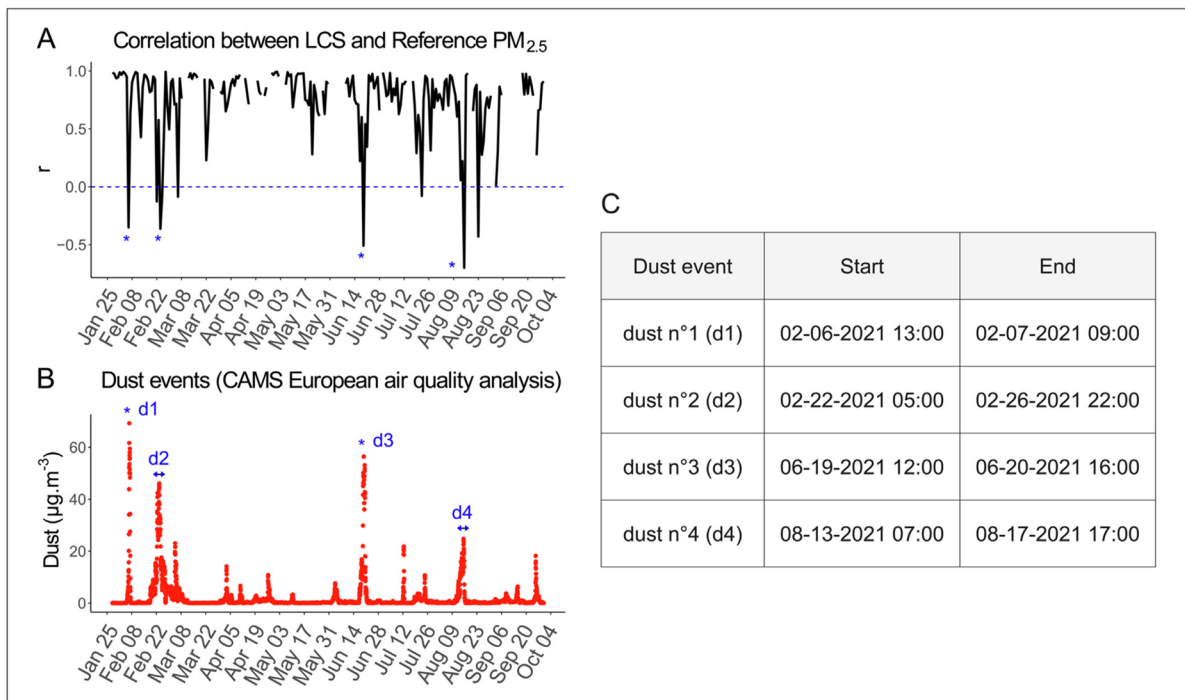


Fig. 2. Removal of dust events from the Sahara Desert: (A) identification of negative daily Pearson correlation coefficients (r), (B) dust events identification, (C) selected dust events to remove.

influence (Wang et al., 2015), the temperature is also mentioned in various works together with RH as a confounding factor (Chakraborty et al., 2020; Giordano et al., 2021). As an extension of Eq. (3), the following equation involving both  $RH_{int}$  and  $T_{int}$  is used (Chakraborty et al., 2020; Streibl, 2017):

$$PM_{2.5\ ref} = \alpha_0 + \alpha_1 \frac{PM_{2.5\ lcs}}{g(RH_{int})} + \alpha_2 T_{int} \quad (4)$$

where  $g(RH_{int})$ , the hygroscopic growth factor, defined as the ratio of wet to dry particle diameters at a given RH, is determined by Di Antonio et al. (2018):

$$g(RH_{int}) = \left( 1 + \kappa \frac{RH_{int}}{100 - RH_{int}} \right)^{\frac{1}{3}} \quad (5)$$

in which  $\kappa$  refers to the degree of hygroscopicity of a particle, depending on the local aerosol. The parameters  $\alpha_0$ ,  $\alpha_1$ ,  $\alpha_2$  and  $\kappa$  were estimated with the nls() function (R Core Team, 2022).

2.4.2. Schmitz methodology

The Schmitz open-source method is a 7-step methodology (see blue boxes in Fig. 4) initially developed to calibrate gas-phase pollutants such as nitrogen dioxide (NO<sub>2</sub>) or ozone (O<sub>3</sub>). An open-access code can be found online (Schmitz et al., 2020). Step 1 aims to provide a better understanding of the data by analyzing distributions and identifying potential quality issues to be addressed before calibration. This includes checking the distributions of the reference concentrations, LCS data, and weather variables. This is done on both training and testing sets through histograms, violin plots, and time series plots. Step 2 involves removing outliers as they

Calibration technique	Dataset
Linear regression	75% TRAIN   25% TEST
Mechanistic	75% TRAIN   25% TEST
Multivariate Linear Regression (Schmitz et al.)	Sliding window → 75% TRAIN   25% TEST
Random Forest Regression (Schmitz et al.)	75% TRAIN   25% TEST

Fig. 3. Calibration techniques implemented in this study.



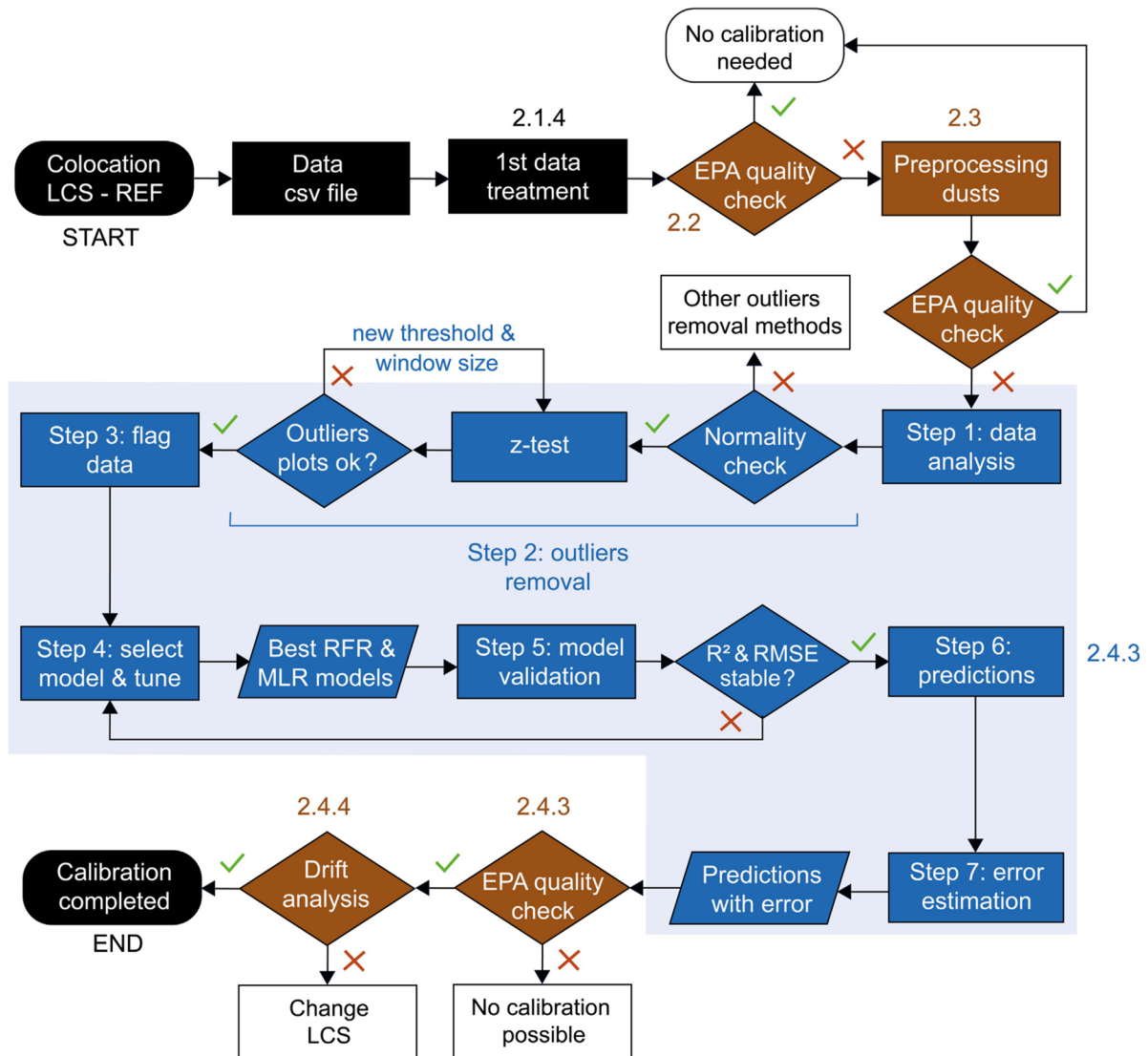


Fig. 4. Methodology flowchart. In blue, the Schmitz method (Section 2.4.2 of the manuscript). In brown, the adaptations made for this PM related study. The numbers (for example 2.1.4) refer to the corresponding Materials and methods subsections.

can affect calibration models. Data normality is checked with a Shapiro-Wilk test, followed by a z-test with running mean and standard deviation to detect outliers. Visualization of the outliers on a time-series aids in ensuring a meaningful time window and z-test threshold. Step 3 involves flagging test data falling outside the range of the training data, as well as training data outside the range of the test data. The objective is to identify data points that may be less reliable for prediction and assign them a higher level of uncertainty. Step 4 selects and optimizes the best calibration models, dividing the training dataset into smaller sets using a moving window. In their case-study, Schmitz et al. use a 5 days window, with the models trained on four days and tested on the fifth day. Models with the smaller average RMSE over the various fifth-day predictions are selected. Subsequently, measures of AIC (Akaike Information Criterion) for the MLR model and VI (Variable Importance) for the RFR model are assessed to determine which predictors should remain. VI assesses the relative

importance of each predictor variable in predicting the target variable and AIC quantifies the balance between model goodness of fit and complexity. Finally, models are tested on the test subset and assessed using RMSE and  $R^2$ . The most accurate MLR and RFR models are then sent to the next step. Step 5 allows to validate models by splitting the training set into training and testing subsets at a 75/25 ratio. Those continuous blocks of data allow accounting for autocorrelation in the data. Stability across blocks is then checked using  $R^2$ , RMSE and VI. Step 6 is about exporting predictions given by the best MLR and RFR models and plotting them using time series. Step 7 evaluates the overall error and confidence intervals associated with the predictions. The reference instrument's technical error is merged with the statistical error associated with the model's predictions. The former is derived from reference specifications, while the latter is computed as the median mean absolute error (MAE) across all blocks during model validation. We adapted this method to our PM dataset (Fig. 5):

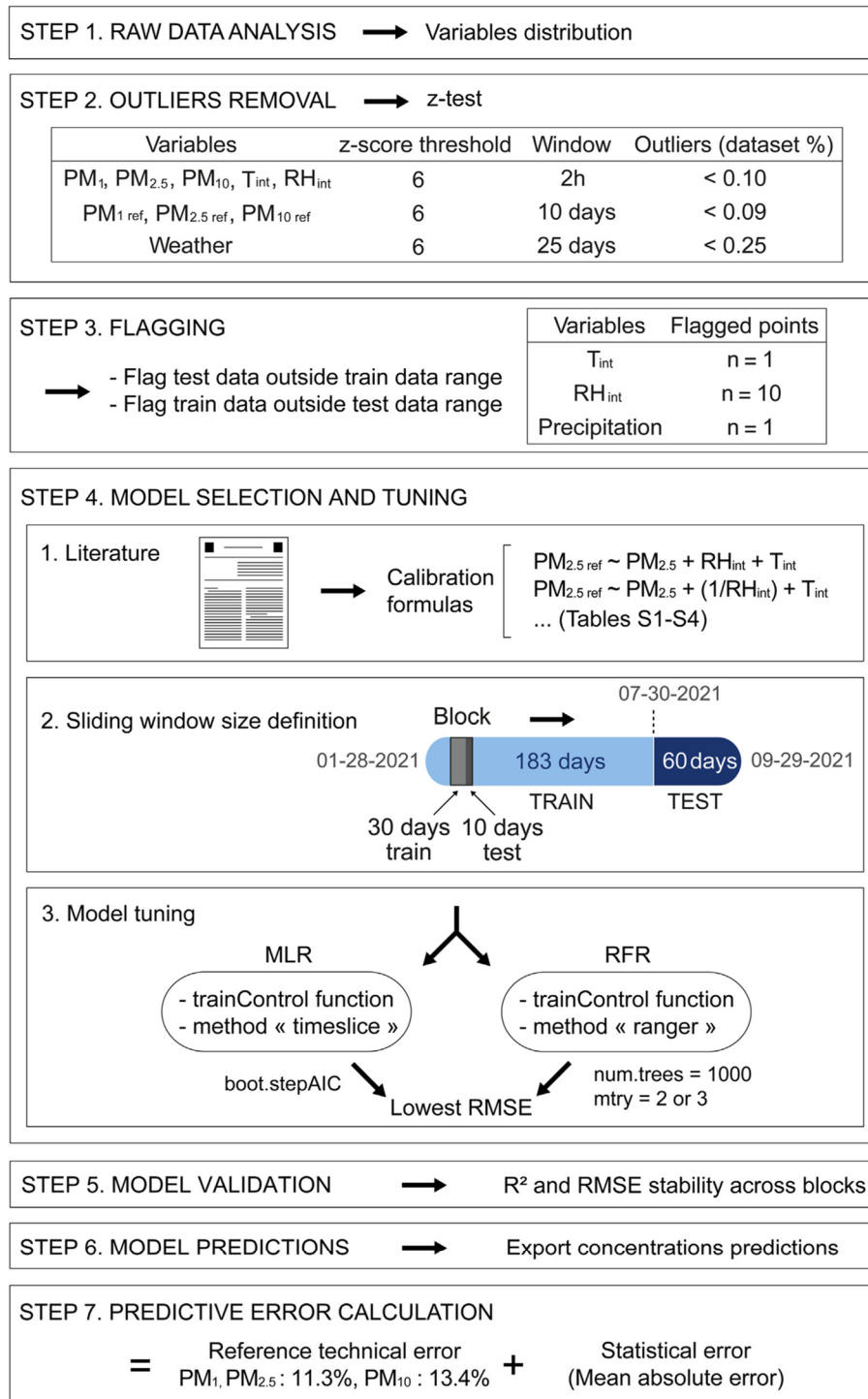


Fig. 5. Flowchart of adapting the Schmitz method.

(Step 1) Data analysis. Distributions of weather and PM data were similar (Fig. S3) in both training and testing datasets allowing us to continue the analysis.

(Step 2) Outliers removal. Before running the z-test, normality was checked on each sliding window by the detectOutlier function. For PM<sub>10</sub>, between 6.8 % and 9 % of the data failed the normality test



depending on the device. For  $PM_{2.5}$ , between 7.9 % and 9.9 % of the data did not pass the normality test, while between 8.6 % and 10.8 % of  $PM_1$  data failed the test. Furthermore, between 2.2 % and 3 % of the RH data and between 2.6 % and 3.3 % of the temperature data failed the test. We assumed that most of the data aligned sufficiently with the normal distribution for the z-test to be applicable and we conducted a visual inspection of outliers (Fig. S3) to ensure that the function did not erroneously flag the extreme values of typical data spikes as outliers. Outliers represented <0.1 % of the LCS data.

(Step 3) Flagging. 12 out-of-bounds points were flagged for  $RH_{int}$  ( $n = 10$ ),  $T_{int}$  ( $n = 1$ ), and rain ( $n = 1$ ), all occurring during the first two weeks of August (Fig. S3).

(Step 4) Model selection and tuning.

- After conducting an extensive literature search on calibration for LCS measuring PM, we identified key variables and the most promising calibration formulas to be tested (models in Tables S1, S2, S3 and S4).
- To find the best RFR and MLR models, a moving window of 30 days was used to train models and 10 days to test (Step 4.2 in Fig. 5). This ratio was chosen proportionally to what was done by Schmitz et al.
- The trainControl function (caret R package) was used on all blocks.
- The models with the lowest RMSE averaged over the various sliding windows were kept. For RFR, the number of features to be considered at each node of trees (mtry) was adjusted by selecting the best performing in terms of RMSE.

(Step 5) Model validation. RMSE and  $R^2$  were considered stable enough (Fig. S4) compared to what was observed in Schmitz et al.'s work, so we decided to go further.

(Step 6) Model predictions. Final concentrations predictions were exported.

(Step 7) Predictive error calculation (see output example in Fig. S4). Regarding technical errors in the reference instrument, it was found that the Fidas 200 datasheet (Palas GmbH, 2020) had an uncertainty of 10 % for  $PM_{2.5}$  and 8 % for  $PM_{10}$ . However, local official comparison tests performed with the gold-standard gravimetric method on the Fidas 200 in Grenoble revealed an expanded uncertainty ( $k = 2$ ) of 11.3 % for  $PM_{2.5}$  and 13.4 % for  $PM_{10}$  (LCSQA, 2020) so we applied this expanded uncertainty. We assumed that  $PM_1$  had an 11.3 % uncertainty like  $PM_{2.5}$ .

#### 2.4.3. Calibrations performances metrics

After having used both traditional and Schmitz approaches to generate calibration formulas, we tested these formulas on the test dataset. To select the best models, we used both  $R^2$  (coefficient of determination) and RMSE:

$$R^2 = 1 - \frac{\sum_{i=1}^n (y_i - x_i)^2}{\sum_{i=1}^n (y_i - \bar{y})^2} \quad (6)$$

where  $y_i$  are the PM concentrations measured by the reference,  $x_i$  represents PM values predicted by the various correction models and  $\bar{y}$  is the mean of reference values.

$$RMSE = \sqrt{\frac{\sum_{i=1}^n (y_i - x_i)^2}{n}} \quad (7)$$

And after having chosen the best models according to those two criteria, we checked EPA accuracy metrics again. Nonzero intercepts and nonunity slopes are less concerning for optical LCS due to their sensitivity to aerosol characteristics like shape and refractive index. They just have to be calibrated for specific aerosol conditions when accuracy is needed (Giordano et al., 2021; Molina Rueda et al., 2023).  $R^2$  indicates the prediction quality of a model and RMSE the accuracy. These two metrics should be given a higher priority to choose the best models. Once the best calibration models have been selected and predictions made, it may be important to ensure the stability of the corrected values over time.

#### 2.4.4. Drift in the corrected measurements over time

An assessment of potential degradation in the corrected measurements over time was conducted using a methodology proposed by deSouza et al. (2023a). To this end, we used PM values from the best calibration formulas (see Table 1, formulas in bold) and called them  $PM_{Corrected}$ . A drift error was then computed for  $PM_{10}$ ,  $PM_{2.5}$  and  $PM_1$  using this formula:

$$Drift = PM_{Corrected} - PM_{Ref} \quad (8)$$

The goal was to investigate the time-dependence of the error between corrected LCS data and reference values.

### 3. Results

#### 3.1. Raw data analysis

In line with the EPA guidelines, we started our data analysis by drawing scatterplots showing measured LCS values against the reference concentrations with a regression line (Fig. 1A). The  $R^2$  did not meet EPA compliance standards for  $PM_{10}$ , and the NRMSE was non-conforming for all PM sizes. During the analysis of the scatterplots, some clusters of points were observed to deviate from the overall trend of the dataset, particularly for  $PM_{2.5}$  and  $PM_{10}$ . These clusters exhibited a smaller slope compared to the majority of the dataset, and further examination revealed that they were associated with Saharan dust events.

#### 3.2. Preprocessing with dust events removal

The dust events pre-processing, previously explained in Section 2.3, allowed us to color-code the dust events on the scatterplot (Fig. 1B) which visually demonstrated that these outliers would be eliminated with our technique. We then removed all those dust events in the dataset and proceeded with a new quality check according to EPA standards (Fig. 1C). Dust events removal yielded notable improvements in  $R^2$  values, with a significant 93 % increase for  $PM_{10}$  and a 23 % increase for  $PM_{2.5}$ . After preprocessing, data from LCS for  $PM_1$  and  $PM_{2.5}$  already explained 93 % and 90 % variability of the reference data respectively, whereas  $PM_{10}$  had a much lower  $R^2$  (0.52), reflecting a poor correlation with REF. NRMSE remained non-compliant for all PM sizes, indicating a need for further calibration. A statistical analysis of the dataset cleared of dust events (Table S5) showed that mean  $PM_{10}$  reference concentrations were higher than mean LCS concentrations, unlike  $PM_{2.5}$  and  $PM_1$  where the LCS tended to overestimate the concentrations. ROMMA temperature values were smaller than LCS values, which was not unexpected as the LCS temperature sensor was located inside the device and therefore subject to heating. This might as well have been enhanced by the southern orientation of the collocation site.

#### 3.3. Performance of calibration protocols

A range of correction formulas (Table 1) was generated using the different calibration methods. The best RFR formulas included wind speed for  $PM_{2.5}$  and  $PM_{10}$ . However, the accuracy improvement was not significant compared to formulas solely involving  $RH_{int}$  and  $T_{int}$ . Therefore, we pursued with RF formulas using  $RH_{int}$  and  $T_{int}$  only. This would make the

**Table 1**  
Model performances on the test dataset, using hourly values.

Method	Correction formula	R <sup>2</sup>	RMSE <sup>a</sup>	NRMSE <sup>b</sup>	Slope	Intercept
PM <sub>1</sub>						
LR	PM <sub>1 Ref</sub> = 0.70 PM <sub>1</sub> + 0.93	0.80	1.00	21.70	1.06	0.12
Mechanistic	PM <sub>1 Ref</sub> = 0.08 + 0.83 $\frac{PM_1}{(1+0.13\frac{RH_{int}}{100-RH_{int}})^{\frac{1}{3}}}$ + 0.03 T <sub>int</sub>	0.92	0.62	13.42	1.05	-0.05
<b>MLR</b>	<b>PM<sub>1 Ref</sub> = PM<sub>1</sub> * RH<sub>int</sub></b>	<b>0.94</b>	<b>0.55</b>	<b>11.95</b>	<b>1.07</b>	<b>-0.33</b>
RFR	PM <sub>1 Ref</sub> = PM <sub>1</sub> + RH <sub>int</sub> + T <sub>int</sub>	0.92	0.62	13.45	0.98	0.33
PM <sub>2.5</sub>						
LR	PM <sub>2.5 Ref</sub> = 0.49 PM <sub>2.5</sub> + 2.49	0.83	1.03	17.75	0.86	1.12
Mechanistic	PM <sub>2.5 Ref</sub> = 0.50 + 0.65 $\frac{PM_{2.5}}{(1+0.25\frac{RH_{int}}{100-RH_{int}})^{\frac{1}{3}}}$ + 0.08 T <sub>int</sub>	0.87	0.90	15.57	0.88	0.84
MLR	PM <sub>2.5 Ref</sub> = PM <sub>2.5</sub> * RH <sub>int</sub>	0.90	0.78	13.46	0.86	0.48
RFR	PM <sub>2.5 Ref</sub> = PM <sub>2.5</sub> + RH <sub>int</sub> + T <sub>int</sub> + WS	0.92	0.70	12.02	0.96	0.46
	<b>PM<sub>2.5 Ref</sub> = PM<sub>2.5</sub> + RH<sub>int</sub> + T<sub>int</sub></b>	<b>0.92</b>	<b>0.70</b>	<b>12.02</b>	<b>0.96</b>	<b>0.44</b>
PM <sub>10</sub>						
LR	PM <sub>10 Ref</sub> = 0.45 PM <sub>10</sub> + 7.71	0.39	3.42	31.45	0.33	7.63
Mechanistic	PM <sub>10 Ref</sub> = 1.75 + 1.12 $\frac{PM_{10}}{(1+2.68\frac{RH_{int}}{100-RH_{int}})^{\frac{1}{3}}}$ + 0,23 T <sub>int</sub>	0.43	3.31	30.40	0.53	5.40
MLR	PM <sub>10 Ref</sub> = 1.15 + 0.89 $\frac{PM_{10}}{(1+\frac{RH_{int}}{100-RH_{int}})^{\frac{1}{3}}}$ + 0,27 T <sub>int</sub>	0.42	3.33	30.61	0.54	5.53
RFR	PM <sub>10 Ref</sub> = PM <sub>10</sub> + RH <sub>int</sub> + T <sub>int</sub> + WS	0.54	2.96	27.21	0.64	4.29
	<b>PM<sub>10 Ref</sub> = PM<sub>10</sub> + RH<sub>int</sub> + T<sub>int</sub></b>	<b>0.54</b>	<b>2.98</b>	<b>27.36</b>	<b>0.66</b>	<b>4.02</b>

PM<sub>1 Ref</sub> = PM<sub>1</sub> concentrations in µg/m<sup>3</sup> measured by the reference, PM<sub>1</sub> = PM<sub>1</sub> concentrations in µg/m<sup>3</sup> measured by the LCS, RH<sub>int</sub> = internal relative humidity in % measured by the LCS, T<sub>int</sub> = internal (LCS) temperature in °C, WS = average wind speed in km/h, \* = the model has interactions.

<sup>a</sup> In µg/m<sup>3</sup>.

<sup>b</sup> NRMSE or normalized RMSE (in %) = RMSE divided by the mean of the observed (reference) concentrations and multiplied by 100.

calibration simpler because LCS systematically provide RH<sub>int</sub> and T<sub>int</sub>. Moreover, ambient parameters from external weather stations do not represent the local LCS environment, so it is better to use internal LCS parameters for calibration.

PM<sub>1</sub> models were performing the best in terms of precision, and all metrics for PM<sub>1</sub> and PM<sub>2.5</sub>, including those obtained through the LR technique, were found to be conform with the EPA checklist. However, the Schmitz protocol outperformed the traditional methods for all PM sizes. Simple LR always performed significantly less well than the other techniques. Compared to LR, mechanistic models brought a 38 % accuracy improvement for PM<sub>1</sub> and a 13 % accuracy improvement for PM<sub>2.5</sub>. MLR worked better for PM<sub>1</sub> but RFR performed better (lowest RMSE and highest R<sup>2</sup>) for PM<sub>2.5</sub> and PM<sub>10</sub>. None of the methods used to calibrate PM<sub>10</sub> produced results that met EPA standards. To compare the four model's fitting more in detail, we regressed reference PM concentrations against predicted values on the test dataset (Fig. 6). It highlights the difficulty in accurately predicting PM<sub>10</sub> levels, as the scatter in the data is large and R<sup>2</sup> does not comply with EPA standards. Corrected PM<sub>2.5</sub> and PM<sub>1</sub> gave more accurate results with a better fit.

### 3.4. PM<sub>10</sub> calibration improvement essay

To investigate the lower performance of LCS compared to the reference station for PM<sub>10</sub>, we considered the concentration difference between PM<sub>10</sub> and PM<sub>2.5</sub> for both reference and LCS as PM<sub>(10-2.5) Ref</sub> = PM<sub>10 Ref</sub> - PM<sub>2.5 Ref</sub> and PM<sub>10-2.5</sub> = PM<sub>10</sub> - PM<sub>2.5</sub>. The reasoning was to try to estimate the concentration of PM<sub>2.5</sub> counted as PM<sub>10</sub>. We found that the scatterplot of PM<sub>(10-2.5) Ref</sub> versus PM<sub>2.5 Ref</sub> shows almost no relationship with a rather high variability (Fig. S5, A) whereas PM<sub>10-2.5</sub> versus PM<sub>2.5</sub> exhibits a two-slope linear relation with a breakpoint at 28 µg/m<sup>3</sup> (Fig. S5, B). This clearly indicates that although the reference and the LCS both use optical probes, the PM<sub>10</sub> counting methods (and the transcription algorithms used) lead to qualitatively and quantitatively different results. These two profiles are so different that they cannot be superimposed by making simple transformations such as regressions. The regressions obtained are the best we can do.

### 3.5. The importance of combining preprocessing with the Schmitz method

To evaluate the efficacy of dust events pre-processing, we calibrated our LCS without removing dust events (Fig. 7C) and we compared performances with the full combined method (Fig. 7A). The RFR and MLR methods used the same predictor variables regardless of whether dust events were present in the dataset or not. Removing dust events was highly beneficial for PM<sub>2.5</sub>, as all metrics exhibited significant improvement. We observed an 11 % increase in R<sup>2</sup> and a 49 % decrease in RMSE for PM<sub>2.5</sub>. The situation was more nuanced for PM<sub>1</sub>, as dust events removal led to a slight degradation of R<sup>2</sup> (-1 %) and NRMSE (+3 %). For PM<sub>10</sub>, all metrics improved by removing dust events, apart from R<sup>2</sup>, decreasing by 10 %. We also observed that relying solely on dust events processing without using the Schmitz method would not be sufficient to meet the EPA standards (Fig. 7B).

### 3.6. Long-term stability of corrected PM measurements

The degradation over the course of the experiment is shown in Fig. S6. No bias over time was observed on the drift. The mean drift over the whole 8 months period was 0.069 (95 % CI: -0.020, 0.157) µg/m<sup>3</sup> for PM<sub>10</sub>, 0.042 (95 % CI: 0.018, 0.066) µg/m<sup>3</sup> for PM<sub>2.5</sub> and -0.001 (95 % CI: -0.028, 0.026) µg/m<sup>3</sup> for PM<sub>1</sub>. Therefore, degradation over time was not an issue in our study.

## 4. Discussion

Our findings indicate that PMS7003 is more effective in measuring PM<sub>1</sub> compared to PM<sub>2.5</sub>, with a lower NRMSE and higher R<sup>2</sup>. This is consistent with previous research by Molina Rueda et al. (2023) on PMS5003, with similar raw metrics observed. Our results showed an R<sup>2</sup> correlation of 0.73 for PM<sub>2.5</sub> and 0.93 for PM<sub>1</sub>, which are consistent with their findings of 0.76 and 0.9, respectively. In line with their research, our study also confirms that PMS7003 is a poor probe for measuring PM<sub>10</sub>. First, PMS7003 clearly underestimated increases in PM<sub>10</sub> as already shown (Sayahi et al., 2019; Vogt et al., 2021). This discrepancy in the PM<sub>10</sub> between the

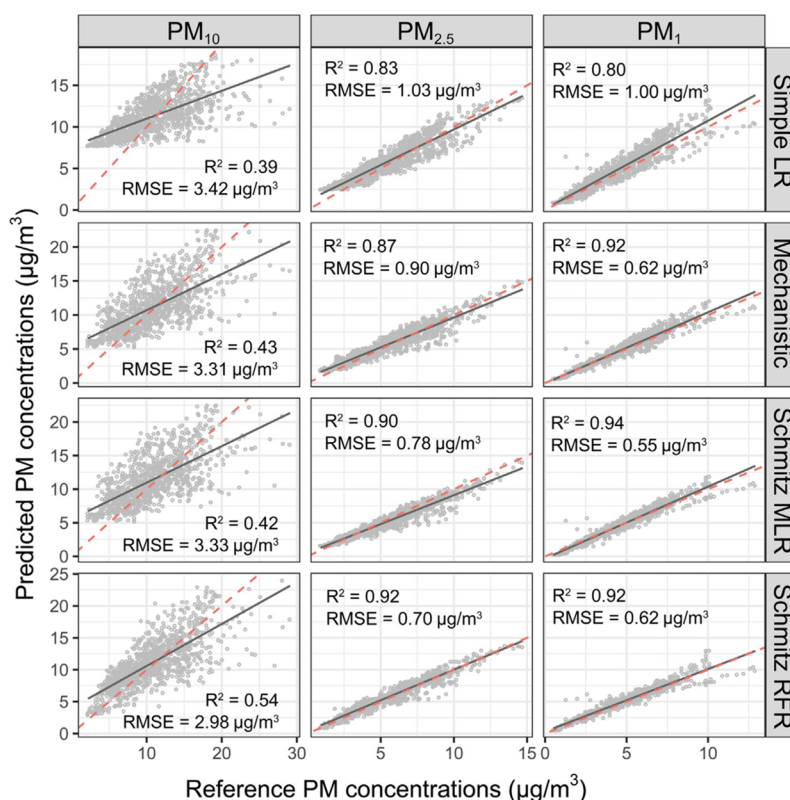


Fig. 6. Scatterplot of hourly PM reference concentrations versus predicted PM concentrations (test dataset). The red dashed line shows the parity line ( $y = x$ ) and the black solid line shows the fitted linear regressions.

reference and the LCS is linked to the size distribution of the particles detected as a function of both the optical wavelength of the PMS7003 and the angles of diffusion toward the photodiode. Second, it seems hardly feasible to predict the coarse fraction (PM<sub>10-2.5</sub>) by using the PM<sub>2.5</sub> cumulative concentrations. The LCS is technically limited to detect PM<sub>10</sub> so our calibrations could not improve performances tremendously. It is reassuring that models for PM<sub>1</sub> and PM<sub>2.5</sub> are the best performing since these small particles penetrate the respiratory and circulatory system more deeply than PM<sub>10</sub> and can have stronger toxicity (Valavanidis et al., 2008).

To achieve better alignment with the reference concentrations, four calibration techniques were used to enhance the accuracy of LCS measurements. None of the methods used for PM<sub>10</sub> produced results that met EPA compliance standards, while all PM<sub>1</sub> and PM<sub>2.5</sub> performance metrics, including those obtained via the LR technique, met EPA criteria. Among the four tested methods, RFR was the best for PM<sub>2.5</sub> whereas MLR performed better for PM<sub>1</sub>. Recently, deSouza et al. (2023b) calibrated a LCS for PM<sub>2.5</sub> measurement and also stated that RFR gave better results than MLR in a stationary setting. Interestingly, for PM<sub>1</sub> we found that a mechanistic approach could perform as well as a bootstrap RFR technique (RMSE = 0.62 µg/m<sup>3</sup> for both approaches). But bootstrap MLR still performed better for PM<sub>1</sub> (RMSE = 0.55 µg/m<sup>3</sup>). The best RMSEs found in our study (0.55 µg/m<sup>3</sup> for PM<sub>1</sub> and 0.70 µg/m<sup>3</sup> for PM<sub>2.5</sub>) were excellent compared to what can be seen in the literature. It is difficult to compare RMSEs from one study to another because experimental conditions are different, but we believe that the dust events preprocessing brought a competitive advantage as it is seldom used before calibrating LCS in ambient conditions. We only found a study from Kosmopoulos et al. (2020) removing dust events before calibration, but they only used LR afterwards. Our dust events removal method using satellite analyses could be further automated using

CAMS API. In our study, dust events removal immediately increased R<sup>2</sup> for PM<sub>10</sub> and PM<sub>2.5</sub> but this preprocessing had less influence on PM<sub>1</sub>. These observations were similar to what had been observed by Kosmopoulos et al. (2020). They stated that the impact of dust events on LCS was more important for PM<sub>2.5</sub> than for PM<sub>1</sub>, due to a considerable portion of the smaller-sized particles falling within the 1–2.5 µm range. It would be interesting to develop algorithms to calibrate PM measurements during dust events without discarding them. Stavroulas et al. (2020) used polynomial regression using ratios related to the presence of dust events (PM<sub>1</sub>/PM<sub>2.5</sub> or PM<sub>2.5</sub>/PM<sub>10</sub>) and had good performances (40 % NRMSE improvement) predicting PM<sub>2.5</sub> with a quadratic equation. Regarding PM<sub>1</sub>, removing dust events led to a slight degradation of R<sup>2</sup> (–1 %) and NRMSE (+3 %), so we could use the PM<sub>1</sub> dataset without discarding dust events. However, for PM<sub>2.5</sub>, dust events removal brought an 11 % increase in R<sup>2</sup>, a 49 % decrease in RMSE, and all other metrics improved as well. Therefore, we recommend checking the presence of dust events by considering scatterplot linearity before step 1 of the Schmitz method. Other types of LCS might react differently to dust events, and the occurrence of dust events may not be consistent across all regions and seasons. However, in this case-study, removing dust events improved considerably the LCS accuracy for PM<sub>2.5</sub>, which was further enhanced by the Schmitz method. Only a few studies had similar accuracy metrics. Puttaswamy et al. (2022) found a 15 % NRMSE for PM<sub>2.5</sub> using LR with temperature, but their study only lasted 100 days. Kelly et al. (2021) had NRMSEs ranging from 13.1 % to 22.9 % for wildfires using a Gaussian process model. Model accuracy is considered as good when 10 % < NRMSE < 20 % (Li et al., 2013) and we found NRMSE = 12 % for the best PM<sub>2.5</sub> and PM<sub>1</sub> models. As also found by Schmitz et al. on their experimental dataset, models with internal parameters coming from LCS performed better than models using external weather



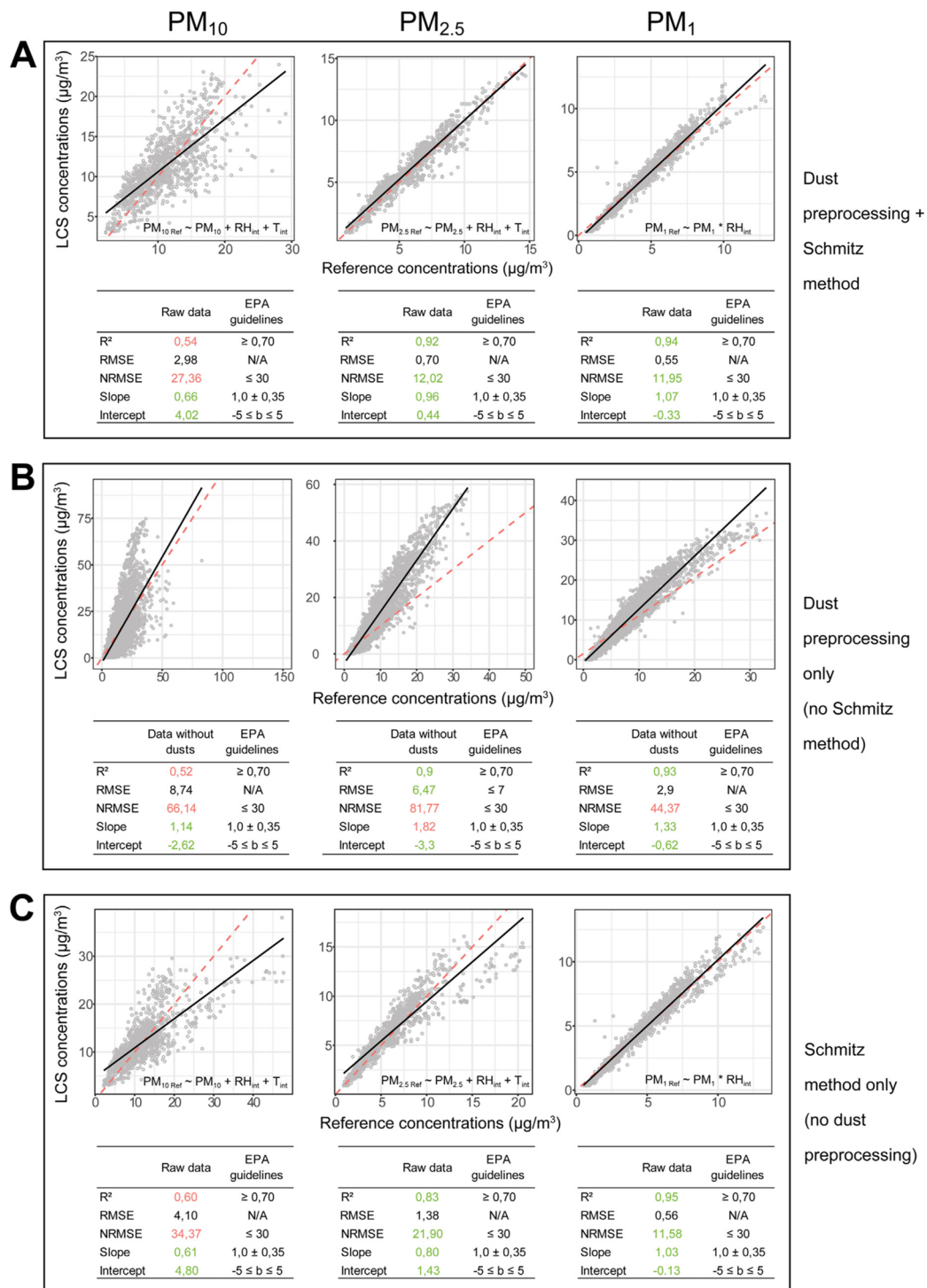


Fig. 7. Calibration performances: (A) complete method involving the Schmitz technique and dust event preprocessing, (B) with removal of dust events but without having yet applied the Schmitz method, (C) with the Schmitz method but without dust event removal. The green color indicates EPA compliant metrics, while red values denote non-EPA compliant metrics.

variables. There is an exception yet with WS playing an important role in the first retrieved RFR models for  $PM_{2.5}$  and  $PM_{10}$ . WS was implicated in many LCS studies (Báthory et al., 2021; Hua et al., 2021; Tian et al., 2022). Wind influence seems logical as official measurement stations of PM draw the air inside a pipe at a constant flow rate while the LCS air intake is subject to more variability. It would be interesting to place an anemometer close to the LCS for a more local measure of WS. It seems important to use RH when correcting LCS PM concentrations. Kosmopoulos et al. (2020) found the effects of RH and temperature to be negligible, but their study took place in the Eastern Mediterranean, where RH is smaller than in Grenoble and temperatures are warmer. Many studies concluded that involving RH and temperature can improve models (Badura et al., 2019; Magi et al., 2020). Moreover, RH and temperature might have synergistic effects on sensor performance (Wu et al., 2022a). A switch from LR to mechanistic regression involving  $RH_{int}$  and  $T_{int}$  led to a significant improvement in accuracy (13 % for  $PM_{2.5}$  and 38 % for  $PM_{10}$ ). This implies that temperature and humidity sensors should work properly. Maintenance on MaxDetect DHT22 devices should be considered, especially after 6 months. Another suggestion for improvement would be to replace MaxDetect DHT22 sensor with possibly more robust low-cost sensors like Bosch BME280 or Sensirion SHT85. Even if we did not find any evidence of a significant correlation between rainy days and MaxDetect DHT22 degradation, we could hypothesize that it was enhanced by an unusually humid 2021 summer (Météo-France, 2021). This was flagged during step 3, where out-of-bound points were found during the first two August weeks for  $RH_{int}$ ,  $T_{int}$ , and rain. In the case study conducted by Schmitz et al. on gas-phase pollutants, the most precise models for predicting  $NO_2$  or  $O_3$  concentrations on a longer experimental dataset involved  $T_{int}$ , while  $O_3$  models also included  $RH_{int}$  and ToD. These findings are consistent with our study, where we observed that internal parameters outperformed ambient parameters. However, ToD had no significant impact on our predictions. In their study, RFR was found to be the better predictor of gas concentrations, albeit only slightly, compared to MLR. Our results showed the same, except for  $PM_{10}$ , where RFR models performed substantially better than MLR.

Degradation over time did not seem to be an issue in this study, in consistency with the 15-month stability reported by Báthory et al. (2021). However, we recommend performing a degradation check because drift might be sensor dependent. It is also important to remind that all these calibration functions remain site-dependent because LCS performance depends on the site-specific PM source mixture (Malyan et al., 2023). We did not perform a validation across different sites, but we had a wide range of weather conditions covered during the 8 months experiment. We do not recommend to blindly transpose these formulas to other sites with different characteristics and aerosols compositions. The applicability of the models stays geographically limited but the Schmitz calibration protocol itself is available online (Schmitz et al., 2020) and can be applied to any location. We recommend coupling it with the aforementioned preprocessing and drift analysis steps (flowchart in Fig. 4, see brown boxes). Further research might explore Gaussian Mixture Regression (GMR) to further improve our methodology. This probabilistic technique handles well nonlinear relationships in non-identically distributed explanatory variables. GMR models already demonstrated better  $R^2$  and mean absolute error in comparison to MLR and RFR (McFarlane et al., 2021b).

## 5. Conclusion

Taken together, our results show that combining dust events preprocessing with the Schmitz approach can lead to highly accurate results for low-cost sensors measuring PM. Here this combined framework yielded excellent results for  $PM_{2.5}$  ( $R^2 = 0.92$ ,  $RMSE = 0.70 \mu g/m^3$ ,  $NRMSE = 12\%$ ) and performed even better for  $PM_{10}$  ( $R^2 = 0.94$ ,  $RMSE = 0.55 \mu g/m^3$ ,  $NRMSE = 12\%$ ), although the preprocessing step did not significantly improve  $PM_{10}$  results.  $PM_{10}$  could not be properly measured and calibrated due to the technical limitations of the PMS7003. This work represents a novel approach that has not been previously reported in the literature. It demonstrates that without dust events preprocessing,  $PM_{2.5}$  data may

comply with the EPA guidelines but fall short of achieving optimal accuracy. On the other hand, relying solely on dust events processing without using the Schmitz method would not be sufficient to meet the EPA target metrics. These findings underscore the importance of taking a holistic approach to PM data measurement, which involves integrating multiple techniques to achieve optimal accuracy and compliance with regulatory standards. Moving forward, it may be worthwhile to explore ways to calibrate PM measurements during dust events without discarding them from the dataset, as this could further improve the usefulness of LCS.

## Code availability

The code for the Schmitz methodology can be found in this open-access Zenodo repository: <https://doi.org/10.5281/zenodo.4317521> (Schmitz et al., 2020).

The code used to retrieve data from the Copernicus API can be found here:

<https://doi.org/10.5281/zenodo.7795898> (Aix et al., 2023).

## CRediT authorship contribution statement

**Marie-Laure Aix:** Conceptualization, Data curation, Formal analysis, Investigation, Software, Visualization, Writing – original draft. **Seán Schmitz:** Investigation, Methodology, Writing – review & editing, Validation. **Dominique J. Bicout:** Conceptualization, Formal analysis, Funding acquisition, Investigation, Methodology, Project administration, Supervision, Validation, Writing – review & editing.

## Data availability

Data will be made available on request.

## Declaration of competing interest

The authors declare that they have no known competing financial interests or personal relationships that could have appeared to influence the work reported in this paper.

## Acknowledgment

Marie-Laure Aix is a PhD student supported by a grant from the Ministry of Education and Research of France through the Ecole Doctorale Ingénierie pour la Santé, la Cognition et l'Environnement (ED-ISCE) of Grenoble Alpes University. This work has been partially supported by MIAI@Grenoble Alpes (ANR-19-P3IA-0003). We would like to warmly thank Atmo Auvergne Rhône-Alpes for their help and assistance in assembling and collocating the AQSS as part of our collaboration agreement. The dust results were generated using the Copernicus Atmosphere Monitoring Service Information [2021]. We also thank ROMMA for the local weather data.

## Appendix A. Supplementary data

Supplementary data to this article can be found online at <https://doi.org/10.1016/j.scitotenv.2023.164063>.

## References

- Adams, K., Greenbaum, D.S., Shaikh, R., van Erp, A.M., Russell, A.G., 2015. Particulate matter components, sources, and health: systematic approaches to testing effects. *J. Air Waste Manage. Assoc.* 65 (5), 544–558. <https://doi.org/10.1080/10962247.2014.1001884>.
- Aix, M.L., Schmitz, S., Bicout, D.J., 2023. Calibration Methodology of Low-Cost Sensors for High-Quality Monitoring of Fine Particulate Matter (1.0.0). Zenodo [code under embargoed Access] <https://doi.org/10.5281/zenodo.7795898>.
- Badura, M., Batog, P., Drzeniecka-Osiadacz, A., Modzel, P., 2019. Regression methods in the calibration of low-cost sensors for ambient particulate matter measurements. *SN Appl. Sci.* 1 (6), 622. <https://doi.org/10.1007/s42452-019-0630-1>.



- Barcelo-Ordinas, J.M., Doudou, M., Garcia-Vidal, J., Badache, N., 2019. Self-calibration methods for uncontrolled environments in sensor networks: a reference survey. *Ad Hoc Netw.* 88, 142–159. <https://doi.org/10.1016/j.adhoc.2019.01.008>.
- Barkjohn, K.K., Gantt, B., Clements, A.L., 2021. Development and application of a United States wide correction for PM<sub>2.5</sub> data collected with the PurpleAir sensor. *Atmos. Meas. Tech.* 4 (6), 4617–4637. <https://doi.org/10.5194/amt-14-4617-2021>.
- Báthory, C., Dobo, Z., Garami, A., Palotas, A., Toth, P., 2021. Low-cost monitoring of atmospheric PM-development and testing. *J. Environ. Manag.* 304, 114158. <https://doi.org/10.1016/j.jenvman.2021.114158>.
- Bauerová, P., Šindelářová, A., Rychlík, Š., Novák, Z., Keder, J., 2020. Low-cost air quality sensors: one-year field comparative measurement of different gas sensors and particle counters with reference monitors at Tušimice observatory. *Atmosphere (Basel)* 11 (5), 492. <https://doi.org/10.3390/atmos11050492>.
- Bi, J., Wildani, A., Chang, H.H., Liu, Y., 2020. Incorporating low-cost sensor measurements into high-resolution PM<sub>2.5</sub> modeling at a large spatial scale. *Environ. Sci. Technol.* 54 (4), 2152–2162. <https://doi.org/10.1021/acs.est.9b06046>.
- Chakraborty, R., Heydon, J., Mayfield, M., Mihaylova, L., 2020. Indoor air pollution from residential stoves: examining the flooding of particulate matter into homes during real-world use. *Atmosphere (Basel)* 11 (12), 1326. <https://doi.org/10.3390/atmos11121326>.
- Chojer, H., Branco, P.T.B.S., Martins, F.G., Alvim-Ferraz, M.C.M., Sousa, S.I.V., 2022. Can data reliability of low-cost sensor devices for indoor air particulate matter monitoring be improved? – an approach using machine learning. *Atmos. Environ.* 286. <https://doi.org/10.1016/j.atmosenv.2022.119251>.
- Crilly, L.R., Singh, A., Kramer, L.J., Shaw, M.D., Alam, M.S., Apte, J.S., Bloss, W.J., Hildebrandt Ruiz, L., Fu, P., Fu, W., Gani, S., Gatari, M., Ilyinskaya, E., Lewis, A.C., Ng'ang'a, D., Sun, Y., Whitty, R.C.W., Yue, S., Young, S., Pope, F.D., 2020. Effect of aerosol composition on the performance of low-cost optical particle counter correction factors. *Atmos. Meas. Tech.* 13 (3), 1181–1193. <https://doi.org/10.5194/amt-13-1181-2020>.
- Danesh Yazdi, M., Wang, Y., Di, Q., Requia, W.J., Wei, Y., Shi, L., Sabath, M.B., Dominici, F., Coull, B., Evans, J.S., Koutrakis, P., Schwartz, J.D., 2021. Long-term effect of exposure to lower concentrations of air pollution on mortality among US Medicare participants and vulnerable subgroups: a doubly-robust approach. *Lancet Planet. Health* 5 (10), e689–e697. [https://doi.org/10.1016/S2542-5196\(21\)00204-7](https://doi.org/10.1016/S2542-5196(21)00204-7).
- deSouza, P., Kahn, R.A., Limbacher, J.A., Marais, E.A., Duarte, F., Ratti, C., 2020. Combining low-cost, surface-based aerosol monitors with size-resolved satellite data for air quality applications. *Atmos. Meas. Tech.* 13 (10), 5319–5334. <https://doi.org/10.5194/amt-13-5319-2020>.
- deSouza, P., Barkjohn, K., Clements, A., Lee, J., Kahn, R., Crawford, B., Kinney, P., 2023a. An analysis of degradation in low-cost particulate matter sensors. *Environ. Sci. Atmos.* 3 (3), 521–536. <https://doi.org/10.1039/d2ea00142j>.
- deSouza, P., Wang, A., Machida, Y., Duhl, T., Mora, S., Kumar, P., Kahn, R., Ratti, C., Durant, J.L., Hudda, N., 2023b. Evaluating the Performance of Low-Cost PM<sub>2.5</sub> Sensors in Mobile Settings. *arXiv preprint* <https://doi.org/10.48550/arXiv.2301.03847>.
- Di Antonio, A., Popoola, O.A.M., Ouyang, B., Saffell, J., Jones, R.L., 2018. Developing a relative humidity correction for low-cost sensors measuring ambient particulate matter. *Sensors (Basel)* 18 (9), 2790. <https://doi.org/10.3390/s18092790>.
- Di Mauro, B., Garzonio, R., Rossini, M., Filippa, G., Pogliotti, P., Galvagno, M., Morra di Cella, U., Migliavacca, M., Baccolo, G., Clemenza, M., Delmonte, B., Maggi, V., Dumont, M., Tuzet, F., Lafayse, M., Morin, S., Cremonese, E., Colombo, R., 2019. Saharan dust events in the European Alps: role in snowmelt and geochemical characterization. *Cryosphere* 13 (4), 1147–1165. <https://doi.org/10.5194/tc-13-1147-2019>.
- Duvall, R., Clements, A., Hagler, G., Kamal, A., Vasu Kilaru, L., Goodman, S., Frederick, K., Johnson, Barkjohn, I., VonWald, D., Greene, Dye, T., 2021. Performance Testing Protocols, Metrics, and Target Values for Fine Particulate Matter Air Sensors: Use in Ambient, Outdoor, Fixed Site, Non-Regulatory Supplemental and Informational Monitoring Applications. EPA/600/R-20/280. U.S. Environmental Protection Agency, Office of Research and Development, Washington, DC, USA. [https://cfpub.epa.gov/si/si\\_public\\_record\\_Report.cfm?dirEntryId=350785&Lab=CEMM](https://cfpub.epa.gov/si/si_public_record_Report.cfm?dirEntryId=350785&Lab=CEMM) (accessed 2023.01.23).
- Duyzer, J., van den Hout, D., Zandveld, P., van Ratingen, S., 2015. Representativeness of air quality monitoring networks. *Atmos. Environ.* 104, 88–101. <https://doi.org/10.1016/j.atmosenv.2014.12.067>.
- European Environment Agency, 2020. Air Quality in Europe - 2020 Report, EEA Report No 09/2020. <https://www.eea.europa.eu/publications/air-quality-in-europe-2020-report> (accessed 2023.01.23).
- Fishbain, B., Lerner, U., Castell, N., Cole-Hunter, T., Popoola, O., Broday, D.M., Iñiguez, T.M., Nieuwenhuijsen, M., Jovasevic-Stojanovic, M., Topalovic, D., Jones, R.L., Galea, K.S., Etzion, Y., Kizel, F., Golumbic, Y.N., Baram-Tsabari, A., Yacobi, T., Draher, D., Robinson, J.A., Kocman, D., Horvat, M., Svevova, V., Arpaci, A., Bartonova, A., 2017. An evaluation tool kit of air quality micro-sensing units. *Sci. Total Environ.* 575, 639–648. <https://doi.org/10.1016/j.scitotenv.2016.09.061>.
- Fuller, R., Landrigan, P.J., Balakrishnan, K.,athan, G., Bose-O'Reilly, S., Brauer, M., Caravanos, J., Chiles, T., Cohen, A., Corra, L., Cropper, M., Ferraro, G., Hanna, J., Hanrahan, D., Hu, H., Hunter, D., Janata, G., Kupka, R., Lanphear, B., Lichtveld, M., Martin, K., Mustapha, A., Sanchez-Triana, E., Sandilya, K., Schaeffli, L., Shaw, J., Seddon, J., Suk, W., Téllez-Rojo, M.M., Yan, C., 2022. Pollution and health: a progress update. *Lancet Planet. Health* 6 (6), e535–e547. [https://doi.org/10.1016/S2542-5196\(22\)00090-0](https://doi.org/10.1016/S2542-5196(22)00090-0).
- Giordano, M.R., Malings, C., Pandis, S.N., Presto, A.A., McNeill, V.F., Westervelt, D.M., Beekmann, M., Subramanian, R., 2021. From low-cost sensors to high-quality data: a summary of challenges and best practices for effectively calibrating low-cost particulate matter mass sensors. *J. Aerosol Sci.* 158, 105833. <https://doi.org/10.1016/j.jaerosci.2021.105833>.
- Hong, G.-H., Le, T.-C., Tu, J.-W., Wang, C., Chang, S.-C., Yu, J.-Y., Lin, G.-Y., Aggarwal, S.G., Tsai, C.-J., 2021. Long-term evaluation and calibration of three types of low-cost PM<sub>2.5</sub> sensors at different air quality monitoring stations. *J. Aerosol Sci.* 157. <https://doi.org/10.1016/j.jaerosci.2021.105829>.
- Hua, J., Zhang, Y., de Foy, B., Mei, X., Shang, J., Zhang, Y., Sulaymon, I.D., Zhou, D., 2021. Improved PM<sub>2.5</sub> concentration estimates from low-cost sensors using calibration models categorized by relative humidity. *Aerosol Sci. Technol.* 55 (5), 600–613. <https://doi.org/10.1080/02786826.2021.1873911>.
- Jiang, Y., Zhu, X., Chen, C., Ge, Y., Wang, W., Zhao, Z., Cai, J., Kan, H., 2021. On-field test and data calibration of a low-cost sensor for fine particles exposure assessment. *Ecotoxicol. Environ. Saf.* 211, 111958. <https://doi.org/10.1016/j.ecoenv.2021.111958>.
- Kang, Y., Aye, L., Ngo, T.D., Zhou, J., 2021. Performance evaluation of low-cost air quality sensors: a review. *Sci. Total Environ.* 818, 151769. <https://doi.org/10.1016/j.scitotenv.2021.151769>.
- Kelly, K.E., Whitaker, J., Petty, A., Widmer, C., Dybwad, A., Sleeth, D., Martin, R., Butterfield, A., 2017. Ambient and laboratory evaluation of a low-cost particulate matter sensor. *Environ. Pollut.* 221, 491–500. <https://doi.org/10.1016/j.envpol.2016.12.039>.
- Kelly, K.E., Xing, W.W., Sayahi, T., Mitchell, L., Becnel, T., Gaillardon, P.E., Meyer, M., Whitaker, R.T., 2021. Community-based measurements reveal unseen differences during air pollution episodes. *Environ. Sci. Technol.* 55 (1), 120–128. <https://doi.org/10.1021/acs.est.0c02341>.
- Kosmopoulos, G., Salamalikis, V., Pandis, S.N., Yannopoulos, P., Bloutsos, A.A., Kazantzidis, A., 2020. Low-cost sensors for measuring airborne particulate matter: field evaluation and calibration at a South-Eastern European site. *Sci. Total Environ.* 748, 141396. <https://doi.org/10.1016/j.scitotenv.2020.141396>.
- Kumar, V., Sahu, M., 2021. Evaluation of nine machine learning regression algorithms for calibration of low-cost PM<sub>2.5</sub> sensor. *J. Aerosol Sci.* 157, 105809. <https://doi.org/10.1016/j.jaerosci.2021.105809>.
- Kuula, J., Mäkelä, T., Aurela, M., Teinilä, K., Varjonen, S., González, Ó., Timonen, H., 2020. Laboratory evaluation of particle-size selectivity of optical low-cost particulate matter sensors. *Atmos. Meas. Tech.* 13 (5), 2413–2423. <https://doi.org/10.5194/amt-13-2413-2020>.
- Languille, B., Gros, V., Bonnaire, N., Pommier, C., Honoré, C., Debort, C., Gauvin, L., Srairi, S., Annesi-Maesano, I., Chaix, B., Zeitouni, K., 2020. A methodology for the characterization of portable sensors for air quality measurements with the goal of deployment in citizen science. *Sci. Total Environ.* 708, 134698. <https://doi.org/10.1016/j.scitotenv.2019.134698>.
- LCSQA, 2017. Conformité technique des appareils de mesure pour la surveillance des polluants réglementaires – bilan 2016. <https://www.lcsqa.org/fr/rapport/2016/ineris-imit-ld/conformite-technique-appareils-mesure-surveillance-polluants-reglementaire> (accessed 2023.03.19).
- LCSQA, 2020. Suivi de l'adéquation des analyseurs automatiques de PM à la méthode de référence: bilan réglementaire 2016–2019 et synthèse des travaux menés depuis 2013. <https://www.lcsqa.org/fr/rapport/suivi-de-ladequation-des-analyseurs-automatiques-de-pm-la-methode-de-reference-bilan> (accessed 2023.03.19).
- Li, M.-F., Tang, X.-P., Wu, W., Liu, H.-B., 2013. General models for estimating daily global solar radiation for different solar radiation zones in mainland China. *Energy Convers. Manag.* 70, 139–148. <https://doi.org/10.1016/j.enconman.2013.03.004>.
- Loomis, D., Grosse, Y., Lauby-Secretan, B., Ghisassi, F.E., Bouvard, V., Benbrahim-Tallaa, L., Guha, N., Baan, R., Mattock, H., Straif, K., 2013. The carcinogenicity of outdoor air pollution. *Lancet Oncol.* 14 (13), 1262–1263. [https://doi.org/10.1016/S1470-2045\(13\)70487-X](https://doi.org/10.1016/S1470-2045(13)70487-X).
- Lua, Y., Giuliano, G., Habre, R., 2021. Estimating hourly PM<sub>2.5</sub> concentrations at the neighborhood scale using a low-cost air sensor network: a Los Angeles case study. *Environ. Res.* 195, 110653. <https://doi.org/10.1016/j.envres.2020.110653>.
- Magi, B.I., Cupini, C., Francis, J., Green, M., Hauser, C., 2020. Evaluation of PM<sub>2.5</sub> measured in an urban setting using a low-cost optical particle counter and a Federal Equivalent Method Beta Attenuation Monitor. *Aerosol Sci. Technol.* 54 (2), 147–159. <https://doi.org/10.1080/02786826.2019.1619915>.
- Malings, C., Tanzer, R., Hauriyluk, A., Saha, P.K., Robinson, A.L., Presto, A.A., Subramanian, R., 2020. Fine particle mass monitoring with low-cost sensors: corrections and long-term performance evaluation. *Aerosol Sci. Technol.* 54 (2), 160–174. <https://doi.org/10.1080/02786826.2019.1623863>.
- Malyan, V., Kumar, V., Sahu, M., 2023. Significance of sources and size distribution on calibration of low-cost particle sensors: evidence from a field sampling campaign. *J. Aerosol Sci.* 168, 106114. <https://doi.org/10.1016/j.jaerosci.2022.106114>.
- McFarlane, C., Isevalambire, P.K., Lumbuenamo, R.S., Ndinga, A.M.E., Dhammapala, R., Jin, X., McNeill, V.F., Malings, C., Subramanian, R., Westervelt, D.M., 2021a. First measurements of ambient PM<sub>2.5</sub> in Kinshasa, Democratic Republic of Congo and Brazzaville, Republic of Congo using field-calibrated low-cost sensors. *Aerosol Air Qual. Res.* 21, 200619. <https://doi.org/10.4209/aaqr.200619>.
- McFarlane, C., Raheja, G., Malings, C., Appoh, E.K.E., Hughes, A.F., Westervelt, D.M., 2021b. Application of Gaussian mixture regression for the correction of low cost PM<sub>2.5</sub> monitoring data in Accra, Ghana. *ACS Earth Space Chem.* 5 (9), 2268–2279. <https://doi.org/10.1021/acsearthspacechem.1c00217>.
- Météo-France, 2021. Un été 2021 assez maussade. <https://meteofrance.com/actualites-et-dossiers/actualites/un-ete-2021-assez-maussade> (accessed 2023.01.23).
- Météo-France, Institut National de l'Environnement Industriel et des Risques (Ineris), Aarhus University, Norwegian Meteorological Institute (MET Norway), Jülich Institut für Energie- und Klimaforschung (IEK), Institute of Environmental Protection – National Research Institute (IEP-NRI), Koninklijk Nederlands Meteorologisch Instituut (KNMI), Nederlandse Organisatie voor toepast-natuurwetenschappelijk onderzoek (TNO), Swedish Meteorological and Hydrological Institute (SMHI), Finnish Meteorological Institute (FMI), 2020. CAMS European air quality forecasts, ENSEMBLE data. Copernicus Atmosphere Monitoring Service (CAMS) Atmosphere Data Store (ADS) <https://ads.atmosphere.copernicus.eu/cdsapp#!/dataset/cams-europe-air-quality-forecasts?tab=overview> (accessed 2023.01.23).
- Molina Rueda, E., Carter, E., L'Orange, C., Quinn, C., Volkens, J., 2023. Size-resolved field performance of low-cost sensors for particulate matter air pollution. *Environ. Sci. Technol. Lett.* <https://doi.org/10.1021/acs.estlett.3c00030>.

- Mousavi, A., Wu, J., 2021. Indoor-generated PM<sub>2.5</sub> during COVID-19 shutdowns across California: application of the PurpleAir indoor-outdoor low-cost sensor network. *Environ. Sci. Technol.* 55 (9), 5648–5656. <https://doi.org/10.1021/acs.est.0c06937>.
- Noble, C.A., Vanderpool, R.W., Peters, T.M., McElroy, F.F., Gemmill, D.B., Wiener, R.W., 2001. Federal reference and equivalent methods for measuring fine particulate matter. *Aerosol Sci. Technol.* 34 (5), 457–464. <https://doi.org/10.1080/02786820121582>.
- Nowack, P., Konstantinovskiy, L., Gardiner, H., Cant, J., 2021. Machine learning calibration of low-cost NO<sub>2</sub> and PM<sub>10</sub> sensors: non-linear algorithms and their impact on site transferability. *Atmos. Meas. Tech.* 14 (8), 5637–5655. <https://doi.org/10.5194/amt-14-5637-2021>.
- Palas GmbH, 2020. Fidas® 200 S technical datasheet. <https://www.palas.de/en/product/download/fidas200s/datasheet/pdf> (accessed 2023.03.19).
- Patra, S.S., Ramsisaria, R., Du, R., Wu, T., Boor, B.E., 2021. A machine learning field calibration method for improving the performance of low-cost particle sensors. *Build. Environ.* 190, 107457. <https://doi.org/10.1016/j.buildenv.2020.107457>.
- Plantower, 2016. PMS7003 technical datasheet. [https://www.plantower.com/en/products\\_33/76.html](https://www.plantower.com/en/products_33/76.html).
- Puttaswamy, N., Sreekanth, V., Pillariseti, A., Upadhyaya, A.R., Saidam, S., Veerappan, B., Mukhopadhyay, K., Sambandam, S., Sutaria, R., Balakrishnan, K., 2022. Indoor and ambient air pollution in Chennai, India during COVID-19 lockdown: an affordable sensors study. *Aerosol Air Qual. Res.* 22 (1), 210170. <https://doi.org/10.4209/aaqr.210170>.
- R Core Team, 2022. R: A Language and Environment for Statistical Computing. R Foundation for Statistical Computing, Vienna, Austria. <https://www.R-project.org/> (accessed 2023.01.23).
- Raheja, G., Sabi, K., Sonla, H., Gbedjangni, E.K., McFarlane, C.M., Hodoli, C.G., Westervelt, D.M., 2022. A network of field-calibrated low-cost sensor measurements of PM<sub>2.5</sub> in Lomé, Togo, over one to two years. *ACS Earth Space Chem.* 6 (4), 1011–1021. <https://doi.org/10.1021/acsearthspacechem.1c00391>.
- Rai, P.K., 2016. Impacts of particulate matter pollution on plants: implications for environmental biomonitoring. *Ecotoxicol. Environ. Saf.* 129, 120–136. <https://doi.org/10.1016/j.ecoenv.2016.03.012>.
- Réseau d'Observation Météo du Massif Alpin, 2022. Données Station de Saint-Martin-d'Hères [Members dataset]. <https://romma.fr/> (accessed 2023.01.23).
- Sayahi, T., Butterfield, A., Kelly, K.E., 2019. Long-term field evaluation of the Plantower PMS low-cost particulate matter sensors. *Environ. Pollut.* 245, 932–940. <https://doi.org/10.1016/j.envpol.2018.11.065>.
- Schmitz, S., Towers, S., Villena, G., Caseiro, A., Wegener, R., Klemp, D., Langer, I., Meier, F., Von Schneidmesser, E., 2020. Unraveling a Black Box: An Open-source Methodology for the Field Calibration of Small Air Quality Sensors (1.0.0). Zenodo [code] <https://doi.org/10.5281/zenodo.4317521>.
- Schmitz, S., Towers, S., Villena, G., Caseiro, A., Wegener, R., Klemp, D., Langer, I., Meier, F., Von Schneidmesser, E., 2021. Unravelling a black box: an open-source methodology for the field calibration of small air quality sensors. *Atmos. Meas. Tech.* 4, 7221–7241. <https://doi.org/10.5194/amt-2020-489>.
- Smith, K.R., Edwards, P.M., Evans, M.J., Lee, J.D., Shaw, M.D., Squires, F., Wilde, S., Lewis, A.C., 2017. Clustering approaches to improve the performance of low cost air pollution sensors. *Faraday Discuss.* 200, 621–637. <https://doi.org/10.1039/c7fd00020k>.
- Smith, K.R., Edwards, P.M., Ivatt, P.D., Lee, J.D., Squires, F., Dai, C., Peltier, R.E., Evans, M.J., Sun, Y., Lewis, A.C., 2019. An improved low-power measurement of ambient NO<sub>2</sub> and O<sub>3</sub> combining electrochemical sensor clusters and machine learning. *Atmos. Meas. Tech.* 12 (2), 1325–1336. <https://doi.org/10.5194/amt-12-1325-2019>.
- Stavroulas, I., Grivas, G., Michalopoulos, P., Liakakou, E., Bougiatioti, A., Kalkavouras, P., Famelí, K., Hatzianastassiou, N., Mihalopoulos, N., Gerasopoulos, E., 2020. Field evaluation of low-cost PM sensors (purple air PA-II) under variable urban air quality conditions, in Greece. *Atmosphere* 11 (9). <https://doi.org/10.3390/atmos11090926>.
- Streibl, N., 2017. Influence of Humidity on the Accuracy of Low-Cost Particulate Matter Sensors. Technical report. [https://www.researchgate.net/publication/320474792\\_Influence\\_of\\_Humidity\\_on\\_the\\_Accuracy\\_of\\_Low-Cost\\_Part particulate\\_Matter\\_Sensors?channel=doi&linkId=59e7ad15aca272bc423d0b97&showFulltext=true](https://www.researchgate.net/publication/320474792_Influence_of_Humidity_on_the_Accuracy_of_Low-Cost_Part particulate_Matter_Sensors?channel=doi&linkId=59e7ad15aca272bc423d0b97&showFulltext=true) (accessed 2023.01.23). <https://doi.org/10.13140/RG.2.2.21095.75683>.
- Tian, Y., deSouza, P., Mora, S., Yao, X., Duarte, F., Norford, L.K., Lin, H., Ratti, C., 2022. Evaluating the meteorological effects on the urban form-air quality relationship using mobile monitoring. *Environ. Sci. Technol.* 56 (11), 7328–7336. <https://doi.org/10.1021/acs.est.1c04854>.
- Valavanidis, A., Fiotakis, K., Vlachogianni, T., 2008. Airborne particulate matter and human health: toxicological assessment and importance of size and composition of particles for oxidative damage and carcinogenic mechanisms. *J. Environ. Sci. Health C Environ. Carcinog. Ecotoxicol. Rev.* 26 (4), 339–362. <https://doi.org/10.1080/10590500802494538>.
- Vogt, M., Schneider, P., Castell, N., Hamer, P., 2021. Assessment of low-cost particulate matter sensor systems against optical and gravimetric methods in a field co-location in Norway. *Atmosphere (Basel)* 12 (8), 961. <https://doi.org/10.3390/atmos12080961>.
- Wallace, L., Hopke, P.K., 2022. Measuring particle concentrations and composition in indoor air. In: Zhang, Y., Hopke, P.K., Mandin, C. (Eds.), *Handbook of Indoor Air Quality*. Springer Nature Singapore, Singapore, pp. 517–567. [https://doi.org/10.1007/978-981-16-7680-2\\_19](https://doi.org/10.1007/978-981-16-7680-2_19).
- Wang, Y., Li, J., Jing, H., Zhang, Q., Jiang, J., Biswas, P., 2015. Laboratory evaluation and calibration of three low-cost particle sensors for particulate matter measurement. *Aerosol Sci. Technol.* 49 (11), 1063–1077. <https://doi.org/10.1080/02786826.2015.1100710>.
- World Health Organization, 2021. WHO global air quality guidelines: particulate matter (PM<sub>2.5</sub> and PM<sub>10</sub>), ozone, nitrogen dioxide, sulfur dioxide and carbon monoxide. <https://apps.who.int/iris/handle/10665/345329> (accessed 2023.01.23).
- Wu, D., Zhang, G., Liu, J., Shen, S., Yang, Z., Pan, Y., Zhao, X., Yang, S., Tian, Y., Zhao, H., Li, J., Cai, L., 2022a. Influence of particle properties and environmental factors on the performance of typical particle monitors and low-cost particle sensors in the market of China. *Atmos. Environ.* 268, 118825. <https://doi.org/10.1016/j.atmosenv.2021.118825>.
- Wu, H., Zhang, B., Wei, J., Lu, Z., Zhao, M., Liu, W., Bovet, P., Guo, X., Xi, B., 2022b. Short-term effects of exposure to ambient PM<sub>1</sub>, PM<sub>2.5</sub>, and PM<sub>10</sub> on ischemic and hemorrhagic stroke incidence in Shandong Province, China. *Environ. Res.* 212 (Pt C), 113350. <https://doi.org/10.1016/j.envres.2022.113350>.
- Zhang, Y., Ding, Z., Xiang, Q., Wang, W., Huang, L., Mao, F., 2020a. Short-term effects of ambient PM<sub>1</sub> and PM<sub>2.5</sub> air pollution on hospital admission for respiratory diseases: case-crossover evidence from Shenzhen, China. *Int. J. Hyg. Environ. Health* 224, 113418. <https://doi.org/10.1016/j.ijheh.2019.11.001>.
- Zhang, Y., Fang, J., Mao, F., Ding, Z., Xiang, Q., Wang, W., 2020b. Age- and season-specific effects of ambient particles (PM<sub>1</sub>, PM<sub>2.5</sub>, and PM<sub>10</sub>) on daily emergency department visits among two Chinese metropolitan populations. *Chemosphere* 246, 125723. <https://doi.org/10.1016/j.chemosphere.2019.125723>.
- Zimmerman, N., 2022. Tutorial: guidelines for implementing low-cost sensor networks for aerosol monitoring. *J. Aerosol Sci.* 159, 105872. <https://doi.org/10.1016/j.jaerosci.2021.105872>.

## Supporting information of

# Calibration methodology of low-cost sensors for high-quality monitoring of fine particulate matter

*Marie-Laure Aix<sup>a</sup>, Seán Schmitz<sup>b</sup>, Dominique J. Bicout<sup>c,\*</sup>*

<sup>a</sup> Univ. Grenoble Alpes, CNRS, UMR 5525, VetAgro Sup, Grenoble INP, TIMC, 38000 Grenoble, France, [marie-laure.aix@univ-grenoble-alpes.fr](mailto:marie-laure.aix@univ-grenoble-alpes.fr)

<sup>b</sup> Institute for Advanced Sustainability Studies e. V. (IASS), Berliner Strasse 130, 14467 Potsdam, Germany, [Sean.Schmitz@iass-potsdam.de](mailto:Sean.Schmitz@iass-potsdam.de)

<sup>c</sup> Univ. Grenoble Alpes, CNRS, UMR 5525, VetAgro Sup, Grenoble INP, TIMC, 38000 Grenoble, France, [dominique.bicout@univ-grenoble-alpes.fr](mailto:dominique.bicout@univ-grenoble-alpes.fr)

\* Corresponding author at : Laboratoire TIMC, Domaine de la Merci, 38706 La Tronche – France

E-mail address: [dominique.bicout@univ-grenoble-alpes.fr](mailto:dominique.bicout@univ-grenoble-alpes.fr)



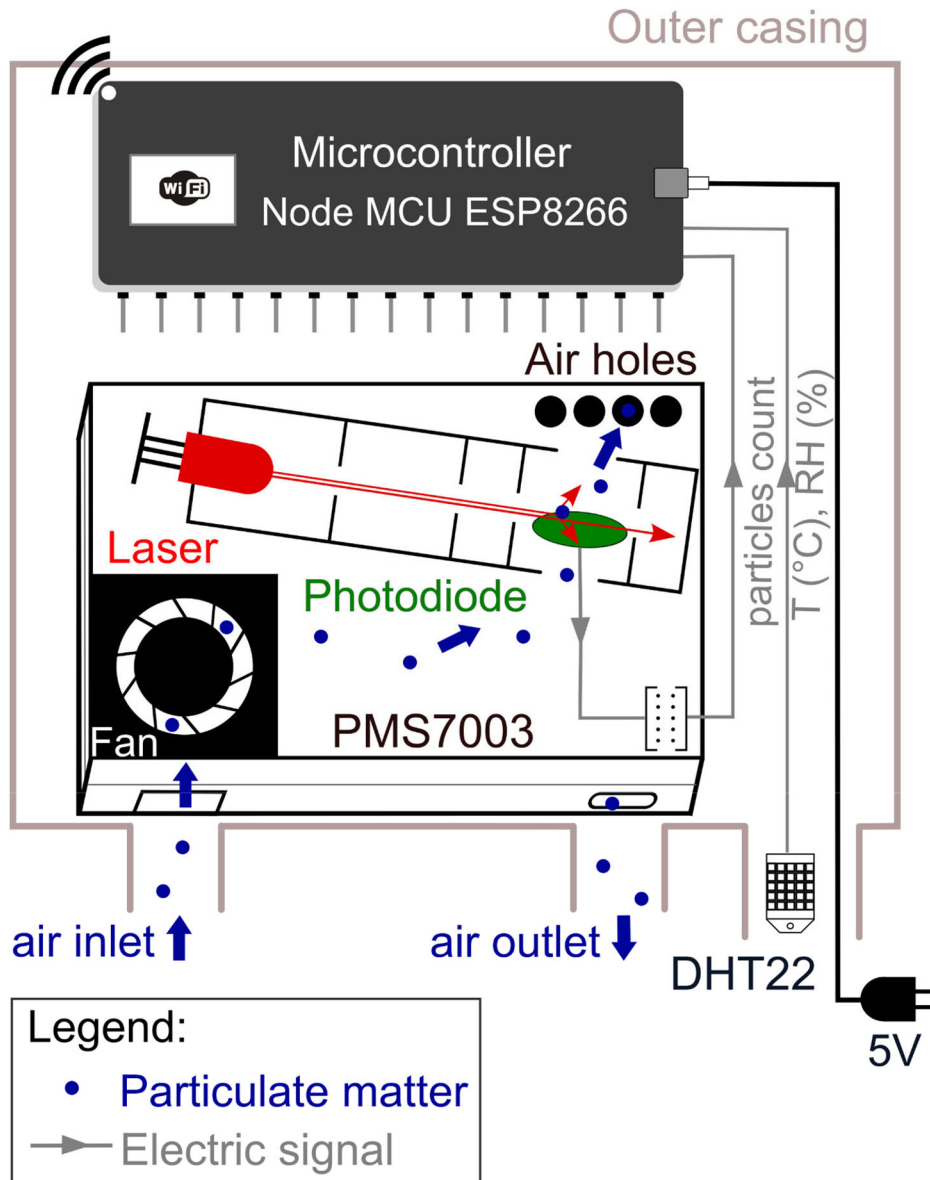


Figure S1. Air quality station schematic description.

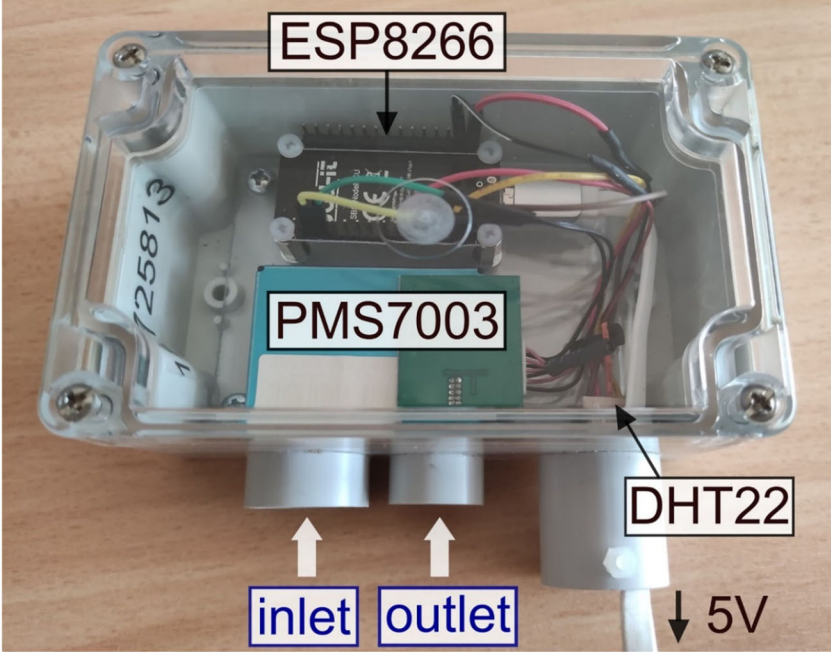
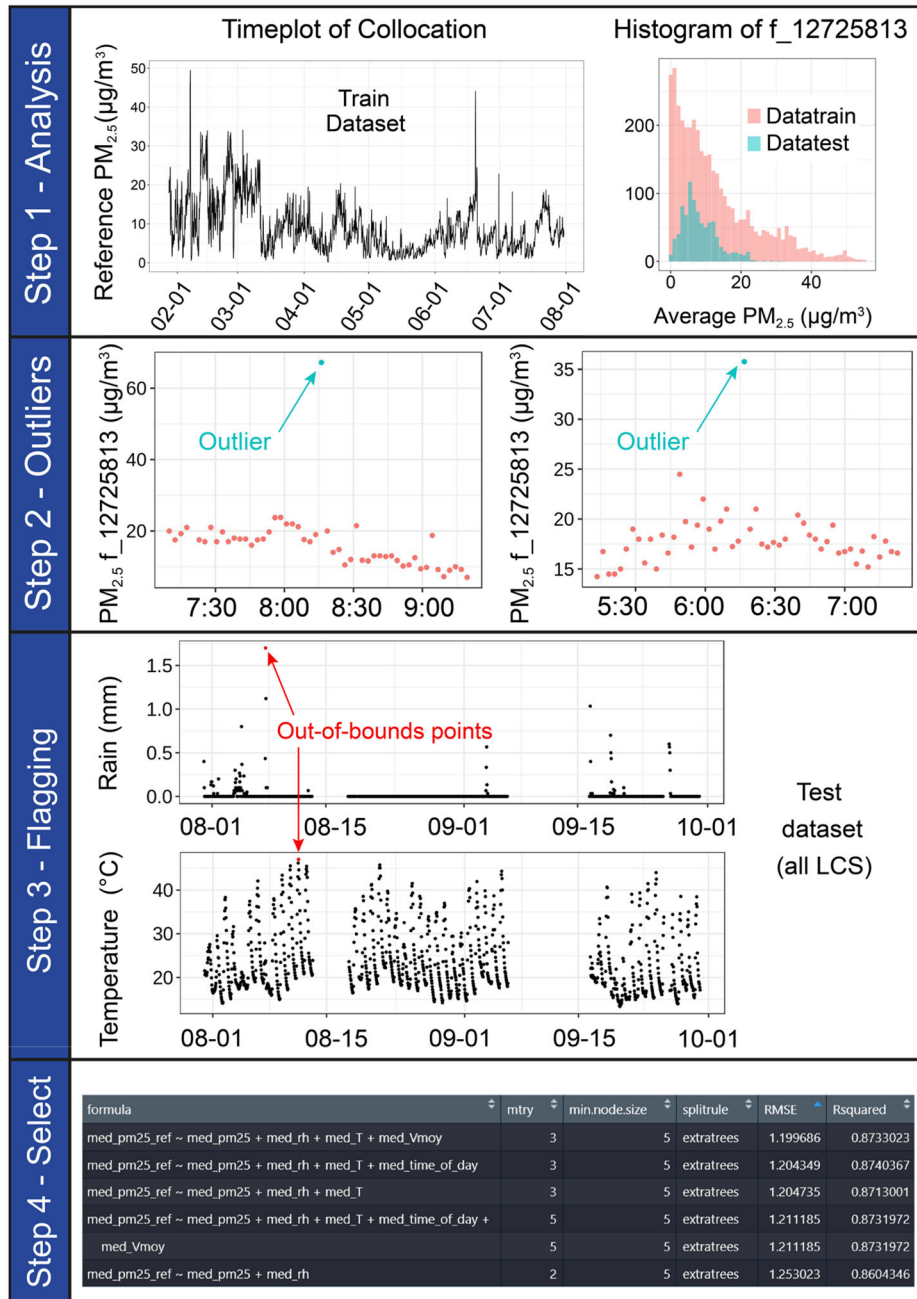
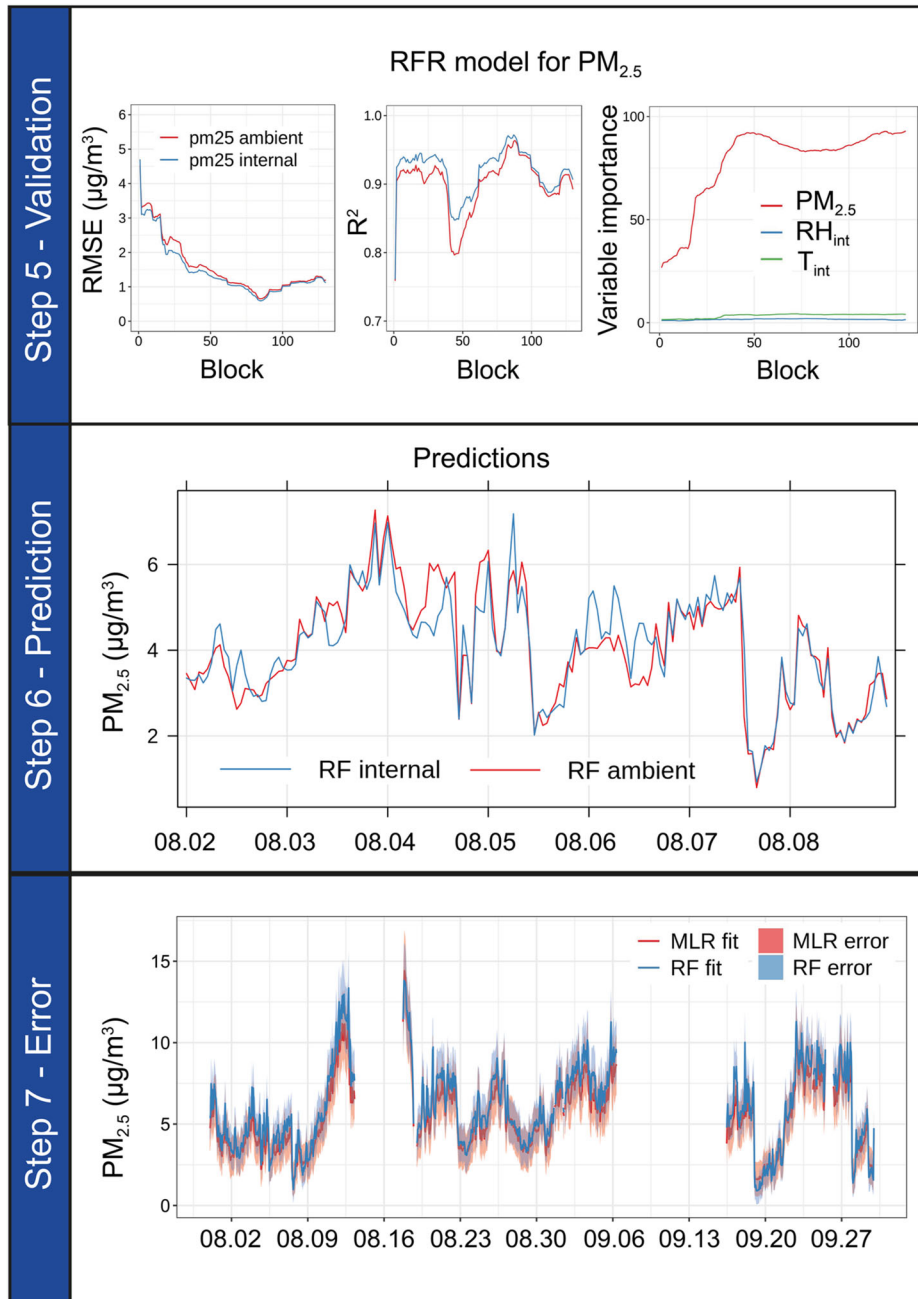


Figure S2. Air quality station picture.



**Figure S3.** Seven-step protocol outputs examples (steps 1 to 4) (f\_12725813: identification number of one LCS)



**Figure S4.** Seven-step protocol outputs examples (steps 5 to 7) (f\_12725813: identification number of one LCS)

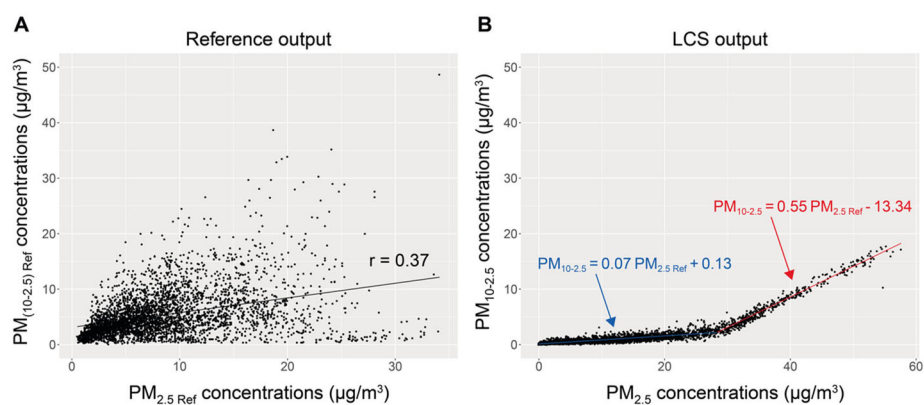


**Figure S5.** (A) Scatterplot of  $PM_{(10-2.5)\text{ Ref}}$  and  $PM_{2.5\text{ Ref}}$  on the train dataset.  $r$  is the Pearson correlation coefficient between  $PM_{(10-2.5)\text{ Ref}}$  and  $PM_{2.5\text{ Ref}}$ . (B) Scatterplot of  $PM_{10-2.5}$  and  $PM_{2.5}$  on the train dataset. The linear equations of the two best-fitting regression lines are shown.

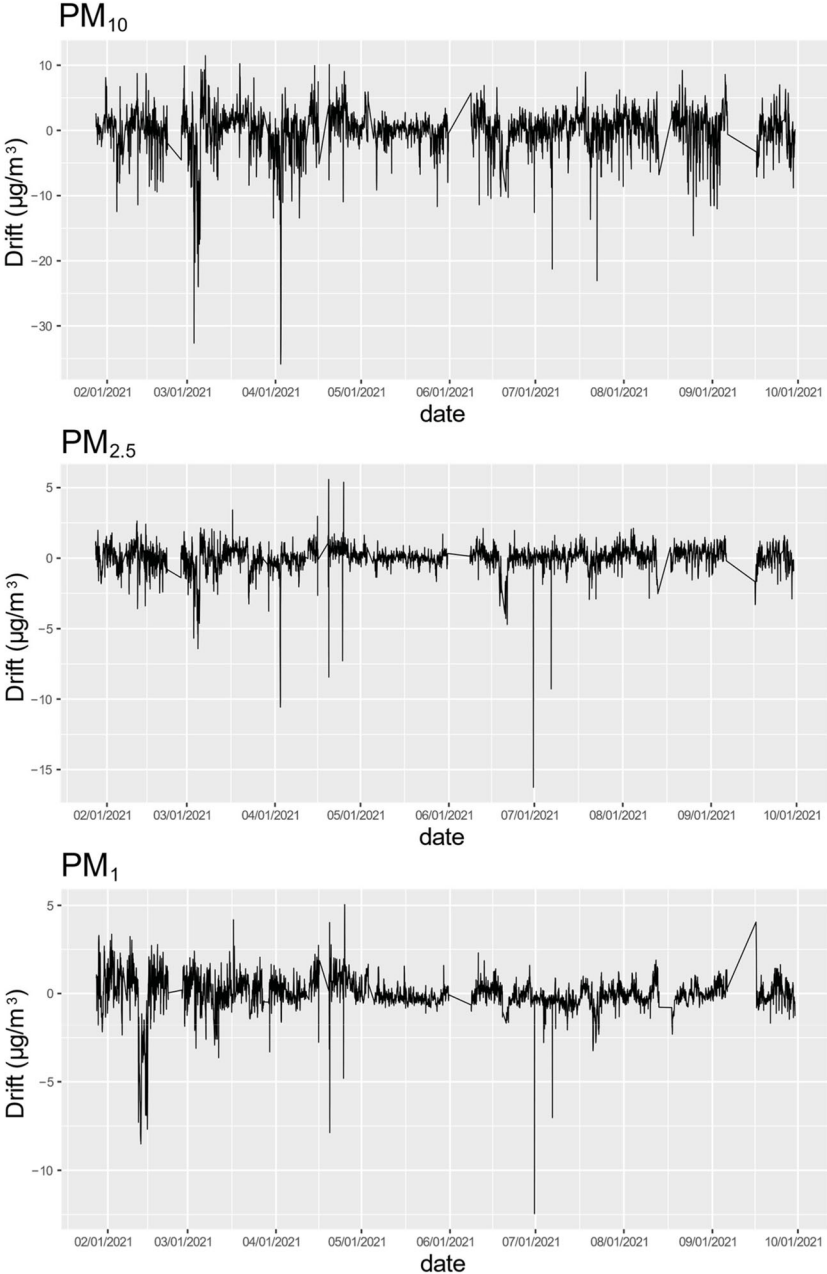


**Figure S6.** Drift evaluation: difference between the corrected LCS median measurements (given by the best regression models) and the corresponding hourly reference measurements.

**Table S1.** List of tested calibration formulas (as entered in RStudio) for Multiple Linear Regression using LCS temperature and relative humidity.

Formula
$PM_{1\ Ref} \sim PM_1 * RH_{int} * T_{int} * ToD * WS$
$PM_{1\ Ref} \sim PM_1 * RH_{int} * T_{int} * ToD$
$PM_{1\ Ref} \sim PM_1 * RH_{int} * T_{int} * WS$
$PM_{1\ Ref} \sim PM_1 * RH_{int} * T_{int}$
$PM_{1\ Ref} \sim PM_1 * RH_{int}$
$PM_{1\ Ref} \sim PM_1$
$PM_{1\ Ref} \sim PM_1 * RH_{int} * I(1 / RH_{int}) * ToD * WS$
$PM_{1\ Ref} \sim PM_1 * T_{int} * I(1 / RH_{int}) * ToD$
$PM_{1\ Ref} \sim PM_1 * T_{int} * I(1 / RH_{int}) * WS$
$PM_{1\ Ref} \sim PM_1 * T_{int} * I(1 / RH_{int})$
$PM_{1\ Ref} \sim PM_1 + RH_{int} + T_{int} + ToD + WS$
$PM_{1\ Ref} \sim PM_1 + RH_{int} + T_{int} + ToD$
$PM_{1\ Ref} \sim PM_1 + RH_{int} + T_{int} + WS$
$PM_{1\ Ref} \sim PM_1 + RH_{int} + T_{int}$
$PM_{1\ Ref} \sim PM_1 + RH_{int}$
$PM_{1\ Ref} \sim PM_1 + T_{int} + I(1 / RH_{int}) + ToD + WS$
$PM_{1\ Ref} \sim PM_1 + T_{int} + I(1 / RH_{int}) + ToD$
$PM_{1\ Ref} \sim PM_1 + T_{int} + I(1 / RH_{int}) + WS$
$PM_{1\ Ref} \sim PM_1 + T_{int} + I(1 / RH_{int})$
$PM_{1\ Ref} \sim I(PM_1 / ((1 + 0.251 * (RH_{int} / (100 - RH_{int}))) ^ (1/3))) + T_{int}$
$PM_{1\ Ref} \sim I(PM_1 / ((1 + (RH_{int} / (100 - RH_{int}))) ^ (1/3))) + T_{int}$
$PM_{1\ Ref} \sim I(PM_1 / ((1 + 0.251 * (RH_{int} / (100 - RH_{int}))) ^ (1/3)))$
$PM_1 \sim PM_{1\ Ref} + RH_{int} + I(RH_{int} * PM_{1\ Ref})$
$PM_1 \sim PM_{1\ Ref} + RH_{int} + T_{int} + I(RH_{int} * PM_{1\ Ref}) + I(T_{int} * PM_{1\ Ref}) + I(RH_{int} * T_{int}) + I(RH_{int} * PM_{1\ Ref} * T_{int})$

$PM_1$  are chosen as an example. The same equations were tested for  $PM_{10}$  and  $PM_{2.5}$ . These formulas were inspired by different works (Barkjohn et al., 2021; Chakrabarti et al., 2004; Chakraborty et al., 2020).  $PM_{1\ Ref}$  =  $PM_1$  concentrations in  $\mu g/m^3$  measured by the reference,  $PM_1$  =  $PM_1$  measured by the LCS,  $RH_{int}$  = internal relative humidity measured by the LCS,  $T_{int}$  = internal (LCS) temperature,  $WS$  = average wind speed,  $ToD$  = binary time of day factor (zero for night, 1 for daytime).  $I()$  isolates a part of the formula and allows it to serve as a predictor in the model.

**Table S2.** List of tested calibration formulas (as entered in RStudio) for Multiple Linear Regression using ambient parameters.

Formula
$PM_{1\text{ Ref}} \sim PM_1 * RH_{amb} * T_{amb} * ToD * WS$
$PM_{1\text{ Ref}} \sim PM_1 * RH_{amb} * T_{amb} * ToD$
$PM_{1\text{ Ref}} \sim PM_1 * RH_{amb} * T_{amb} * WS$
$PM_{1\text{ Ref}} \sim PM_1 * RH_{amb} * T_{amb}$
$PM_{1\text{ Ref}} \sim PM_1 * RH_{amb}$
$PM_{1\text{ Ref}} \sim PM_1$
$PM_{1\text{ Ref}} \sim PM_1 * RH_{amb} * I(1 / RH_{amb}) * ToD * WS$
$PM_{1\text{ Ref}} \sim PM_1 * T_{amb} * I(1 / RH_{amb}) * ToD$
$PM_{1\text{ Ref}} \sim PM_1 * T_{amb} * I(1 / RH_{amb}) * WS$
$PM_{1\text{ Ref}} \sim PM_1 * T_{amb} * I(1 / RH_{amb})$
$PM_{1\text{ Ref}} \sim PM_1 + RH_{amb} + T_{amb} + ToD + WS$
$PM_{1\text{ Ref}} \sim PM_1 + RH_{amb} + T_{amb} + ToD$
$PM_{1\text{ Ref}} \sim PM_1 + RH_{amb} + T_{amb} + WS$
$PM_{1\text{ Ref}} \sim PM_1 + RH_{amb} + T_{amb}$
$PM_{1\text{ Ref}} \sim PM_1 + RH_{amb}$
$PM_{1\text{ Ref}} \sim PM_1 + T_{amb} + I(1 / RH_{amb}) + ToD + WS$
$PM_{1\text{ Ref}} \sim PM_1 + T_{amb} + I(1 / RH_{amb}) + ToD$
$PM_{1\text{ Ref}} \sim PM_1 + T_{amb} + I(1 / RH_{amb}) + WS$
$PM_{1\text{ Ref}} \sim PM_1 + T_{amb} + I(1 / RH_{amb})$
$PM_{1\text{ Ref}} \sim I(PM_1 / ((1 + 0.251 * (RH_{amb} / (100 - RH_{amb})))^{(1/3)})) + T_{amb}$
$PM_{1\text{ Ref}} \sim I(PM_1 / ((1 + (RH_{amb} / (100 - RH_{amb})))^{(1/3)})) + T_{amb}$
$PM_{1\text{ Ref}} \sim I(PM_1 / ((1 + 0.251 * (RH_{amb} / (100 - RH_{amb})))^{(1/3)}))$
$PM_1 \sim PM_{1\text{ Ref}} + RH_{amb} + I(RH_{amb} * PM_{1\text{ Ref}})$
$PM_1 \sim PM_{1\text{ Ref}} + RH_{amb} + T_{amb} + I(RH_{amb} * PM_{1\text{ Ref}}) + I(T_{amb} * PM_{1\text{ Ref}}) + I(RH_{amb} * T_{amb}) + I(RH_{amb} * PM_{1\text{ Ref}} * T_{amb})$

$PM_1$  are chosen as an example. The same equations were tested for  $PM_{10}$  and  $PM_{2.5}$ . These formulas were inspired by different works (Barkjohn et al., 2021; Chakrabarti et al., 2004; Chakraborty et al., 2020).  $T_{amb}$  and  $RH_{amb}$  are ambient variables given by ROMMA (GPS coordinates: latitude = 45.169°, longitude = 5.768°).  $PM_{1\text{ Ref}}$  =  $PM_1$  concentrations in  $\mu\text{g}/\text{m}^3$  measured by the reference,  $PM_1$  =  $PM_1$  measured by the LCS,  $WS$  = average wind speed,  $ToD$  = binary time of day factor (zero for night, 1 for daytime).  $I()$  isolates a part of the formula and allows it to serve as a predictor.



**Table S3.** List of tested calibration equations (as entered in RStudio) for Random Forest Regression involving LCS internal temperature and relative humidity.  $PM_1$  are chosen as an example. The same equations were tested for  $PM_{10}$  and  $PM_{2.5}$ .

Models using LCS internal temperature and relative humidity
$PM_{1\text{ Ref}} \sim PM_1 + RH_{\text{int}} + T_{\text{int}} + \text{ToD} + \text{WS}$
$PM_{1\text{ Ref}} \sim PM_1 + RH_{\text{int}} + T_{\text{int}} + \text{ToD}$
$PM_{1\text{ Ref}} \sim PM_1 + RH_{\text{int}} + T_{\text{int}} + \text{WS}$
$PM_{1\text{ Ref}} \sim PM_1 + RH_{\text{int}} + T_{\text{int}}$
$PM_{1\text{ Ref}} \sim PM_1 + RH_{\text{int}}$

$PM_{1\text{ Ref}} = PM_1$  concentrations in  $\mu\text{g}/\text{m}^3$  measured by the reference,  $PM_1 = PM_1$  measured by the LCS,  $RH_{\text{int}} =$  internal relative humidity measured by the LCS,  $T_{\text{int}} =$  internal (LCS) temperature,  $\text{WS} =$  average wind speed,  $\text{ToD} =$  binary time of day factor (zero for night, 1 for day).

**Table S4.** List of tested calibration equations for Random Forest Regression using ambient parameters.  $PM_1$  are chosen as an example. The same equations were tested for  $PM_{10}$  and  $PM_{2.5}$ .

Models using ambient temperature and relative humidity
$PM_{1\text{ Ref}} \sim PM_1 + RH_{\text{amb}} + T_{\text{amb}} + \text{ToD} + \text{WS}$
$PM_{1\text{ Ref}} \sim PM_1 + RH_{\text{amb}} + T_{\text{amb}} + \text{ToD}$
$PM_{1\text{ Ref}} \sim PM_1 + RH_{\text{amb}} + T_{\text{amb}} + \text{WS}$
$PM_{1\text{ Ref}} \sim PM_1 + RH_{\text{amb}} + T_{\text{amb}}$
$PM_{1\text{ Ref}} \sim PM_1 + RH_{\text{amb}}$

$T_{\text{amb}}$  and  $RH_{\text{amb}}$  are ambient variables given by ROMMA (GPS coordinates: latitude =  $45.169^\circ$ , longitude =  $5.768^\circ$ ).  $PM_{1\text{ Ref}} = PM_1$  concentrations in  $\mu\text{g}/\text{m}^3$  measured by the reference,  $PM_1 = PM_1$  measured by the LCS,  $\text{WS} =$  average wind speed,  $\text{ToD} =$  binary time of day factor (zero for night, 1 for day).

**Table S5.** Descriptive statistics for hourly PM concentrations, temperature and relative humidity. The dataset is cleared of dusts and points corresponding to RH > 98%.

	PM <sub>10</sub>		PM <sub>2.5</sub>		PM <sub>1</sub>		Temperature (°C)		RH %	
	LCS	REF <sup>a</sup>	LCS	REF <sup>a</sup>	LCS	REF <sup>a</sup>	LCS	ROMMA	LCS	ROMMA
<b>Min</b>	0	1.0	0	0.5	0	0.3	-1.8	-2.8	10.9	13.7
<b>Q1</b>	3.9	7.6	3.5	4.0	2.8	2.9	11.7	9.4	43.8	59.2
<b>Median</b>	8.6	11.6	8.0	6.6	6.3	5.4	18.7	15.7	67.0	79.2
<b>Mean</b>	12.4	13.2	11.1	7.9	8.1	6.5	19.1	15.2	64.25	74.0
<b>Q3</b>	16.1	17.0	14.9	10.0	11.2	8.3	24.8	20.4	87.2	90.3
<b>Max</b>	74.8	82.8	57.6	34.1	36.8	32.9	47.0	34.6	96.8	97

<sup>a</sup>REF: Reference station “Les Frênes”, Atmo Auvergne-Rhône-Alpes

## REFERENCES

- Barkjohn, K. K., Gantt, B., Clements, A. L., 2021. Development and Application of a United States wide correction for PM<sub>2.5</sub> data collected with the PurpleAir sensor. *Atmos. Meas. Tech.* 4 (6), 4617–4637. <https://doi.org/10.5194/amt-14-4617-2021>.
- Chakrabarti, B., Fine, P. M., Delfino, R., Sioutas, C., 2004. Performance evaluation of the active-flow personal DataRAM PM<sub>2.5</sub> mass monitor (Thermo Anderson pDR-1200) designed for continuous personal exposure measurements. *Atmos. Environ.* 38 (20), 3329-3340. <https://doi.org/10.1016/j.atmosenv.2004.03.007>.
- Chakraborty, R., Heydon, J., Mayfield, M., Mihaylova, L., 2020. Indoor Air Pollution from Residential Stoves: Examining the Flooding of Particulate Matter into Homes during Real-World Use. *Atmosphere* (Basel). 11 (12), 1326. <https://doi.org/10.3390/atmos11121326>.

**Summary – Conclusion Article n°3**

A conclusion drawn from this paper is that excluding dusts substantially improves the performance of calibration algorithms, consequently improving LCS accuracy. In the future, allocating research resources to rectify sensor values during these episodes would be of interest, as this would avoid removing this data from exposure studies. It would also be interesting to further work on improving dust detection. In the future, it may become feasible to completely rely on satellite observations for dust detection, eliminating the need for in-field assessments. This is not currently possible due the coarse 10 km x 10 km resolution of CAMS satellite data for dusts detection (Météo-France, 2020). Our study shows the significance of preprocessing data before trying various calibration models. Finally, another notable aspect of Schmitz et al.'s (2021) method is its approach to address uncertainties in LCS measurements, including guidelines to calculate them.

### 3.4 CONCLUSION

The correction formulas for the different PM sizes, along with their associated uncertainties, are summarized in Table 2. Given the importance of accounting for uncertainties in both reference and LCS (Koritsoglou et al., 2020; Schmitz et al., 2021), a reference's technical error of 11% for PM<sub>2.5</sub> or PM<sub>1</sub>, and 13% for PM<sub>10</sub> is also added (LCSQA, 2020). Uncertainties were computed as follows:

- For MLR and RFR algorithms, the median mean absolute error (MAE) across test blocks with the reference instrument's technical error were merged as recommended by Schmitz et al. (2021)
- For linear and mechanistic regressions formulas, we calculated the MAE of the test dataset and added it to the reference's technical error.

The MAE was calculated as follows:

$$\text{MAE} = \frac{\sum_{i=1}^n |y_i - x_i|}{n} \quad (2)$$

Where  $y_i$  is the predicted (corrected) value,  $x_i$  the observed value, and  $n$  the number of values in the test dataset.

**Table 2. Calibration formulas for  $\text{PM}_{10}$ ,  $\text{PM}_{2.5}$ , and  $\text{PM}_1$ , along with their uncertainties.** Example (LR calibration): if  $\text{PM}_{2.5} = 10 \mu\text{g}/\text{m}^3$ ,  $\text{PM}_{2.5 \text{ Cal}} = 7.39 \pm 1.68 \mu\text{g}/\text{m}^3$ .

Method	Formula	Uncertainty
<b><math>\text{PM}_1</math></b>		
LR	$\text{PM}_{1 \text{ Cal}} = 0.70 \text{ PM}_1 + 0.93$	$\pm (0.11 \text{ PM}_{1 \text{ Cal}} + 0.79)$
Mechanistic	$\text{PM}_{1 \text{ Cal}} = 0.08 + 0.83 \frac{\text{PM}_1}{\left(1 + 0.13 \frac{\text{RH}_{\text{int}}}{100 - \text{RH}_{\text{int}}}\right)^{\frac{1}{3}}} + 0.03 \text{ T}_{\text{int}}$	$\pm (0.11 \text{ PM}_{2.5 \text{ Cal}} + 0.44)$
MLR	$\text{PM}_{1 \text{ Cal}} = 1.29 + 0.96 \text{ PM}_1 - 0.01 \text{ RH}_{\text{int}} - 0.003 \text{ PM}_1 * \text{RH}_{\text{int}}$	$\pm (0.11 \text{ PM}_{1 \text{ Cal}} + 0.61)$
RFR	$\text{PM}_{1 \text{ Cal}} = \text{PM}_1 + \text{RH}_{\text{int}} + \text{T}_{\text{int}}$	$\pm (0.11 \text{ PM}_{1 \text{ Cal}} + 0.43)$
<b><math>\text{PM}_{2.5}</math></b>		
LR	$\text{PM}_{2.5 \text{ Cal}} = 0.49 \text{ PM}_{2.5} + 2.49$	$\pm (0.11 \text{ PM}_{2.5 \text{ Cal}} + 0.87)$
Mechanistic	$\text{PM}_{2.5 \text{ Cal}} = 0.5 + 0.65 \frac{\text{PM}_{2.5}}{\left(1 + 0.25 \frac{\text{RH}_{\text{int}}}{100 - \text{RH}_{\text{int}}}\right)^{\frac{1}{3}}} + 0.08 \text{ T}_{\text{int}}$	$\pm (0.11 \text{ PM}_{2.5 \text{ Cal}} + 0.72)$
MLR	$\text{PM}_{2.5 \text{ Cal}} = 2.86 + 0.79 \text{ PM}_{2.5} - 0.01 \text{ RH}_{\text{int}} - 0.004 \text{ PM}_{2.5} * \text{RH}_{\text{int}}$	$\pm (0.11 \text{ PM}_{2.5 \text{ Cal}} + 0.87)$
RFR	$\text{PM}_{2.5 \text{ Cal}} = \text{PM}_{2.5} + \text{RH}_{\text{int}} + \text{T}_{\text{int}}$	$\pm (0.11 \text{ PM}_{2.5 \text{ Cal}} + 0.73)$
<b><math>\text{PM}_{10}</math></b>		
LR	$\text{PM}_{10 \text{ Cal}} = 0.45 \text{ PM}_{10} + 7.71$	$\pm (0.13 \text{ PM}_{10 \text{ Cal}} + 2.72)$
Mechanistic	$\text{PM}_{10 \text{ Cal}} = 1.75 + 1.12 \frac{\text{PM}_{10}}{\left(1 + 2.68 \frac{\text{RH}_{\text{int}}}{100 - \text{RH}_{\text{int}}}\right)^{\frac{1}{3}}} + 0.23 \text{ T}_{\text{int}}$	$\pm (0.13 \text{ PM}_{10 \text{ Cal}} + 2.53)$
MLR	$\text{PM}_{10 \text{ Cal}} = 1.15 + 0.89 \frac{\text{PM}_{10}}{\left(1 + \frac{\text{RH}_{\text{int}}}{100 - \text{RH}_{\text{int}}}\right)^{\frac{1}{3}}} + 0.27 \text{ T}_{\text{int}}$	$\pm (0.13 \text{ PM}_{10 \text{ Cal}} + 2.86)$
RFR	$\text{PM}_{10 \text{ Cal}} = \text{PM}_{10} + \text{RH}_{\text{int}} + \text{T}_{\text{int}}$	$\pm (0.13 \text{ PM}_{10 \text{ Cal}} + 2.73)$

Overall, although linear or mechanistic regression models may be adequate to meet US EPA's performance guidelines, machine learning calibration models demonstrated promising results in our study. This is in alignment with the literature, as we observe a growing number of articles using machine learning in the field of LCS calibration (Liang, 2021). Calibration formulas reported in Table 2 can be directly transposed to sites with similar aerosol compositions and environments. Careful use and recalibration are needed when dealing with sites different from the calibration sites. This work also aligns with recent research showing that calibrated low-cost PM sensors can effectively complement reference stations, even though they may have technical limitations in measuring coarse PM, which is of minor concern, given the lower health effects of coarse PM. The inability of LCS to measure Saharan dust events may be attributed to various factors, dusts predominantly consisting of  $PM_{10}$  and  $PM_{2.5}$  (Alonso-Pérez & López-Solano, 2023; Querol et al., 2019). Some studies suggested that coarse PM could not perform the complete trajectory till the photodiode inside the PMS7003, especially the 90-degree turns (Sayahi et al., 2019). Others point out that PM size might influence light scattering and that bigger PM could diffract less light. This could also result from a difference in the refractive index related to the composition of dust or from its transparent nature, which might allow the signal to pass through. In summary, there are several hypotheses, some related to the sensor itself, while others are linked to the composition of dust particles. More research is needed to explore this topic. A recent study (Alonso-Pérez and López-Solano, 2023) demonstrated that a LCS, the SDS011, could detect Saharan dust. Hence, it can be inferred that the SDS011 might provide a more direct path for PM than the PMS7003, or it may have a different wavelength enabling better PM distinction. This needs to be confirmed by further research. Badura et al. (2018) noted slightly weaker correlations with a reference for the SDS 011 ( $r = 0.88$ ) than for the PMS7003 ( $r = 0.90-0.92$ ). Combining both sensors like the SDS 011 and the PMS 7003 could offer a synergistic approach, potentially yielding more dependable data.

The poor performance of LCS on  $PM_{10}$  led us to disregard  $PM_{10}$  and focus only on  $PM_1$  or  $PM_{2.5}$  in the next chapters. The absence of drift and the good results from our calibration study encouraged us to deploy a LCS network in Grenoble and further analyse the data as detailed in the next chapter. A limitation of this calibration study resides in the range of collocation concentrations, i.e., the test dataset only features low PM concentrations (e.g.,  $PM_{2.5}$  less than  $15 \mu\text{g}/\text{m}^3$ ). As explained in the next chapter, it would have been valuable to conduct a more extended collocation experiment entailing episodes of extreme PM levels.

### Summary - Results Chapter 3

- Excluding dust events improves calibration algorithms performance;
- For  $PM_1$ , MLR calibration gave better results than LR or mechanistic methods;
- For  $PM_{2.5}$ , RFR calibration gave the best results;
- Performance of PMS7003 is poor for coarse PM like  $PM_{10}$ .

# 4 AN EXPERIMENTAL NETWORK OF LOW-COST PARTICULATE MATTER SENSORS IN GRENOBLE

## Summary - Introduction Chapter 4

- Background: LCS networks measuring PM are becoming increasingly popular and offer research opportunities. However, only a limited number of studies analyse their outputs.
- Objectives:
  1. Assess PM levels provided by a LCS network in Grenoble;
  2. Study their relationship with the background reference to explore localized variations;
  3. Locate PM hot-spots where individuals could face excessive PM exposure.
  4. Identify time periods when local PM levels are higher

## 4.1 INTRODUCTION

The use of low-cost sensors is growing, and there are now tens of thousands of LCS worldwide (Searle et al., 2023). Two of the most prominent stationary LCS networks are PurpleAir (2023) and Sensor.Community (2023). The LCS are deployed by citizens themselves, and their data is freely



accessible to everyone via an API, making their use more straightforward. Interestingly, scientists recently started to use these massive citizen science data to quantify LCS degradation (deSouza et al., 2023), develop calibration techniques (Barkjohn et al., 2021; deSouza et al., 2022; Searle et al., 2023), especially for wildfires evaluation (Barkjohn et al., 2022). The PurpleAir network had more than 12,000 sensors in January 2022 (Barkjohn et al., 2022), and the Sensor.Community currently comprises around 13,000 sensors worldwide. In recent years, smaller networks emerged, such as Breathe London (2023) and “Love My Air” in Denver (Li et al., 2023). All of these networks provide unparalleled research opportunities, as long as reference stations are available in close proximity to calibrate LCS. Scientists also deploy their own LCS networks but there are currently more studies related to calibration than papers aiming at analysing deployed LCS outputs. This approach is prudent, as data reliability is crucial before starting network deployment and analysing results. Nonetheless, there are limited studies available for us to compare our research to when it comes to analysing LCS networks. Raheja et al. (2022) deployed five sensors using PMS5003 in Lomé (Togo) and compared their PM levels with WHO guidelines. However, they missed an on-site reference monitor against which to compare LCS measurements. Gitahi and Hahn (2022) used crowd sourced Sensor.Community measurements and compared them to reference monitors located close to the LCS. However, they emphasized the lack of standardization in LCS placement by citizens, which might lead to non-representative measurements. They found good correlations between LCS and reference stations located within a 1km radius, with almost half of the Pearson correlation coefficients bigger than 0,7. LCS measurements were impacted by their proximity to roads and road types. Dimitriou et al. (2023) established an LCS network across 5 Greek cities and observed strong correlations in daily PM<sub>2.5</sub> levels across locations. Peak concentrations were primarily linked to regional northern airflows, underscoring the significance of long-distance transportation. Their objective was to get insights into more localized contributions that can add to the background levels measured by the central reference. In this study, we are going to analyse PM levels given by different LCS placed in Grenoble, as well as their relationship with the background reference values, in order to better understand localized variations. Conducting a spatio-temporal analysis, we will compare the sensors between each other, and try to identify potential hot-spots in Grenoble where individuals might be overexposed to PM.

## 4.2 MATERIALS AND METHODS

### 4.2.1 Measuring instruments

The measurements were conducted with the calibrated air quality stations (Aix et al., 2023) depicted in Figure 18. These stations consist of three main components: a Wi-Fi microcontroller, an optical PM sensor (PMS 7003) and a humidity/temperature sensor (DHT 22). The detailed components list can be found in Appendix C.

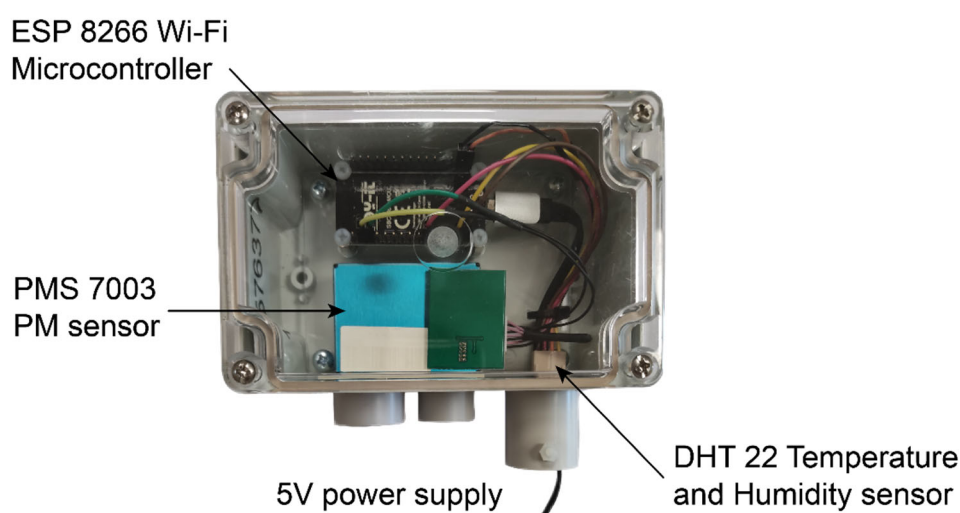


Figure 18. Layout of a PM monitoring station

At the beginning of the experiment, all DHT22 sensors were replaced by new ones because some of them exhibited relative humidity deviations. In total, 8 air quality stations were deployed in Grenoble and Saint-Martin d'Hères (adjacent city to Grenoble). PM concentrations were measured at a frequency of approximately 150 s (2mn 30 s).

### 4.2.2 Sampling locations and time period

Sampling locations were selected to provide comprehensive coverage of the city, in addition to the official background station. The criteria for sensor placement were stringent, as our objective was to closely align the sensors deployment conditions with those of the calibration. Since the

sensors were calibrated in background conditions, they had to be deployed under similar environments. Moreover, we aimed to measure PM close to ground level, in order to be as representative as possible of what individuals breathe. The location criteria given to the volunteers willing to host a station, were as follows:

- In Grenoble or Saint-Martin d'Hères;
- Between 1.5 and 4 meters above the ground (upper levels were prohibited);
- Away from smoking areas or construction sites;
- Avoid south-facing positions (or ensuring shelter if facing south);
- Ensure no obstacle within a circle of 1 meter, aside from the sensor support.

These criteria were crucial as they would influence the quality of the data we would gather later on. Table 3 displays the characteristics of the locations, together with their deployment time period. We named the stations using the name of the neighbourhood or street where they were located.

**Table 3. Sampling sites description and deployment time period**

Name	Characteristics	Deployment time period
Abbaye	Residential area with houses, in a garden	2022-06-30 to 2023-08-08
Aigle	Residential area with houses, facing towards the street	2022-06-29 to 2023-08-08
Bachelard	Residential area with houses, in a garden	2022-07-19 to 2023-08-08
City center	Public housing, pedestrian street with shops and restaurants	2022-09-03 to 2023-08-08
Clemenceau	Public housing, courtyard-side	2022-01-17 to 2023-08-08
Mistral	School facade, facing a courtyard near a street	2022-07-19 to 2023-08-08
Saint-Bruno	Residential building, private terrace	2022-07-25 to 2023-08-08
Saint-Martin d'Hères	Public housing, facing a garden	2022-09-05 to 2023-06-08

Figure 19 illustrates the stations distribution throughout the urban area.

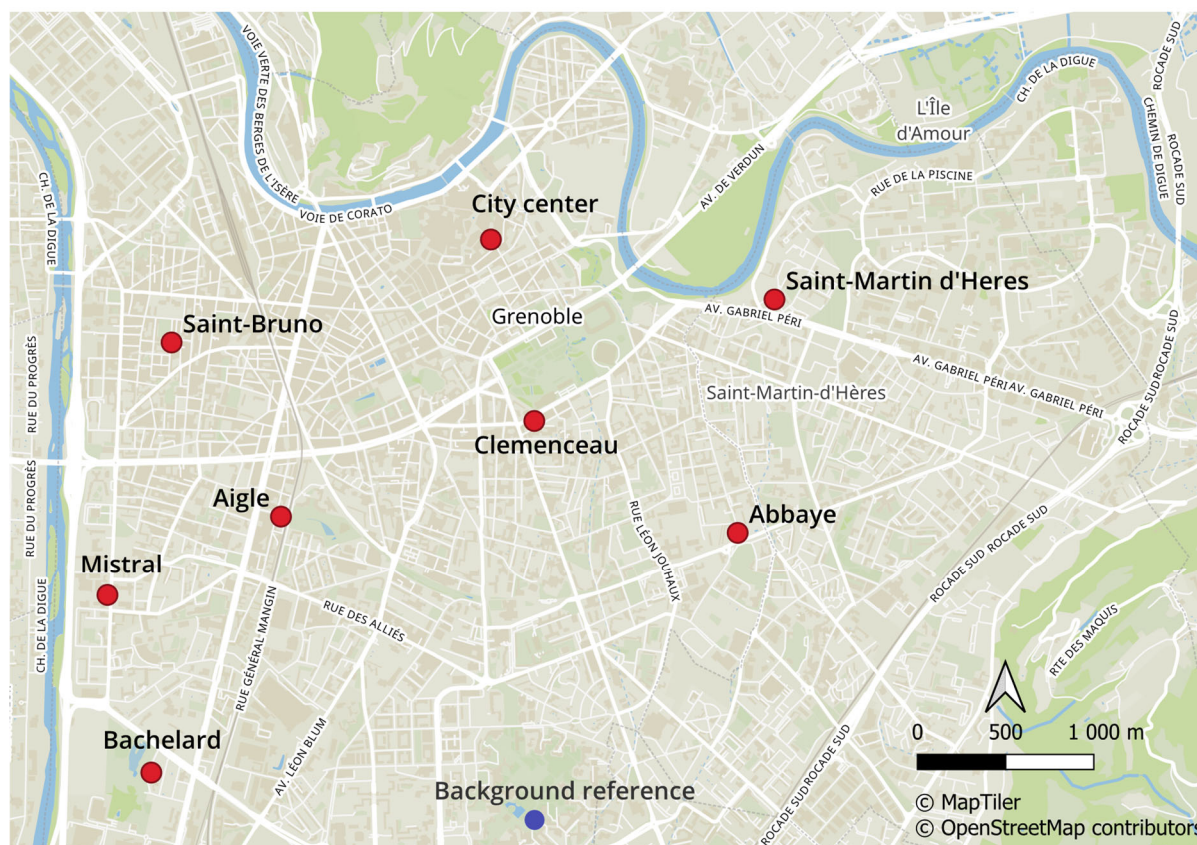


Figure 19. Map of the network of LCS showing sensors locations (red) and the official background reference station from Atmo AuRA (blue).

The station in Saint-Martin d’Hères could not be regularly sampled because of frequent Wi-Fi connectivity issues. 80% of the PM records were missing, so this station had to be removed from the analysis.

### 4.2.3 Data cleaning

PM<sub>2.5</sub> raw data were fused with temperature and RH measurements made at the same time. All PM<sub>2.5</sub> values greater than 500µg/m<sup>3</sup> were also removed because of PMS7003 efficiency range (Bauerová et al., 2020; Plantower, 2016). This applied to a negligible fraction of the dataset, ranging from 0.0005% to 0.09%, depending on the sensor. Outliers were not removed from the datasets to assess individual exposures. The sensor values were subsequently converted into hourly averages

to facilitate comparison with hourly reference values. All data cleaning steps, as well as the following selection procedure, are schematized in Figure 20.

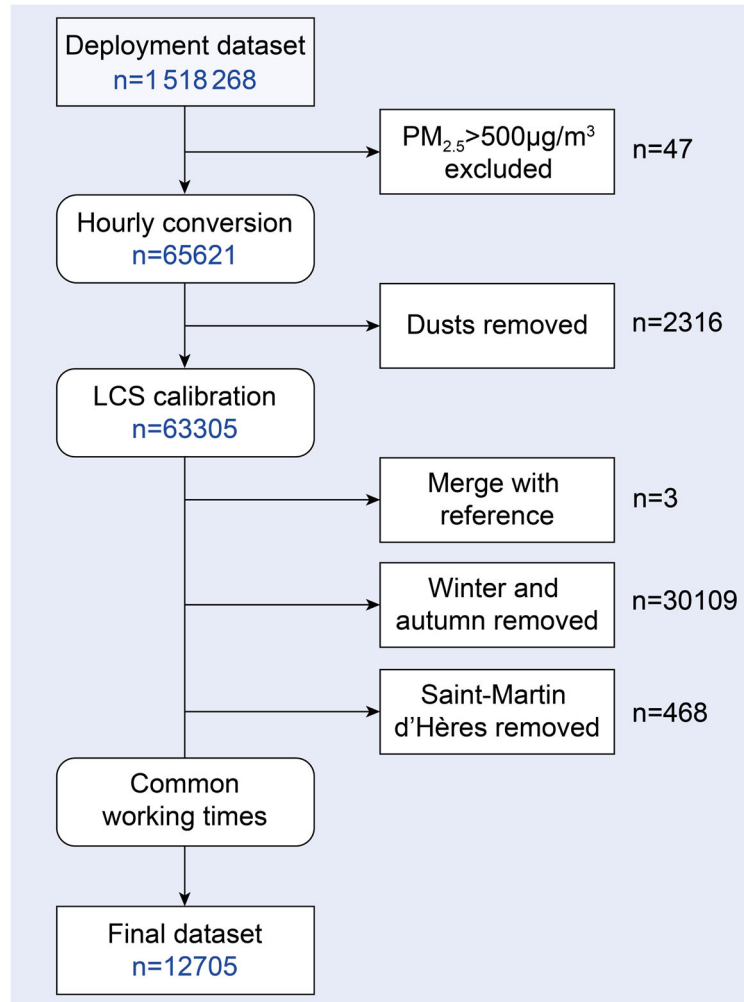


Figure 20. Flowchart of the data cleaning and selection procedure

The hourly conversion was then followed by a dust removal step. In general, LCS readings are well correlated to reference values except during dusts when LCS do not capture well large PM like  $PM_{10}$  or  $PM_{2.5}$  (Jaffe et al., 2023; Kosmopoulos et al., 2020; Molina Rueda et al., 2023). Therefore, we applied the technique developed in Chapter 3 (Aix et al., 2023) to detect dust events. First, we checked daily correlations between the reference and the LCS. Second, we uploaded dust values from Copernicus (Météo-France, 2020). PM values were removed from the dataset when both the correlation was negative and Copernicus showed a dust (Figure 21).

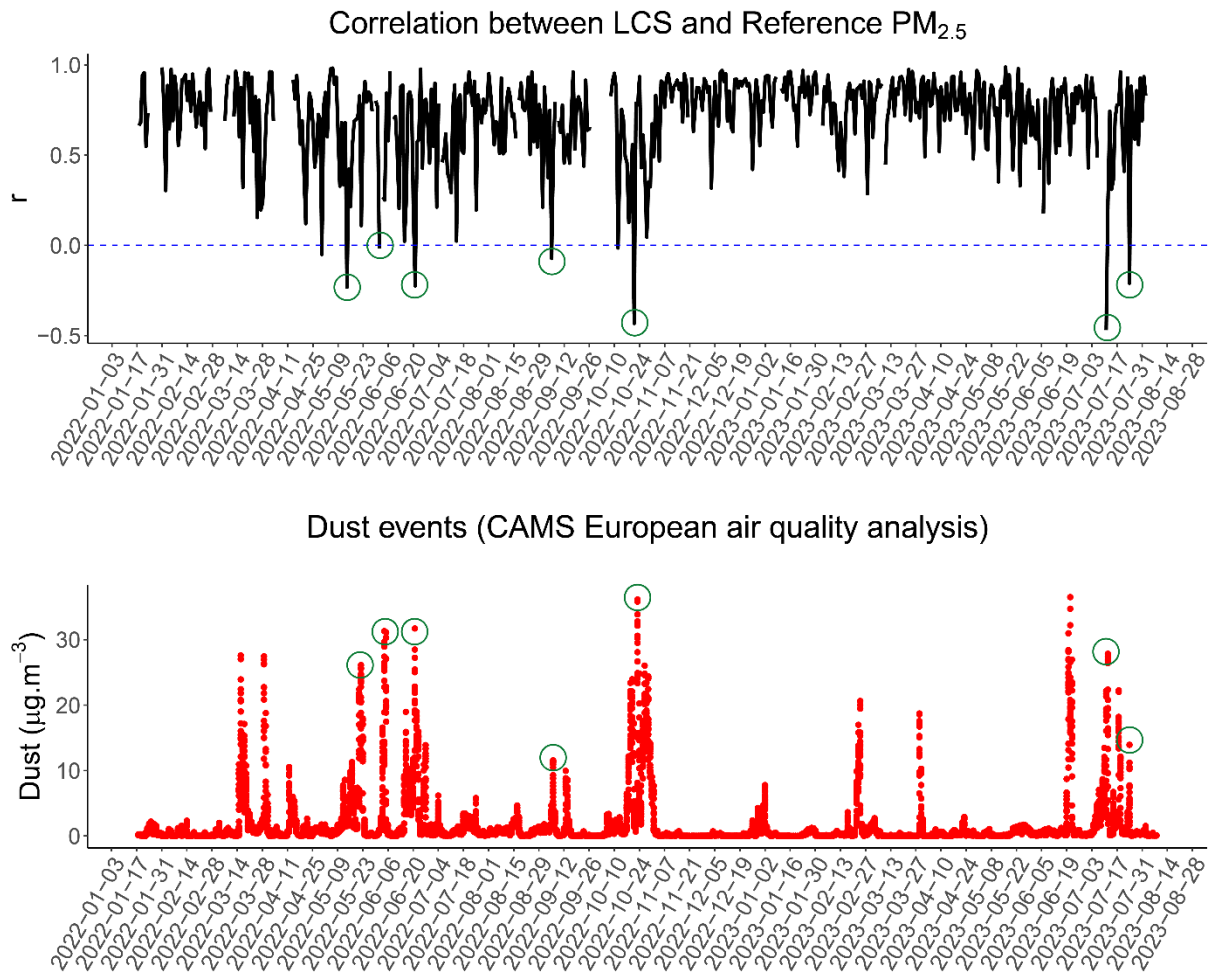


Figure 21. Dust identification steps

After a thorough dataset analysis, 7 dust events were identified (Table 4) and removed from the dataset.

Table 4. Dust events time periods discarded from the dataset

	start	end
dust1	2022-05-09	2022-05-16
dust2	2022-06-01	2022-06-05
dust3	2022-06-19	2022-06-24
dust4	2022-09-05	2022-09-06
dust5	2022-10-17	2022-10-21
dust6	2023-07-11	2023-07-12
dust7	2023-07-23	2023-07-25

After dust removal (5.6% of the dataset), PM values were corrected using the different correction algorithms developed by Aix et al. (2023).



#### 4.2.4 Calibration and time period selection

The calibration formulas use temperature and relative humidity measured by the air quality station (Appendix 1 and 2). First, the calibrated  $PM_{1\text{ LCS}}$  values were examined with respect to  $PM_{1\text{ Ref}}$  measurements (Figure 22). For all LCS stations, an inflexion occurred around  $PM_{1\text{ Ref}} = 15\text{--}20\ \mu\text{g}/\text{m}^3$ .

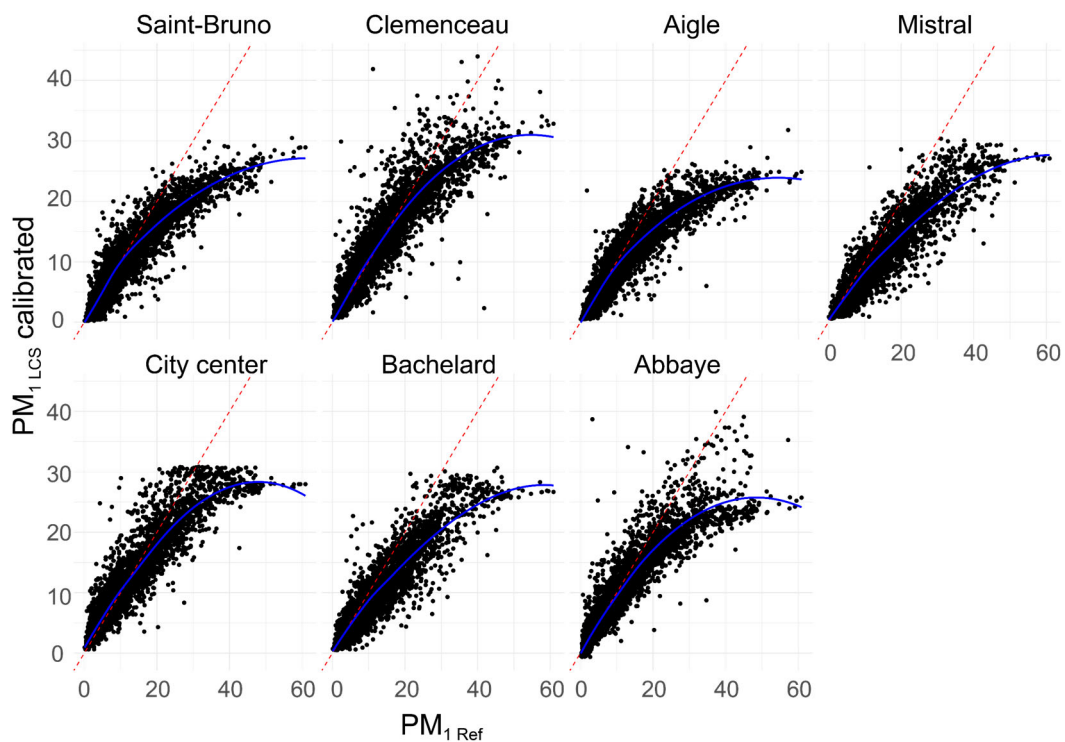


**Figure 22.** Scatterplots showing calibrated  $PM_{1\text{ LCS}}$  levels versus  $PM_{1\text{ Ref}}$ . 4 outliers were removed for presentation purposes. The dashed red lines indicate the parity and the blue lines the loess regression curve.

This was intriguing and we therefore checked the LCS raw values (Figure 23). This inflection was associated with high PM levels observed during autumn and winter. By examining the relationship between  $PM_{1\text{ Ref}}$  and  $PM_{1\text{ LCS}}$  raw values during these two seasons, we found that the scatterplot could be divided into two distinct parts. The linear regression of  $PM_{1\text{ LCS}}$  for  $PM_{1\text{ Ref}}$  values greater than  $20\ \mu\text{g}/\text{m}^3$  was different from those below  $20\ \mu\text{g}/\text{m}^3$ .



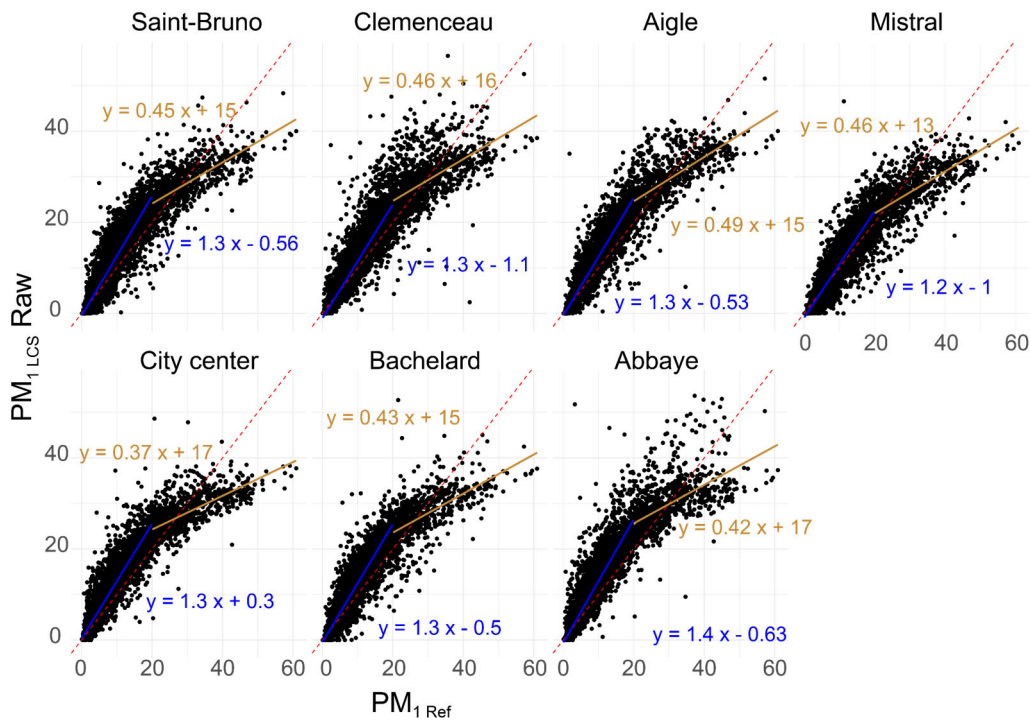


**Figure 23.** Scatterplots showing raw PM<sub>1</sub> levels versus PM<sub>1</sub> Ref for winter and autumn. 5 outliers were removed for presentation purposes. In blue, the regression lines for PM<sub>1</sub> Ref < 20 µg/m<sup>3</sup>, in orange, for PM<sub>1</sub> Ref > 20 µg/m<sup>3</sup>. The dashed red lines indicate the parity line.

Everything indicated that our calibration formulas were unable to correct PM<sub>1</sub> LCS values corresponding to PM<sub>1</sub> Ref values greater than 15-20 µg/m<sup>3</sup>. We attempted to implement a dedicated winter correction algorithm by focusing on the winter portion of the colocation data. Additionally, we explored the application of an algorithm tailored to PM<sub>1</sub> Ref co-location values > 15 µg/m<sup>3</sup>. We also tried to calibrate the LCS individually using a simple linear regression, in order to see if humidity could be responsible for this phenomenon. Polynomial equations were also tested. None of these methods produced successful results, as all scatterplots still exhibited a distinct inflection point. Figure 24 displays the colocation PM<sub>1</sub> levels, and highlights the reason why we struggled to calibrate these extreme data points. The colocation study took place between the 28<sup>th</sup> of January 2021 and the 29<sup>th</sup> of September 2021. As a result, the dataset had limited winter and autumn data. The primary issue was that the highest level of PM measured during the colocation was 30 µg/m<sup>3</sup>, whereas our fixed sensors recorded levels of up to 60 µg/m<sup>3</sup> during deployment. The colocation exhibited considerably lower PM levels than the deployment phase, which made the calibration of extreme values observed on deployed LCS uncertain. This raises the question of validity range of colocation.

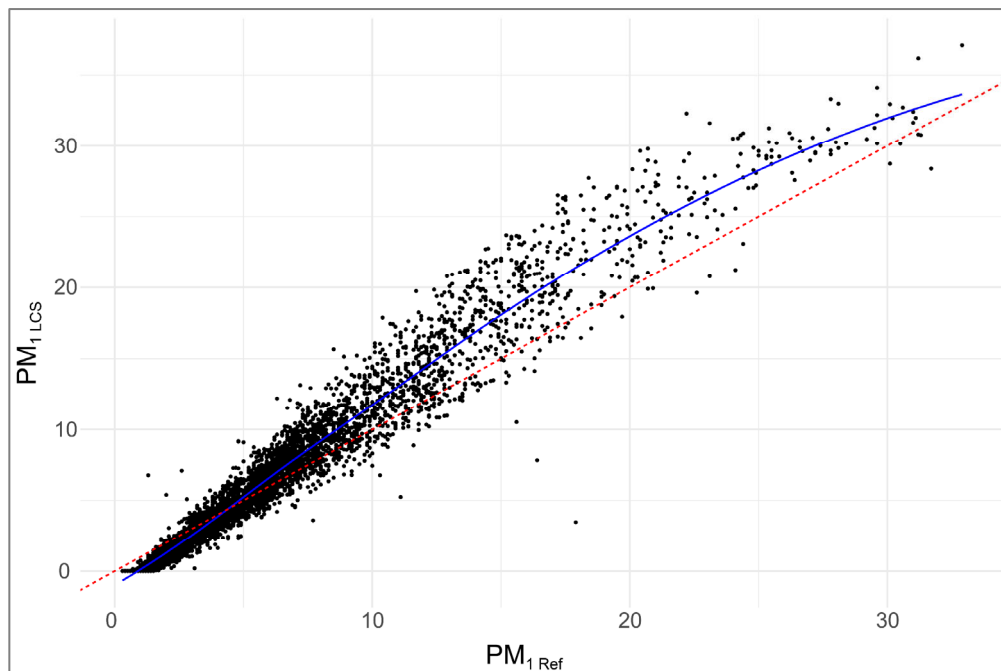


**Figure 24. Scatterplot of hourly LCS average  $PM_1$  concentrations versus  $PM_1$  reference concentrations during the colocation study (8-month dataset).** As reported by Aix et al. (2023)

This flattening of the curve phenomenon was also highlighted by Stampfer et al. (2020). In their study, the relationship between  $PM_{2.5\text{ LCS}}$  and  $PM_{2.5\text{ Ref}}$  changed at  $PM_{2.5\text{ Ref}}$  values above around  $25\ \mu\text{g}/\text{m}^3$  (which, in our study, corresponds to  $PM_1$  values exceeding  $16\ \mu\text{g}/\text{m}^3$ ). Wang et al. (2023) acknowledged the same limitations, having too low  $PM_{2.5}$  levels during their colocation. They highlighted the need for more research on PM levels higher than  $20\ \mu\text{g}/\text{m}^3$  and emphasized the risk of deploying LCS in an environment differing from the calibration conditions. As we required precision for our exposure calculations, we opted to limit our analysis to spring and summer periods where measured levels are consistent with the colocation. Lastly, we chose to focus on the overlapping operational periods of the sensors to allow meaningful comparisons. As a result, all time slots during which one or more LCS did not work were removed for further analysis. This included removing times when the reference did not deliver results. In total, 61% of the dataset was discarded during this operation. We had 12705 hourly values remaining in the dataset. The removed values are left for a different analysis.

### 4.2.5 Exposure calculations

We first conducted a descriptive analysis of PM concentrations, temperature and humidity measured by the air quality stations. Subsequently, we focused on ratios of PM measurements in relation to their corresponding background reference levels. This normalization technique helps to identify excessive local PM concentrations above reference levels and allows to compare different times or days when background concentrations are different. The following ratios were computed:

$$PM_1 \text{ ratio} = \frac{PM_1}{PM_{1 \text{ Ref}}} \quad (3)$$

$$PM_{2.5} \text{ ratio} = \frac{PM_{2.5}}{PM_{2.5 \text{ Ref}}} \quad (4)$$

In these equations,  $PM_1$  and  $PM_{2.5}$  refer to hourly LCS concentrations while  $PM_{1 \text{ Ref}}$  and  $PM_{2.5 \text{ Ref}}$  denote hourly reference concentrations. The objective was to identify locations where individuals might experience PM overexposure in contrast to background reference levels, which were regarded as a baseline scenario. Following Boulter (2020), within a city, there is a basis of regional background pollution covering a wide area and relatively stable (Figure 25). Atop this first layer, there is an urban background, resulting from traffic, residential heating, and industries. The reference station can capture this urban background, as well as the regional background. Lastly, as a third layer, there are additional local contributions (hot-spots), such as those coming from traffic. Our research aimed to evaluate these local contributions. All calculations were made with RStudio 2023.06.2 (R Core Team, 2023).

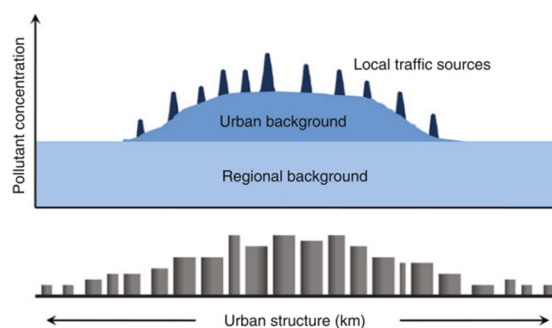


**Figure 25. Simplified representation of urban structure and pollution levels** Extracted from Boulter (2020) and adapted from Keuken et al. (2005).

## 4.3 RESULTS

### 4.3.1 Descriptive statistics

Statistics conducted for each LCS, as well as for the reference station are displayed in Table 5. The sensor located in the city center exhibits the highest levels of PM, along with the largest standard deviations. For PM<sub>1</sub>, the least exposed sensor was in Mistral, while for PM<sub>2.5</sub>, it was the Aigle sensor, both exhibiting the lowest standard deviations. Generally, the LCS displayed lower PM levels than the reference, except for the city center sensor, as well as Clemenceau for PM<sub>1</sub>.

**Table 5. Descriptive statistics for calibrated LCS and reference hourly PM concentrations, temperature and relative humidity. SD: Standard deviation.**

Location	PM <sub>1</sub> ( $\mu\text{g}/\text{m}^3$ )		PM <sub>2.5</sub> ( $\mu\text{g}/\text{m}^3$ )		Relative humidity (%)		Temperature (°C)	
	Mean	SD	Mean	SD	Mean	SD	Mean	SD
Reference	5,5	3,3	6,9	3,8	-	-	-	-
Aigle	4,9	3,0	5,7	2,8	74,5	23,3	18,7	6,6
Mistral	4,6	2,7	5,8	3,1	68,9	21,7	18,2	6,6
Bachelard	5,0	3,0	6,1	3,3	73,9	19,8	18,2	7,3
Abbaye	5,0	3,3	6,2	3,4	75,3	23,2	18,7	7,4
Saint-Bruno	5,3	3,5	6,4	3,4	59,7	24,6	20,7	7,5
Clemenceau	5,5	3,5	6,7	3,4	51,7	14,9	21,0	6,9
City center	6,2	5,3	7,5	3,9	57,3	15,8	19,8	6,9

Depending on the LCS, humidity values ranged between 52% and 75%, while temperature varied between 18°C and 21°C. The sensors oriented towards the south or southwest (Saint-Bruno, Clemenceau, City Center) exhibited higher temperatures (20-21°C compared to 18-19°C for the others), and lower relative humidity values (52-60% versus 69-75% for the others).

### 4.3.2 PM concentrations

When checking distances between sensors and correlations between them, we observed that the most correlated sensors were generally close to each other. Figure 26 shows a distance matrix (A) and correlation matrices for PM<sub>2.5</sub> (B) and PM<sub>1</sub> (C) between sensors. The closest stations

(Bachelard and Mistral) were the ones that were the most correlated with each other for PM<sub>2.5</sub>, with a Pearson correlation coefficient indicating a strong association ( $r=0.95$ ). For some of the LCS, such as Clemenceau, City Center, or Abbaye, the distance did not seem to influence the correlation with other LCS.

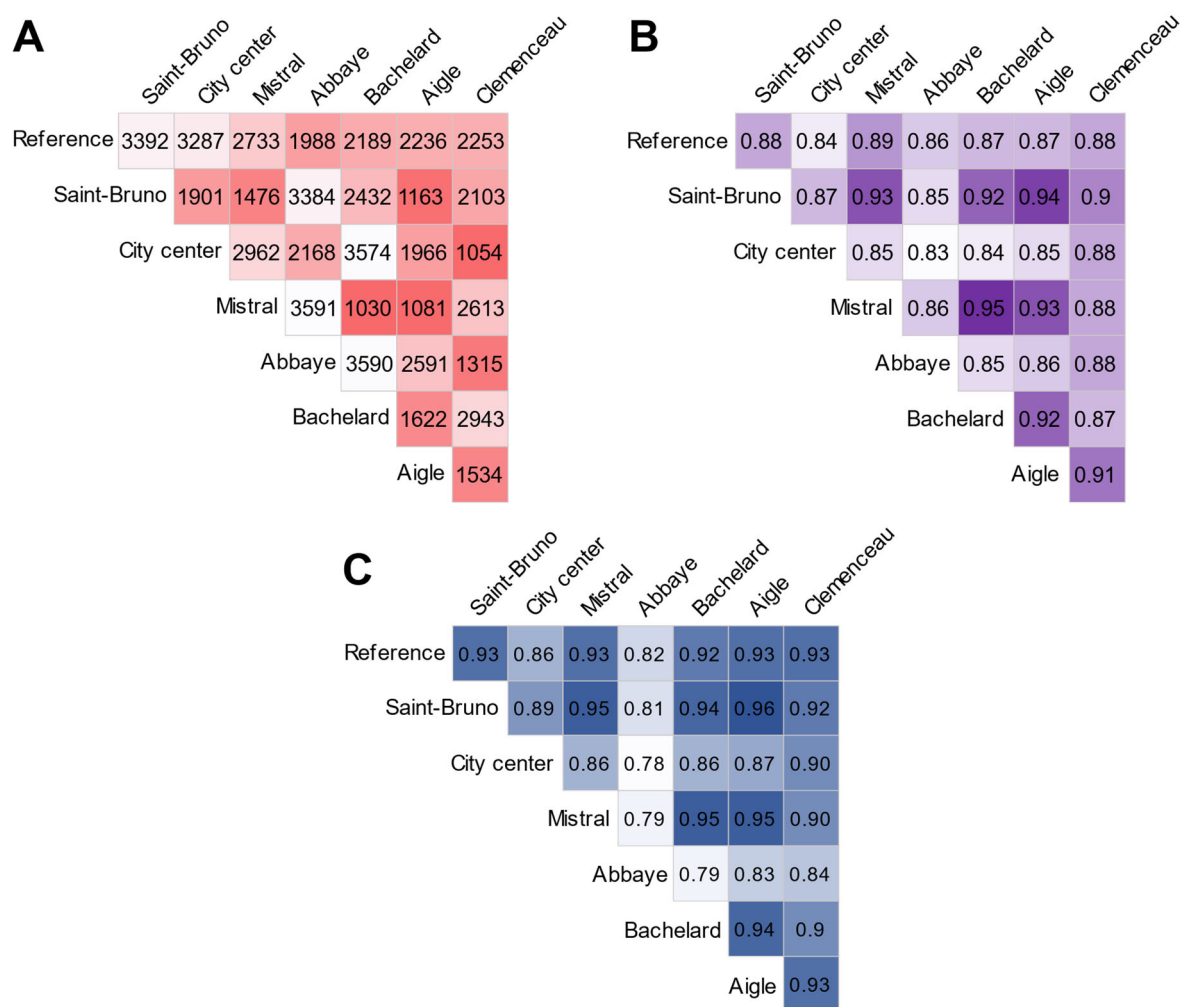
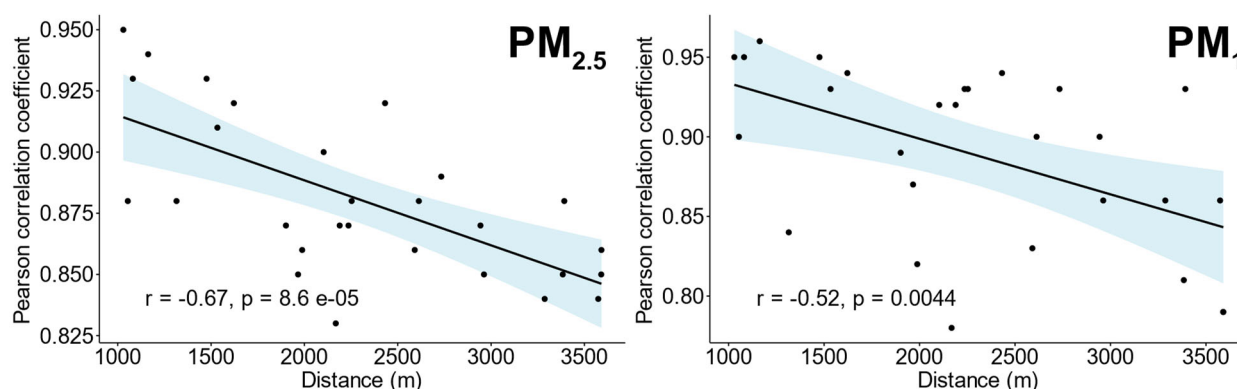


Figure 26. Distances in meters (A), PM<sub>2.5</sub> (B) and PM<sub>1</sub> (C) correlation matrixes for the LCS and the reference (hourly values).

Strong correlations were found between the sensors' PM levels and the reference, ranging from 0.84 to 0.89 for PM<sub>2.5</sub> and from 0.82 to 0.93 for PM<sub>1</sub>. The sensors showing the weakest correlations with the reference were Abbaye and City center. The correlations between the PM values of two sensors were associated with the distance between them, specifically for PM<sub>2.5</sub> (Figure 27).



**Figure 27. Scatterplot of Pearson correlation coefficient between sensors (including reference monitor) for PM levels versus distance between them, with linear regression and 95% confidence interval.**

We observed that the correlation was weaker for  $PM_1$  ( $r = -0.52$ ,  $p\text{-value}=0.0044$ ) than for  $PM_{2.5}$ .

### 4.3.3 PM ratios

In order to calculate PM ratios, PM concentrations were compared with reference values to standardize PM concentrations. This allowed us to focus on local variations in relation to the reference, in order to identify potential concentration hotspots within specific urban areas. When checking the average hourly distribution of PM by sensor (Figure 28), we observed diurnal variations with a minimum between 7-9 a.m. and a maximum around 7-8 p.m. for most LCS. We also observed that there was more heterogeneity among sensors during the evening peak than during the morning peak. In the morning, the peaks occurred at 6 a.m., whereas, in the afternoon, they were more spread out. For Clemenceau, there was an evening peak at 4 p.m., whereas for other sensors, such as Bachelard or Saint-Bruno, the peak occurred later. The Mistral sensor showed very few diurnal variations, and its signal remained relatively constant, except during the 6 a.m. morning peak.

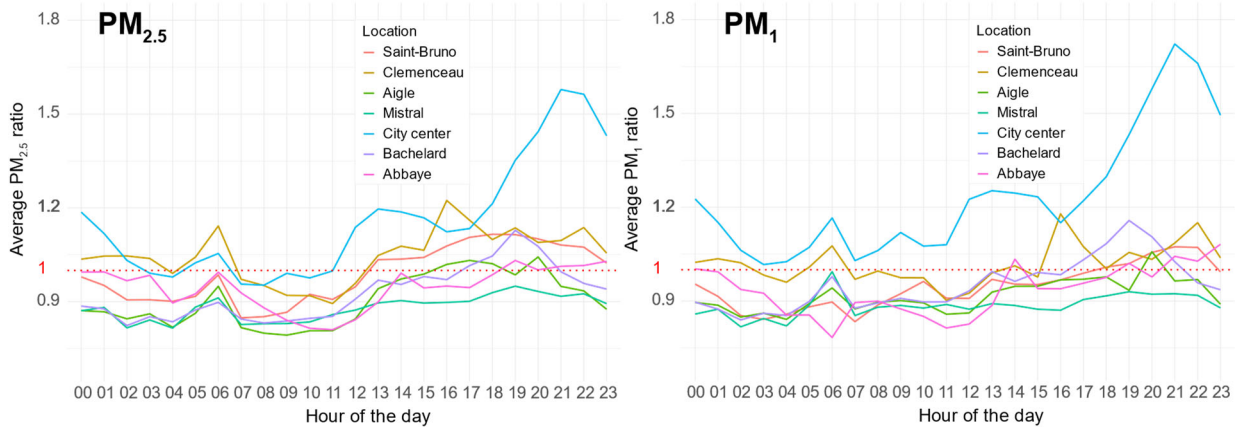


Figure 28. Average hourly  $PM_{2.5}$  ratios across all deployment locations

On the city center sensor, we observed two important peaks, one at 1 pm and one at 9 pm. They seemed to correspond to the operational hours of a nearby restaurant. The 9 pm peak was 30% more important than the 1 pm spike. These peaks disappeared on Sundays when the restaurant was closed. In the same street, there was also a bakery that might have contributed to some emissions. These PM spikes seemed to influence PM concentrations throughout the day and night, especially for  $PM_1$ . This was likely due to the lack of pollutant dispersion in this narrow street. The LCS in Clemenceau might have been influenced by traffic, as we observed a first evening peak at 4 p.m., which might have been associated with commuting from work. The sensor was located on one of Grenoble's main boulevard but on the courtyard side. Clemenceau and City center sensors appeared to stand out from the rest, as confirmed by a spatial clustering analysis using the k-means method. Figure 29 illustrates the categorization of LCS into three clusters where, for  $PM_{2.5}$ , Clemenceau and City center sensors appeared to behave differently from the rest of the network, while for  $PM_1$ , Abbaye and City center were separated from the others.

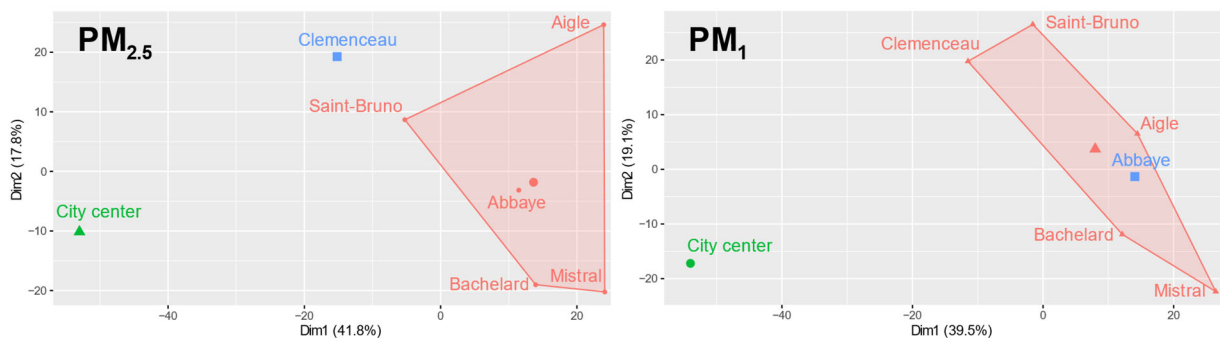
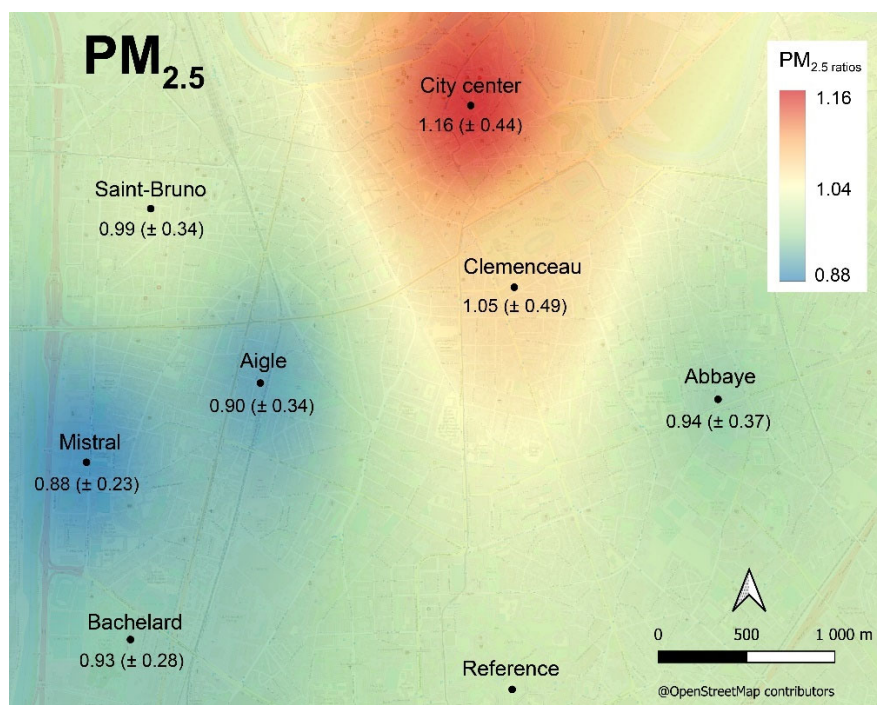


Figure 29. Sensors clustering using k-means on PM ratios.



The average  $PM_{2.5}$  ratios per LCS were placed on a map (Figure 30) where ratios were interpolated using Inverse Distance Weighting (IDW) in QGIS 3.28.3. This technique enabled the identification of elevated local PM concentrations surpassing reference background levels, potentially resulting in PM overexposure for individuals. It seemed that the proximity to the city center could be a factor in determining ratios. Ratios for the different LCS were compared using a Wilcoxon test, and the results were placed under Figure 30.



**Figure 30.  $PM_{2.5}$  ratio landscape by IDW interpolation** The numbers represent the mean  $PM_{2.5}$  ratios per sensor (with their standard deviation into brackets). All devices exhibited significantly different ratios ( $p < 0.05$ , Wilcoxon's test) except Mistral, statistically similar with Aigle. Bachelard was also similar with Abbaye.

When considering  $PM_1$  (Figure 31), LCS close to the city center also appeared to be more exposed, with the Bachelard sensor showing values equivalent to that of Saint-Bruno. These maps confirmed the existence of a hotspot in the city center, as well as low PM levels areas around Aigle and Mistral, meaning that there was a low contribution of local sources in these areas.



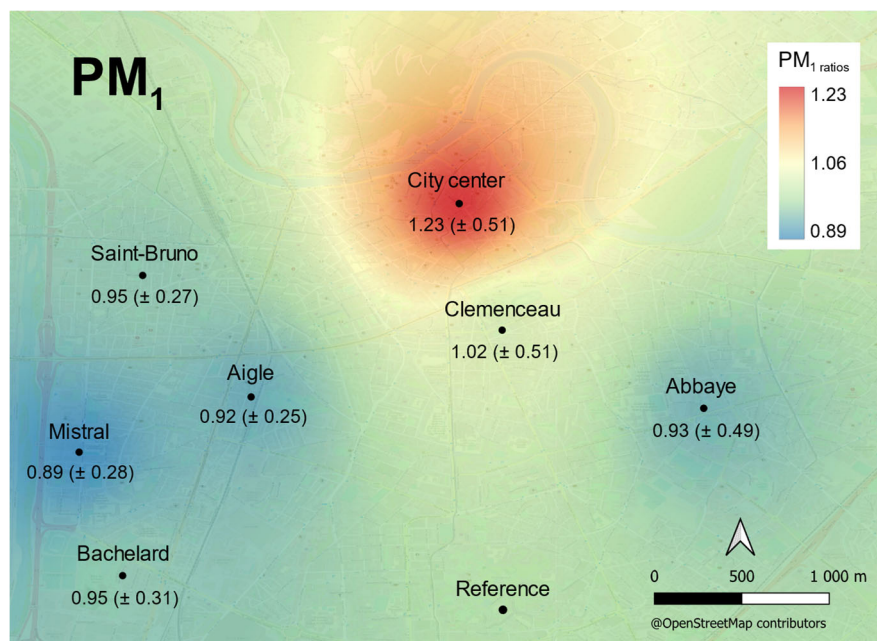


**Figure 31. PM<sub>1</sub> ratio landscape by IDW interpolation.** The numbers represent the mean PM<sub>1</sub> ratios per sensor (with their standard deviation into brackets). All devices exhibited significantly different ratios ( $p < 0.05$ , Wilcoxon's test) except Bachelard, statistically similar with Saint-Bruno or Abbaye. Aigle was also statistically similar with Abbaye.

Depending on the neighbourhood, significant exposure differences could be observed, with average PM ratios varying by a factor of 1.4 (28%) for PM<sub>1</sub> and 1.3 (24%) for PM<sub>2.5</sub>.

## 4.4 DISCUSSION

### 4.4.1 Main findings

In this study, we found that the correlation between the PM values of two sensors was generally influenced by the distance between them. The most correlated sensors were generally in close proximity to each other. However, the proximity effect on the correlation between sensors was weaker for PM<sub>1</sub> ( $r = -0.52$ ) than for PM<sub>2.5</sub> ( $r = -0.67$ ), which might suggest higher local contributions for PM<sub>1</sub> than for PM<sub>2.5</sub>. Dimitriou et al. (2023) also found significant correlations between sensors within a city ( $r$  from 0.62 to 0.97), and between different cities ( $r$  from 0.31 to 0.72), but they did not study distances between LCS. They attributed these strong intra-city

correlations to similar pollution sources, transport and dispersion conditions. Kosmopoulos et al. (2022) underlined that, in the warm season, regional transport played a significant role, accounting for around 80-85% of  $PM_{2.5}$  in the city center. This could explain the good correlations between sensors. Perillo et al. (2022) also found good correlations ( $r > 0.71$ ) for  $PM_{2.5}$  among multiple sites in Dublin (Ireland). The high correlations we observed between the sensors and the background reference (from 0.84 to 0.89 for  $PM_{2.5}$  and from 0.82 to 0.93 for  $PM_1$ ) highlight the low influence of local factors, with a substantial impact of urban and regional background. These values were higher compared to those observed by Gitahi and Hahn (2022), whose maximum correlations between LCS and references ranged between 0.68 and 0.78. This could be due to the lack of standardization in the installation criteria for their LCS, installed by citizens. In our study, the city center emerged as a hotspot, exhibiting elevated levels of  $PM_1$  and  $PM_{2.5}$ , along with higher ratios when compared to the reference. Zuurbier et al. (2010) analysed commuters' exposure to PM and found that particle number counts were higher than background levels in the city center, which they attributed to street canyon effect caused by high buildings. In our case, these high exposure levels seemed to be associated with specific time intervals, suggesting a link with a restaurant activity. In a similar LCS network study, Kosmopoulos et al. (2022) also observed that locations experiencing the highest  $PM_{2.5}$  levels were not situated in high traffic density areas, but in pedestrian-only zones with high concentrations of restaurants. PM spikes caused by restaurants also seemed to influence PM concentrations throughout the day and night, as  $PM_{2.5}$  concentrations in these areas were higher than elsewhere. In the same city, Siouti et al. (2021) found the highest concentration of cooking organic aerosols in an area with high restaurant density. They also calculated that half of the daily cooking organic aerosol occurred during diner time (from 9 pm to midnight), while approximately 25% during lunch time (1-4 pm). This distribution appears similar to what we observed in Grenoble with the city center sensor, although the peak occurred earlier in the evening. The elevated PM values could also be attributed to a mountain-side stagnation phenomenon, as elucidated by Le Bouëdec (2021). The PM levels appeared to persist at lower, yet still significant, values outside of the restaurant's operating hours. Regarding PM ratios, we observed two distinct areas with a hotspot in the city center and low local emissions areas in the western part of the city. Ventilation could play a role, as a  $PM_{10}$  stagnation area was identified in the foothills of the Chartreuse mountain, not far from the city center, by Le Bouëdec (2021). To further confirm or refute this hypothesis, additional sensors would need to be deployed across this area. In our study, the spatial variabilities of the ratios did not seem to be associated with traffic or

proximity to major roads. For instance, Mistral, Bachelard and Aigle sensors were located in areas with major traffic arteries, but brought few local contributions to PM levels, eventually suggesting a protective effect from the barrier of trees or buildings. Clemenceau however could be influenced by traffic. Gitahi and Hahn (2022) found that sensors located near major roads presented higher PM levels than the ones situated in the background areas. We also noticed a greater PM concentrations heterogeneity during the evening peak compared to the morning peak. This variability could be associated with ventilation patterns or proximity to major roads. Levels of PM exposure can vary considerably based on residential location, with ratios spanning from 0.89 to 1.23 for  $PM_1$  and 0.88 to 1.16 for  $PM_{2.5}$ . This accounts for a 28% difference in exposure to  $PM_1$  and a 24% difference for  $PM_{2.5}$ , which is significant when calculating health risks. An interesting outcome of this study was that urban hotspots can be non-related to traffic. This was also highlighted by ElSharkawy and Ibrahim (2022) measuring high levels of pollutants ( $CO$ ,  $CO_2$ , VOCs,  $NO_2$ ,  $SO_2$ ) close to grilling restaurants. However, they did not measure PM in their study. Robinson et al. (2018) measured organic aerosol (OA), a major component of  $PM_{2.5}$  and detected high concentrations of OAs hundreds of meters downwind from certain restaurants, underscoring the potential of these sources to impact air quality at the neighbourhood level. Our observations further confirm those results, highlighting the importance of improving emission control measures.

#### 4.4.2 Study limitations

Our work emphasizes the importance of calibration that should be comprehensive to minimize data losses. In our case, restricting the study to summer and spring seasons resulted in half of the dataset being not included in the analyses. It is crucial to consider similar PM levels during the calibration process to those encountered during deployment. Proper calibration across a wide range of conditions is important (Gitahi & Hahn, 2022), otherwise, a significant portion of the dataset may become difficult to analyse. Molina Rueda et al. (2023) also recommended calibrating sensors with similar environmental conditions (temperature, relative humidity...), and resembling pollution sources to the ones under which the LCS will be deployed. Regarding our calibration, the changing shape of the scatterplots at  $PM_{2.5}$  levels of 30-40  $\mu g/m^3$  (Figure 23) was also observed in other studies using PMS7003 (Cowell et al., 2022; Dejchanchaiwong et al., 2023). Searle et al. (2023) identified a bias in  $PM_{2.5}$  concentrations below 16  $\mu g/m^3$ , further confirming our observations suggesting a diverging behaviour between values below and above that threshold.

Kelly et al. (2017) reported that some LCS begin to exhibit a non-linear response at high PM concentrations ( $>40 \mu\text{g}/\text{m}^3$ ). Specific calibration algorithms seem to be needed for those values. Wang et al. (2023) acknowledged the same limitations in their study, and recommended having the broadest possible air quality range during calibration to address air pollution variability in deployments. Our research also underscored the importance of minimizing LCS downtime and optimizing sensor maintenance to ensure an adequate dataset for meaningful comparisons. Implementing automatic alerts notifying us when a sensor malfunctions and providing users training can be valuable in reducing offline times. Increasing common sensors operational time periods is an assurance of quality for data analysis. Lastly, in order to improve our study, it would be beneficial to upgrade the relative humidity sensors. They had to be changed at the beginning of the deployment and using more robust sensors would be recommended. We also attempted to calibrate PM readings using an external relative humidity monitor from ROMMA (Réseau d'Observation Météo du Massif Alpin, 2022). However, the use of internal humidity sensors yielded better results, likely because they were located within the air quality station near the PM optical sensor. There is an urgent need for research on humidity sensors, as they may also introduce uncertainties in calibrated values.

## 4.5 CONCLUSION

This work underscores the critical importance of ensuring the quality of preliminary calibration to achieve accurate predictions and a comprehensive data analysis. In this study, focussing on spring and summer, PM levels measured by the LCS and the reference monitor were strongly correlated. LCS exhibited high correlations with each other, which seemed to be related to distance between them, especially for  $\text{PM}_{2.5}$ . These findings highlight a significant regional impact on PM levels during spring and summer. Moreover, diurnal fluctuations in PM ratios were seen with a 7-9 am minimum and a 7-8 pm maximum. The city center exhibited the highest PM levels and ratios, with evening spikes around 9 pm, probably due to restaurant activities. LCS seem appropriate to identify air pollution hotspots, not necessarily related to traffic, and diurnal variations. In summary, LCS networks allow to collect more comprehensive spatiotemporal data, facilitating the identification of exposure disparities within a city. These differences must be considered when conducting a health risk analysis.

## 4.6 ACKNOWLEDGEMENTS

We warmly thank all individuals who have agreed to host a sensor. We would also like to warmly acknowledge Atmo Auvergne-Rhône-Alpes for our collaboration.

### Summary - Results Chapter 4

- Calibration should be as wide as possible to cover deployment conditions;
- In this spring – summer study:
  - Diurnal variations: 7-9 am minimum & 7-8 pm maximum (9 pm in city center);
  - Spatial variations: city center sensor exhibited highest PM levels and ratios due to aerosols emitted by restaurants;
- LCS enable a finer spatiotemporal mapping of PM exposure.

## 4.7 APPENDIX

Appendix 1. Calibration formulas for PM<sub>2.5</sub> concentrations (in bold, the formula used for this chapter)

Metrics on the test dataset					
Sensor	Technique	Formula	R <sup>2</sup>	RMSE (µg/m <sup>3</sup> )	NRMSE (%)
14504557_clemenceau	<b>MLR</b>	<b>PM<sub>2.5</sub> Ref ~ PM<sub>2.5</sub> * RH</b>	<b>0.91</b>	<b>0.73</b>	<b>12.6</b>
	RFR	PM <sub>2.5</sub> Ref ~ PM <sub>2.5</sub> + RH + T	0.90	0.78	13.4
14507343_smh	<b>MLR</b>	<b>PM<sub>2.5</sub> Ref ~ PM<sub>2.5</sub> * RH</b>	<b>0.92</b>	<b>0.69</b>	<b>12.0</b>
	RFR	PM <sub>2.5</sub> Ref ~ PM <sub>2.5</sub> + RH + T	0.90	0.81	14.0
14576390_aigle	<b>MLR</b>	<b>PM<sub>2.5</sub> Ref ~ PM<sub>2.5</sub> * RH</b>	<b>0.93</b>	<b>0.66</b>	<b>11.4</b>
	RFR	PM <sub>2.5</sub> Ref ~ PM <sub>2.5</sub> + RH + T	0.9	0.76	13.2
6816708_bachelard	MLR	PM <sub>2.5</sub> Ref ~ PM <sub>2.5</sub> * RH	0.9	0.76	13.1
	<b>RFR</b>	<b>PM<sub>2.5</sub> Ref ~ PM<sub>2.5</sub> + RH + T</b>	<b>0.93</b>	<b>0.65</b>	<b>11.3</b>
7823097_abbaye	MLR	PM <sub>2.5</sub> Ref ~ PM <sub>2.5</sub> * RH	0.89	0.80	13.9
	<b>RFR</b>	<b>PM<sub>2.5</sub> Ref ~ PM<sub>2.5</sub> + RH + T</b>	<b>0.93</b>	<b>0.64</b>	<b>11.0</b>
6813993_mistral	MLR	PM <sub>2.5</sub> Ref ~ PM <sub>2.5</sub> * RH	0.90	0.75	12.8
	<b>RFR</b>	<b>PM<sub>2.5</sub> Ref ~ PM<sub>2.5</sub> + RH + T</b>	<b>0.92</b>	<b>0.68</b>	<b>11.7</b>
6814689_citycenter	<b>MLR</b>	<b>PM<sub>2.5</sub> Ref ~ PM<sub>2.5</sub> * RH * T</b>	<b>0.93</b>	<b>0.62</b>	<b>10.6</b>
	RFR	PM <sub>2.5</sub> Ref ~ PM <sub>2.5</sub> + RH + T	0.93	0.65	11.2
12725813_stbruno	<b>MLR</b>	<b>PM<sub>2.5</sub> Ref ~ PM<sub>2.5</sub> * RH</b>	<b>0.93</b>	<b>0.65</b>	<b>11.1</b>
	RFR	PM <sub>2.5</sub> Ref ~ PM <sub>2.5</sub> + RH + T	0.91	0.73	12.5

Appendix 2. Calibration formulas for PM<sub>1</sub> concentrations (in bold, the formula used for this chapter)

Sensor	Technique	Formula	Metrics on the test dataset		
			R <sup>2</sup>	RMSE (µg/m <sup>3</sup> )	NRMSE (%)
14504557_clemenceau	<b>MLR</b>	<b>PM<sub>1,Ref</sub> ~ PM<sub>1</sub> * RH</b>	<b>0.94</b>	<b>0.53</b>	<b>11.4</b>
	RFR	PM <sub>1,Ref</sub> ~ PM <sub>1</sub> + RH	0.93	0.59	12.8
14507343_smh	<b>MLR</b>	<b>PM<sub>1,Ref</sub> ~ PM<sub>1</sub> * RH * T</b>	<b>0.93</b>	<b>0.57</b>	<b>12.4</b>
	RFR	PM <sub>1,Ref</sub> ~ PM <sub>1</sub> + RH	0.93	0.58	12.6
14576390_aigle	<b>MLR</b>	<b>PM<sub>1,Ref</sub> ~ PM<sub>1</sub> * RH</b>	<b>0.94</b>	<b>0.51</b>	<b>11.1</b>
	RFR	PM <sub>1,Ref</sub> ~ PM <sub>1</sub> + RH + T	0.92	0.59	12.7
6816708_bachelard	MLR	PM <sub>1,Ref</sub> ~ PM <sub>1</sub> * RH * T	0.93	0.56	12.0
	<b>RFR</b>	<b>PM<sub>1,Ref</sub> ~ PM<sub>1</sub> + RH + T</b>	<b>0.94</b>	<b>0.51</b>	<b>11.1</b>
7823097_abbaye	<b>MLR</b>	<b>PM<sub>1,Ref</sub> ~ PM<sub>1</sub> * RH * T</b>	<b>0.92</b>	<b>0.60</b>	<b>12.9</b>
	RFR	PM <sub>1,Ref</sub> ~ PM <sub>1</sub> + RH + T	0.91	0.63	13.5
6813993_mistral	MLR	PM <sub>1,Ref</sub> ~ PM <sub>1</sub> * RH * T	0.95	0.49	10.5
	<b>RFR</b>	<b>PM<sub>1,Ref</sub> ~ PM<sub>1</sub> + RH + T</b>	<b>0.95</b>	<b>0.47</b>	<b>10.1</b>
6814689_citycentre	MLR	PM <sub>1,Ref</sub> ~ PM <sub>1</sub> * RH * T	0.94	0.52	11.2
	<b>RFR</b>	<b>PM<sub>1,Ref</sub> ~ PM<sub>1</sub> + RH + T</b>	<b>0.94</b>	<b>0.52</b>	<b>11.1</b>
12725813_stbruno	<b>MLR</b>	<b>PM<sub>1,Ref</sub> ~ PM<sub>1</sub> * RH</b>	<b>0.92</b>	<b>0.58</b>	<b>12.3</b>
	RFR	PM <sub>1,Ref</sub> ~ PM <sub>1</sub> + RH + T	0.91	0.63	13.4

# 5 EXPOSURE TO PARTICULATE MATTER WHEN COMMUTING IN THE URBAN AREA OF GRENOBLE (FRANCE)

## 5.1 INTRODUCTION

- Background: Commuting contributes significantly to daily PM exposure, and more research is needed to understand how transport mode and locations affect PM exposure.
- Objectives:
  1. Compare PM<sub>1</sub> and PM<sub>2.5</sub> exposure across 4 transport modes (bike, walk, bus, tramway) in different 4 urban microenvironments;
  2. Investigate commuting mode, location, and time effects;
  3. Study the impact of street configuration and traffic;
  4. Compare inhaled PM doses across transport modes.

## 5.2 ARTICLE N°4

The following paper (Article n°4) is in preparation for journal submission. The bibliography is located at the end of the article (pp. 141-152), not at the end of the thesis manuscript.



# Exposure to particulate matter when commuting in the urban area of Grenoble (France)

*Marie-Laure Aix<sup>a</sup>, Méline Claitte<sup>b</sup>, Dominique J. Bicout<sup>c,\*</sup>*

<sup>a</sup> Univ. Grenoble Alpes, CNRS, UMR 5525, VetAgro Sup, Grenoble INP, TIMC, 38000  
Grenoble, France, [marie-laure.aix@univ-grenoble-alpes.fr](mailto:marie-laure.aix@univ-grenoble-alpes.fr)

<sup>b</sup> Univ. Grenoble Alpes, CNRS, UMR 5525, VetAgro Sup, Grenoble INP, TIMC, 38000  
Grenoble, France, [melaine.claitte@etu.univ-grenoble-alpes.fr](mailto:melaine.claitte@etu.univ-grenoble-alpes.fr)

<sup>c</sup> Univ. Grenoble Alpes, CNRS, UMR 5525, VetAgro Sup, Grenoble INP, TIMC, 38000  
Grenoble, France, [dominique.bicout@univ-grenoble-alpes.fr](mailto:dominique.bicout@univ-grenoble-alpes.fr)

## ABSTRACT.

Air pollution is a major contributor to mortality and chronic diseases worldwide. Particulate matter (PM) is one of the most dangerous air pollutants, contributing to an important part of mortality globally. It is well known that heterogeneity can be seen in urban PM concentrations, but few papers investigate the influence of transportation mode versus commuting times or locations in reducing PM exposure. Using low-cost sensors (LCS), we measured PM<sub>1</sub> (PM < 1 μm) and PM<sub>2.5</sub> (PM < 2.5 μm) levels in four different transport modes (bicycle, walk, bus, and tramway), across four different streets at three different times of the day. The goal was to better understand factors driving personal exposure to PM. During this study, conducted in spring with low PM levels, the transport mode had a greater impact on exposure to PM compared to the time of day or site. Whether considering PM concentrations ratios to reference levels (PM<sub>ratios</sub> = PM / PM<sub>Ref</sub>) or inhalation, active transport modes (bike, walk) were the most exposed, followed by bus and tramway. For PM<sub>ratios</sub>, the exposure order was the following: bike > walk > bus > tramway, but when considering inhalation, the rank changed to walk > bike > bus > tramway. The difference between active and passive modes also increased when examining inhalation, due to higher ventilation values for active commuters. Segregated bike lanes seemed to reduce cyclists' exposure to PM<sub>1</sub> by 16%. Separating bicycle lanes from roadways and facilitating access to the tramway should be prioritized. LCS can provide insights on PM exposure and their use should be encouraged for prevention purposes.

**KEYWORDS.** Particulate matter, Low-cost sensors, Inhaled dose, Mobility, Urban microenvironments.

## 1. INTRODUCTION.

### 1.1. Background information

About 70 to 90% of chronic health issues are probably due to environmental differences (Rappaport and Smith, 2010; Willett, 2002). Air pollution is a major contributor to those chronic diseases, responsible for 26% of respiratory infection fatalities, 25% of deaths from chronic obstructive pulmonary disease, and 16% of lung cancer-related deaths (World Health Organization, 2022). Urban development may amplify exposure to air pollution (Zhang et al., 2022), while vulnerability could rise due to aging populations and climate warming (United States Environmental Protection Agency, 2022; Xu et al., 2023).

Particulate matter (PM) is considered as one of the most dangerous components of air pollution (Borja-Aburto et al., 1997; Dockery et al., 1993; Raaschou-Nielsen et al., 2013; Samet et al., 2000). Studies support the significance of considering PM size, demonstrating that adverse effects are most pronounced when it comes to the smallest particles (Kim et al., 2015; Meng et al., 2013; Schraufnagel, 2020). People and decision makers would greatly benefit from gaining more knowledge about PM exposure. Unfortunately, official stations are not always representative of what individuals breathe, especially when placed in a background area (Kumar et al., 2017). The primary advantage of mobile PM sensors is to provide information about local sources affecting individual exposure. Real-time PM monitoring solutions offer people the opportunity to consciously adapt their behaviours, in order to reduce daily exposure. Addressing travel habits can be more convenient for individuals than changing their place of residence. Transport microenvironments often expose individuals to significantly higher pollutant levels than other places, resulting in a rapid and substantial increase in their daily exposure (Kaur and Nieuwenhuijsen, 2009). Chaney et al. (2017) found that commuting, while occupying 6-10% of the day, could contribute up to 12% of daily PM<sub>2.5</sub> exposure. Therefore, studying individuals' exposure during their journeys is crucial.

## 1.2. Research gap

Kaur et al. (2007) acknowledged that heterogeneity in air quality can be seen, even within a local urban area. They recognized that many studies focus on the transport mode, overlooking the potential impact of individual behavior on exposure. Intermodal comparison studies seem to be the main seminal work (Gelb and Apparicio, 2021). While numerous papers compare different transport modes (de Nazelle et al., 2012; Peng et al., 2021; Yu et al., 2012), very few specifically address site effects in comparison to mode influence. They do not directly investigate the comparative significance of transport mode versus specific locations in reducing PM exposure. Chaney et al. (2017) also highlighted the fact that few studies compared multiple modes of transportation simultaneously along a common route, making inter-modal comparisons difficult. But studies comparing multiple transport modes along various routes are even scarcer. A few papers were found that compared PM concentrations between different routes and transport modes. deSouza et al. (2021) conducted a study in Zhengzhou (China) that closely aligns with our research objective. They examined four modes (bike, taxi, subway, and bus) along diverse commuting routes. However, their study took place in China, where PM<sub>2.5</sub> levels were about 3.5 times higher than ours, they focused solely on rush hours, and they did not investigate PM<sub>1</sub>. A strength of their study was that they controlled for background PM<sub>2.5</sub>

variations by simultaneously monitoring transport modes on the same route, enabling direct mode-to-mode pollutant comparisons. Int Panis et al. (2010) also used a pairwise design along three different routes, assessing both busy and quiet areas but they only studied car drivers and cyclists. They observed location-driven differences : on one street, PM<sub>2.5</sub> concentration was significantly higher for the bike, while on another street, the concentrations were higher for the car. Hertel et al. (2008) and Li et al. (2017) assessed different routes but used different modes on each route. Qiu et al. (2019) studied different routes and modes, finding that traffic volume was significant for black carbon, but not for PM<sub>2.5</sub> or ultrafine particles. Zuurbier et al. (2010) compared PM concentrations between two routes with different traffic levels for several transport modes. Cyclists on the high-traffic route experienced 40% higher particle number counts than those on the low-traffic route. No significant difference was found in exposure to PM<sub>10</sub> and PM<sub>2.5</sub> but no measurement was made on PM<sub>1</sub>. Kaur et al. (2005) observed different PM<sub>2.5</sub> and ultrafine particle counts between a heavily trafficked route and a nearby backstreet, despite their proximity within 100m of each other. They attributed this difference to traffic density. Adams et al. (2001) also noted a significant difference in cyclists' exposure to PM<sub>2.5</sub> between the main route and a side street route. Further research is necessary to assess the relative importance of transportation mode and site in reducing exposure to PM, especially to PM<sub>1</sub>. It is now well known that transport mode plays a very important role in determining exposure to PM (Chan et al., 2002; Kaur and Nieuwenhuijsen, 2009), but few field studies have been considering the influence of modes and specific locations. The current literature on urban exposure in mobility also lacks research on PM<sub>1</sub> (Borghgi et al., 2021; Gelb and Apparicio, 2021; Guo et al., 2021), probably because few regulatory air quality authorities routinely measure PM<sub>1</sub>. Yet, Chen et al. (2017) indicated that most health effects of PM<sub>2.5</sub> can be attributed to PM<sub>1</sub> and emerging research suggests that PM<sub>1</sub> plays a more significant role in respiratory diseases (Song et al., 2022; C. Wu et al., 2022; Yang et al., 2020; Zwozdziak et al., 2016) or cardiovascular illnesses (Lin et al., 2016; Han Wu et al., 2022). Furthermore, there is a significant lack of air pollution studies comparing tramways with other modes, as already highlighted by Borghgi et al. (2021) in a systematic review. After searching over 150 mobility-related articles, we found only 3 studies focusing on PM in tramways (Asmi et al., 2009; Moreno et al., 2015; Strasser et al., 2018). Moreover, very few research papers take ventilation or inhalation into account, leading to poor exposure estimation (Gelb and Apparicio, 2021; Singh et al., 2021).

To our knowledge, this is the first study trying to investigate transport mode and site related variability on PM<sub>1</sub>. It seems important to better estimate PM<sub>1</sub> variability, especially because it's

known that higher levels of fine PM can be found near roadways (Lall and Thurston, 2006; Lee et al., 2006). Understanding transport mode and site-specific influence on PM levels could also help individuals adapt their travel behaviors. Chaney et al. (2019) highlighted a disparity between public assumptions and real PM<sub>2.5</sub> exposure levels in transport micro-environments. Ueberham et al. (2019) found an exposure awareness gap where most people underestimated PM exposure. They observed that knowledge about health impacts or road characteristics affected route choices and they recommended using smart sensing for exposure assessment.

### 1.3. Study objectives

The objective of this paper is to use portable sensors to better understand factors influencing personal exposure to PM. PM measurements were conducted with low-cost sensors, especially useful and popular for personal or local sources monitoring (Oyola et al., 2022). Our goal was to explore the impact of the transport mode and site on PM concentrations. This research analysed individual exposure levels to PM<sub>1</sub> and PM<sub>2.5</sub> in four urban microenvironments in Grenoble (France) across four commuting modes (bicycle, walk, bus, and tramway) at low PM levels (spring season). Additionally, we computed the inhaled dose of PM associated with each transport mode. Each site exhibited distinct traffic levels, and the study also aimed to explore the influence of street configuration. To achieve this goal, streets with medium-sized buildings and narrow streets with close proximity buildings were selected. In summary, the study aimed to compare different routes using various transport modes and identify the most significant variable: time of day, site or transportation mode.

## 2. MATERIALS AND METHODS.

### 2.1. Sampling design

#### 2.1.1. Sampling periods

The study was conducted in the urban area of Grenoble (France) in spring, during working days from April 25, 2022, to May 12, 2022. Ambient temperature recorded by sensors ranged from 14°C to 34°C (mean: 24°C), and relative humidity between 39% and 97% (mean: 58%). PM levels from background reference station were lower than during winter, with an average PM<sub>1 Ref</sub> value of 6.3 µg/m<sup>3</sup> and an average PM<sub>2.5 Ref</sub> value of 8.2 µg/m<sup>3</sup>. Measurements were recorded during three sessions: S1 in the morning (8-9 am), S2 at noon (12 pm -1 am), and S3 in the afternoon (4-5 pm). The sessions were selected to cover a broad range of traffic conditions and PM concentrations, while also aligning with displacement peaks in Grenoble. Figure 1 (A) illustrates the chosen experimental time slots (S1, S2, S3) along with travel statistics for

Grenoble residents from the 2019-2020 Household Travel Survey (CEREMA, 2022). These data provide an hourly count of individuals using different transport modes (walk, bicycle or public transport) for their journeys in Grenoble. Figure 1 (A) also includes local congestion statistics for car drivers depicted as travel times per kilometer sourced from TomTom (2022a).

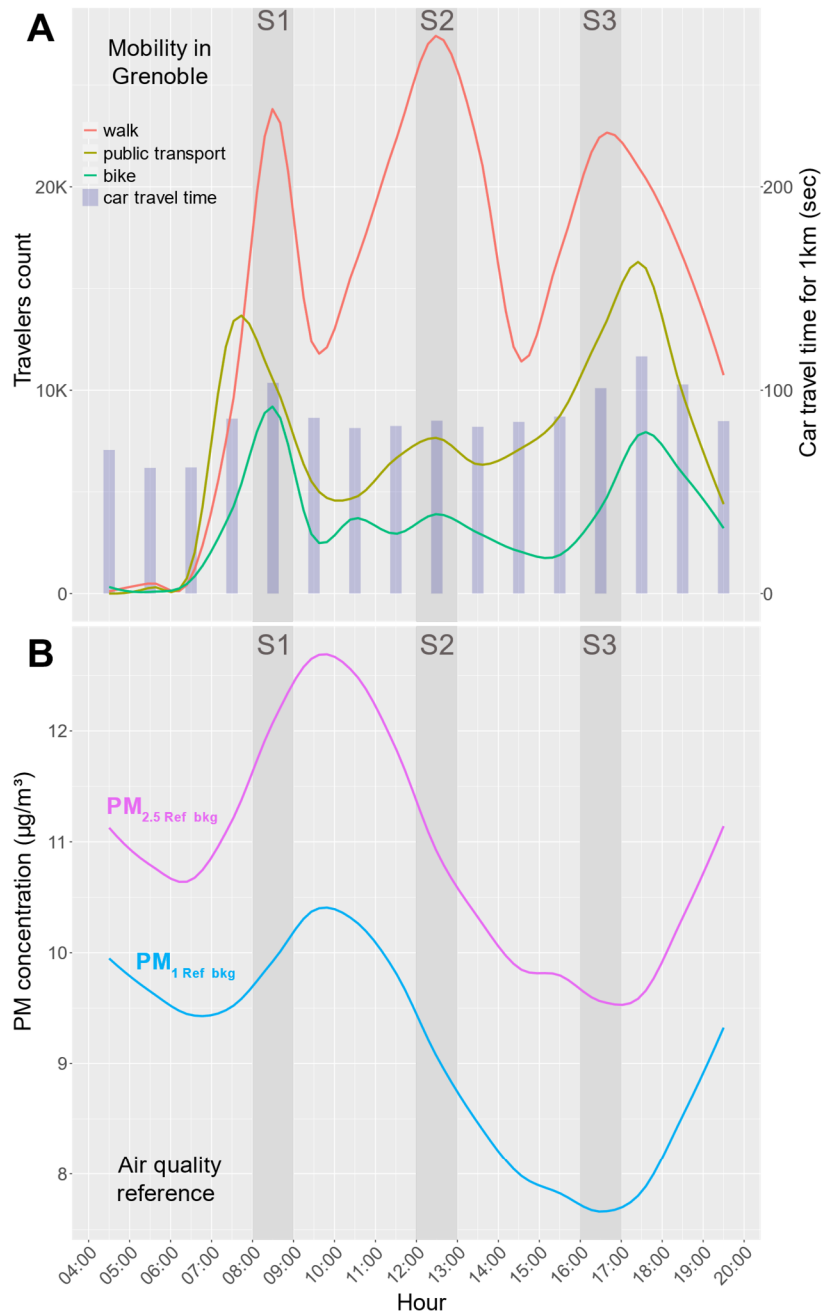


Figure 1. Temporal trends of hourly individual mobilities, car traffic and PM reference background concentrations in Grenoble. Data sources: (A) Number of travels by foot, bike or public transport: CEREMA (2022). Average travel time to drive 1km by car in Grenoble (in seconds : TomTom (2022a). (B) PM concentrations at background reference station (called “Les Frênes”): Atmo AuRA (2023).



Figure 1 (B) displays PM reference concentrations measured by Atmo Auvergne-Rhône-Alpes (Atmo AuRA), the local regulatory instance measuring air quality.

### 2.1.2. Characterization of study location and sampling routes

Grenoble (latitude: 45.188529, longitude: 5.724524) is a mountain valley city with 450,000 inhabitants. Focused on sustainable mobility, Grenoble is recognized as the leading major city in France for cycling (FUB, 2022). The train, often used to enter or leave Grenoble, provides connections between Grenoble and neighboring towns. For the purpose of this study, we chose to focus on four modes of transportation: bicycle, walk, bus, and tramway. The measurement routes were carefully chosen to include as much as possible transport modes and street configurations (Figure 2). However, covering all four transport modes was not always possible, as two roads (Abbé Grégoire or Raoul Blanchard streets) only had three transport modes available. Two major routes, Jean Pain Boulevard (JP) and Cours Jean Jaurès (JA), and two narrow streets, Abbé Grégoire (AG) and Raoul Blanchard (BL), were examined (see Table 1).

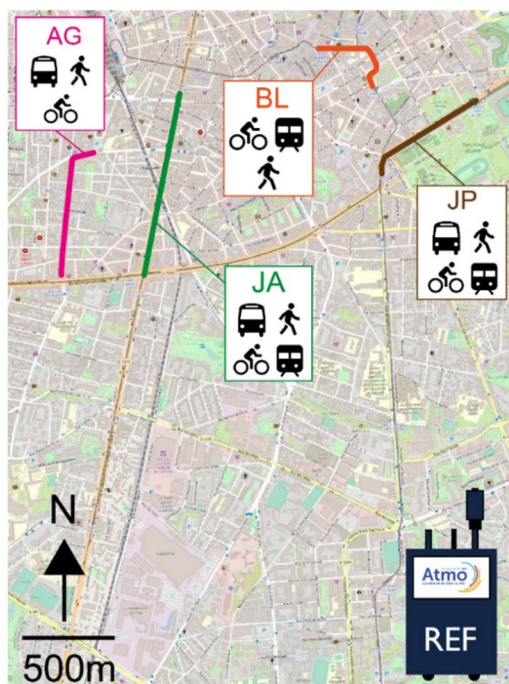


Figure 2. Map of sampling routes with transport modes and reference location. REF designates the background reference monitor (Atmo AuRA, station name: “Les Frênes”). JP refers to “Jean Pain boulevard”, JA to “Cours Jean Jaurès”, AG to “Abbé Grégoire street”, and BL to “Raoul Blanchard street”.

These four routes were carefully selected to enable a comprehensive comparison of the four transport modes and to represent different neighborhoods of Grenoble with both canyon and



non-canyon streets, low and high traffic streets. Urban science studies commonly use the street aspect ratio, defined as the ratio of the buildings (mean) height (H) by street (mean) width (W). Street canyons can be classified into three categories based on their depth-to-width (H/W) ratio: shallow ( $H/W \leq 0.5$ ), medium ( $0.5 < H/W < 2$ ), and deep ( $H/W \geq 2$ ) (Tomson et al., 2021). This street aspect ratio might affect pollutants distribution (Fu et al., 2017; Zhou et al., 2022). In our study, two sites displayed a shallow H/W ratio and two others had a medium street aspect ratio (Table 1). In Grenoble, it was not possible to find a deep canyon where we could compare the different transport modes. Traffic values were extracted from TomTom Traffic Stats (TomTom, 2022b) and represented the number of cars per working day from 7 am to 6 pm for the time period spanning from October 17, 2022, to October 28, 2022. Those traffic values were then recalibrated using a regression technique from Gilardi et al. (2023) using a multiplying factor of 0.075. The results were close to the values from the Grenoble metropolitan area for 2018 (Infogram, 2021).

Table 1. Routes characteristics with street dimensions, H/W ratio, lanes number, street length, number of dedicated lanes, and traffic (number of cars from 7 am to 6 pm).

Site	Mean width (m)	Mean height (m)	H/W	Lanes number <sup>1</sup>	Street length <sup>2</sup> (m)	Dedicated lanes	Traffic <sup>3</sup>
AG	10	11	1.09 (medium)	3	700	walk	2331
BL	12	9	0.76 (medium)	5	480	walk	3933
JA	40	16	0.39 (shallow)	8	1000	walk, tramway	12655
JP	45	4	0.08 (shallow)	10	550	bicycle, tramway, walk, bus	27089

<sup>1</sup>"Lane numbers" refer to the count of traffic lanes specifically allocated for bicycles, pedestrians, buses, tramways, and cars in each street. <sup>2</sup>Street length refers to average distances between trips start and end points per route for all transport modes, measured in meters. <sup>3</sup>Number of cars per working day from 7 am to 6 pm (TomTom, 2022b).

Being the narrowest streets, AG and BL had no dedicated lanes, except sidewalks for pedestrians, and all transport modes were mixed. On JA, we had a dedicated tramway lane and on JP, the widest street, all transport modes had dedicated lanes. On JP, the lanes for bicycles and pedestrians were far from the cars compared to the other sites. In summary, AG is a residential street with a low traffic volume and high buildings. BL is a street with low circulation, surrounded by high buildings. JA is Grenoble's longest boulevard, with lighter

traffic than JP, but it is surrounded by buildings. It features numerous intersections, shops and restaurants. JP is Grenoble’s most trafficked arterial road, surrounded by low-rise buildings and a large park, featuring an open street configuration. Figure 3 depicts the different routes.

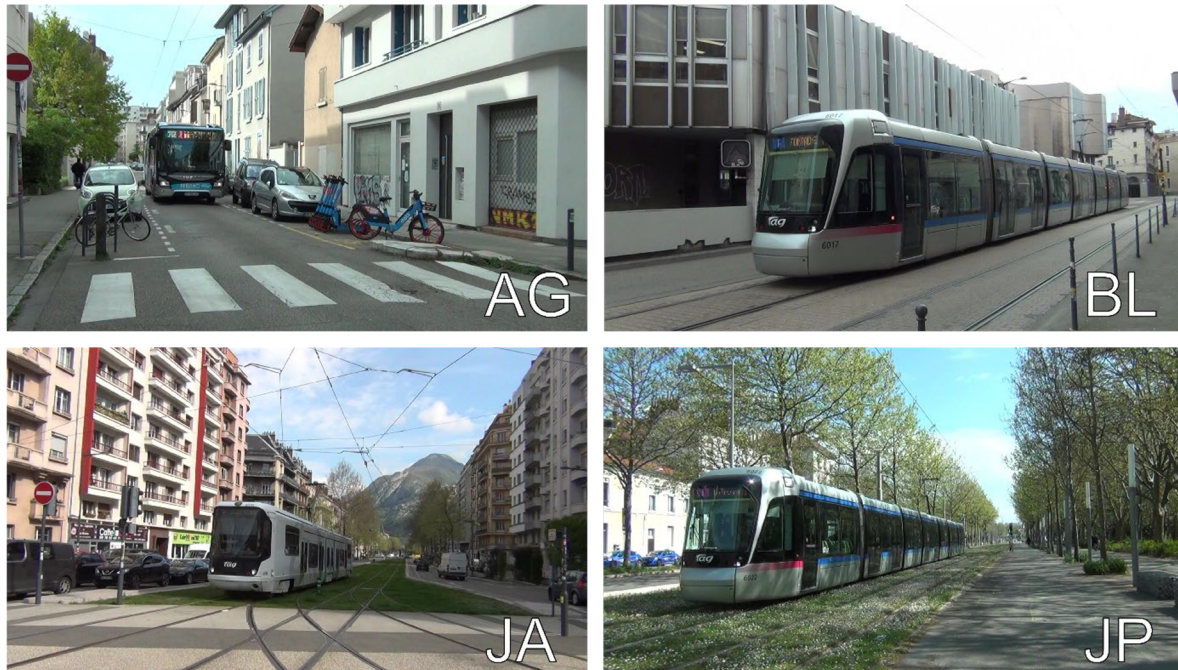



Figure 3. Typical pictures of the four routes. AG refers to “Abbé Grégoire street” (H/W ratio = 1.09). BL stands for “Raoul Blanchard street” (H/W ratio = 0.76). JA refers to “Cours Jean Jaurès” (H/W ratio = 0.39), and JP to “Jean Pain boulevard” (H/W ratio = 0.08).

### 2.1.3. Protocol

Two researchers, equipped with PM and heart rate sensors, conducted measurements while traveling simultaneously along identical routes with distinct transport modes. Each sampling trip consisted of traveling from the starting point to the endpoint on the designated route. A trip did not include waiting times at bus or tramway stops. Measurements were collected for 3 to 4 non-consecutive days at each site. This was influenced by the time constraints of the study, allowing for a total duration of two weeks (10 working days), as well as the limited number of experimenters available (two operators). Few measurement sessions had to be cancelled due to rainy conditions and were rescheduled accordingly (Table 2).

Table 2. Sampling design with dates, timings (S1, S2, S3) and sites (AG, BL, JA, JP).

	S1 8:00 - 9:00	S2 12:00 - 13:00	S3 16:00 - 17:00
2022-04-25	JP	JP	JP
2022-04-26	JA	JA	JA
2022-04-27	BL	BL	BL
	AG	AG	AG
2022-04-28	JP	JP	JP
2022-04-29	JA	JA	JA
2022-05-02	AG	AG	AG
	BL	BL	BL
2022-05-03	JA	JA	JA
2022-05-04	Canceled 		
2022-05-05			
2022-05-06	JP	JP	JP
2022-05-11	JA	JA	JA
2022-05-12	AG	AG	AG
	BL	BL	BL

A total of 410 trips were monitored by both experimenters (Table 3), with durations ranging from 50 seconds to approximately 18 minutes. Studies explored the required number of repetitions on an axis to achieve representative sampling (Anowar et al., 2017; Van den Bossche et al., 2015). Both reached similar conclusions, indicating that 17 passages are needed to obtain a representative sample (Gelb and Apparicio, 2021). In our experimental design, we ensured a minimum of 18 passages per site and per mode.

Table 3. Number of trips (with percentage), trip duration in seconds and trip length in meters (mean  $\pm$  standard deviation) by commuting mode

Transport mode	Number of trips	Trip duration (s)	Trip length (m)
Walk	138 (34%)	533 $\pm$ 168	718 $\pm$ 189
Bike	104 (25%)	179 $\pm$ 61	722 $\pm$ 235
Bus	82 (20%)	224 $\pm$ 106	797 $\pm$ 228
Tramway	86 (21%)	170 $\pm$ 65	745 $\pm$ 246

We used a time activity diary alongside sensors measurements to document the transport modes used (Table S.1). In this diary, we also reported the presence of idling cars, smokers, smells from restaurants, waiting times at traffic lamps or intersections, along with their respective timestamps.



## 2.2. Measuring instruments

PM concentrations were measured with two AirBeam2 portable air monitors, each costing about 350 euros and manufactured by HabitatMap, a non-profit environmental organization (HabitatMap, 2022). AirBeam2 devices were attached to the experimenters' backpacks at a height of 135cm above the ground, recording PM concentrations ( $PM_1$ ,  $PM_{2.5}$ ,  $PM_{10}$ ), temperature, and humidity every second. All the measurements were displayed on an open-source platform ([www.aircasting.org/map](http://www.aircasting.org/map)). AirBeam2 is built in with a PMS7003 sensor, which has been demonstrated to provide quality measurements for  $PM_{2.5}$  and  $PM_1$  but less reliable for  $PM_{10}$  (Aix et al., 2023). Thus, this study mainly focuses on  $PM_{2.5}$  and  $PM_1$ . AirBeam2 has been successfully used in studies, demonstrating good correlation with reference devices (Mukherjee et al., 2019; South Coast Air Quality Management District, 2018). Lim et al. (2019) used AirBeam2 to model urban street-level air quality with high spatial resolution using machine learning and reached a  $R^2$  value of 0.80. Both mobile sensors were calibrated independently with the "Golden Sensor method", where a carefully calibrated sensor ("gold pod") is used to calibrate the other sensors within the network (Bean, 2021). The first step of the calibration process was the gold pod calibration with an official reference station from Atmo AuRA. The gold-pod used the same PM optical sensor as the AirBeam2 (PMS 7003). More details on the calibration methodology can be found in (Aix et al., 2023) and results can be seen in Table S.2 (Step 1). In a second step, the AirBeam2 were collocated with the gold-pod from September 20, 2022 to November 3, 2022. We tested Random Forest Regression (RFR) and Multilinear Regression (MLR), and the best models involved RFR with temperature and humidity (see Table S.2, Step 2).  $R^2$  and RMSE (Root Mean Square Error) served as performance metrics, RMSE reflecting the accuracy as the closeness between the AirBeam2 and the calibrated gold-pod. For  $PM_1$ , we achieved an  $R^2 = 0.99$  for both devices, with RMSE of  $0.29 \mu\text{g}/\text{m}^3$  and  $0.28 \mu\text{g}/\text{m}^3$ . For  $PM_{2.5}$ , we obtained an  $R^2$  of 0.99 or 0.98 depending on the device, with RMSE of  $0.37 \mu\text{g}/\text{m}^3$  and  $0.32 \mu\text{g}/\text{m}^3$ . All those metrics reflected good accuracy and overall sensors performance. Those calibration algorithms were further used to correct raw data obtained from AirBeam2. Hourly PM reference values were retrieved from a background reference monitor (Fidas Palas GmbH 200) from Atmo AuRA situated in a park of Grenoble, 3km away from the experimental sites (see Figure 2). The reference data were collected using an online and publicly accessible Application Programming Interface (Atmo AuRA, 2023). In addition, we also used heart rate sensors (Polar OH1) to estimate ventilation, capturing heart rate (HR) measurements every second, and coupled with a GPS device.

### 2.3. Data cleaning

AirBeam2 sensors measurements had a 1-s resolution and did not exhibit any noise. Therefore, AirBeam2 raw data were used as such. The heartbeats measurements were also recorded at a 1-second resolution, and could be readily synchronized with the sensor's measurements. The reference PM concentrations were provided at an hourly frequency. By interpolating the reference values down to a 1-second scale, continuity with other datasets was ensured, resulting in a unified dataset with 1-second resolution. Transport modes were manually assigned to PM measurements based on the time activity diary (Table S.1), since the sensors did not automatically provide that information. Recorded heartbeats were associated with PM measurements and all the timestamps were converted to local (Paris) time. Before starting calculations involving PM<sub>2.5</sub>, a methodology developed by Aix et al. (2023) was applied to check the presence of dusts through Copernicus data (Météo-France, 2020) given the acknowledged impact of dusts on PM<sub>2.5</sub> measurements when using low-cost sensors (Giordano et al., 2021; Hassani et al., 2023; Molina Rueda et al., 2023).

### 2.4. Data treatment

After cleaning, raw PM values were calibrated as explained in Section 2.2. Most of the calculations were done without removing outliers because the study objective was to assess the complete exposure burden experienced by commuters. However, for specific calculations assessing traffic or street configuration influence (section 3.2.4), outliers were temporarily removed using the 1.5 times the interquartile range (IQR) method. Outliers were identified as data points exceeding 1.5 times the IQR above the third quartile (Q3) or below 1.5 times the IQR beneath the first quartile (Q1), and subsequently excluded. This approach allowed to mitigate the potential influence of extreme values, like those associated with smokers or restaurants.

### 2.5. Exposure calculations

In a first descriptive part (section 3.1), PM<sub>1</sub> concentrations were analysed. In a second part (section 3.2), we computed the ratio of each PM<sub>1</sub> measurement to the corresponding background reference level (PM<sub>1 Ref</sub>), following a methodology already used by various authors (Adams et al., 2001; Chaney et al., 2017; Huang et al., 2012; Larson et al., 2007). This approach helps characterize excess PM concentrations above the reference and normalize data to remove day-to-day variations, especially those related to weather. This allows to attribute any variation in PM to local sources, topography or microscale meteorology (Thai et al., 2008). Accounting

for background pollution is crucial in studying local variations of exposure (Gelb and Apparicio, 2021), and this method is especially suitable for assessing the importance of sites or modes. The ratios of each PM concentration to the corresponding background levels for each second were computed:

$$PM_{1\ ratio} = \frac{PM_1}{PM_{1\ Ref}} \quad (1)$$

$$PM_{2.5\ ratio} = \frac{PM_{2.5}}{PM_{2.5\ Ref}} \quad (2)$$

To better assess the PM mixture in different commuting microenvironments, we also calculated the  $PM_{1/2.5}$  fraction per second:

$$PM_{1/2.5} = \frac{PM_1}{PM_{2.5}} \quad (3)$$

Then, we normalized it with respect to the reference fraction using a specific formula:

$$PM_{1/2.5\ ratio} = \frac{PM_1}{PM_{2.5}} \bigg/ \frac{PM_{1\ Ref}}{PM_{2.5\ Ref}} \quad (4)$$

Following data visualization using boxplots, nonparametric rank sum Wilcoxon tests were employed to compare various groups. This facilitated the identification of significant differences between sessions, modes, or sites, with p-values below 0.05 being considered statistically significant. In the boxplots, where useful, we included geometric means to mitigate the influence of outliers.

## 2.6. Inhalation doses assessment

PM concentration measurements provide insights into the amount of PM present in an individual's environment. However, these measurements do not directly indicate the actual quantity of PM entering the body. To estimate the inhaled dose accurately, factors like activity and ventilation levels must be considered (Int Panis et al., 2010).

### 2.6.1. Estimation of ventilation values

Ventilations values can be estimated using HR (Ramos et al., 2015; Zhu et al., 2022; Zuurbier et al., 2009). In their study, Cruz et al. (2020) observed strong correlation values ( $R^2 = 0.92$ ) between ventilation and HR, successfully deriving an equation that was close to a previously proposed formula by Zuurbier et al. (2009). However, Cruz et al. (2020) considered their equation more precise as it incorporated a wider range of exercise intensities and a larger dataset. As a result, they formulated the following equation:

$$VE = e^{1.16 + 0.021 * HR} \quad (5)$$

where VE is the minute ventilation in  $L \cdot \text{min}^{-1}$  and HR the heart rate in beats per minute (bpm). Heart rates measured from the experimenters served as a basis to estimate minute ventilations with this formula. Both experimenters had different heart rates, even when using the same transport mode. Heart rates can depend on factors like age, fitness level, hormones or stress. An experimenter consistently had lower heart rates and, consequently, lower ventilations than the other. Therefore, it was necessary to compute average ventilation values per modes. However, the experimenters did not use each transport mode an equal number of times. One experimenter might have used a specific mode more frequently than the other, leading to a greater number of heart rate measurements for that user in this particular mode. To mitigate these effects and harmonize the number of ventilations assigned to each experimenter per mode, ventilation values were derived with the `sample()` R function. This adjustment aimed to achieve parity in the number of minute ventilations assigned to each experimenter per transport mode. Following this adjustment, four mode-specific average ventilation values were extracted.

### 2.6.2. Inhaled dose calculation

Furthermore, we calculated the duration in time and kilometers per trip, along with the average PM values. We then applied the mean ventilations previously computed using the following formula to derive an average inhaled dose per minute (Boniardi et al., 2021; Borghi et al., 2020) :

$$D_{min} = C * VE \quad (6)$$

Where D is the PM inhaled dose per minute ( $\mu\text{g}/\text{min}$ ), C the PM concentration ( $\mu\text{g}/\text{m}^3$ ), and VE the minute ventilation ( $\text{m}^3/\text{min}$ ). Inhalation was computed for each 410 individual trips. All data analyses were performed with RStudio 2023.06.1 (R Core Team, 2023).

## 3. RESULTS

### 3.1. $\text{PM}_{10}$ concentrations

To smooth out inter-day differences, the results from various days were aggregated by session and transport mode to examine the impact of those variables.

#### 3.1.1. Transport mode effect

This first part aimed to better understand the effect of the transport mode on the exposure to  $\text{PM}_{10}$ . From Figure 4, we see that bikes had the highest exposure levels, followed by pedestrians (-3% compared to bike), bus users (-11% versus bike) and tramway commuters (-15%).



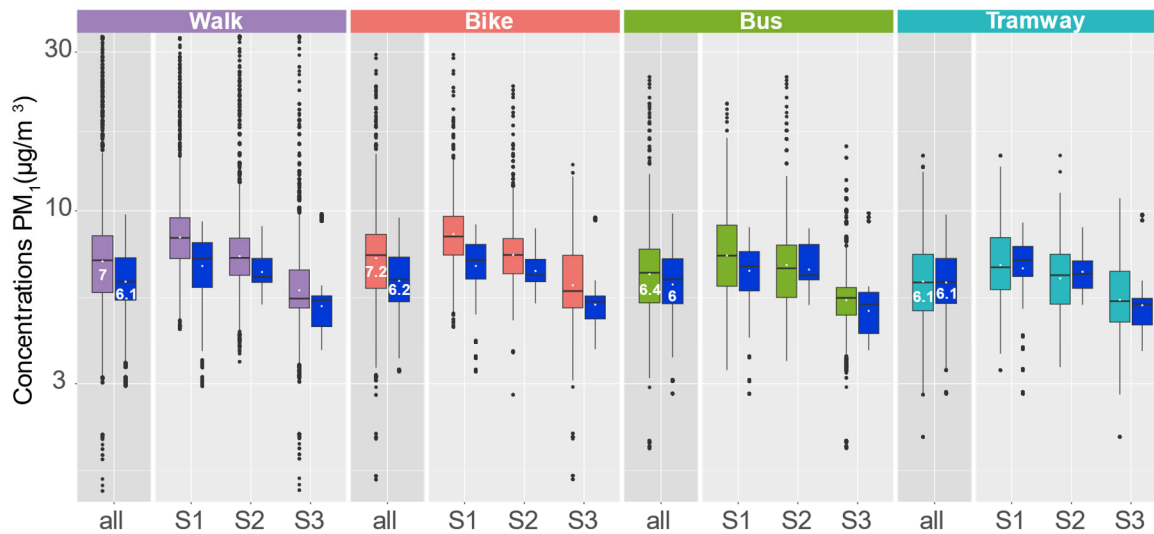


Figure 4. Boxplots of  $PM_1$  concentrations measured by the AirBeam2 and the reference station (darkblue) for the different transport modes and sessions. A logarithmic ( $\log_{10}$ ) scale was applied to the y-axis. Boxes represent 25th to 75th percentiles, and the central line the median. White points indicate geometric means, bars outside the box represent  $1.5 \times IQR$ , and points denote outliers. All differences between modes or sessions are highly significant ( $p < 0.0001$ ).

The differences between transport modes were highly significant ( $p < 0.0001$ ) according to a Wilcoxon test. A large number of outliers were observed, particularly for pedestrians, and few for the tramway.

### 3.1.2. Session effect

In Figure 4,  $PM_1$  concentrations show a daytime decrease with  $S1 > S2 > S3$ , and a noticeable difference in geometric means among sessions. Active transportation modes (walk and bike) exhibited higher inter-session variability and tramway the lowest. S3 geometric mean was 30% lower than S1 geometric mean for pedestrians, 29% lower for bikers, 26% lower for bus users, and 22% lower for tramway commuters (Table S.3). Differences between sessions were all highly significant ( $p < 0.0001$ ) using Wilcoxon test.

### 3.1.3. Comparison with reference concentrations

Local  $PM$  concentrations followed a parallel trend to background reference values, but with higher geometric means than the reference, at the exception of tramway observations where the geometric means were almost equal to that of reference. Background levels seemed to influence local  $PM$  concentrations, and they varied from day to day (Figure S.1). Next, we consider the  $PM_1$  ratio (see Eq.(1)) to normalize the local concentration variations with respect to reference variations and gain better insights into the local conditions.

### 3.2. Ratios $PM_1 / PM_{1 Ref}$

#### 3.2.1. Transport mode effect

In relation to transport mode, it can be seen on Figure 5 that the ratios rank is the same than for the concentrations. Bicycles exhibit the highest ratio of  $PM_1$  to background station, followed by pedestrians (- 2% compared to bike), bus (-9% versus bike), and tramway (-14%).

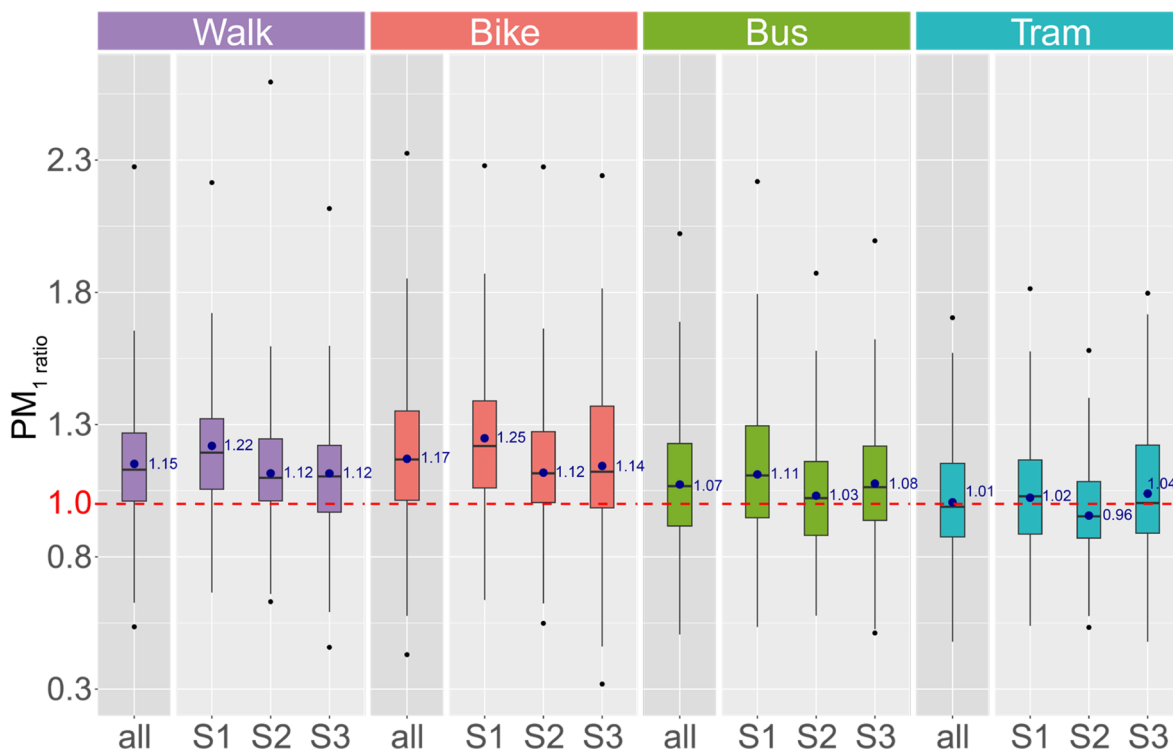


Figure 5.  $PM_1$  ratios for different modes and sessions (geometric means in blue). Upper and lower outliers were replaced by mean points. The differences between modes were all highly significant ( $p < 0.0001$ ) for all combined sessions (“all”). Within a mode, ratios were all highly significantly different ( $p < 0.0001$ ), apart from S1 - S3 for tramway (significant,  $p < 0.05$ ) and S2 - S3 for walk (non-significant,  $p > 0.05$ ). The horizontal red dotted line represents ratios equal to 1.

Differences between modes were highly significant ( $p < 0.0001$ ). Apart from tramway, all transport modes showed higher average exposure concentrations than at the background station. Tramway users were close to background levels, with a ratio close to 1 (Figure 5).

#### 3.2.2. Session effect

Differences between sessions were significant (except for walk S2 - S3), but less pronounced than differences previously seen between  $PM_1$  concentrations (Figure 4). For active commuters and bus users, S1 always had higher ratios than the other sessions. Overall, minimum ratios were observed during S2, with S3 ratios equal to or greater than S2. The differences between

S1 and S2 ranged from 10% for bike, 8% for walk to 7% for bus and 6% for tramway. These differences remained well below those observed for the concentrations, ranging from 22 to 30%. This showed the importance of background pollution in determining local concentrations.

### 3.2.3. Site effect

The site seemed to influence  $PM_{10}$  ratios, as seen on Figure 6. Within each mode, differences between sites were consistently significant ( $p < 0.0001$ ) except for AG and JP in the case of bike users. The ratios for the active (non-protected or opened) modes seemed to follow traffic intensity, AG being the less trafficked route and JP the road with the highest congestion (refer Table 1). There was an exception for bicycle on JP, where the ratio was lower than expected. JP was the only street having an off-road designated bike lane, well separated from the main road (refer Figure 3). To quantify the difference in cyclist exposure related to the dedicated bike lane on JP, we established a linear relationship between traffic and  $PM_{10}$  ratios for all streets except JP (Figure S.2). Using the linear regression formula between traffic and  $PM_{10}$  ratio ( $PM_{10} \text{ ratio} = 8.04 * 10^{-6} * \text{traffic} + 1.14$ ), we found that the  $PM_{10}$  ratio for JP was 16% lower than expected.

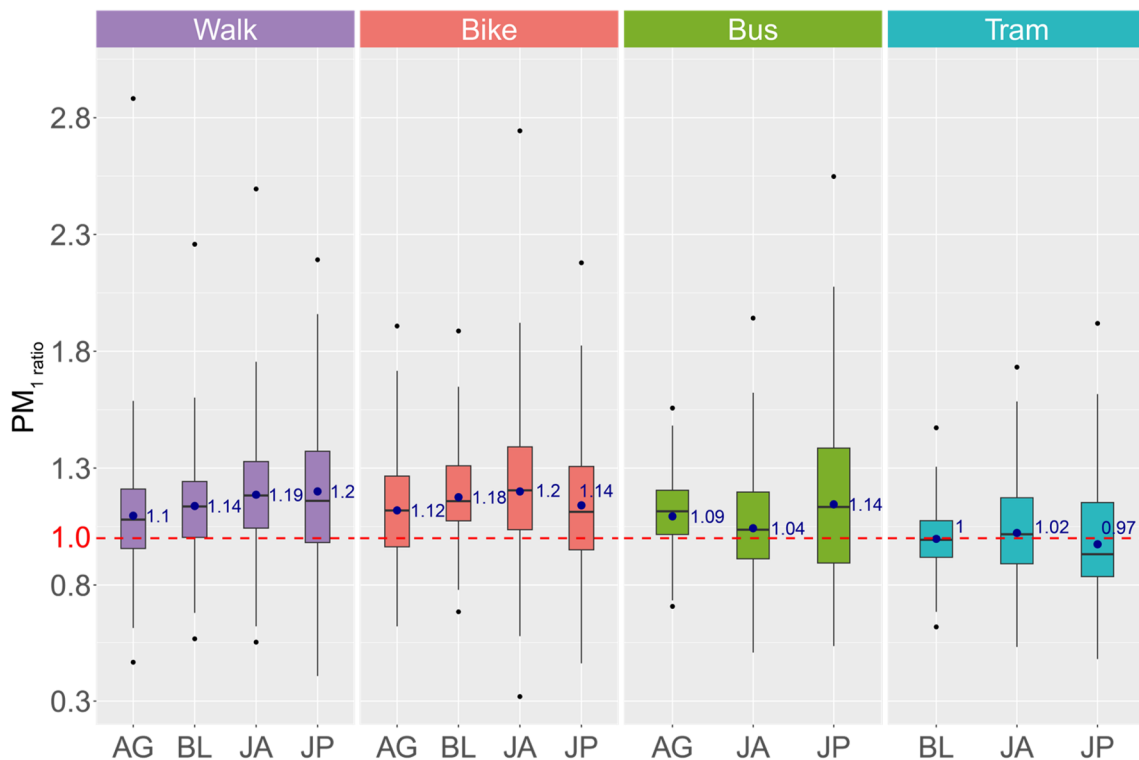


Figure 6. Ratios  $PM_{10} / PM_{10 \text{ Ref}}$  for various modes and sites. In blue, the geometric means. Upper and lower outliers were replaced by mean points. Within each mode, differences between sites were always highly significant ( $p < 0.0001$ ) except for bus, AG - JP (significant,  $p < 0.001$ ) and bike, AG - JP (non-significant).

Taking a less trafficked road (AG) versus a higher trafficked roadway (JA) decreased the ratio by 8% for pedestrians, and 7% for cyclists. For those active modes, even on the less trafficked street (AG), we see a 10% to 12% PM<sub>1</sub> excess compared to the background reference (PM<sub>1</sub> ratios of 1.1 and 1.12 for walk and bike, respectively). Having a tramway line in a street would allow pedestrians to reduce their exposure ratios by 12 to 19%, depending on the site size. For JP, the widest and more trafficked street, the use of tramway could reduce pedestrian exposure by 19%, while for JA, the reduction was 14%, and for BL, it was 12%.

### 3.2.4. Street configuration and / or traffic effect

When plotting traffic as a function of street height/width configuration ratio, a strong negative correlation was observed between these two variables, as evidenced by a Pearson coefficient ( $r = -0.94$ ,  $p\text{-value}=0.059$ ) suggesting collinearity due to a potential influence of street width in determining traffic patterns.

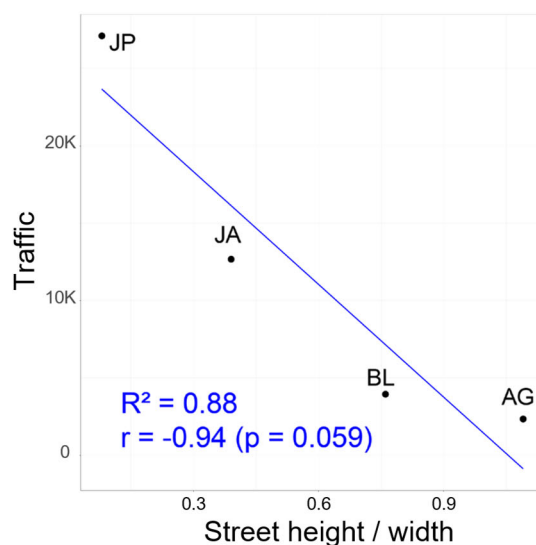


Figure 7. Traffic (TomTom, 2022b) as a function of street height/width ratio.  $R^2$  is the determination coefficient.

We further attempted to correlate the average PM<sub>1</sub> ratios experienced by pedestrians with traffic and the H/W ratio. When correlating the mean PM<sub>1</sub> ratio with traffic (Figure 8, A), we found a Pearson coefficient  $r = 0.94$  ( $p\text{-value} = 0.059$ ), which seemed to indicate a traffic influence. When removing outliers in the dataset (Figure 8, B), the Pearson coefficient was improved to a value of  $r = 0.97$  ( $p\text{-value}=0.025$ ). The determination coefficient ( $R^2$ ) of 0,95 indicated that 95% of the variance in the mean PM<sub>1</sub> ratio could be explained by traffic.

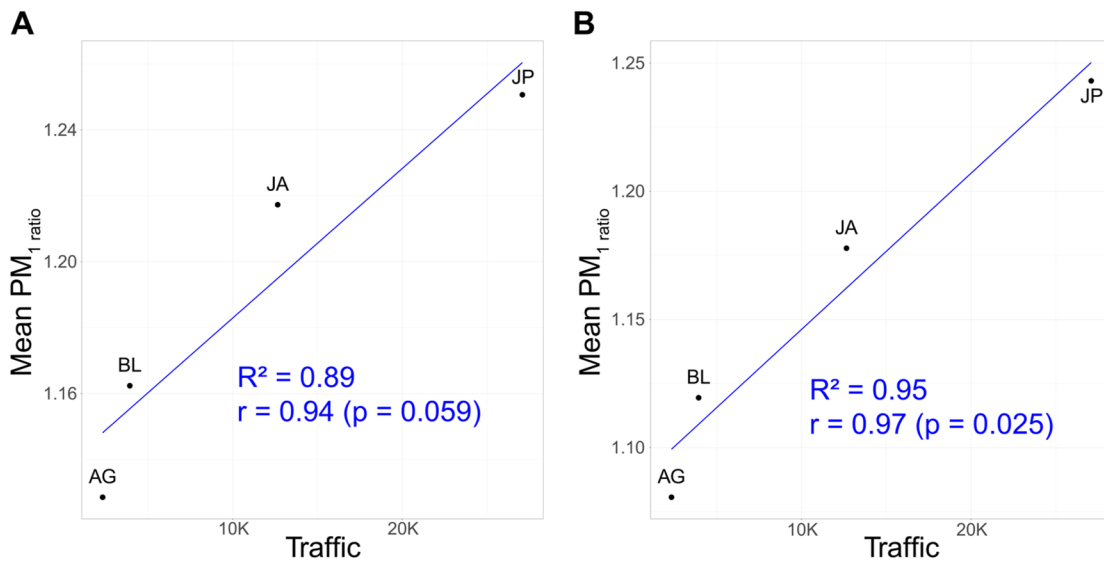


Figure 8. Mean PM<sub>1</sub> ratio for pedestrians as a function of traffic (number of cars per working day, from 7a.m. to 6p.m.). A/ dataset with outliers, B/ dataset without outliers (linear regression output in Table S.4). R<sup>2</sup> represents the determination coefficient.

When considering the H/W ratio (Figure 9), good significant correlations ( $r = -1$ ,  $p = 0.003$ ) were found for the dataset with outliers and  $r = -0.99$  ( $p = 0.007$ ) for the dataset without outliers.

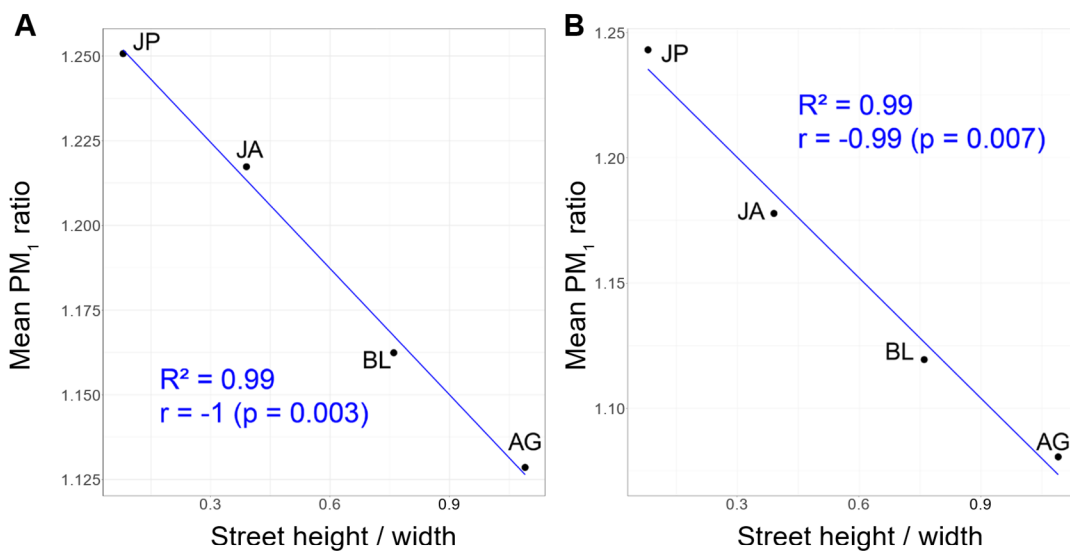


Figure 9. Mean PM<sub>1</sub> ratio for pedestrians as a function of street H / W ratio. A/ dataset with outliers, B/ dataset without outliers. R<sup>2</sup> represents the coefficient of determination. Adjustment formula for the dataset without outliers:  $\log(\text{PM}_{1 \text{ ratio}}) = 0.22 - 0.14 * (\text{street H/W})$ . Regression output in Table S.5.

Having identified key factors influencing the PM<sub>1</sub> ratio, namely transport mode, session, and site (through the influence of traffic and/or street configuration), we will now hierarchize these

factors to confirm the primary drivers responsible for street level exposure. The aim is to provide practical recommendations for individuals seeking to reduce their exposure to PM.

### 3.2.5. Mode vs. session and site induced variabilities

To better understand the relative influence of mode, session, and site, we compiled the average PM<sub>1</sub> ratios for each scenario into a table (Table 4). In this table, we categorized the sites into two groups: the shallow (H/W ≤ 0.5) high-traffic sites (JP and JA) and the medium (0.5 < H/W < 2), less frequented sites (AG and BL). We also illustrated the amplitude range in one's exposure that could occur by changing mode, session, or street configuration. The objective was to focus on changes enabling individuals to decrease their exposure ratio (negative amplitude ranges). To achieve this, we identified the lowest and highest PM<sub>1</sub> ratios in each scenario, subtracted them, and then calculated a percentage, which we referred to as "amplitude range":

$$Amplitude\ range\ (\%) = \frac{Minimum\ PM_1\ ratio - Maximum\ PM_1\ ratio}{Maximum\ PM_1\ ratio} * 100 \quad (7)$$

For example (Table 4), when travelling during S1 in a medium street with low traffic, the maximum PM<sub>1</sub> ratio was 1,24. By changing the transportation mode, PM<sub>1</sub> ratio can be lowered to 0.96, which gave an amplitude range of, (0.96-1.24)/1.24\*100 = -23%.

Table 4. Average PM<sub>1</sub> ratios per mode, session and sites (shallow or medium streets) with amplitude ranges observed. The last column “All streets - Site amplitude range” refers to a change in street configuration (i.e., from shallow street to medium street) for a same session and mode.

Mode	Ventilation (L/min)	Shallow street / High traffic (JP and JA)			Session amplitude range	Medium street / Low traffic (AG and BL)			Site amplitude range	All streets
		PM <sub>1</sub> ratios				PM <sub>1</sub> ratios				
Bike	28	1,31	1,16	1,19	-11%	1,24	1,11	1,15	-10%	-5%
Bus	23	1,14	1,06	1,12	-7%	1,2	1,03	1,08	-14%	-5%
Tramway	23	1,06	0,97	1,06	-8%	0,96	0,97	1,09	-12%	-9%
Walk	29,4	1,31	1,19	1,17	-11%	1,18	1,11	1,11	-6%	-10%
Session		S1	S2	S3		S1	S2	S3		
Mode amplitude range		-19%	-18%	-11%		-23%	-13%	-6%		

Generally, we observed that highest amplitude ranges were associated with a change in transportation mode (amplitude range from -23% to -6%, average of -15%), followed by session changes (amplitude range: -14% to -6%, average: -10%), and then changes related to the site



(from -10% to -5%, average of -7%). The most effective way to reduce exposure was typically by using the tramway, with bus rides being less predictable in terms of  $PM_{1 \text{ ratio}}$ .

When examining  $PM_{1 \text{ ratios}}$  per site, without considering the session (Table 5), AG had a lower amplitude range (-3%) compared to the other sites, which we attributed to the absence of a tramway option in this street. The presence of a tramway lane in a street was a way to reduce exposure to  $PM_1$ . Taking the tramway instead of cycling reduced the exposure ratios by 15% for all sites.

Table 5. Average  $PM_1$  ratios per mode and site with amplitude range observed

	Walk	Bike	Bus	Tramway	Amplitude range
AG	1,13	1,14	1,11	-	-3%
BL	1,16	1,19	-	1,01	-15%
JA	1,22	1,24	1,07	1,05	-15%
JP	1,25	1,18	1,21	1	-20%
Amplitude range	-10%	-8%	-12%	-5%	

In summary, the mode remained the most important variable to reduce exposure. The tramway appeared to be the less exposed way to travel most of the time, the bus showed more variability, while active transport modes had higher exposure ratios.

### 3.3. The case of $PM_{2.5}$

#### 3.3.1. Dust event

Throughout the study,  $PM_{2.5}$  concentrations displayed a similar behaviour to  $PM_1$  (see, Figure S.3 for  $PM_1$  and Figure S.4 for  $PM_{2.5}$ ), apart from day 10 (D10 or May 12, 2022) when a dust event was identified. On this day,  $PM_{2.5 \text{ Ref}}$  exceeded the measured  $PM_{2.5}$  levels (Figure S.4). Additionally, Copernicus (Météo-France, 2020) measured about of  $8 \mu\text{g}/\text{m}^3$  of dust (Figure S.5), which was a bit higher than during the rest of the experiment. The necessary conditions were satisfied to confirm the presence of dust, following the methodology established by Aix et al. (2023). Therefore, we removed this day from the dataset for calculations involving  $PM_{2.5}$ .

#### 3.3.2. $PM_{2.5}$ concentrations and $PM_{2.5 \text{ ratios}}$

Regarding  $PM_{2.5}$  concentrations (Table S.6), as for  $PM_1$ , bikes had the highest exposure levels, followed by pedestrians (-3% compared to bike), bus users (-13% versus bike) and tramway commuters (-16%).  $PM_{2.5}$  ratios for different modes and sessions can be seen in Figure S.6. Bicycles exhibited the highest ratio of  $PM_{2.5}$  to background station, followed by pedestrians (-3% compared to bike), bus (-11% versus bike), and tramway (-15%). Regarding the influence



of a dedicated line on  $PM_{2.5}$  ratios experimented by cyclists, we could not draw conclusions as the average  $PM_{2.5}$  ratios and traffic were not significantly correlated when removing Jean Pain (see Figure S.7). This might have been linked to the removal of D10 (dust event) in the dataset leaving the experimental design unbalanced due to missing experimental values on AG and BL. We confirmed this when checking the relationship between mean  $PM_{2.5}$  ratios and traffic (Figure S.8), or the relationship between mean  $PM_{2.5}$  ratios and street configuration (Figure S.9). Even if the  $PM_{2.5}$  ratios were still correlated to traffic or street H/W, all p-values were non-significant ( $p > 0.05$ ). We also compiled the average  $PM_{2.5}$  ratios for each scenario into a table (Table 6). As for  $PM_1$  ratios, we found that highest amplitude ranges were associated with a change in transportation mode (amplitude range from -20% to -13%, average of -16%), followed by session changes (amplitude range: -13% to -5%, average: -8%), and then changes related to the site (from -9% to -5%, average of -7%).

Table 6. Average  $PM_{2.5}$  ratios per mode and site with amplitude range observed. The last column “site amplitude range” refers to a change in street configuration for a same session and mode.

Mode	Ventilation (L/min)	Shallow street / High traffic (JP and JA)			Session amplitude range	Medium street / Low traffic (AG and BL)			Session amplitude range	Site amplitude range
		$PM_{2.5}$ ratios	$PM_{2.5}$ ratios	$PM_{2.5}$ ratios		$PM_{2.5}$ ratios	$PM_{2.5}$ ratios	$PM_{2.5}$ ratios		
Bike	28	1,2	1,09	1,08	-10%	1,17	1,1	1,15	-6%	-6%
Bus	23	1,05	0,98	0,99	-7%	1,11	1,02	1,03	-8%	-6%
Tramway	23	0,97	0,9	0,95	-7%	0,94	0,92	1	-8%	-5%
Walk	29,4	1,18	1,1	1,03	-13%	1,07	1,05	1,11	-5%	-9%
Session		S1	S2	S3		S1	S2	S3		
Mode amplitude range		-19%	-18%	-12%		-20%	-16%	-13%		

### 3.3.3. $PM_1 / PM_{2.5}$ fraction

The fraction  $PM_{1/2.5}$  (see, Eq.(3)) was considered to characterize the PM mixtures encountered by individuals while breathing. The streets with more traffic seemed to be the ones with larger  $PM_{1/2.5}$ , particularly for active (opened) transport modes (Figure 10).

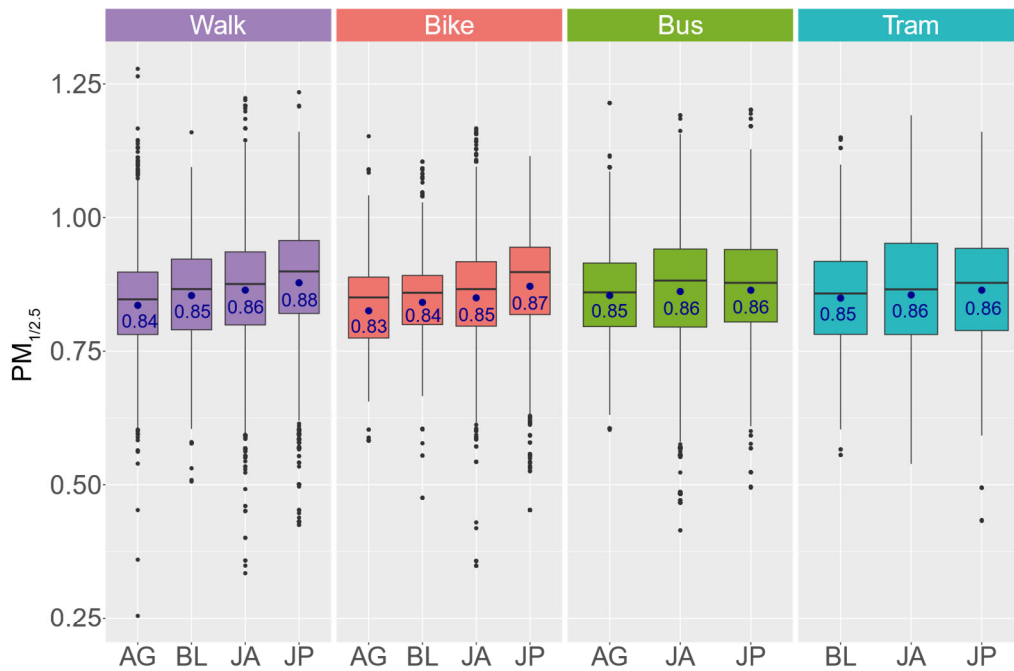


Figure 10.  $PM_{1/2.5}$  fractions for different modes and sites (geometric means in blue). Within a mode, all sites have significantly different ratios, apart from JA and JP for bus.

### 3.3.4. $PM_1 / PM_{2.5}$ ratio to reference

Because measurements were conducted on different days at different times with varying proportions of  $PM_{1\text{ Ref}} / PM_{2.5\text{ Ref}}$  at the reference station, we considered the  $PM_{1/2.5}$  ratio (see, Eq.(4)). On Figure 11, we see that all  $PM_{1/2.5}$  are higher than at the reference ( $PM_{1/2.5}$  ratios  $>1$ ).

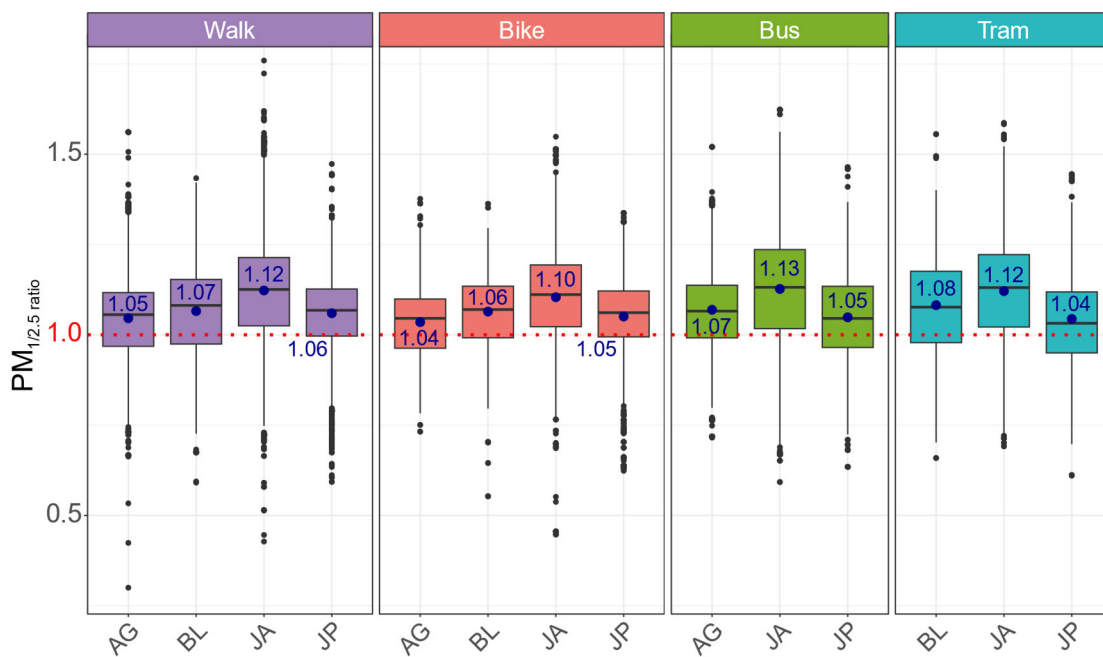


Figure 11.  $PM_{1/2.5}$  ratios for different modes and sites (arithmetic means in blue). Within a mode, all sites had significantly different ratios ( $p < 0.0001$  or  $p < 0.001$ ).

PM<sub>1/2.5</sub> ratios increased with higher traffic, especially for active modes, but not for JP, which could indicate the influence of the distance from the roadway for bikes and pedestrians. Overall, we observed a PM<sub>1/2.5</sub> excess of 4 to 13% depending on the site and mode, compared to the reference ratio. On JP, PM<sub>1/2.5</sub> ratios were smaller than expected for pedestrians and cyclists, which might be related to dedicated lanes. Overall, higher PM<sub>1/2.5</sub> fractions were found close to the traffic than at the reference. In the majority of cases, we had higher PM<sub>1/2.5</sub> ratios in public transports, except on JP. Lastly, we supplemented this study by assessing ventilation and inhalation in order to better understand individual exposure to PM.

### 3.4. Inhaled doses calculation

#### 3.4.1. Ventilation

Using heart rates measured during the experiment, we computed average ventilations per transport mode (Table 7).

Table 7. Average ventilation rates per transport mode

Mode	Ventilation (L/min)
Bike	28.0 ± 6.1
Walk	29.4 ± 11.0
Bus	23.0 ± 8.4
Tramway	23.0 ± 8.4

The results showed that active transportation modes, like walking and cycling, led to higher ventilation estimates compared to public transportation modes.

#### 3.4.2. Concentrations and inhaled doses per minute

In order to compute inhaled doses, ventilations had to be multiplied by concentrations. The graph below (Figure 12, A) shows the PM<sub>1</sub> concentrations for the various transport modes during the 410 trips. The exposure order was as follows: bike > walk > bus > tram.

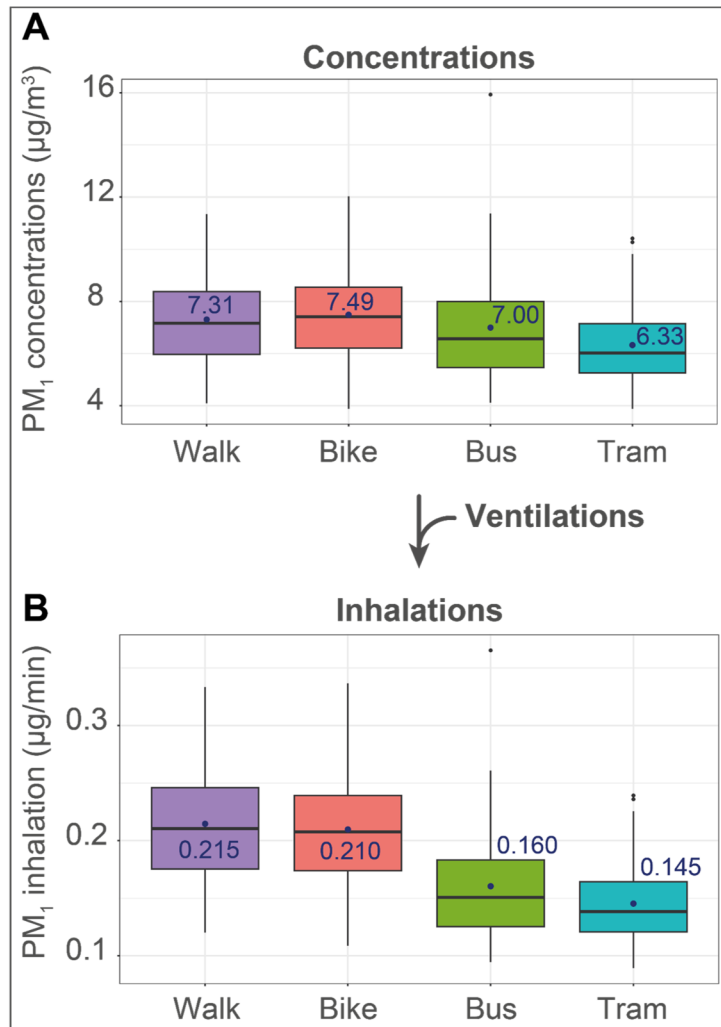


Figure 12. Average  $PM_{10}$  concentrations ( $\mu g/m^3$ ) and inhalations ( $\mu g/min$ ) per transport mode for the 410 experiment trips. Blue points refer to arithmetic means.

When analyzing inhalations (Figure 12, B), the exposure order changed, with cyclists inhaling smaller  $PM_{10}$  doses per minute than pedestrians. Furthermore, the relative difference between active modes and public transports users increased when considering inhalation. All these observations were also true for  $PM_{2.5}$  (see, Figure S.10)

#### 4. DISCUSSION.

##### 4.1. Main results and interpretations versus literature

##### 4.1.1. Mode importance

Our study emphasized that the mode was more crucial than the site to determine exposure to PM. Active commuters were more exposed than bus or tramway users and whether considering ratios or inhalation, tramway was always significantly under the active modes, with an exposure

close to background levels. For active transport modes, even on the less trafficked street, we would see a 10% to 12% PM<sub>1</sub> excess compared to the background reference values. Having a tramway line in a street would allow walkers to reduce their exposure to PM<sub>1</sub> by 12 to 19%. Choosing tramway over bike transportation decreased PM<sub>1</sub> exposure ratios by 15% across all sites, highlighting the substantial benefits of having tramway infrastructure in streets. Regarding buses, we observed a lot of variability, which aligns with prior research (Ma et al., 2020). It would have been interesting to consider whether the air conditioning was in use in buses during our experiment. An interview with a driver revealed the existence of diverse practices, depending on bus operators and weather conditions. Various studies acknowledged the significant influence of the mode on personal exposure levels (Dons et al., 2012; Kaur et al., 2007). Kaur and Nieuwenhuijsen (2009) found that it played a crucial role in determining exposure to PM<sub>2.5</sub>, with an even greater impact on ultrafine particle counts (0.02 -1 µm). deSouza et al. (2021) stated that the mode explained most of the variability in PM concentrations but their measurements were made with 3.5 times higher concentrations than us. Singh et al. (2021) showed in a meta-analysis that open transport modes exhibited higher pollutant exposure than closed transport modes. In a systematic review, Cepeda et al. (2017) also found that active commuters were generally more exposed to pollutants, followed by bus users and massive motorized transport users (train, subway, metro). In a meta-analysis, Gelb and Apparicio (2021) mentioned that cyclists were overexposed compared to other modes. Chaney et al. (2017) and Yu et al. (2012) also found that bus riders had lower inhaled doses and exposure rates than active commuters. We found only four papers in the literature dealing with exposure to PM in tramways. Moreno et al. (2015) stated that it was the cleanest form of public transport compared to bus and subway, but they did not study PM<sub>1</sub>. Strasser et al. (2018) found that tramways had higher ultrafine particle concentrations than subways. Asmi et al. (2009) indicated comparable PM<sub>2.5</sub> concentrations for newly introduced tramways and buses. Motlagh et al. (2021) did not study active modes but observed lower PM<sub>2.5</sub> levels in tramways compared to buses in summer, this order reversing in spring and autumn.

When considering inhalation, similarly to deSouza et al. (2021) and Zhu et al. (2022), we observed that the ranking between modes changed. Pedestrians became more exposed than cyclists. Dons et al. (2012) stated that active modes contributed more to inhaled pollutant dose than overall exposure. They also found that the relative importance of transport mode increased by up to 30% when considering inhalation. Similar to our study, higher PM<sub>1/2.5</sub> fractions in public transports were reported in the literature (Qiu et al., 2017; Rivas et al., 2017; Shen and Gao, 2019), a ventilation system removing more coarse particles than PM<sub>1</sub> (Amouei

Torkmahalleh et al., 2020). In summary, our observations align with the existing literature, which is interesting considering that we used low-cost sensors. Despite the affordability of the equipment, our findings reflected those obtained with more expensive measuring devices. We also present new evidence indicating the tramway as the safest mode of transport for both PM<sub>1</sub> exposure and inhalation.

#### 4.1.2. Session effect

The timing of the trip also appeared to be important to reduce exposure. For PM<sub>1</sub> ratios, we observed session related amplitude ranges varying between 6 and 10% depending on the transport mode. S1 always displayed higher ratios than the other sessions for active modes and buses users. It is therefore advisable to consider avoiding morning times and prioritize timings when traffic is low (e.g., S2). Bereitschaft (2015) also demonstrated that PM levels peaked in the mornings due to higher traffic flow and favorable atmospheric conditions. Chaney et al. (2017) worked on ratios with reference and found higher ratios in the morning than in the afternoon. Dons et al. (2012) stated that higher than average black carbon levels were observed during morning rush hour compared to off-peak hours. As in our study, the evening rush hour peak was less pronounced, likely due to the high-traffic period being spread over more hours. Overall, they identified transport mode and timing as important variables to determine exposure while commuting.

#### 4.1.3. Site role

In our study, the site seemed to have less significance than transport mode and session, but still played an important role. Site-related PM<sub>1</sub> exposure ratio amplitude range within a mode ranged from 5% (tramway) to 12% (bus), while the mode-related variabilities on streets with tramway lines were more significant, ranging from 15% to 20%. Few studies investigated the site influence on PM exposure. Kaur et al. (2007) highlighted substantial intra-mode variations in exposure levels due to factors like geographical location, weather, and traffic parameters but did not quantify the site-related variability. Briggs et al. (2008) found that levels of exposure varied from one route to another for walkers and car drivers. For pedestrians, significant positive associations were seen between ultrafine exposures and street configuration (open, semi-enclosed, enclosed or canyon), or traffic density. But they did not identify any association for PM<sub>1</sub>, contrary to what we observed. More research on this topic would be needed, especially on PM<sub>1</sub>. In summary, we observed a site effect, which could stem from traffic or urban infrastructure factors such as dedicated lanes or street dimensions.

#### 4.1.2.1. Traffic influence

PM<sub>1</sub> ratios seemed to follow traffic intensity for active modes ( $R^2 = 0.89$  for pedestrians,  $R^2 = 0.84$  for cyclists), even if we had a small number of points ( $n=4$ ). We also observed higher PM<sub>1/2.5</sub> fractions close to the traffic than at the reference, which is supported by studies showing that higher levels of fine PM can be found near roadways (Lall and Thurston, 2006; Lee et al., 2006). In a meta-analysis, Gelb and Apparicio (2021), acknowledged that measuring traffic-related pollution exposure was challenging and often relied on indirect indicators. They found studies using road type (major / minor) as indicator, assuming major axes have higher traffic volume. However, they also acknowledged that this approach reflected street morphology as well, leading to complicated interpretations. Dons et al. (2013) observed that exposure to black carbon was higher on highways, in urban areas or during traffic peak hours. According to Kaur and Nieuwenhuijsen (2009), traffic count had a limited effect on PM<sub>2.5</sub> levels but a stronger influence on ultrafine particle count. They found differences in exposure between a heavily trafficked and a quieter street, particularly for ultrafine particle count, suggesting that road users can minimize their exposure by using less busy roads. The increased PM<sub>1/2.5</sub> fractions near traffic could be linked to the substantial emission of ultrafine particles from vehicles (Kaur and Nieuwenhuijsen, 2009).

#### 4.1.2.2. Street configuration

The presence of tramway lanes significantly reduced exposure ratios, with mode-related variability ranging from 3% (on a street without tramway lane) to 15-20% (on streets with tramway lanes). Having a dedicated bike lane proved to be efficient as well as it lowered the ratio by 16% compared to on-road biking. Hofman et al. (2018) observed a 20% higher concentration of ultrafine particles along the roadway compared to the bike highway. Interestingly, Qiu et al. (2022) found that a dedicated lane resulted in a 16.8% PM<sub>2.5</sub> reduction compared to a mixed bike lane without separation from motor vehicles. Although they used a more expensive GRIMM equipment for PM measurement, their observation closely aligned with ours. According to Pattinson et al. (2017), the average exposure to ultrafine particles was found to be approximately 20-30% lower at the sidewalk compared to other locations. Subsequently, numerous scientists recognized the need to increase the distance between road and bicycle paths (Hernández et al., 2021; Qiu et al., 2019). Cepeda et al. (2017), suggest that reducing commuter exposure to pollutants can be achieved by selecting routes with low emissions and high dispersion (ex: parks) or by increasing the distance from traffic emissions. Regarding street configuration and especially canyon effect determined by street H/W ratios, Gelb and Apparicio (2021) acknowledged the fact that the axes' typology considered both traffic



effects and street morphology (width, street-canyon), making result interpretation challenging. In contrast to certain studies (Qiu et al., 2019), we did not observe any “canyon effect”, where local PM levels increase with the street H/W ratio. In our study, the effect was contrary, as exposure ratios decreased with higher street ratios. The influence of traffic may introduce bias and hinder the assessment of the effect of street configuration, thereby complicating the establishment of clear and definitive conclusions.

#### 4.2. Relevance of this study

Our findings offer guidance for reducing personal exposure and health risks during commuting. Optimal strategies include using tramway, favouring smaller streets, and avoid peak hours. While recommendations to avoid certain streets are commonly provided through smartphone applications, in our study, the transport mode seems to play a more critical role in exposure outcomes. Qiu et al. (2019) identified the background concentration as the dominant factor contributing to 40.4% variability in exposure. They found a 13.2% contribution of the time of day, 4.1% for weather and 0.6% for traffic volume. Bereitschaft (2015) observed a 56% variability attributable to background levels and highlighted the need to control for regional background concentrations when comparing PM<sub>2.5</sub> between sites. Dekoninck et al. (2015) stated that background contributions to the total trip exposure were 25% in spring and summer, increasing to 50-60% in winter. However, we cannot control background concentration or weather parameters. These factors are beyond our influence, and individuals must focus on other aspects that they can address to reduce their exposure to PM. One of the strengths of our study is to eliminate background influence, thereby mitigating weather effects and day-to-day variations. This was achieved through different techniques like using PM ratios to reference, simultaneously monitoring transport modes on the same route, and conducting the study at three different times of the day. Another strength is that we measured PM on different sites, which makes our results more generalizable. Lastly, what is noteworthy in our study is that we achieved similar results to studies using more expensive measuring devices.

#### 4.3. Limitations of this study

However, several limitations should be acknowledged. Firstly, the use of heart rate to estimate ventilation may not provide as accurate results as using a spirometer. Moreover, our study included two female experimenters, which could introduce gender-related biases in ventilations calculations. Int Panis et al. (2010) found that women had lower ventilation rates compared to men. Therefore, adjustments may be necessary if we aim for a generalizable approach, although broad generalizations on inhalation were not the study's main focus. It is

also important to recognize that low-cost sensors cannot measure PM smaller than 300 nm accurately (Bulot et al., 2019; Plantower, 2016), whereas more expensive reference stations like Fidas Palas GmbH 200 can reach a detection limit of 180 nm (Palas GmbH, 2020). Kirešová et al. (2023) indicated that, while ultrafine particles had a negligible mass concentration compared to fine and coarse particles, they constituted the dominant component of PM in terms of number concentration, raising health concerns. The use of a gold pod to calibrate mobile sensors may also raise concerns, but the calibration accuracy results were excellent, further strengthening confidence in the analysis. To increase experiment efficiency, it would be interesting to involve more experimenters, enabling simultaneous data collection from different locations. This would avoid normalizing with reference values. Lastly, further investigations are needed during other seasons. This study was only performed in spring, which means that it might not be generalizable to other times of the year.

#### 4.4. Future perspectives

Characterizing Grenoble's streets by their aspect ratio could enable estimation of exposure by simply knowing a street's aspect ratio. However, to fully understand traffic and aspect ratio impacts on exposure, a study involving streets with similar H/W ratios but varying traffic levels, and vice versa, is necessary. It would also be interesting to replicate this study using NO<sub>2</sub> measuring devices to determine whether the site's influence becomes more significant for this pollutant, usually associated with traffic. A winter replication of this experiment would also be highly informative, especially in Grenoble, where wood heating leads to a significant increase in PM levels during cold days. This study is of particular interest as it offers guidance to individuals on reducing their exposure to PM. Additionally, it provides insights for policymakers to create urban spaces that support citizens in minimizing their exposure to pollutants. Gelb and Apparicio (2021) recognized the lack of papers providing practical insights to plan cycling networks. Schmitz et al. (2021) highlighted the first use of low-cost sensors to measure NO<sub>2</sub> in a science-policy context, during the implementation of a dedicated bike lane, resulting in a 22% NO<sub>2</sub> levels reduction. Our study also clearly shows the advantage of dedicated bike lanes, as well as tramway lanes, in an urban environment. The presence of tramway lanes seemed to reduce pedestrian's exposure to PM<sub>1</sub> by 12-19%, emphasizing significant positive impacts. Another interesting finding was that tramway exhibited the lowest site-related amplitude range for PM<sub>1</sub> ratios (5%). Politicians might consider systematically refunding tramway tickets during air pollution alerts or expanding tramway lines. A local study found that extending a tramway line in Grenoble reduced nitrogen oxides by 11% and PM

concentrations by 7 to 9% (Atmo AuRA, 2020). However, it is important to note that the health benefits of active commuting are believed to outweigh the risks of increased air pollution exposure during journeys (Cepeda et al., 2017; Chaney et al., 2017; Gelb and Apparicio, 2021).

## 5. CONCLUSION.

During this study, conducted at relatively low PM levels, it has been found that the transport mode had a greater impact on exposure to PM compared to the time of day or site. These findings highlight the importance of considering transport mode as a primary factor when studying exposure to PM. Taking the tramway appeared to be the safest transport mode for exposure to PM and inhalation, while showing lower site-related amplitude ranges. To reduce cyclists' exposure to PM, implementing more dedicated bike lanes may be beneficial, as our study indicated they could bring a 16% PM<sub>1</sub> exposure reduction. This measure would not only lower exposure but also help fighting sedentary behaviour. Walking resulted in the highest levels of inhaled PM per minute. This is particularly concerning in Grenoble, where walking is the main travel mode, especially among the population aged 65 and older (CEREMA, 2022), more susceptible to adverse effects of air pollution (Health Effects Institute, 2020). Efforts should be directed towards facilitating access to the tramway and segregating bicycle lanes from roadways. Finally, this study emphasizes the significance of low-cost sensors for providing valuable data for citizens, urban planners and scientists. In addition to being easy to use, calibrated low-cost sensors have the capacity to provide valuable insights on particulate matter exposure.

## 6. ACKNOWLEDGEMENTS.

We thank Carole Rolland and the MESP Team who provided the heart rate monitors. We also acknowledge Atmo Auvergne-Rhône-Alpes for our collaboration and Grenoble Alpes Métropole for the mobility data.

7. APPENDIX.

Table S.1. Example of a time activity diary

Date : 4/25/2022

Weather	humid, light rain, clouds
Wind	low
Traffic intensity	low

J1_S1 session	Experimenter	Code	Transport mode	Start "Chavant"	Arrival "Hôtel de Ville"	Start "Hôtel de Ville"	Arrival "Chavant "	Observations			
								Smokers	Idling vehicles	Crosses	Others
Wait 1	mob2	A_VM_CH	Wait at "Chavant"	7:50:18	7:54:08						
	mob2	A_T_CH	Wait at "Chavant"	7:54:09	7:59:12			7:57 smokers			
	mob1	A_VM_CH	Tram wait	7:50:07	7:54:46						
	mob1	A_B_CH	Bus wait	7:54:46	7:57:50						
Trip 1	mob2	T_CH_HV	Tram C	7:59:13	8:01:28						
	mob1	B_CH_HV	Bus C1	7:57:51	7:59:20				7:59 - 8:00 bus		
Waiting 2	mob2	A_B_HV	Bus wait			8:03:44	8:10:32				
	mob1	A_VM_HV	Walk wait			8:03:10	8:06:10				
Trip 2	mob2	B_HV_CH	Bus C1			8:10:33	8:12:00				
	mob1	M_HV_CH	Walk			8:06:11	8:14:25		8:09 garbage truck	8:13 stop	
Wait 3	mob2	A_T_CH	Tram wait	8:15:12	8:20:58						
	mob1	A_VM_CH	Bike wait	8:14:26	8:19:44						
Trip 3	mob2	T_CH_HV	Tram C	8:21:00	8:22:31						
	mob1	VD_CH_HV	Dedicated bike	8:19:45	8:21:51						
Wait 4	mob2	A_VM_HV	Walk wait			8:22:32	8:23:36				
	mob1	A_VM_HV	Walk wait			8:21:52	8:23:36				
Trip 4	mob2	M_HV_CH	Walk			8:23:37	8:30:40				
	mob1	M_HV_CH	Walk			8:23:36	8:30:40				
Wait 5	mob2	A_B_CH	Bus wait	8:31:52	8:34:00						
	mob1	A_VM_CH	Bike wait	8:30:41	8:33:12						
Trip 5	mob2	B_CH_HV	Bus C1	8:34:01	8:35:20						
	mob1	VD_CH_HV	Dedicated bike	8:33:13	8:35:37						
Wait 6	mob2	A_T_HV_RO	Tram wait			8:35:36	8:43:12				
	mob1	A_VM_HV	Walk wait			8:35:38	8:40:37				
Trip 6	mob2	T_HV_CH	Tram C			8:43:13	8:45:28				
	mob1	M_HV_CH	Walk			8:40:38	8:47:50				
Wait 7	mob2	A_VM_CH	Walk wait	8:45:29	8:48:30						
	mob1	A_VM_CH	Bike wait	8:47:51	8:51:45						
Trip 7	mob2	M_CH_HV	Walk	8:48:31	8:55:00			8:53 smoker			
	mob1	VD_CH_HV	Dedicated bike	8:51:46	8:54:10						
Wait 8	mob2	A_B_HV	Bus wait			8:55:20	8:57:49				
	mob1	A_T_HV_RO	Tram wait			8:56:22	8:59:17				
Trip 8	mob2	B_HV_CH	Bus C1			8:57:59	9:00:08				
	mob1	T_HV_CH	Tram C			8:59:18	9:01:02				

Table S.2. AirBeam2 calibration steps and metrics.

□ STEP 1: Gold-pod calibration versus reference

Gold-pod identification: f\_14504557.

Dataset split: 75% train set – 25% test set.

	PM <sub>1</sub>	
Technique	RFR	MLR
Best formula	$PM_{1\text{ Ref}} \sim PM_1 + RH$	$PM_{1\text{ Ref}} \sim PM_1 * RH$
RMSE ( $\mu\text{g}/\text{m}^3$ ), test dataset	0.60	0,53
R <sup>2</sup> , test dataset	0.93	0.94
	PM <sub>2.5</sub>	
Technique	RFR	MLR
Best formula	$PM_{2.5\text{ Ref}} \sim PM_{2.5} + RH + T$	$PM_{2.5\text{ Ref}} \sim PM_{2.5} * RH$
RMSE ( $\mu\text{g}/\text{m}^3$ ), test dataset	0.79	0,74
R <sup>2</sup> , test dataset	0.90	0.91

MLR: Multi Linear Regression, RFR: Random Forest Regression. In bold, the best technique (lowest RMSE).

□ STEP 2: AirBeam2 calibration

○ AirBeam2:0011E400053E (AB1)

	PM <sub>1</sub>	
Technique	RFR	MLR
Best formula	$PM_{1\text{ AB1 Cal}} \sim PM_{1\text{ AB1}} + RH_{\text{AB1}} + T_{\text{AB1}}$	$PM_{1\text{ AB1 Cal}} \sim I (PM_{1\text{ AB1}} / ((1 + (RH_{\text{AB1}} / (100 - RH_{\text{AB1}})))^{1/3})) + T_{\text{AB1}}$
RMSE ( $\mu\text{g}/\text{m}^3$ ), test	0.29	0.36
R <sup>2</sup> , test	0.99	0.98
	PM <sub>2.5</sub>	
Technique	RFR	MLR
Best formula	$PM_{2.5\text{ AB1 Cal}} \sim PM_{2.5\text{ AB1}} + RH_{\text{AB1}} + T_{\text{AB1}}$	$PM_{2.5\text{ AB1 Cal}} \sim I (PM_{2.5\text{ AB1}} / ((1 + (RH_{\text{AB1}} / (100 - RH_{\text{AB1}})))^{1/3})) + T_{\text{AB1}}$
RMSE ( $\mu\text{g}/\text{m}^3$ ), test	0.37	0.41
R <sup>2</sup> , test	0.98	0.98

○ AirBeam2: 0011E40005F9 (AB2)

	PM <sub>1</sub>	
Technique	RFR	MLR
Best formula	$PM_{1\text{ AB2 Cal}} \sim PM_{1\text{ AB2}} + RH_{\text{AB2}} + T_{\text{AB2}}$	$PM_{1\text{ AB2 Cal}} \sim I (PM_{1\text{ AB2}} / ((1 + (RH_{\text{AB2}} / (100 - RH_{\text{AB2}})))^{1/3})) + T_{\text{AB2}}$
RMSE ( $\mu\text{g}/\text{m}^3$ ), test	0.28	0.35
R <sup>2</sup> , test set	0.99	0.99
	PM <sub>2.5</sub>	
Technique	RFR	MLR
Best formula	$PM_{2.5\text{ AB2 Cal}} \sim PM_{2.5\text{ AB2}} + RH_{\text{AB2}} + T_{\text{AB2}}$	$PM_{2.5\text{ AB2 Cal}} \sim I (PM_{2.5\text{ AB2}} / ((1 + (RH_{\text{AB2}} / (100 - RH_{\text{AB2}})))^{1/3})) + T_{\text{AB2}}$
RMSE ( $\mu\text{g}/\text{m}^3$ ), test	0.32	0.41
R <sup>2</sup> , test set	0.99	0.98

Table S.3. Summary statistics for PM<sub>1</sub> concentrations (µg/m<sup>3</sup>) per session and mode. Mean refers to geometric mean and SD to geometric standard deviation.

Mode	Session	Portable sensors		Reference	
		Mean (SD)	Range	Mean (SD)	Range
Walk	All	7.0 (1.3)	1.4 – 33.3	6.1 (1.3)	2.9 – 9.7
	S1	8.2 (1.2)	4.4 – 33.1	6.7 (1.3)	2.9 – 9.3
	S2	7.2 (1.3)	3.5 – 33.3	6.5 (1.1)	5.2 – 8.9
	S3	5.7 (1.3)	1.4 – 33.2	5.1 (1.2)	3.7 – 9.7
Bike	All	7.2 (1.3)	1.5 – 29.5	6.2 (1.3)	3.3 – 9.5
	S1	8.5 (1.2)	4.5 - 29.5	6.8 (1.3)	3.3 – 9.1
	S2	7.4 (1.3)	2.8 – 23.7	6.6 (1.2)	5.3 – 8.8
	S3	6.0 (1.3)	1.5 – 13.7	5.2 (1.2)	3.8 – 9.5
Bus	All	6.4 (1.4)	1.9 – 25.2	6.0 (1.3)	2.8 – 9.8
	S1	7.3 (1.3)	3.3 – 21.0	6.6 (1.3)	2.8 – 8.9
	S2	6.8 (1.3)	3.5 – 25.2	6.6 (1.2)	5.2 – 8.8
	S3	5.4 (1.4)	1.9 – 15.6	5.0 (1.2)	3.8 - 9.8
Tramway	All	6.1 (1.3)	2.1 – 14.7	6.1 (1.3)	2.8 – 9.7
	S1	6.9 (1.3)	3.3 – 14.6	6.7 (1.3)	2.8 – 9.2
	S2	6.3 (1.3)	3.4 – 14.7	6.5 (1.2)	5.2 – 8.9
	S3	5.4 (1.3)	2.1 – 10.9	5.2 (1.2)	3.8 – 9.7

Table S.4. Linear regression output, showing the relationship between PM<sub>1</sub> ratios and traffic.

Dataset without outliers (walk mode). "\*\*\*\*":  $p < 0.001$ , "\*":  $p < 0.05$

Dependant variable: PM<sub>1</sub> ratio

	Estimates	Std.error	t	p-value
(Intercept)	1.09	0.015	72.79	0.00019****
traffic	6.10e-06	9.86e-07	6.18	0.025*
R <sup>2</sup>	0.95			
Adj. R <sup>2</sup>	0.93			
F	38.23			
p-value	0.025			

Table S.5. Regression output, showing the logarithm relationship between PM<sub>1</sub> ratios and street height / width. Dataset without outliers (walk mode). "\*\*\*\*":  $p < 0.001$ , "\*\*\*":  $p < 0.01$ .

Dependant variable: log(PM<sub>1</sub> ratio)

	Estimates	Std.error	t	p-value
(Intercept)	0.22	0.0069	32.28	0.00096****
Street H/W	-0.14	0.010	-13.88	0.0052**
R <sup>2</sup>	0.99			
Adj. R <sup>2</sup>	0.98			
F	192.6			
p-value	0.0052			



Table S.6. Summary statistics for PM<sub>2.5</sub> concentrations (µg/m<sup>3</sup>) per session and mode. Mean refers to geometric mean and SD to geometric standard deviation. Day 10 was discarded from the dataset (dust event).

Mode	Session	Portable sensors		Reference	
		Mean (SD)	Range	Mean (SD)	Range
Walk	All	8.3 (1.3)	2.8 – 38.2	7.7 (1.3)	3.6 – 11.8
	S1	9.3 (1.2)	5.4 – 37.7	8.3 (1.3)	3.6 – 11.8
	S2	8.6 (1.2)	4.6 – 38.2	8.1 (1.1)	6.3 – 10.1
	S3	7.0 (1.3)	2.8 – 38.2	6.8 (1.2)	5.2 – 10.8
Bike	All	8.6 (1.3)	3.7 – 34.7	7.8 (1.2)	3.9 – 11.7
	S1	9.5 (1.2)	5.9 – 34.7	8.3 (1.3)	3.9 – 11.7
	S2	8.8 (1.2)	5.3 – 24.4	8.2 (1.1)	6.4 – 10.2
	S3	7.5 (1.2)	3.7 – 16.8	6.9 (1.2)	5.5 – 10.7
Bus	All	7.5 (1.3)	2.7 – 30.7	7.6 (1.3)	3.4 – 11.6
	S1	8.1 (1.3)	4.8 – 24.0	8.0 (1.3)	3.4 – 11.6
	S2	8.0 (1.3)	4.8 – 30.7	8.3 (1.2)	6.3 – 10.1
	S3	6.5 (1.3)	2.7 – 15.6	6.7 (1.2)	5.4 – 10.9
Tramway	All	7.2 (1.2)	3.5 – 16.9	7.7 (1.3)	3.4 – 11.8
	S1	7.7 (1.3)	3.8 – 16.9	8.1 (1.3)	3.4 – 11.8
	S2	7.4 (1.2)	4.5 – 12.4	8.2 (1.2)	6.3 – 10.2
	S3	6.6 (1.2)	3.5 – 11.7	7.0 (1.2)	5.3 – 10.8

Figure S.1. Variations in measured  $PM_{10}$  concentrations during the full experiment. D1 refers to the first day, and D10 to the 10<sup>th</sup> day (last experiment day).  $PM_{10}$  concentrations measured at the reference ( $PM_{10, Ref}$ ) are represented by a dark blue line.

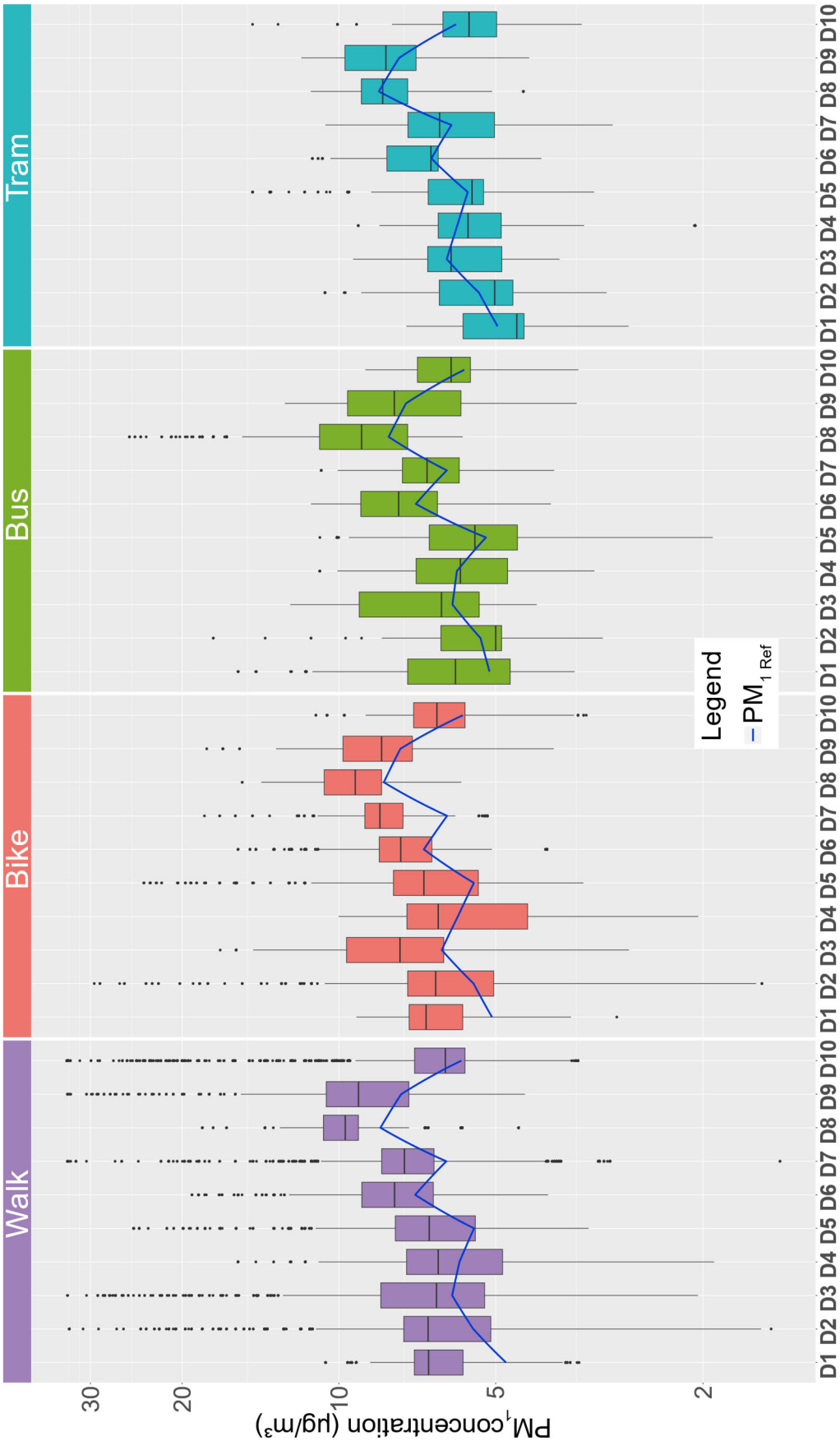


Figure S.2. Mean PM<sub>1</sub> ratio for cyclists (dataset with outliers) as a function of traffic (number of cars per working day, from 7a.m. to 6p.m.). R<sup>2</sup> represents the determination coefficient.

The equation illustrates the linear relationship between the PM<sub>1</sub> ratio and the traffic.

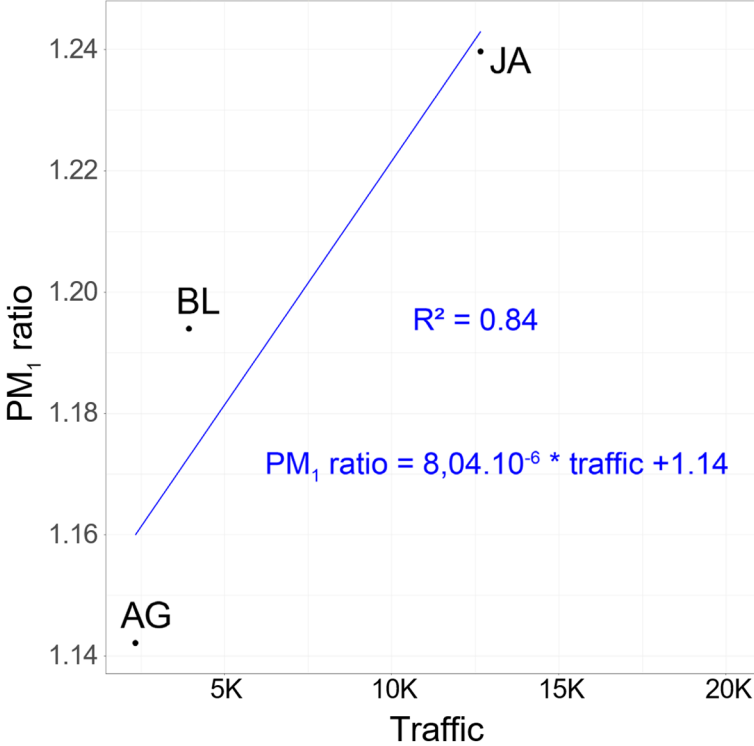


Figure S.3. PM<sub>1</sub> concentrations for pedestrians (pink boxplots) depending on the site, day and session. Dark blue boxplots represent reference values. A logarithmic scale was applied to the Y-axis. Upper and lower outliers were replaced by mean points.

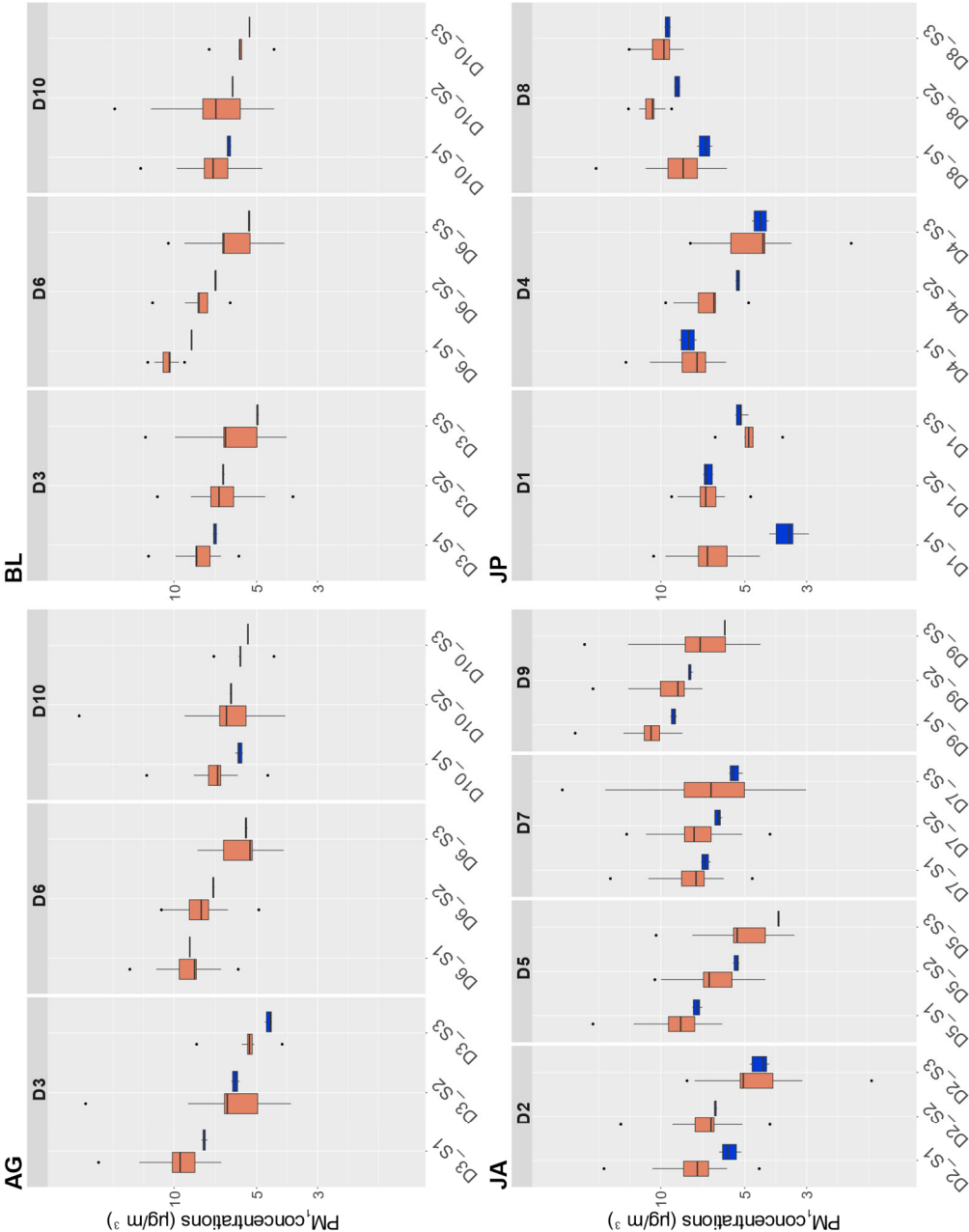


Figure S.4. PM<sub>2.5</sub> concentrations for pedestrians (pink boxplots) depending on the site, day and session. Dark blue boxplots represent reference values. A logarithmic scale is applied to the Y-axis. Upper and lower outliers were replaced by mean points.

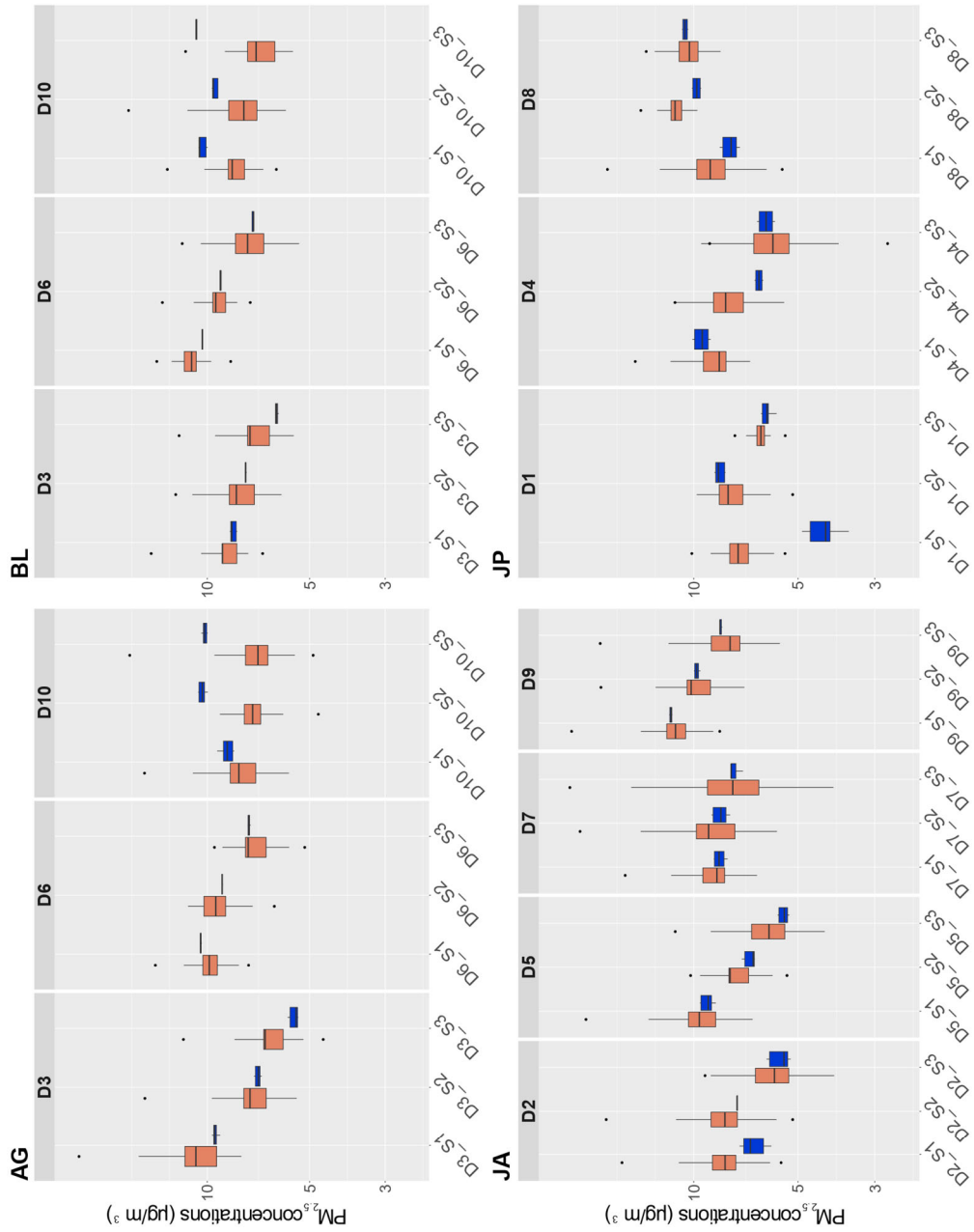


Figure S.5. Copernicus dust values (Météo-France, 2020). The period corresponding to our experiment is highlighted within the blue-bordered frame.

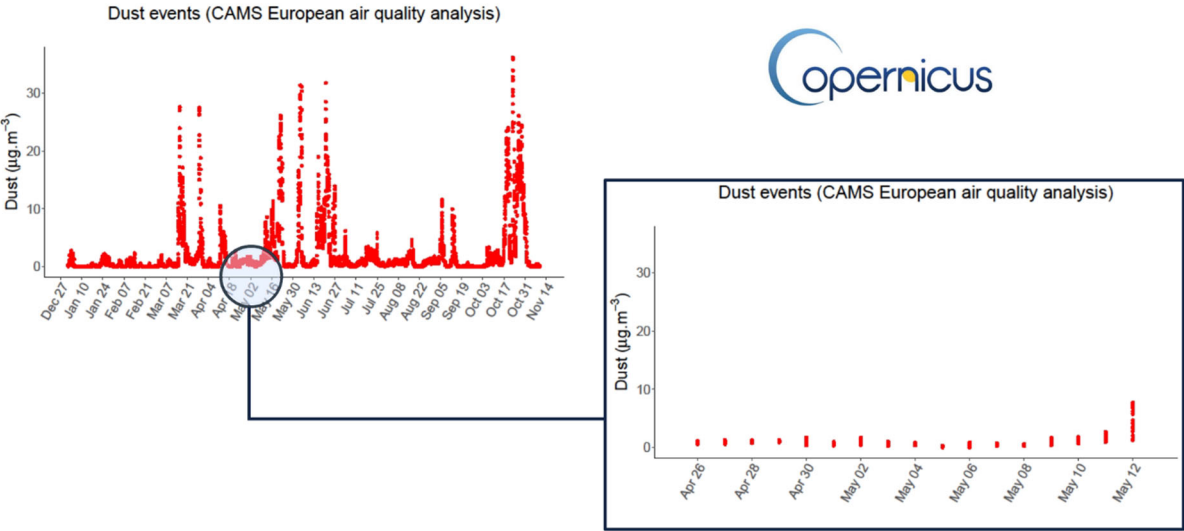


Figure S.6. PM<sub>2.5</sub> ratios for different modes and sessions (geometric means in blue). Upper and lower outliers were replaced by mean points.

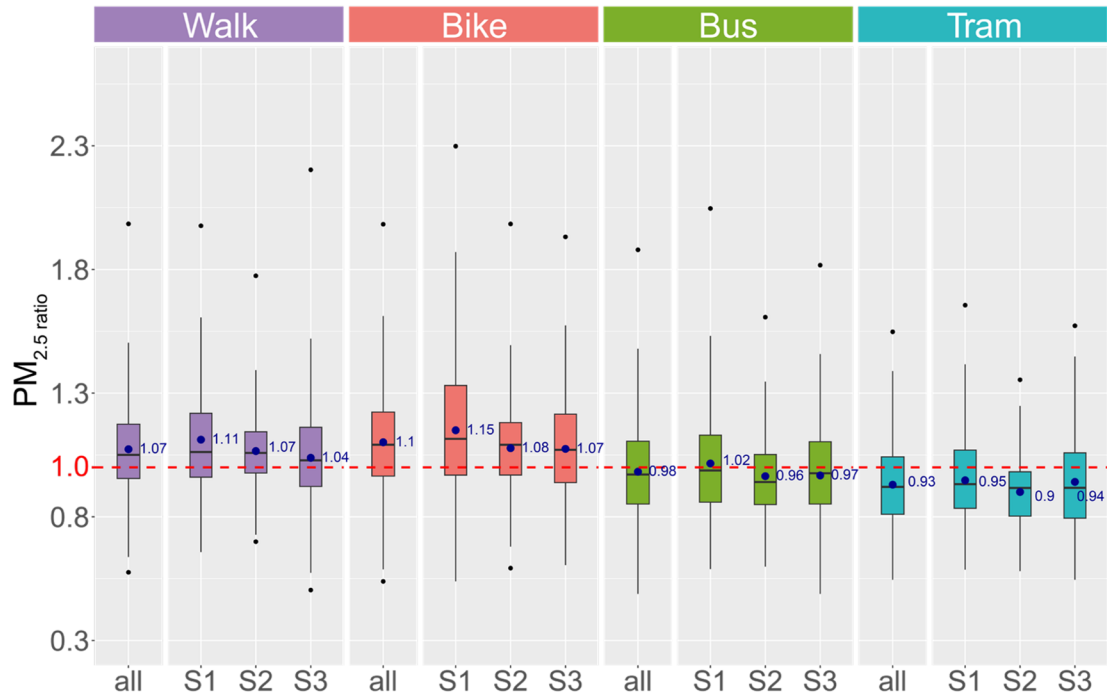


Figure S.7. Mean PM<sub>2.5</sub> ratio for cyclists (dataset with outliers) as a function of traffic (number of cars per working day, from 7a.m. to 6p.m.). R<sup>2</sup> represents the determination coefficient. The equation shows the linear relationship between the PM<sub>2.5</sub> ratio and the traffic.

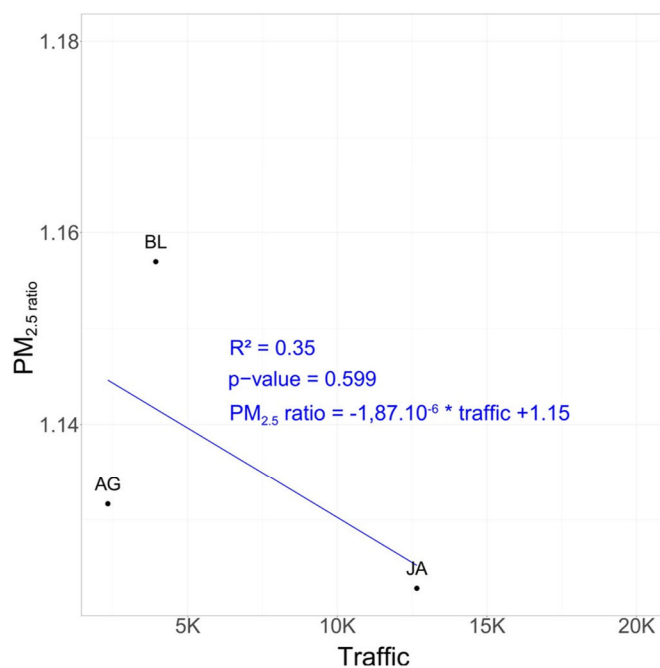




Figure S.8. Mean  $PM_{2.5}$  ratios for pedestrians as a function of traffic (number of cars per working day, from 7a.m. to 6p.m.). A/ dataset with outliers, B/ dataset without outliers.  $R^2$  represents the determination coefficient.

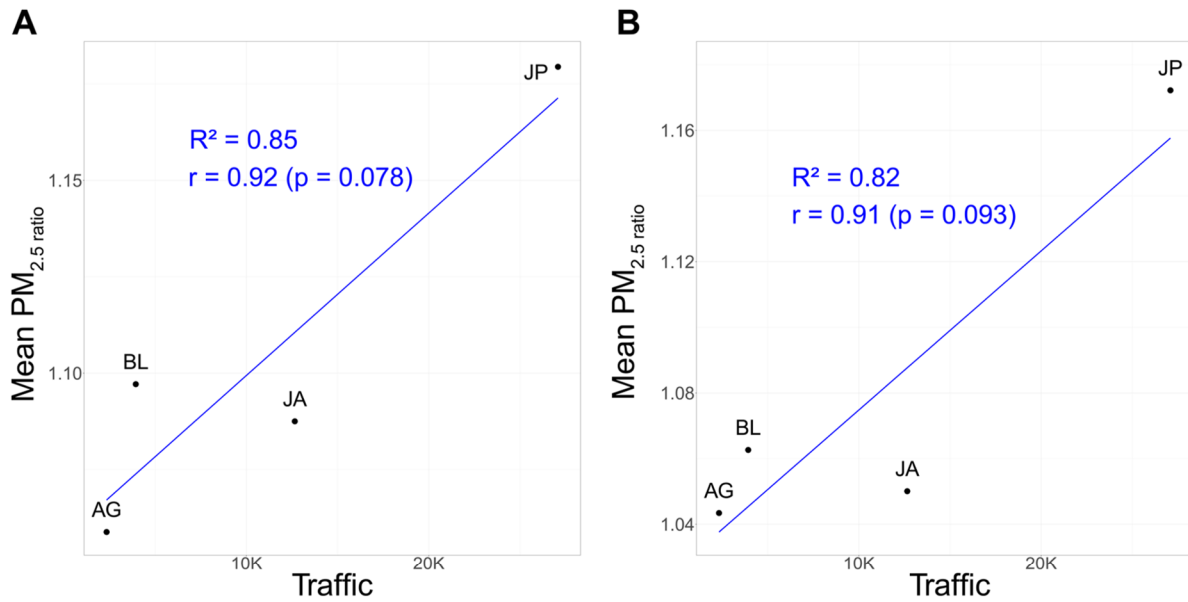


Figure S.9. Mean  $PM_{2.5}$  ratios for pedestrians as a function of street H / W ratio. A/ dataset with outliers, B/ dataset without outliers.  $R^2$  represents the coefficient of determination.

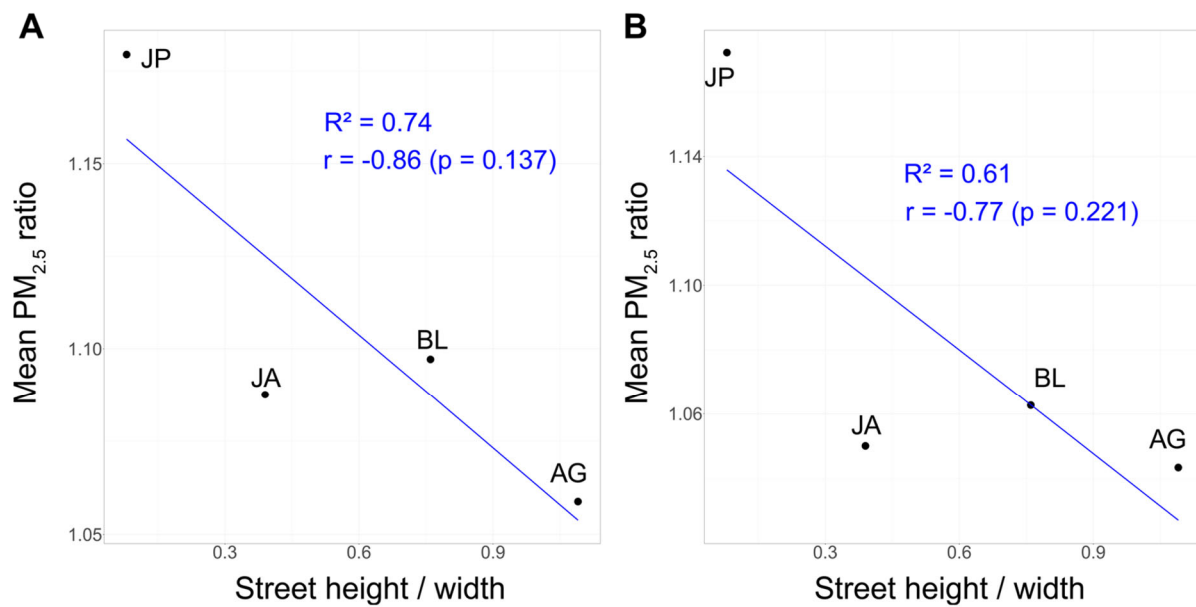
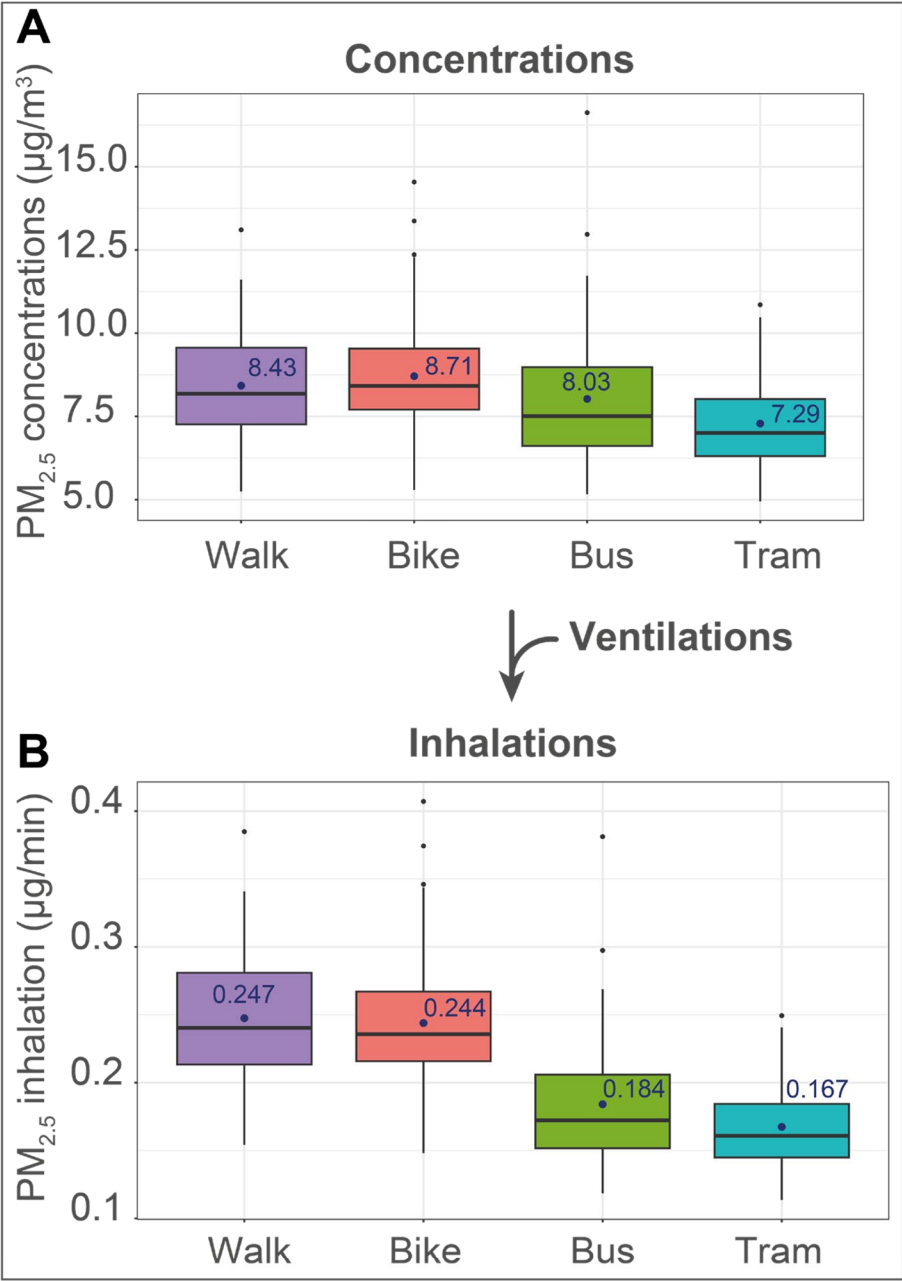


Figure S.10. Average  $PM_{2.5}$  concentrations ( $\mu\text{g}/\text{m}^3$ ) and inhalations ( $\mu\text{g}/\text{min}$ ) per transport mode for the 410 experiment trips. Blue points refer to arithmetic means.



## 8. REFERENCES.

- Adams, H. S., Nieuwenhuijsen, M. J., Colville, R. N., McMullen, M. A., Khandelwal, P., 2001. Fine particle PM<sub>2.5</sub> personal exposure levels in transport microenvironments, London, UK. *Sci Total Environ.* 279 (1-3), 29-44. [https://doi.org/10.1016/s0048-9697\(01\)00723-9](https://doi.org/10.1016/s0048-9697(01)00723-9).
- Aix, M. L., Schmitz, S., Bicout, D. J., 2023. Calibration methodology of low-cost sensors for high-quality monitoring of fine particulate matter. *Sci Total Environ.* 889, 164063. <https://doi.org/10.1016/j.scitotenv.2023.164063>.
- Amouei Torkmahalleh, M., Hopke, P. K., Broomandi, P., Naseri, M., Abdrakhmanov, T., Ishanov, A., et al., 2020. Exposure to particulate matter and gaseous pollutants during cab commuting in Nur-Sultan city of Kazakhstan. *Atmos Pollut Res.* 11 (5), 880-885. <https://doi.org/10.1016/j.apr.2020.01.016>.
- Anowar, S., Eluru, N., Hatzopoulou, M., 2017. Quantifying the value of a clean ride: How far would you bicycle to avoid exposure to traffic-related air pollution? *Transp Res Part A Policy Pract.* 105, 66-78. <https://doi.org/10.1016/j.tra.2017.08.017>.
- Asmi, E., Antola, M., Yli-Tuomi, T., Jantunen, M., Aarnio, P., Makela, T., et al., 2009. Driver and passenger exposure to aerosol particles in buses and trams in Helsinki, Finland. *Sci Total Environ.* 407 (8), 2860-7. <https://doi.org/10.1016/j.scitotenv.2009.01.004>.
- Atmo AuRA, 2020. Évaluation des effets de la mise en place du tram E sur la qualité de l'air de l'agglomération grenobloise. [https://www.atmo-auvergnerhonealpes.fr/sites/aura/files/content/migrated/atoms/files/20201014\\_bilan\\_qa\\_trame.pdf](https://www.atmo-auvergnerhonealpes.fr/sites/aura/files/content/migrated/atoms/files/20201014_bilan_qa_trame.pdf) (accessed 2023-10-10).
- Atmo AuRA, 2023. API Atmo Auvergne-Rhône-Alpes [Data set]. <https://api.atmo-aura.fr/> (accessed 2023-10-10).
- Bean, J. K., 2021. Evaluation methods for low-cost particulate matter sensors. *Atmos Meas Tech.* 14 (11), 7369-7379. <https://doi.org/10.5194/amt-14-7369-2021>.

- Bereitschaft, B., 2015. Pedestrian exposure to near-roadway PM<sub>2.5</sub> in mixed-use urban corridors: A case study of Omaha, Nebraska. *Sustain Cities Soc.* 15, 64-74. <https://doi.org/10.1016/j.scs.2014.12.001>.
- Boniardi, L., Borghi, F., Straccini, S., Fanti, G., Campagnolo, D., Campo, L., et al., 2021. Commuting by car, public transport, and bike: Exposure assessment and estimation of the inhaled dose of multiple airborne pollutants. *Atmos Environ.* 262. <https://doi.org/10.1016/j.atmosenv.2021.118613>.
- Borghi, F., Spinazze, A., Fanti, G., Campagnolo, D., Rovelli, S., Keller, M., et al., 2020. Commuters' Personal Exposure Assessment and Evaluation of Inhaled Dose to Different Atmospheric Pollutants. *Int J Environ Res Public Health.* 17 (10). <https://doi.org/10.3390/ijerph17103357>.
- Borghi, F., Spinazze, A., Mandaglio, S., Fanti, G., Campagnolo, D., Rovelli, S., et al., 2021. Estimation of the Inhaled Dose of Pollutants in Different Micro-Environments: A Systematic Review of the Literature. *Toxics.* 9 (6). <https://doi.org/10.3390/toxics9060140>.
- Borja-Aburto, V. H., Loomis, D. P., Bangdiwala, S. I., Shy, C. M., Rascon-Pacheco, R. A., 1997. Ozone, suspended particulates, and daily mortality in Mexico City. *Am J Epidemiol.* 145 (3), 258-68. <https://doi.org/10.1093/oxfordjournals.aje.a009099>.
- Briggs, D. J., de Hoogh, K., Morris, C., Gulliver, J., 2008. Effects of travel mode on exposures to particulate air pollution. *Environ Int.* 34 (1), 12-22. <https://doi.org/10.1016/j.envint.2007.06.011>.
- Bulot, F. M. J., Johnston, S. J., Basford, P. J., Easton, N. H. C., Apetroaie-Cristea, M., Foster, G. L., et al., 2019. Long-term field comparison of multiple low-cost particulate matter sensors in an outdoor urban environment. *Sci Rep.* 9 (1). <https://doi.org/10.1038/s41598-019-43716-3>.
- Cepeda, M., Schoufour, J., Freak-Poli, R., Koolhaas, C. M., Dhana, K., Brammer, W. M., et al., 2017. Levels of ambient air pollution according to mode of transport: a systematic review. *Lancet Public Health.* 2 (1), e23-e34. [https://doi.org/10.1016/s2468-2667\(16\)30021-4](https://doi.org/10.1016/s2468-2667(16)30021-4).
- CEREMA, Syndicat mixte des transports en commun de l'agglomération grenobloise, 2022. Enquête Ménages Déplacements, Grenoble / Grande région grenobloise - 2019-2020. <https://www.data.gouv.fr/fr/datasets/enquetes-menages-deplacements-emd/> (accessed 2023-10-10).

- Chan, L. Y., Lau, W. L., Lee, S. C., Chan, C. Y., 2002. Commuter exposure to particulate matter in public transportation modes in Hong Kong. *Atmos Environ.* 36 (21), 3363-3373. [https://doi.org/10.1016/S1352-2310\(02\)00318-7](https://doi.org/10.1016/S1352-2310(02)00318-7).
- Chaney, R. A., Sloan, C. D., Cooper, V. C., Robinson, D. R., Hendrickson, N. R., McCord, T. A., et al., 2017. Personal exposure to fine particulate air pollution while commuting: An examination of six transport modes on an urban arterial roadway. *PLoS One.* 12 (11), e0188053. <https://doi.org/10.1371/journal.pone.0188053>.
- Chen, G., Li, S., Zhang, Y., Zhang, W., Li, D., Wei, X., et al., 2017. Effects of ambient PM<sub>1</sub> air pollution on daily emergency hospital visits in China: an epidemiological study. *Lancet Planet Health.* 1 (6), e221-e229. [https://doi.org/10.1016/s2542-5196\(17\)30100-6](https://doi.org/10.1016/s2542-5196(17)30100-6).
- Cruz, R., Alves, D. L., Rumenig, E., Goncalves, R., Degaki, E., Pasqua, L., et al., 2020. Estimation of minute ventilation by heart rate for field exercise studies. *Sci Rep.* 10 (1), 1423. <https://doi.org/10.1038/s41598-020-58253-7>.
- de Nazelle, A., Fruin, S., Westerdahl, D., Martinez, D., Ripoll, A., Kubesch, N., et al., 2012. A travel mode comparison of commuters' exposures to air pollutants in Barcelona. *Atmos Environ.* 59, 151-159. <https://doi.org/10.1016/j.atmosenv.2012.05.013>.
- Dekoninck, L., Botteldooren, D., Panis, L. I., 2015. Using city-wide mobile noise assessments to estimate bicycle trip annual exposure to Black Carbon. *Environ Int.* 83, 192-201. <https://doi.org/10.1016/j.envint.2015.07.001>.
- deSouza, P., Lu, R., Kinney, P., Zheng, S., 2021. Exposures to multiple air pollutants while commuting: Evidence from Zhengzhou, China. *Atmos Environ.* 247, 118168. <https://doi.org/10.1016/j.atmosenv.2020.118168>.
- Dockery, D. W., Pope, C. A., Xu, X., Spengler, J. D., Ware, J. H., Fay, M. E., et al., 1993. An Association between Air Pollution and Mortality in Six U.S. Cities. *N Engl J Med.* 329 (24), 1753-1759. <https://doi.org/10.1056/nejm199312093292401>.
- Dons, E., Int Panis, L., Van Poppel, M., Theunis, J., Wets, G., 2012. Personal exposure to Black Carbon in transport microenvironments. *Atmos Environ.* 55, 392-398. <https://doi.org/10.1016/j.atmosenv.2012.03.020>.



- Dons, E., Temmerman, P., Van Poppel, M., Bellemans, T., Wets, G., Int Panis, L., 2013. Street characteristics and traffic factors determining road users' exposure to black carbon. *Sci Total Environ.* 447, 72-9. <https://doi.org/10.1016/j.scitotenv.2012.12.076>.
- Fu, X., Liu, J., Ban-Weiss, G. A., Zhang, J., Huang, X., Ouyang, B., et al., 2017. Effects of canyon geometry on the distribution of traffic-related air pollution in a large urban area: Implications of a multi-canyon air pollution dispersion model. *Atmos Environ.* 165, 111-121. <https://doi.org/10.1016/j.atmosenv.2017.06.031>.
- FUB, 2022. Baromètre des villes cyclables 2021 - Palmarès et résultats. [https://www.fub.fr/sites/fub/files/fub/dossier\\_de\\_presse\\_barometre\\_2021\\_numerique\\_vf.pdf](https://www.fub.fr/sites/fub/files/fub/dossier_de_presse_barometre_2021_numerique_vf.pdf) (accessed 2023-10-10).
- Gelb, J., Apparicio, P., 2021. Cyclists' exposure to atmospheric and noise pollution: a systematic literature review. *Transp Rev.* 41 (6), 742-765. <https://doi.org/10.1080/01441647.2021.1895361>.
- Gilardi, A., Borgoni, R., Presicce, L., Mateu, J., 2023. Measurement error models for spatial network lattice data: Analysis of car crashes in Leeds. *Journal of the Royal Statistical Society Series A: Statistics in Society.* 186 (3), 313-334. <https://doi.org/10.1093/jrssa/qnad057>.
- Giordano, M. R., Malings, C., Pandis, S. N., Presto, A. A., McNeill, V. F., Westervelt, D. M., et al., 2021. From low-cost sensors to high-quality data: A summary of challenges and best practices for effectively calibrating low-cost particulate matter mass sensors. *Journal of aerosol science.* 158, 105833. <https://doi.org/10.1016/j.jaerosci.2021.105833>.
- Guo, H., Li, X., Li, W., Wu, J., Wang, S., Wei, J., 2021. Climatic modification effects on the association between PM<sub>1</sub> and lung cancer incidence in China. *BMC Public Health.* 21 (1), 880. <https://doi.org/10.1186/s12889-021-10912-8>.
- HabitatMap, 2022. AirBeam2 Technical Specifications, Operation & Performance. <https://www.habitatmap.org/blog/airbeam2-technical-specifications-operation-performance> (accessed 2023-10-10).

- Hassani, A., Castell, N., Watne, Å. K., Schneider, P., 2023. Citizen-operated mobile low-cost sensors for urban PM<sub>2.5</sub> monitoring: field calibration, uncertainty estimation, and application. *Sustain Cities Soc.* 95. <https://doi.org/10.1016/j.scs.2023.104607>.
- Hernández, M. A., Ramírez, O., Benavides, J. A., Franco, J. F., 2021. Urban cycling and air quality: Characterizing cyclist exposure to particulate-related pollution. *Urban Climate.* 36. <https://doi.org/10.1016/j.uclim.2020.100767>.
- Hertel, O., Hvidberg, M., Ketzel, M., Storm, L., Stausgaard, L., 2008. A proper choice of route significantly reduces air pollution exposure--a study on bicycle and bus trips in urban streets. *Sci Total Environ.* 389 (1), 58-70. <https://doi.org/10.1016/j.scitotenv.2007.08.058>.
- Hofman, J., Samson, R., Joosen, S., Blust, R., Lenaerts, S., 2018. Cyclist exposure to black carbon, ultrafine particles and heavy metals: An experimental study along two commuting routes near Antwerp, Belgium. *Environ Res.* 164, 530-538. <https://doi.org/10.1016/j.envres.2018.03.004>.
- Huang, J., Deng, F., Wu, S., Guo, X., 2012. Comparisons of personal exposure to PM<sub>2.5</sub> and CO by different commuting modes in Beijing, China. *Sci Total Environ.* 425, 52-9. <https://doi.org/10.1016/j.scitotenv.2012.03.007>.
- Infogram, G.-A. M., 2021. L'usage de la voiture dans la métropole grenobloise - Infogram. <https://infogram.com/lusage-de-la-voiture-dans-la-metropole-grenobloise-1h9j6q8jzp756gz> (accessed 2023-10-10).
- Int Panis, L., de Geus, B., Vandenbulcke, G., Willems, H., Degraeuwe, B., Bleux, N., et al., 2010. Exposure to particulate matter in traffic: A comparison of cyclists and car passengers. *Atmos Environ.* 44 (19), 2263-2270. <https://doi.org/10.1016/j.atmosenv.2010.04.028>.
- Kaur, S., Nieuwenhuijsen, M., Colvile, R., 2005. Personal exposure of street canyon intersection users to PM<sub>2.5</sub>, ultrafine particle counts and carbon monoxide in Central London, UK. *Atmos Environ.* 39 (20), 3629-3641. <https://doi.org/10.1016/j.atmosenv.2005.02.046>.
- Kaur, S., Nieuwenhuijsen, M. J., 2009. Determinants of Personal Exposure to PM<sub>2.5</sub>, Ultrafine Particle Counts, and CO in a Transport Microenvironment. *Environ Sci Technol.* 43 (13), 4737-4743. <https://doi.org/10.1021/es803199z>.



- Kaur, S., Nieuwenhuijsen, M. J., Colvile, R. N., 2007. Fine particulate matter and carbon monoxide exposure concentrations in urban street transport microenvironments. *Atmos Environ.* 41 (23), 4781-4810. <https://doi.org/10.1016/j.atmosenv.2007.02.002>.
- Kim, K. H., Kabir, E., Kabir, S., 2015. A review on the human health impact of airborne particulate matter. *Environ Int.* 74, 136-43. <https://doi.org/10.1016/j.envint.2014.10.005>.
- Kirešová, S., Guzan, M., Sobota, B., 2023. Using Low-Cost Sensors for Measuring and Monitoring Particulate Matter with a Focus on Fine and Ultrafine Particles. *Atmosphere.* 14 (2). <https://doi.org/10.3390/atmos14020324>.
- Kumar, P., Rivas, I., Sachdeva, L., 2017. Exposure of in-pram babies to airborne particles during morning drop-in and afternoon pick-up of school children. *Environ Pollut.* 224, 407-420. <https://doi.org/10.1016/j.envpol.2017.02.021>.
- Lall, R., Thurston, G. D., 2006. Identifying and quantifying transported vs. local sources of New York City PM<sub>2.5</sub> fine particulate matter air pollution. *Atmos Environ.* 40, 333-346. <https://doi.org/10.1016/j.atmosenv.2006.04.068>.
- Larson, T., Su, J., Baribeau, A.-M., Buzzelli, M., Setton, E., Brauer, M., 2007. A Spatial Model of Urban Winter Woodsmoke Concentrations. *Environ Sci Technol.* 41 (7), 2429-2436. <https://doi.org/10.1021/es0614060>.
- Lee, S. C., Cheng, Y., Ho, K. F., Cao, J. J., Louie, P. K. K., Chow, J. C., et al., 2006. PM<sub>1.0</sub> and PM<sub>2.5</sub> Characteristics in the Roadside Environment of Hong Kong. *Aerosol Science and Technology.* 40 (3), 157-165. <https://doi.org/10.1080/02786820500494544>.
- Li, H. C., Chiueh, P. T., Liu, S. P., Huang, Y. Y., 2017. Assessment of different route choice on commuters' exposure to air pollution in Taipei, Taiwan. *Environ Sci Pollut Res Int.* 24 (3), 3163-3171. <https://doi.org/10.1007/s11356-016-8000-7>.
- Lim, C. C., Kim, H., Vilcassim, M. J. R., Thurston, G. D., Gordon, T., Chen, L.-C., et al., 2019. Mapping urban air quality using mobile sampling with low-cost sensors and machine learning in Seoul, South Korea. *Environ Int.* 131, 105022. <https://doi.org/10.1016/j.envint.2019.105022>.

- Lin, H., Tao, J., Du, Y., Liu, T., Qian, Z., Tian, L., et al., 2016. Particle size and chemical constituents of ambient particulate pollution associated with cardiovascular mortality in Guangzhou, China. *Environ Pollut.* 208, 758-766. <https://doi.org/10.1016/j.envpol.2015.10.056>.
- Ma, X., Longley, I., Gao, J., Salmond, J., 2020. Assessing schoolchildren's exposure to air pollution during the daily commute - A systematic review. *Sci Total Environ.* 737, 140389. <https://doi.org/10.1016/j.scitotenv.2020.140389>.
- Meng, X., Ma, Y., Chen, R., Zhou, Z., Chen, B., Kan, H., 2013. Size-fractionated particle number concentrations and daily mortality in a Chinese city. *Environ Health Perspect.* 121 (10), 1174-8. <https://doi.org/10.1289/ehp.1206398>.
- Météo-France, Institut National de l'Environnement Industriel et des Risques (Ineris), Aarhus University, Norwegian Meteorological Institute (MET Norway), Jülich Institut für Energie- und Klimaforschung (IEK), Institute of Environmental Protection – National Research Institute (IEP-NRI), Koninklijk Nederlands Meteorologisch Instituut (KNMI), Nederlandse Organisatie voor toegepast-natuurwetenschappelijk onderzoek (TNO), Swedish Meteorological and Hydrological Institute (SMHI), Finnish Meteorological Institute (FMI), 2020. CAMS European air quality forecasts, ENSEMBLE data. Copernicus Atmosphere Monitoring Service (CAMS) Atmosphere Data Store (ADS). <https://ads.atmosphere.copernicus.eu/cdsapp#!/dataset/cams-europe-air-quality-forecasts?tab=overview> (accessed 2023-10-10).
- Molina Rueda, E., Carter, E., L'Orange, C., Quinn, C., Volckens, J., 2023. Size-Resolved Field Performance of Low-Cost Sensors for Particulate Matter Air Pollution. *Environ Sci Technol Lett.* 10 (3), 247-253. <https://doi.org/10.1021/acs.estlett.3c00030>.
- Moreno, T., Reche, C., Rivas, I., Cruz Minguillon, M., Martins, V., Vargas, C., et al., 2015. Urban air quality comparison for bus, tram, subway and pedestrian commutes in Barcelona. *Environ Res.* 142, 495-510. <https://doi.org/10.1016/j.envres.2015.07.022>.
- Motlagh, N. H., Zaidan, M. A., Fung, P. L., Lagerspetz, E., Aula, K., Varjonen, S., et al., 2021. Transit pollution exposure monitoring using low-cost wearable sensors. *Transp Res D Transp Environ.* 98, 102981. <https://doi.org/10.1016/j.trd.2021.102981>.
- Mukherjee, A., Brown, S. G., McCarthy, M. C., Pavlovic, N. R., Stanton, L. G., Snyder, J. L., et al., 2019. Measuring Spatial and Temporal PM<sub>2.5</sub> Variations in Sacramento, California,

- Communities Using a Network of Low-Cost Sensors. *Sensors (Basel)*. 19 (21), 4701. <https://doi.org/10.3390/s19214701>.
- Oyola, P., Carbone, S., Timonen, H., Torkmahalleh, M., Lindén, J., 2022. Editorial: Rise of Low-Cost Sensors and Citizen Science in Air Quality Studies. *Front Environ Sci*. 10. <https://doi.org/10.3389/fenvs.2022.868543>.
- Palas GmbH, 2020. Fidas® 200 S technical datasheet. <https://www.palas.de/en/product/download/fidas200s/datasheet/pdf> (accessed 2023-10-10).
- Pattinson, W., Kingham, S., Longley, I., Salmond, J., 2017. Potential pollution exposure reductions from small-distance bicycle lane separations. *J Transp Health*. 4, 40-52. <https://doi.org/10.1016/j.jth.2016.10.002>.
- Peng, L., Shen, Y., Gao, W., Zhou, J., Pan, L., Kan, H., et al., 2021. Personal exposure to PM<sub>2.5</sub> in five commuting modes under hazy and non-hazy conditions. *Environ Pollut*. 289, 117823. <https://doi.org/10.1016/j.envpol.2021.117823>.
- Plantower, 2016. PMS7003 technical datasheet. [https://www.plantower.com/en/products\\_33/76.html](https://www.plantower.com/en/products_33/76.html) (accessed 2023-10-10).
- Qiu, Z., Lv, H., Zhang, F., Wang, W., Hao, Y., 2019. Pedestrian exposure to PM<sub>2.5</sub>, BC and UFP of adults and teens: A case study in Xi'an, China. *Sustain Cities Soc*. 51. <https://doi.org/10.1016/j.scs.2019.101774>.
- Qiu, Z., Song, J., Xu, X., Luo, Y., Zhao, R., Zhou, W., et al., 2017. Commuter exposure to particulate matter for different transportation modes in Xi'an, China. *Atmos Pollut Res*. 8 (5), 940-948. <https://doi.org/10.1016/j.apr.2017.03.005>.
- Qiu, Z., Wang, X., Liu, Z., Luo, J., 2022. Quantitative assessment of cyclists' exposure to PM and BC on different bike lanes. *Atmos Pollut Res*. 13 (11). <https://doi.org/10.1016/j.apr.2022.101588>.
- R Core Team, 2023. R: A language and environment for statistical computing. R Foundation for Statistical Computing, Vienna, Austria. <https://www.R-project.org/> (accessed 2023-10-10).
- Raaschou-Nielsen, O., Andersen, Z. J., Beelen, R., Samoli, E., Stafoggia, M., Weinmayr, G., et al., 2013. Air pollution and lung cancer incidence in 17 European cohorts: prospective analyses from the

- European Study of Cohorts for Air Pollution Effects (ESCAPE). *Lancet Oncol.* 14 (9), 813-822.  
[https://doi.org/10.1016/S1470-2045\(13\)70279-1](https://doi.org/10.1016/S1470-2045(13)70279-1).
- Ramos, C. A., Reis, J. F., Almeida, T., Alves, F., Wolterbeek, H. T., Almeida, S. M., 2015. Estimating the inhaled dose of pollutants during indoor physical activity. *Sci Total Environ.* 527-528, 111-8. <https://doi.org/10.1016/j.scitotenv.2015.04.120>.
- Rappaport, S. M., Smith, M. T., 2010. Epidemiology. Environment and disease risks. *Science.* 330 (6003), 460-1. <https://doi.org/10.1126/science.1192603>.
- Rivas, I., Kumar, P., Hagen-Zanker, A., 2017. Exposure to air pollutants during commuting in London: Are there inequalities among different socio-economic groups? *Environ Int.* 101, 143-157.  
<https://doi.org/10.1016/j.envint.2017.01.019>.
- Samet, J. M., Dominici, F., Currier, I., Coursac, I., Zeger, S. L., 2000. Fine Particulate Air Pollution and Mortality in 20 U.S. Cities, 1987–1994. *N Engl J Med.* 343 (24), 1742-1749.  
<https://doi.org/10.1056/NEJM200012143432401>.
- Schmitz, S., Caseiro, A., Kerschbaumer, A., Von Schneidmesser, E., 2021. Do new bike lanes impact air pollution exposure for cyclists?—a case study from Berlin. *Environ Res Lett.* 16 (8), 084031.  
<https://doi.org/10.3402/gha.v7.23574>.
- Schraufnagel, D. E., 2020. The health effects of ultrafine particles. *Exp Mol Med.* 52 (3), 311-317.  
<https://doi.org/10.1038/s12276-020-0403-3>.
- Shen, J., Gao, Z., 2019. Commuter exposure to particulate matters in four common transportation modes in Nanjing. *Build Environ.* 156, 156-170. <https://doi.org/10.1016/j.buildenv.2019.04.018>.
- Singh, V., Meena, K. K., Agarwal, A., 2021. Travellers' exposure to air pollution: A systematic review and future directions. *Urban Climate.* 38, 100901. <https://doi.org/10.1016/j.uclim.2021.100901>.
- Song, J., Ding, Z., Zheng, H., Xu, Z., Cheng, J., Pan, R., et al., 2022. Short-term PM<sub>1</sub> and PM<sub>2.5</sub> exposure and asthma mortality in Jiangsu Province, China: What's the role of neighborhood characteristics? *Ecotoxicol Environ Saf.* 241, 113765.  
<https://doi.org/10.1016/j.ecoenv.2022.113765>.



- South Coast Air Quality Management District, 2018. Field Evaluation - AirBeam2 PM Sensor, AQ-SPEC. <http://www.aqmd.gov/docs/default-source/aq-spec/summary/habitatmap-airbeam2---summary-report.pdf?sfvrsn=16> (accessed 2023-10-10).
- Strasser, G., Hiebaum, S., Neuberger, M., 2018. Commuter exposure to fine and ultrafine particulate matter in Vienna. *Wien Klin Wochenschr.* 130 (1-2), 62-69. <https://doi.org/10.1007/s00508-017-1274-z>.
- Thai, A., McKendry, I., Brauer, M., 2008. Particulate matter exposure along designated bicycle routes in Vancouver, British Columbia. *Sci Total Environ.* 405 (1-3), 26-35. <https://doi.org/10.1016/j.scitotenv.2008.06.035>.
- Tomson, M., Kumar, P., Barwise, Y., Perez, P., Forehead, H., French, K., et al., 2021. Green infrastructure for air quality improvement in street canyons. *Environ Int.* 146. <https://doi.org/10.1016/j.envint.2020.106288>.
- TomTom, 2022a. Grenoble traffic in 2022. <https://www.tomtom.com/traffic-index/grenoble-traffic/> (accessed 2023-10-10).
- TomTom, 2022b. Traffic Data & Traffic Stats. <https://www.tomtom.com/products/traffic-stats/> (accessed 2023-10-10).
- Ueberham, M., Schlink, U., Dijst, M., Weiland, U., 2019. Cyclists' Multiple Environmental Urban Exposures—Comparing Subjective and Objective Measurements. *Sustainability.* 11 (5). <https://doi.org/10.3390/su11051412>.
- United States Environmental Protection Agency, 2022. Climate Change and the Health of Older Adults. <https://www.epa.gov/climateimpacts/climate-change-and-health-older-adults> (accessed 2023-10-10).
- Van den Bossche, J., Peters, J., Verwaeren, J., Botteldooren, D., Theunis, J., De Baets, B., 2015. Mobile monitoring for mapping spatial variation in urban air quality: Development and validation of a methodology based on an extensive dataset. *Atmos Environ.* 105, 148-161. <https://doi.org/10.1016/j.atmosenv.2015.01.017>.
- Willett, W. C., 2002. Balancing Life-Style and Genomics Research for Disease Prevention. *Science.* 296 (5568), 695-698. <https://doi.org/10.1126/science.1071055>.

- World Health Organization, 2022. Ambient air pollution. <https://www.who.int/data/gho/data/themes/topics/indicator-groups/indicator-group-details/GHO/ambient-air-pollution> (accessed 2023-10-10).
- Wu, C., Zhang, Y., Wei, J., Zhao, Z., Norback, D., Zhang, X., et al., 2022. Associations of Early-Life Exposure to Submicron Particulate Matter With Childhood Asthma and Wheeze in China. *JAMA Netw Open*. 5 (10), e2236003. <https://doi.org/10.1001/jamanetworkopen.2022.36003>.
- Wu, H., Zhang, B., Wei, J., Lu, Z., Zhao, M., Liu, W., et al., 2022. Short-term effects of exposure to ambient PM<sub>1</sub>, PM<sub>2.5</sub>, and PM<sub>10</sub> on ischemic and hemorrhagic stroke incidence in Shandong Province, China. *Environ. Res.* 212 (Pt C), 113350. <https://doi.org/10.1016/j.envres.2022.113350>.
- Xu, R., Huang, S., Shi, C., Wang, R., Liu, T., Li, Y., et al., 2023. Extreme Temperature Events, Fine Particulate Matter, and Myocardial Infarction Mortality. *Circulation*. 148 (4), 312-323. <https://doi.org/10.1161/circulationaha.122.063504>.
- Yang, M., Guo, Y. M., Bloom, M. S., Dharmagee, S. C., Morawska, L., Heinrich, J., et al., 2020. Is PM<sub>1</sub> similar to PM<sub>2.5</sub>? A new insight into the association of PM<sub>1</sub> and PM<sub>2.5</sub> with children's lung function. *Environ Int*. 145, 106092. <https://doi.org/10.1016/j.envint.2020.106092>.
- Yu, Q., Lu, Y., Xiao, S., Shen, J., Li, X., Ma, W., et al., 2012. Commuters' exposure to PM<sub>1</sub> by common travel modes in Shanghai. *Atmos Environ*. 59, 39-46. <https://doi.org/10.1016/j.atmosenv.2012.06.001>.
- Zhang, L., You, S., Zhang, M., Zhang, S., Yi, S., Zhou, B., 2022. The effects of urbanization on air pollution based on a spatial perspective: Evidence from China. *Front Environ Sci*. 10. <https://doi.org/10.3389/fenvs.2022.1058009>.
- Zhou, J., Liu, J., Xiang, S., Zhang, Y., Wang, Y., Ge, W., et al., 2022. Evaluation of the Street Canyon Level Air Pollution Distribution Pattern in a Typical City Block in Baoding, China. *Int J Environ Res Public Health*. 19 (16). <https://doi.org/10.3390/ijerph191610432>.
- Zhu, C., Xue, Y., Li, Y., Yao, Z., Li, Y., 2022. Assessment of particulate matter inhalation during the trip process with the considerations of exercise load. *Sci Total Environ*. 866, 161277. <https://doi.org/10.1016/j.scitotenv.2022.161277>.

- Zuurbier, M., Hoek, G., Oldenwening, M., Lenters, V., Meliefste, K., van den Hazel, P., et al., 2010. Commuters' exposure to particulate matter air pollution is affected by mode of transport, fuel type, and route. *Environ Health Perspect.* 118 (6), 783-9. <https://doi.org/10.1289/ehp.0901622>.
- Zuurbier, M., Hoek, G., van den Hazel, P., Brunekreef, B., 2009. Minute ventilation of cyclists, car and bus passengers: an experimental study. *Environ Health.* 8, 48. <https://doi.org/10.1186/1476-069X-8-48>.
- Zwozdziak, A., Sowka, I., Willak-Janc, E., Zwozdziak, J., Kwiecinska, K., Balinska-Miskiewicz, W., 2016. Influence of PM<sub>1</sub> and PM<sub>2.5</sub> on lung function parameters in healthy schoolchildren-a panel study. *Environ Sci Pollut Res Int.* 23 (23), 23892-23901. <https://doi.org/10.1007/s11356-016-7605-1>.



## 5.3 CONCLUSION

- Key variables to reduce PM exposure: transport mode > travel time and site;
- PM<sub>1</sub> ratios: bike > walk (-2%) > bus (-9%) > tramway (-14%);
- PM<sub>2.5</sub> ratios: bike > walk (-3%) > bus (-11%) > tramway (-15%);
- PM<sub>1</sub> inhaled doses: walk > bike (-2%) > bus (-26%) > tramway (-33%);
- PM<sub>2.5</sub> inhaled doses: walk > bike (-1%) > bus (-26%) > tramway (-32%);
- Observations made with low-cost sensors align with studies using more expensive devices

# 6 CONCLUSIONS AND PERSPECTIVES

## 6.1 MAIN RESULTS OF THE THESIS

### 6.1.1 What are health risks related to air pollutants in Grenoble?

This thesis started with an analysis of health risks associated with air pollutants in Grenoble during the COVID-19 crisis. Table 6 summarizes them, showing that the most pronounced health effects happen due to PM<sub>2.5</sub>.

Table 6. Main pollutants changes and related health outcomes in Grenoble during the COVID-19

	LEVELS	SHORT-TERM	LONG-TERM
<b>NO<sub>2</sub></b>	-31%	-2% respiratory hospitalizations	-1% mortality
<b>PM<sub>2.5</sub></b>	-14%	-3% child asthma emergency visits	-3% mortality -2% lung cancer -8% low-birth weight
<b>PM<sub>10</sub></b>	-11%	Almost no effect	
<b>O<sub>3</sub></b>	+11%	Almost no effect	

Most pronounced health effects with PM<sub>2.5</sub>

Therefore, we chose to focus on PM<sub>2.5</sub>, however, the scarcity of reference stations can make the precise measurement of PM<sub>2.5</sub> challenging. In this context, LCS appeared to be valuable tools to obtain finer measurements, both spatially and geographically.

## 6.1.2 How to accurately measure exposure to PM in Grenoble?

### 6.1.2.1 LCS calibration

To assess LCS' performance in accurately measuring PM, we compared their readings to those of a reference. Initially, LCS' measurement quality did not meet EPA's performance standards, highlighting the need for prior LCS' calibration. A key finding was that excluding dust events enhanced the performance of calibration algorithms. The most effective calibration methods were:

- Multi-Linear Regression (MLR) for  $PM_{10}$  with  $R^2 = 0.94$ ,  $RMSE = 0.55 \mu\text{g}/\text{m}^3$ ;
- Random Forest Regression (RFR) for  $PM_{2.5}$  with  $R^2 = 0.92$ ,  $RMSE = 0.70 \mu\text{g}/\text{m}^3$ ;

These metrics, in accordance with EPA's standards, allowed us to validate LCS' accuracy. We confirmed, as demonstrated in existing literature, that LCS with PMS7003 should not be used to measure  $PM_{10}$ . The algorithms developed in this work should not be applied in other geographical areas or under different aerosol conditions, but the method can be used in various contexts.

### 6.1.2.2 Fixed measurements

A measurement campaign using fixed LCS highlighted the importance of broad calibration conditions. Deployment settings should match those during calibration, especially in terms of PM levels and relative humidity. Therefore, we specifically analyzed deployed LCS' measurements during spring and summer in order to match calibration's conditions. We observed diurnal variations with a minimum between 7-9 am and a maximum between 7-8 pm (9 pm in the city center), while spatial variations revealed highest PM levels and ratios in the city center. These findings illustrate the advantages of using LCS for accurate spatiotemporal mapping of PM exposure.

### 6.1.2.3 Mobile measurements

Finally, we performed mobile PM measurements in spring (low PM levels), using four transport modes (bike, walk, bus, and tramway), across four different sites (streets). This study

revealed that the transport mode had a greater impact on individuals' encountered PM ratios than the timing or the street they traversed. Exposure orders were as follows:

- $PM_{1 \text{ ratios}}$ : bike > walk (-2%) > bus (-9%) > tramway (-14%);
- $PM_{2.5 \text{ ratios}}$ : bike > walk (-3%) > bus (-11%) > tramway (-15%).

When considering inhalation, the order changed to the following:

- $PM_{1 \text{ inhaled doses}}$ : walk > bike (-2%) > bus (-26%) > tramway (-33%);
- $PM_{2.5 \text{ inhaled doses}}$ : walk > bike (-1%) > bus (-26%) > tramway (-32%).

This study demonstrated that it is crucial to consider commuting when studying individual exposure to PM, as well as inhalation.

## 6.2 LIMITATIONS OF THE STUDY

### 6.2.1 The importance of LCS electronic components

#### 6.2.1.1 Humidity sensors

Improving electronic components quality will improve the reliability of LCS studies. Relative humidity sensors may introduce bias in the results, as they are used to calibrate PM data, and they are therefore very important. While the DHT22 sensor is commonly used in LCS networks, especially in citizen science, it does not appear to be reliable for long-term deployment studies. Alonso-Pérez and López-Solano (2023) performed an almost 4 years experiment and noted that the DHT22 had to be replaced twice. The SHT35 sensor, manufactured by a Swiss company (Sensirion, 2023a), is gaining popularity in the scientific community (Bulot, Russell, et al., 2023; Hassani et al., 2023), as well as the SHT85 (Sensirion, 2023b). The BME280 could also be an interesting candidate, although a study reported noise and communication issues between the BME280 and the micro-controller (Anagnostopoulos et al., 2023). Adalakun and Akano (2023) found good correlations between the BME280 and reference humidity instruments. Deploying two humidity sensors in an air quality station could also enable data comparison, anomaly detection, and the derivation of an average RH value.

### 6.2.1.2 PM sensors

New optical sensors are starting to be used to measure PM, especially the SPS30 (Gabel et al., 2022; Hassani et al., 2023; Sensirion, 2023c). It would be interesting to assemble this sensor together with the PMS7003, as they may complement each other in terms of measured PM sizes (Kuula et al., 2020). The SDS011, which was recently found to detect dust events (Alonso-Pérez & López-Solano, 2023), could also be added. A key limitation of this thesis was the necessity to focus on PM measurement, because gas sensors measuring O<sub>3</sub> or NO<sub>2</sub> are not yet fully reliable. There is a need for research in the domain of gas sensors, especially because O<sub>3</sub> levels are expected to increase with climate warming, and also because of the health consequences associated with NO<sub>2</sub>.

### 6.2.2 The significance of an extensive calibration

As mentioned earlier, calibration is key and should be as wide as possible for PM levels, relative humidity and temperature (Levy Zamora et al., 2023). Similar to our experience, Koehler et al. (2023) also had calibrations performing better when concentrations were low (< 30 µg/m<sup>3</sup>), likely due to the majority of training data falling within this range. This is particularly important because raw data are considered to be highly inaccurate when PM<sub>2.5</sub> levels are high, these periods generally corresponding to high relative humidity levels (Datta et al., 2020). Calibrating high PM concentrations seems to present the most significant challenge in calibration studies.

## 6.3 RECOMMENDATIONS FOR FUTURE USE OF LCS

It is likely that in the coming years, researchers will accumulate sufficient data to further develop and use LCS for epidemiology research. However, progress in LCS calibration and development is hindered by the scarcity of reference stations worldwide. Figure 32 displays various recommendations for conducting PM studies using LCS.

The first question to be answered is whether there is a reference station for sensor calibration in the study area. If not, using calibration formulas from studies with similar sensors under comparable aerosol conditions can be considered. This implies that, ideally, calibration should have

occurred with the same weather conditions as the deployment, with matching PM levels, under similar conditions (traffic/background). While not optimal, this approach is feasible and has been used by scientists in different situations (Anagnostopoulos et al., 2023; Coker et al., 2022; Koehler et al., 2023; Phung & Wagstrom, 2023). With this aim in mind, Barkjohn et al. (2021) developed a multiple linear regression equation using RH that could be applicable across the United-States in public health contexts. Koehler et al. (2023) used this formula for an indoor study, and found that predicted values were close to gravimetric gold-standard levels for concentrations under  $20 \mu\text{g}/\text{m}^3$ . Performance was reduced at high concentrations, a local calibration resulting in a lower RMSE. This calibration method is not optimal, but can help addressing the scarcity of reference stations, especially in less developed countries. Machine learning should be better suited than linear regression and it would be highly informative to check how a machine learning calibration could perform country-wide. A nice example is a study by Raheja et al. (2022) using a Gaussian Mixture Regression calibration model developed for Accra, Ghana, to calibrate a LCS network in Togo.

If a reference station is available but an official collocation is not possible, open data from a sensor network covering the area can be used to develop calibration formulas as already done by Gitahi and Hahn (2022) or deSouza et al. (2023). The benefit of using open sensor networks lies in the vast amount of data provided, networks like Sensor.Community or PurpleAir hosting more than 10,000 sensors worldwide. This calibration method involves finding relevant reference stations within the study area and comparing their results to those of nearby citizen sensors. A drawback of this technique is that sensors are not always uniformly installed by citizens, for instance in terms of height, potentially introducing biases. However, an advantage lies in the fact that no additional deployment is required, which saves significant time and effort.

The criteria for LCS assembly and deployment are also very important to perform successful PM measurement studies. Regarding assembly, the use of multiple sensors on the same air quality station offers important research perspectives. This could help optimize calibration, for instance by making dusts identification easier. In summary, the optimal protocol, highlighted in green in Figure 32, helps eliminate uncertainty in the measurements. Moreover, combination with satellite observations could also offer further improvement perspectives.

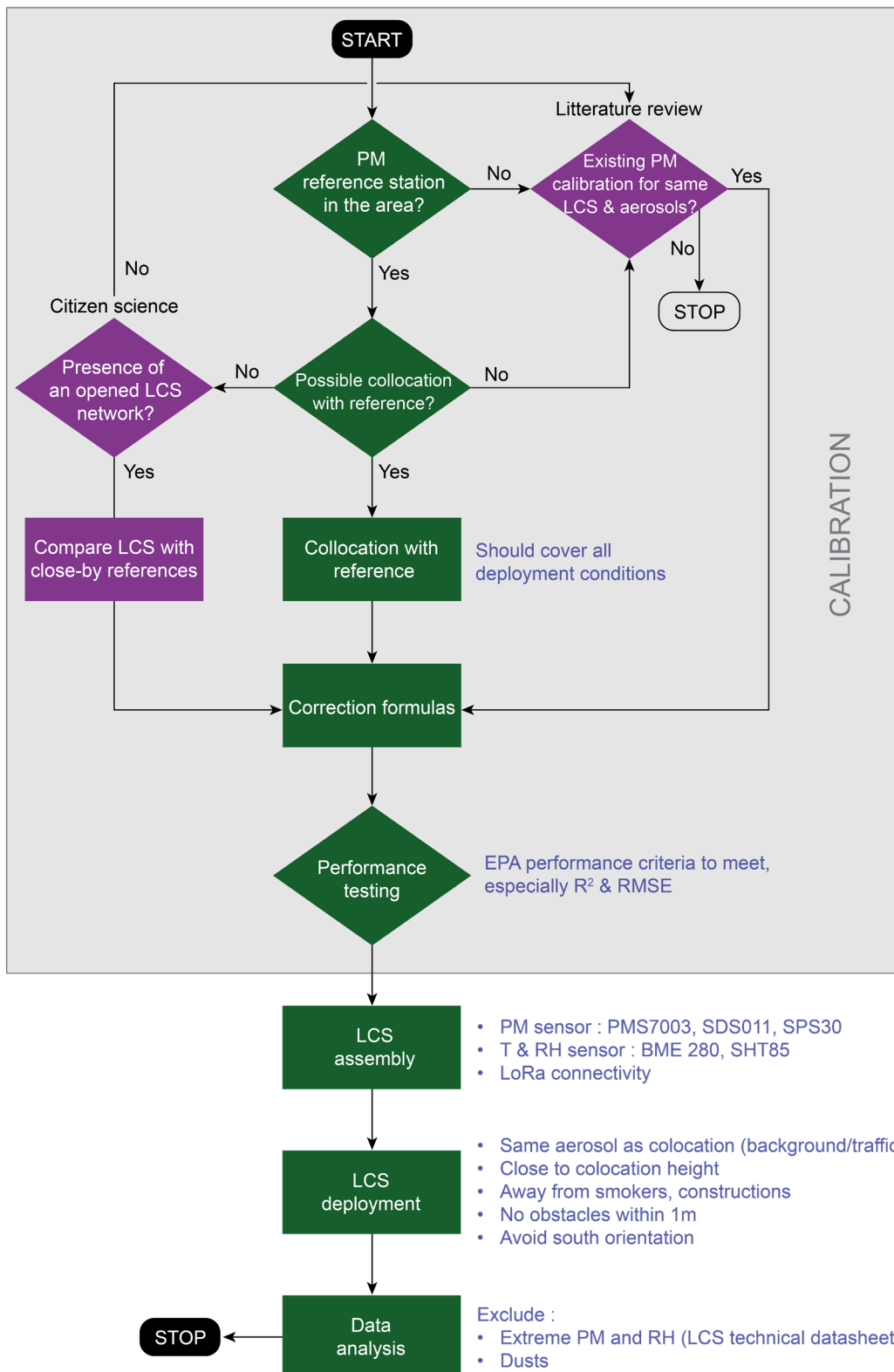


**Figure 32. Framework proposal for individuals interested in low-cost PM measurement** The green boxes represent the optimal scenario in which a reference station is accessible for direct comparison, while the purple boxes indicate less favorable situations.



## 6.4 FUTURE RESEARCH PERSPECTIVES

### 6.4.1 Autonomy and connectivity

Another interesting topic to address is the autonomy of low-cost air quality stations, which could be improved by incorporating solar-powered batteries. Efforts should be made to develop solar systems remaining effective during winter or when cloud cover is important. Such systems would allow deployment in places where there is no electricity. Working on the connectivity of air quality stations is also important to enable broader deployment and reduce the number of missing values. Wi-Fi connectivity was a limitation during our stationary study, especially when deploying air quality stations. Certain users did not have a Wi-Fi at home, and we encountered difficulties accessing Wi-Fi in public buildings such as universities, schools or libraries due to network security. To address this issue, we later developed a LoRaWAN air quality station (see Appendix C). This prototype offers a promising solution for future deployments.

### 6.4.2 Holistic air pollution monitoring

This thesis primarily focused on outdoor air pollution, but it would also be valuable to investigate indoor air pollution in order to gain an overall understanding of individual exposure. This could be done by measuring indoor pollutants within homes, and/or by estimating the infiltration of pollutants from the outside environment. To comprehensively assess individual exposure, it is necessary to consider exposure during commutes, as well as exposure at home and in the workplace. Various tools are available to measure pollutants, Figure 33 summarizing their advantages and disadvantages. These tools should be used complementarily to get a holistic view of air pollution.

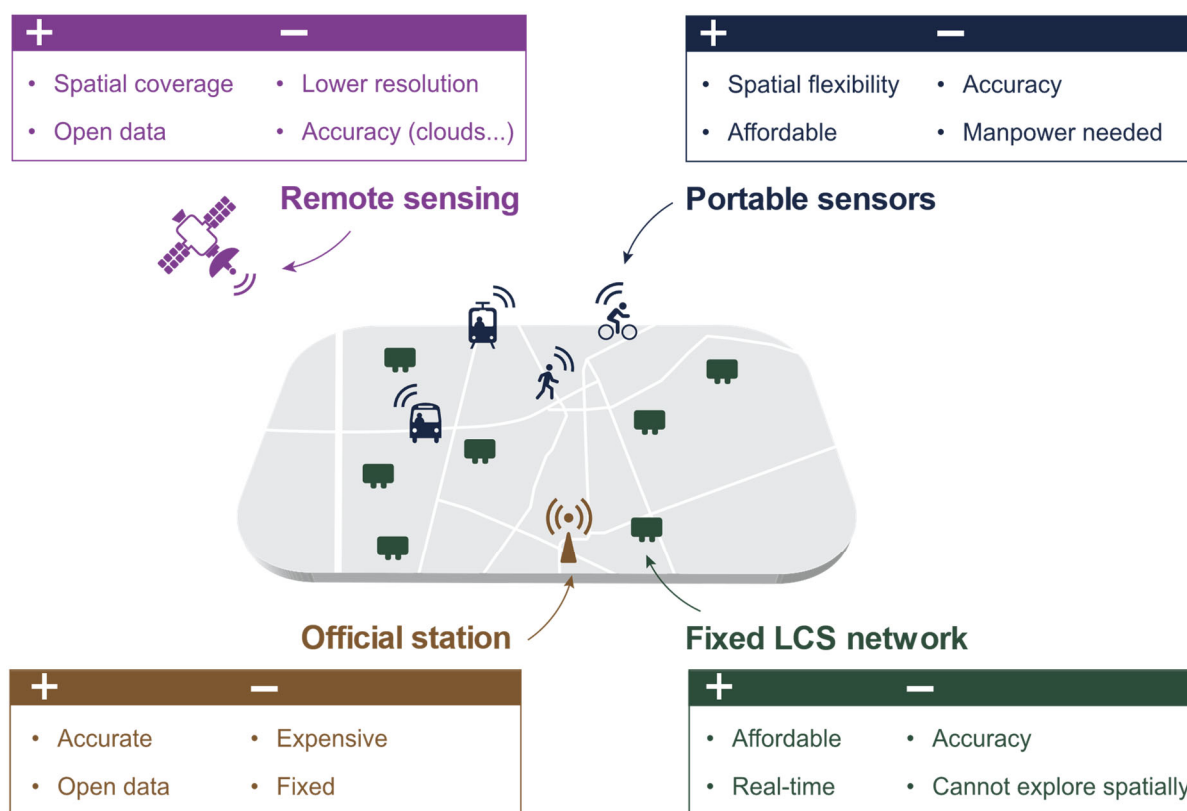


Figure 33. Advantages and disadvantages of different measuring approaches.

Mobile LCS allow spatial exploration, but only provide a brief spatiotemporal overview of pollutant concentrations, and are sensitive to accidental variations or biases (Peters et al., 2013). Another issue with mobile measurements is that replicates must be done to allow representativity, which consumes time and resources. However, while fixed sensors are considered better to measure temporal variations in pollutants (Chambliss et al., 2020), mobile sensors represent optimal solutions to capture spatial fluctuations (Munir et al., 2022). Various studies highlighted that LCS could supplement official monitors for precise spatial and temporal measurements (Bulot, Ossont, et al., 2023; Roberts et al., 2022). LCS could help scientists finding new associations, especially when combined with other sources of information like satellite or ground-based cameras observations. Using a LCS network and Google Street View images, O'Regan et al. (2022) observed that increased urban greenspace levels were linked to reductions in PM concentrations. Similarly, the combination of satellite and LCS network observations can be used to highlight air quality anomalies during wildfires (Wendt et al., 2023).

### 6.4.3 Growing importance of wildfires monitoring

Wildfires are going to become more frequent and intense because of climate change, which means that global population will be increasingly exposed to landscape fire-sourced PM<sub>2.5</sub> (Xu, Ye, et al., 2023). Burke et al. (2023) used both field and satellite PM measurements and found that since 2016, wildfire smoke eroded 4 years of air quality progress in nearly 75% of contiguous USA states and even more in western states. Li et al. (2023) highlighted the need to improve prediction models by incorporating dynamic variables like remote sensing fine-level aerosol data. LCS could also play a role in wildfire prevention, which is particularly important given that forest fires are responsible for significant CO<sub>2</sub> emissions, further aggravating climate warming (Zheng et al., 2023). This is also crucial because wildfires can affect the health of populations even at considerable distances from the fires as air pollutants travel across countries. As showed by Aguilera et al. (2021), smoke from wildfires could have more pronounced impacts on respiratory health compared to PM from other sources. According to Gutierrez et al. (2021) the surface of burned land is expected to increase by 25% by the 2040s, wildfires being very sensitive to small temperature changes, a 1°C rise in temperature corresponding to a 22% fire risk increase. Due to these factors, tracking wildfire events will be crucial, and LCS will likely play a key role in gaining further insights into wildfire monitoring.

### 6.4.4 Proposals for future research on calibration

As already explained, field calibration with a collocation should always be the preferred scenario, but recently some works have been done using LCS networks and showed good performances compared to a local calibration (Koehler et al., 2023). It would be interesting to validate those findings by placing LCS close to a gravimetric reference (gold-standard) along with other LCS positioned at a greater distance (e.g., 200 meters), to evaluate their respective performances compared to the gold-standard. Following Barkjohn et al. (2021) study, it would also be valuable to work on generic calibrations at a country wide scale. Working on algorithms using machine learning and make them available to the community seems to be a promising approach to address the shortage of reference monitors in some areas. Lastly, work should also focus on calibrating high concentrations. Winter is very often the season when citizens are more exposed to PM. It is therefore urgent to develop calibration algorithms adapted to these aerosols' conditions.

### 6.4.5 Simplify PM measurement

Exploring ways to make the use of LCS easier appears to be a promising research direction for simplifying the measurement process and collect more PM data. Minimizing interference with individuals' daily habits should be considered (Steinle et al., 2013; Zauli-Sajani et al., 2022). Exploring sensors miniaturization represents a potential research direction that could revolutionize the assessment of individuals' exposure to PM. Simplifying the deployment and use of LCS seems crucial to increase citizen engagement and develop citizen science. However, it's equally important to remain vigilant about the ecological impact of these sensors, and we should minimize their carbon footprint.

## 6.5 LAST WORDS ON AIR POLLUTION AND HEALTH

As a conclusion, it is important to remind that improved air quality should bring greater health benefits compared to its implementation costs (Hoffmann et al., 2021; Schraufnagel et al., 2019). The US EPA (2011) found that the health benefits of the Clean Air Act outweighed the costs by a factor of 32. In China, improving air quality with the nationwide "Air Plan" yielded public health benefits exceeding the implementation cost by a 1.5 factor (J. Zhang et al., 2019). In this context, low-cost sensors are especially useful to allow citizens to avoid, or at least decrease, their exposure. This is particularly important in highly polluted areas where reference monitors are rare.

# 7 REFERENCES

- Adelakun, A. O., & Akano, O. (2023). Development of an alternative device for measurement and characterization of selected meteorological parameters. *Scientific Reports*, *13*(1), 10992. <https://doi.org/10.1038/s41598-023-35839-5>
- Aguilera, R., Corringham, T., Gershunov, A., & Benmarhnia, T. (2021). Wildfire smoke impacts respiratory health more than fine particles from other sources: observational evidence from Southern California. *Nature communications*, *12*(1), 1493. <https://doi.org/10.1038/s41467-021-21708-0>
- Aix, M. L., Petit, P., & Bicout, D. J. (2022). Air pollution and health impacts during the COVID-19 lockdowns in Grenoble, France. *Environmental Pollution*, *303*, 119134. <https://doi.org/10.1016/j.envpol.2022.119134>
- Aix, M. L., Schmitz, S., & Bicout, D. J. (2023). Calibration methodology of low-cost sensors for high-quality monitoring of fine particulate matter. *Science of the Total Environment*, *889*, 164063. <https://doi.org/10.1016/j.scitotenv.2023.164063>
- Al-Kindi, S. G., Brook, R. D., Biswal, S., & Rajagopalan, S. (2020). Environmental determinants of cardiovascular disease: lessons learned from air pollution. *Nature Reviews Cardiology*, *17*(10), 656-672. <https://doi.org/10.1038/s41569-020-0371-2>
- Alas, H. D. C., Weinhold, K., Costabile, F., Di Ianni, A., Müller, T., Pfeifer, S., Di Liberto, L., Turner, J. R., & Wiedensohler, A. (2019). Methodology for high-quality mobile measurement with focus on black carbon and particle mass concentrations. *Atmospheric Measurement Techniques*, *12*(9), 4697-4712. <https://doi.org/10.5194/amt-12-4697-2019>

- Alfano, B., Barretta, L., Del Giudice, A., De Vito, S., Di Francia, G., Esposito, E., Formisano, F., Massera, E., Miglietta, M. L., & Polichetti, T. (2020). A Review of Low-Cost Particulate Matter Sensors from the Developers' Perspectives. *Sensors*, 20(23), 6819. <https://doi.org/10.3390/s20236819>
- Alonso-Pérez, S., & López-Solano, J. (2023). Long-Term Analysis of Aerosol Concentrations Using a Low-Cost Sensor: Monitoring African Dust Outbreaks in a Suburban Environment in the Canary Islands. *Sensors*, 23(18). <https://doi.org/10.3390/s23187768>
- Altman, M. C., Kattan, M., O'Connor, G. T., Murphy, R. C., Whalen, E., LeBeau, P., Calatroni, A., Gill, M. A., Gruchalla, R. S., Liu, A. H., Lovinsky-Desir, S., Pongracic, J. A., Kerckmar, C. M., Khurana Hershey, G. K., Zoratti, E. M., Teach, S. J., Bacharier, L. B., Wheatley, L. M., Sigelman, S. M., Gergen, P. J., Togias, A., Busse, W. W., Gern, J. E., Jackson, D. J., National Institute of, A., & Infectious Disease's Inner City Asthma, C. (2023). Associations between outdoor air pollutants and non-viral asthma exacerbations and airway inflammatory responses in children and adolescents living in urban areas in the USA: a retrospective secondary analysis. *The Lancet Planetary Health*, 7(1), e33-e44. [https://doi.org/10.1016/S2542-5196\(22\)00302-3](https://doi.org/10.1016/S2542-5196(22)00302-3)
- Amrani, F., Prud'homme, J., Maesano, C., & Annesi-Maesano, I. (2019). Évolution de la pollution atmosphérique urbaine dans 13 grandes villes françaises entre 2008 et 2015 [Evolution of urban air pollution in metropolitan France between 2008 and 2015]. *Revue des Maladies Respiratoires*, 36(10), 1096-1106. <https://doi.org/10.1016/j.rmr.2019.09.003>
- Anagnostopoulos, F. K., Rigas, S., Papachristou, M., Chaniotis, I., Anastasiou, I., Tryfonopoulos, C., & Raftopoulou, P. (2023). A Novel AI Framework for PM Pollution Prediction Applied to a Greek Port City. *Atmosphere*, 14(9). <https://doi.org/10.3390/atmos14091413>
- Apte, J. S., Kirchstetter, T. W., Reich, A. H., Deshpande, S. J., Kaushik, G., Chel, A., Marshall, J. D., & Nazaroff, W. W. (2011). Concentrations of fine, ultrafine, and black carbon particles in auto-rickshaws in New Delhi, India. *Atmospheric Environment*, 45(26), 4470-4480. <https://doi.org/10.1016/j.atmosenv.2011.05.028>
- Araujo, J. A. (2010). Particulate air pollution, systemic oxidative stress, inflammation, and atherosclerosis. *Air Quality, Atmosphere & Health*, 4(1), 79-93. <https://doi.org/10.1007/s11869-010-0101-8>
- Atmo AuRA. (2022a). *Emissions | Contribution des différentes activités humaines aux émissions de polluants atmosphériques en pourcentages - Pour l'EPCI Grenoble-Alpes-Métropole - Données pour les PM<sub>2,5</sub>, PM<sub>10</sub>, et NO<sub>x</sub> (Inventaire 2022 - Données 2020) [Data set and visualization]*. [https://www.atmo-auvergnerhonealpes.fr/dataviz/emissions?type\\_zone=1&zone\\_id=200040715&code\\_parometre=108](https://www.atmo-auvergnerhonealpes.fr/dataviz/emissions?type_zone=1&zone_id=200040715&code_parometre=108)

- Atmo AuRA. (2022b). *Populations exposées par EPCI en 2021 - Jeu de données [Data set]*. [https://data-atmoaura.opendata.arcgis.com/datasets/ef54227ba5c64621999cc9c17ff3b3fb\\_0/explore](https://data-atmoaura.opendata.arcgis.com/datasets/ef54227ba5c64621999cc9c17ff3b3fb_0/explore)
- Atmo AuRA. (2022c). *Suivi de la qualité de l'air à proximité de l'A480 en phase chantier*. <https://www.atmo-auvergnerhonealpes.fr/sites/aura/files/medias/documents/2022-06/A480%20bilan%202021%20vf.pdf>
- Atmo AuRA. (2023a). *API Atmo Auvergne-Rhône-Alpes [Data set]*. <https://api.atmo-aura.fr/>
- Atmo AuRA. (2023b). *Observatoire de la qualité de l'air à proximité de l'A480 en phase chantier*. [https://www.atmo-auvergnerhonealpes.fr/sites/aura/files/medias/documents/2023-07/Rapport%20A480%20bilan%202022\\_V260523.pdf](https://www.atmo-auvergnerhonealpes.fr/sites/aura/files/medias/documents/2023-07/Rapport%20A480%20bilan%202022_V260523.pdf)
- Atmo AuRA. (2023c). *Portraits des territoires d'Auvergne-Rhône-Alpes en 2022*. [https://www.atmo-auvergnerhonealpes.fr/sites/aura/files/medias/documents/2023-04/ATMO\\_A4\\_Dossier-Portraits\\_territoires\\_VDEF.pdf](https://www.atmo-auvergnerhonealpes.fr/sites/aura/files/medias/documents/2023-04/ATMO_A4_Dossier-Portraits_territoires_VDEF.pdf)
- Atmo AuRA. (2023d). *Rapport annuel 2022*. Retrieved 2023-08-20 from [https://www.atmo-auvergnerhonealpes.fr/sites/aura/files/medias/documents/2023-06/ATMO\\_Rapport-annuel-2022\\_VDEF-WEB.pdf](https://www.atmo-auvergnerhonealpes.fr/sites/aura/files/medias/documents/2023-06/ATMO_Rapport-annuel-2022_VDEF-WEB.pdf)
- Automotive News Europe. (2023). *Eight EU nations call for scrapping of Euro 7 emission rules*. <https://europe.autonews.com/environmentemissions/eight-eu-nations-call-scrapping-euro-7-emission-rules>
- Badura, M., Batog, P., Drzeniecka-Osiadacz, A., & Modzel, P. (2018). Optical particulate matter sensors in PM<sub>2.5</sub> measurements in atmospheric air. *E3S Web of Conferences*, 44. <https://doi.org/10.1051/e3sconf/20184400006>
- Ballester, F., Medina, S., Boldo, E., Goodman, P., Neuberger, M., Iniguez, C., Kunzli, N., & Apheis, n. (2008). Reducing ambient levels of fine particulates could substantially improve health: a mortality impact assessment for 26 European cities. *Journal of Epidemiology and Community Health*, 62(2), 98-105. <https://doi.org/10.1136/jech.2007.059857>
- Barkjohn, K. K., Gantt, B., & Clements, A. L. (2021). Development and Application of a United States wide correction for PM<sub>2.5</sub> data collected with the PurpleAir sensor. *Atmospheric Measurement Techniques*, 4(6), 4617–4637. <https://doi.org/10.5194/amt-14-4617-2021>
- Barkjohn, K. K., Holder, A. L., Frederick, S. G., & Clements, A. L. (2022). Correction and Accuracy of PurpleAir PM<sub>2.5</sub> Measurements for Extreme Wildfire Smoke. *Sensors (Basel)*, 22(24). <https://doi.org/10.3390/s22249669>



- Bates, J. T., Fang, T., Verma, V., Zeng, L., Weber, R. J., Tolbert, P. E., Abrams, J. Y., Sarnat, S. E., Klein, M., Mulholland, J. A., & Russell, A. G. (2019). Review of Acellular Assays of Ambient Particulate Matter Oxidative Potential: Methods and Relationships with Composition, Sources, and Health Effects. *Environmental Science & Technology*, 53(8), 4003-4019. <https://doi.org/10.1021/acs.est.8b03430>
- Báthory, C., Dobo, Z., Garami, A., Palotas, A., & Toth, P. (2021). Low-cost monitoring of atmospheric PM-development and testing. *Journal of Environmental Management*, 304, 114158. <https://doi.org/10.1016/j.jenvman.2021.114158>
- Bauerová, P., Šindelářová, A., Rychlík, Š., Novák, Z., & Keder, J. (2020). Low-Cost Air Quality Sensors: One-Year Field Comparative Measurement of Different Gas Sensors and Particle Counters with Reference Monitors at Tušimice Observatory. *Atmosphere (Basel)*, 11(5), 492. <https://doi.org/10.3390/atmos11050492>
- Beckx, C., Int Panis, L., Arentze, T., Janssens, D., Torfs, R., Broekx, S., & Wets, G. (2009). A dynamic activity-based population modelling approach to evaluate exposure to air pollution: Methods and application to a Dutch urban area. *Environmental Impact Assessment Review*, 29(3), 179-185. <https://doi.org/10.1016/j.eiar.2008.10.001>
- Bell, M. L., Dominici, F., Ebisu, K., Zeger, S. L., & Samet, J. M. (2007). Spatial and temporal variation in PM<sub>2.5</sub> chemical composition in the United States for health effects studies. *Environmental Health Perspectives*, 115(7), 989-995. <https://doi.org/10.1289/ehp.9621>
- Belz, D. C., Woo, H., Putcha, N., Paulin, L. M., Koehler, K., Fawzy, A., Alexis, N. E., Barr, R. G., Comellas, A. P., Cooper, C. B., Couper, D., Dransfield, M., Gasset, A. J., Han, M., Hoffman, E. A., Kanner, R. E., Krishnan, J. A., Martinez, F. J., Paine, R., 3rd, Peng, R. D., Peters, S., Pirozzi, C. S., Woodruff, P. G., Kaufman, J. D., Hansel, N. N., & Investigators, S. (2022). Ambient ozone effects on respiratory outcomes among smokers modified by neighborhood poverty: An analysis of SPIROMICS AIR. *Science of the Total Environment*, 829, 154694. <https://doi.org/10.1016/j.scitotenv.2022.154694>
- Botero, N. (2021). Pollution atmosphérique à la une : visibilité médiatique d'un problème environnemental. *Revue Française des Sciences de l'Information et de la Communication* (21). <https://doi.org/10.4000/rfsic.10230>
- Boulter, P. (2020). Air Quality, Surface Transportation Impacts on. In M. E. Goodsite, M. S. Johnson, & O. Hertel (Eds.), *Air Pollution Sources, Statistics and Health Effects*. Springer US. [https://doi.org/10.1007/978-1-4939-2493-6\\_911-3](https://doi.org/10.1007/978-1-4939-2493-6_911-3)

- Bowatte, G., Erbas, B., Lodge, C. J., Knibbs, L. D., Gurrin, L. C., Marks, G. B., Thomas, P. S., Johns, D. P., Giles, G. G., Hui, J., Dennekamp, M., Perret, J. L., Abramson, M. J., Walters, E. H., Matheson, M. C., & Dharmage, S. C. (2017). Traffic-related air pollution exposure over a 5-year period is associated with increased risk of asthma and poor lung function in middle age. *European Respiratory Journal*, *50*(4). <https://doi.org/10.1183/13993003.02357-2016>
- Bowe, B., Xie, Y., Li, T., Yan, Y., Xian, H., & Al-Aly, Z. (2018). The 2016 global and national burden of diabetes mellitus attributable to PM<sub>2.5</sub> air pollution. *The Lancet Planetary Health*, *2*(7), e301-e312. [https://doi.org/10.1016/S2542-5196\(18\)30140-2](https://doi.org/10.1016/S2542-5196(18)30140-2)
- Breathe London. (2023). *Breathe London the community sensing network*. Retrieved October 11, 2023 from <https://www.breathelondon.org/>
- Brook, R. D., Rajagopalan, S., Pope, C. A., 3rd, Brook, J. R., Bhatnagar, A., Diez-Roux, A. V., Holguin, F., Hong, Y., Luepker, R. V., Mittleman, M. A., Peters, A., Siscovick, D., Smith, S. C., Jr., Whitsel, L., Kaufman, J. D., American Heart Association Council on, E., Prevention, C. o. t. K. i. C. D., Council on Nutrition, P. A., & Metabolism. (2010). Particulate matter air pollution and cardiovascular disease: An update to the scientific statement from the American Heart Association. *Circulation*, *121*(21), 2331-2378. <https://doi.org/10.1161/CIR.0b013e3181dbee1>
- Bulot, F. M. J., Johnston, S. J., Basford, P. J., Easton, N. H. C., Apetroaie-Cristea, M., Foster, G. L., Morris, A. K. R., Cox, S. J., & Loxham, M. (2019). Long-term field comparison of multiple low-cost particulate matter sensors in an outdoor urban environment. *Scientific Reports*, *9*(1). <https://doi.org/10.1038/s41598-019-43716-3>
- Bulot, F. M. J., Ossont, S. J., Morris, A. K. R., Basford, P. J., Easton, N. H. C., Mitchell, H. L., Foster, G. L., Cox, S. J., & Loxham, M. (2023). Characterisation and calibration of low-cost PM sensors at high temporal resolution to reference-grade performance. *Heliyon*, *9*(5), e15943. <https://doi.org/10.1016/j.heliyon.2023.e15943>
- Bulot, F. M. J., Russell, H. S., Rezaei, M., Johnson, M. S., Ossont, S. J., Morris, A. K. R., Basford, P. J., Easton, N. H. C., Mitchell, H. L., Foster, G. L., Loxham, M., & Cox, S. J. (2023). Laboratory Comparison of Low-Cost Particulate Matter Sensors to Measure Transient Events of Pollution - Part B - Particle Number Concentrations. *Sensors (Basel)*, *23*(17). <https://doi.org/10.3390/s23177657>
- Burke, M., Childs, M. L., de la Cuesta, B., Qiu, M., Li, J., Gould, C. F., Heft-Neal, S., & Wara, M. (2023). The contribution of wildfire to PM<sub>2.5</sub> trends in the USA. *Nature*. <https://doi.org/10.1038/s41586-023-06522-6>

- Cai, Y., Zhang, B., Ke, W., Feng, B., Lin, H., Xiao, J., Zeng, W., Li, X., Tao, J., Yang, Z., Ma, W., & Liu, T. (2016). Associations of Short-Term and Long-Term Exposure to Ambient Air Pollutants With Hypertension. *Hypertension*, *68*(1), 62-70. <https://doi.org/10.1161/HYPERTENSIONAHA.116.07218>
- Campolim, C. M., Weissmann, L., Ferreira, C. K. O., Zordao, O. P., Dornellas, A. P. S., de Castro, G., Zanotto, T. M., Boico, V. F., Quaresma, P. G. F., Lima, R. P. A., Donato, J., Jr., Veras, M. M., Saldiva, P. H. N., Kim, Y. B., & Prada, P. O. (2020). Short-term exposure to air pollution (PM<sub>2.5</sub>) induces hypothalamic inflammation, and long-term leads to leptin resistance and obesity via Tlr4/Ikbke in mice. *Scientific Reports*, *10*(1), 10160. <https://doi.org/10.1038/s41598-020-67040-3>
- Castell, N., Dauge, F. R., Schneider, P., Vogt, M., Lerner, U., Fishbain, B., Broday, D., & Bartonova, A. (2017). Can commercial low-cost sensor platforms contribute to air quality monitoring and exposure estimates? *Environment International*, *99*, 293-302. <https://doi.org/10.1016/j.envint.2016.12.007>
- Chambliss, S. E., Preble, C. V., Caubel, J. J., Cados, T., Messier, K. P., Alvarez, R. A., LaFranchi, B., Lunden, M., Marshall, J. D., Szpiro, A. A., Kirchstetter, T. W., & Apte, J. S. (2020). Comparison of Mobile and Fixed-Site Black Carbon Measurements for High-Resolution Urban Pollution Mapping. *Environmental Science & Technology*, *54*(13), 7848-7857. <https://doi.org/10.1021/acs.est.0c01409>
- Chandra, M., Rai, C. B., Kumari, N., Sandhu, V. K., Chandra, K., Krishna, M., Kota, S. H., Anand, K. S., & Oudin, A. (2022). Air Pollution and Cognitive Impairment across the Life Course in Humans: A Systematic Review with Specific Focus on Income Level of Study Area. *International Journal of Environmental Research and Public Health*, *19*(3). <https://doi.org/10.3390/ijerph19031405>
- Chauhan, A. J., Inskip, H. M., Linaker, C. H., Smith, S., Schreiber, J., Johnston, S. L., & Holgate, S. T. (2003). Personal exposure to nitrogen dioxide (NO<sub>2</sub>) and the severity of virus-induced asthma in children. *Lancet*, *361*(9373), 1939-1944. [https://doi.org/10.1016/s0140-6736\(03\)13582-9](https://doi.org/10.1016/s0140-6736(03)13582-9)
- Chen, G., Li, S., Zhang, Y., Zhang, W., Li, D., Wei, X., He, Y., Bell, M. L., Williams, G., Marks, G. B., Jalaludin, B., Abramson, M. J., & Guo, Y. (2017). Effects of ambient PM<sub>1</sub> air pollution on daily emergency hospital visits in China: an epidemiological study. *The Lancet Planetary Health*, *1*(6), e221-e229. [https://doi.org/10.1016/s2542-5196\(17\)30100-6](https://doi.org/10.1016/s2542-5196(17)30100-6)
- Chen, J., & Hoek, G. (2020). Long-term exposure to PM and all-cause and cause-specific mortality: A systematic review and meta-analysis. *Environment International*, *143*, 105974. <https://doi.org/10.1016/j.envint.2020.105974>

- Chen, R., Jiang, Y., Hu, J., Chen, H., Li, H., Meng, X., Ji, J. S., Gao, Y., Wang, W., Liu, C., Fang, W., Yan, H., Chen, J., Wang, W., Xiang, D., Su, X., Yu, B., Wang, Y., Xu, Y., Wang, L., Li, C., Chen, Y., Bell, M. L., Cohen, A. J., Ge, J., Huo, Y., & Kan, H. (2022). Hourly Air Pollutants and Acute Coronary Syndrome Onset in 1.29 Million Patients. *Circulation*, *145*(24), 1749-1760. <https://doi.org/10.1161/CIRCULATIONAHA.121.057179>
- Clifford, H. M., Spaulding, N. E., Kurbatov, A. V., More, A., Korotkikh, E. V., Sneed, S. B., Handley, M., Maasch, K. A., Loveluck, C. P., Chaplin, J., McCormick, M., & Mayewski, P. A. (2019). A 2000 Year Saharan Dust Event Proxy Record from an Ice Core in the European Alps. *Journal of Geophysical Research: Atmospheres*, *124*(23), 12882-12900. <https://doi.org/10.1029/2019jd030725>
- Cohen, A. J., Brauer, M., Burnett, R., Anderson, H. R., Frostad, J., Estep, K., Balakrishnan, K., Brunekreef, B., Dandona, L., Dandona, R., Feigin, V., Freedman, G., Hubbell, B., Jobling, A., Kan, H., Knibbs, L., Liu, Y., Martin, R., Morawska, L., Pope, C. A., Shin, H., Straif, K., Shaddick, G., Thomas, M., van Dingenen, R., van Donkelaar, A., Vos, T., Murray, C. J. L., & Forouzanfar, M. H. (2017). Estimates and 25-year trends of the global burden of disease attributable to ambient air pollution: an analysis of data from the Global Burden of Diseases Study 2015. *Lancet*, *389*, 1907. [https://doi.org/10.1016/S0140-6736\(17\)30505-6](https://doi.org/10.1016/S0140-6736(17)30505-6)
- Coker, E. S., Buralli, R., Manrique, A. F., Kanai, C. M., Amegah, A. K., & Gouveia, N. (2022). Association between PM<sub>2.5</sub> and respiratory hospitalization in Rio Branco, Brazil: Demonstrating the potential of low-cost air quality sensor for epidemiologic research. *Environmental Research*, *214*(Pt 1), 113738. <https://doi.org/10.1016/j.envres.2022.113738>
- Corso, M., Lagarrigue, R., & Medina, S. (2019). *Pollution atmosphérique. Guide pour la réalisation d'une évaluation quantitative des impacts sur la santé (EQIS). EQIS avec une exposition mesurée.* <https://www.santepubliquefrance.fr/determinants-de-sante/pollution-et-sante/air/documents/guide/pollution-atmospherique.-guide-pour-la-realisation-d-une-evaluation-quantitative-des-impacts-sur-la-sante-eqis-.eqis-avec-une-exposition-mesuree>
- Cowell, N., Chapman, L., Bloss, W., & Pope, F. (2022). Field Calibration and Evaluation of an Internet-of-Things-Based Particulate Matter Sensor. *Frontiers in Environmental Science*, *9*. <https://doi.org/10.3389/fenvs.2021.798485>
- Crutzen, P. J. (1979). The Role of NO and NO<sub>2</sub> in the Chemistry of the Troposphere and Stratosphere. *Annual Review of Earth and Planetary Sciences*, *7*(1), 443-472. <https://doi.org/10.1146/annurev.ca.07.050179.002303>

- Daellenbach, K. R., Uzu, G., Jiang, J., Cassagnes, L. E., Leni, Z., Vlachou, A., Stefanelli, G., Canonaco, F., Weber, S., Segers, A., Kuenen, J. J. P., Schaap, M., Favez, O., Albinet, A., Aksoyoglu, S., Dommen, J., Baltensperger, U., Geiser, M., El Haddad, I., Jaffrezo, J. L., & Prévôt, A. S. H. (2020). Sources of particulate-matter air pollution and its oxidative potential in Europe. *Nature*, *587*(7834), 414-419. <https://doi.org/10.1038/s41586-020-2902-8>
- Danesh Yazdi, M., Wang, Y., Di, Q., Requia, W. J., Wei, Y., Shi, L., Sabath, M. B., Dominici, F., Coull, B., Evans, J. S., Koutrakis, P., & Schwartz, J. D. (2021). Long-term effect of exposure to lower concentrations of air pollution on mortality among US Medicare participants and vulnerable subgroups: a doubly-robust approach. *The Lancet Planetary Health*, *5*(10), e689-e697. [https://doi.org/10.1016/S2542-5196\(21\)00204-7](https://doi.org/10.1016/S2542-5196(21)00204-7)
- Datta, A., Saha, A., Zamora, M. L., Buehler, C., Hao, L., Xiong, F., Gentner, D. R., & Koehler, K. (2020). Statistical field calibration of a low-cost PM<sub>2.5</sub> monitoring network in Baltimore. *Atmospheric Environment*, *242*. <https://doi.org/10.1016/j.atmosenv.2020.117761>
- de Nazelle, A. (2021). A conversation on the impacts and mitigation of air pollution. *Nature communications*, *12*(1), 5822. <https://doi.org/10.1038/s41467-021-25518-2>
- Dejchanchaiwong, R., Tekasakul, P., Saejio, A., Limna, T., Le, T.-C., Tsai, C.-J., Lin, G.-Y., & Morris, J. (2023). Seasonal Field Calibration of Low-Cost PM<sub>2.5</sub> Sensors in Different Locations with Different Sources in Thailand. *Atmosphere*, *14*(3). <https://doi.org/10.3390/atmos14030496>
- deSouza, P., Barkjohn, K., Clements, A., Lee, J., Kahn, R., Crawford, B., & Kinney, P. (2023). An analysis of degradation in low-cost particulate matter sensors. *Environmental Science: Atmospheres*, *3*(3), 521-536. <https://doi.org/10.1039/d2ea00142j>
- deSouza, P., Kahn, R., Stockman, T., Obermann, W., Crawford, B., Wang, A., Crooks, J., Li, J., & Kinney, P. (2022). Calibrating networks of low-cost air quality sensors. *Atmospheric Measurement Techniques*, *15*(21), 6309-6328. <https://doi.org/10.5194/amt-15-6309-2022>
- Di, Q., Dai, L., Wang, Y., Zanobetti, A., Choirat, C., Schwartz, J. D., & Dominici, F. (2017). Association of Short-term Exposure to Air Pollution With Mortality in Older Adults. *JAMA*, *318*(24), 2446-2456. <https://doi.org/10.1001/jama.2017.17923>
- Dias, D., & Tchepel, O. (2018). Spatial and Temporal Dynamics in Air Pollution Exposure Assessment. *International Journal of Environmental Research and Public Health*, *15*(3). <https://doi.org/10.3390/ijerph15030558>

- Dimitriou, K., Stavroulas, I., Grivas, G., Chatzidiakos, C., Kosmopoulos, G., Kazantzidis, A., Kourtidis, K., Karagioras, A., Hatzianastassiou, N., Pandis, S. N., Mihalopoulos, N., & Gerasopoulos, E. (2023). Intra- and inter-city variability of PM<sub>2.5</sub> concentrations in Greece as determined with a low-cost sensor network. *Atmospheric Environment*, 301. <https://doi.org/10.1016/j.atmosenv.2023.119713>
- Dockery, D. W., Pope, C. A., Xu, X., Spengler, J. D., Ware, J. H., Fay, M. E., Ferris, B. G., & Speizer, F. E. (1993). An Association between Air Pollution and Mortality in Six U.S. Cities. *The New England Journal of Medicine*, 329(24), 1753-1759. <https://doi.org/10.1056/nejm199312093292401>
- Dominski, F. H., Lorenzetti Branco, J. H., Buonanno, G., Stabile, L., Gameiro da Silva, M., & Andrade, A. (2021). Effects of air pollution on health: A mapping review of systematic reviews and meta-analyses. *Environmental Research*, 201, 111487. <https://doi.org/10.1016/j.envres.2021.111487>
- Dons, E., Int Panis, L., Van Poppel, M., Theunis, J., Willems, H., Torfs, R., & Wets, G. (2011). Impact of time–activity patterns on personal exposure to black carbon. *Atmospheric Environment*, 45(21), 3594-3602. <https://doi.org/10.1016/j.atmosenv.2011.03.064>
- Dons, E., Laeremans, M., Orjuela, J. P., Avila-Palencia, I., de Nazelle, A., Nieuwenhuijsen, M., Van Poppel, M., Carrasco-Turigas, G., Standaert, A., De Boever, P., Nawrot, T., & Int Panis, L. (2019). Transport most likely to cause air pollution peak exposures in everyday life: Evidence from over 2000 days of personal monitoring. *Atmospheric Environment*, 213, 424-432. <https://doi.org/10.1016/j.atmosenv.2019.06.035>
- Dwivedi, A. K., Vishwakarma, D., Dubey, P., & Reddy, S. Y. (2022). Air Pollution and the Heart: Updated Evidence from Meta-analysis Studies. *Current Cardiology Reports*, 24(12), 1811-1835. <https://doi.org/10.1007/s11886-022-01819-w>
- ElSharkawy, M. F., & Ibrahim, O. A. (2022). Impact of the Restaurant Chimney Emissions on the Outdoor Air Quality. *Atmosphere*, 13(2). <https://doi.org/10.3390/atmos13020261>
- European Commission. (2021). *Communication from the Commission to the European Parliament, the Council, the European Economic and Social Committee and the Committee of the Regions - Pathway to a Healthy Planet for All - EU Action Plan: 'Towards Zero Pollution for Air, Water and Soil'* - Document 52021DC0400 - COM/2021/400 final. <https://eur-lex.europa.eu/legal-content/EN/TXT/?uri=CELEX%3A52021DC0400&qid=1623311742827>
- European Commission. (November 10, 2022). *Commission proposes new Euro 7 standards to reduce pollutant emissions from vehicles and improve air quality* [Press release]. [https://ec.europa.eu/commission/presscorner/detail/en/ip\\_22\\_6495](https://ec.europa.eu/commission/presscorner/detail/en/ip_22_6495)



- European Environment Agency. (February 28, 2023). *Air quality in Europe*. Retrieved October 11, 2023 from <https://www.eea.europa.eu/publications/air-quality-in-europe-2022>
- European Environment Agency. (2011). *More efforts required to reduce ozone pollution in Europe*. <https://www.eea.europa.eu/highlights/more-efforts-required-to-reduce>
- European Environment Agency. (2020). *Air Quality in Europe - 2020 Report, EEA Report No 09/2020*. <https://www.eea.europa.eu/publications/air-quality-in-europe-2020-report>
- European Environment Agency. (2022). *Sources and emissions of air pollutants in Europe*. <https://www.eea.europa.eu/publications/air-quality-in-europe-2022/sources-and-emissions-of-air>
- Eze, I. C., Hemkens, L. G., Bucher, H. C., Hoffmann, B., Schindler, C., Kunzli, N., Schikowski, T., & Probst-Hensch, N. M. (2015). Association between ambient air pollution and diabetes mellitus in Europe and North America: systematic review and meta-analysis. *Environmental Health Perspectives*, 123(5), 381-389. <https://doi.org/10.1289/ehp.1307823>
- Faustini, A., Rapp, R., & Forastiere, F. (2014). Nitrogen dioxide and mortality: review and meta-analysis of long-term studies. *The European Respiratory Journal*, 44(3), 744-753. <https://doi.org/10.1183/09031936.00114713>
- Frischer, T., Studnicka, M., Beer, E., & Neumann, M. (1993). The effects of ambient NO<sub>2</sub> on lung function in primary schoolchildren. *Environmental Research*, 62(2), 179-188. <https://doi.org/10.1006/enrs.1993.1103>
- Fusco, D., Forastiere, F., Michelozzi, P., Spadea, T., Ostro, B., Arcà, M., & Perucci, C. A. (2001). Air pollution and hospital admissions for respiratory conditions in Rome, Italy. *The European Respiratory Journal*, 17(6), 1143-1150. <https://doi.org/10.1183/09031936.01.00005501>
- Gabel, P., Koller, C., & Hertig, E. (2022). Development of Air Quality Boxes Based on Low-Cost Sensor Technology for Ambient Air Quality Monitoring. *Sensors (Basel)*, 22(10). <https://doi.org/10.3390/s22103830>
- GBD 2019 Risk Factors Collaborators. (2020). Global burden of 87 risk factors in 204 countries and territories, 1990-2019: a systematic analysis for the Global Burden of Disease Study 2019. *Lancet*, 396(10258), 1223-1249. [https://doi.org/10.1016/s0140-6736\(20\)30752-2](https://doi.org/10.1016/s0140-6736(20)30752-2)
- Gerboles, M., Spinelle, L., & Borowiak, A. (2017). *Measuring air pollution with low-cost sensors*. <https://publications.jrc.ec.europa.eu/repository/handle/JRC107461>



- Giordano, M. R., Malings, C., Pandis, S. N., Presto, A. A., McNeill, V. F., Westervelt, D. M., Beekmann, M., & Subramanian, R. (2021). From low-cost sensors to high-quality data: A summary of challenges and best practices for effectively calibrating low-cost particulate matter mass sensors. *Journal of Aerosol Science*, *158*, 105833. <https://doi.org/10.1016/j.jaerosci.2021.105833>
- Gitahi, J., & Hahn, M. (2022). Evaluation of Crowd-Sourced PM<sub>2.5</sub> Measurements from Low-Cost Sensors for Air Quality Mapping in Stuttgart City. In V. Coors, D. Pietruschka, & B. Zeitler (Eds.), *iCity. Transformative Research for the Livable, Intelligent, and Sustainable City* (pp. 225-240). [https://doi.org/10.1007/978-3-030-92096-8\\_14](https://doi.org/10.1007/978-3-030-92096-8_14)
- Grande, G., Hooshmand, B., Vetrano, D. L., Smith, D., Refsum, H., Fratiglioni, L., Ljungman, P., Wu, J., Bellavia, A., Eneroth, K., Bellander, T., & Rizzuto, D. (2023). Association of Long-term Exposure to Air Pollution and Dementia Risk: The Role of Homocysteine, Methionine, and Cardiovascular Burden. *Neurology*. <https://doi.org/10.1212/WNL.0000000000207656>
- Gulliver, J., & Briggs, D. J. (2004). Personal exposure to particulate air pollution in transport microenvironments. *Atmospheric Environment*, *38*(1), 1-8. <https://doi.org/10.1016/j.atmosenv.2003.09.036>
- Gutierrez, A. A., Hantson, S., Langenbrunner, B., Chen, B., Jin, Y., Goulden, M. L., & Randerson, J. T. (2021). Wildfire response to changing daily temperature extremes in California's Sierra Nevada. *Science Advances*, *7*(47), eabe6417. <https://doi.org/10.1126/sciadv.abe6417>
- HabitatMap. (2022a). *AirBeam2 Technical Specifications, Operation & Performance* [Technical datasheet]. <https://www.habitatmap.org/blog/airbeam2-technical-specifications-operation-performance>
- HabitatMap. (2022b). *AirBeam3 Technical Specifications, Operation & Performance* [Technical datasheet]. <https://www.habitatmap.org/blog/airbeam3-technical-specifications-operation-performance>
- HabitatMap. (2023). *AirCasting Map*. Retrieved October 11, 2023 from [http://aircasting.habitatmap.org/mobile\\_map](http://aircasting.habitatmap.org/mobile_map)
- Hagan, D., Lewis, A., von Schneidemesser, E., Peltier, R., Lung, S. C., Jones, R., Zellweger, C., Karppinen, A., Penza, M., Dye, T., Huglin, C., Ning, Z., Leigh, R., Laurent, O., Carmichael, G., Beig, G., Cohen, R., Cross, E., Gentner, D., & Tarasova, O. (2018). *Low-cost sensors for the measurement of atmospheric composition: overview of topic and future applications*. [https://eprints.whiterose.ac.uk/135994/1/WMO\\_Low\\_cost\\_sensors\\_post\\_review\\_final.pdf](https://eprints.whiterose.ac.uk/135994/1/WMO_Low_cost_sensors_post_review_final.pdf)

- Hamra, G. B., Guha, N., Cohen, A., Laden, F., Raaschou-Nielsen, O., Samet, J. M., Vineis, P., Forastiere, F., Saldiva, P., Yorifuji, T., & Loomis, D. (2014). Outdoor particulate matter exposure and lung cancer: a systematic review and meta-analysis. *Environmental Health Perspectives*, 122(9), 906-911. <https://doi.org/10.1289/ehp/1408092>
- Han, Y., Chatzidiakou, L., Yan, L., Chen, W., Zhang, H., Krause, A., Xue, T., Chan, Q., Liu, J., Wu, Y., Barratt, B., Jones, R., Zhu, T., & Kelly, F. J. (2021). Difference in ambient-personal exposure to PM<sub>2.5</sub> and its inflammatory effect in local residents in urban and peri-urban Beijing, China: results of the AIRLESS project. *Faraday Discussions*, 226, 569-583. <https://doi.org/10.1039/d0fd00097c>
- Harrison, R. M. (2020). Airborne particulate matter. *Philosophical Transactions of the Royal Society A*, 378(2183). <https://doi.org/10.1098/rsta.2019.0319>
- Hassani, A., Castell, N., Watne, Å. K., & Schneider, P. (2023). Citizen-operated mobile low-cost sensors for urban PM<sub>2.5</sub> monitoring: field calibration, uncertainty estimation, and application. *Sustainable Cities and Society*, 95. <https://doi.org/10.1016/j.scs.2023.104607>
- Heindel, J. J., Newbold, R., & Schug, T. T. (2015). Endocrine disruptors and obesity. *Nature Reviews: Endocrinology*, 11(11), 653-661. <https://doi.org/10.1038/nrendo.2015.163>
- Hill, W., Lim, E. L., Weeden, C. E., Lee, C., Augustine, M., Chen, K., Kuan, F. C., Marongiu, F., Evans, E. J., Jr., Moore, D. A., Rodrigues, F. S., Pich, O., Bakker, B., Cha, H., Myers, R., van Maldegem, F., Boumelha, J., Veeriah, S., Rowan, A., Naceur-Lombardelli, C., Karasaki, T., Sivakumar, M., De, S., Caswell, D. R., Nagano, A., Black, J. R. M., Martinez-Ruiz, C., Ryu, M. H., Huff, R. D., Li, S., Fave, M. J., Magness, A., Suarez-Bonnet, A., Priestnall, S. L., Luchtenborg, M., Lavelle, K., Pethick, J., Hardy, S., McRonald, F. E., Lin, M. H., Troccoli, C. I., Ghosh, M., Miller, Y. E., Merrick, D. T., Keith, R. L., Al Bakir, M., Bailey, C., Hill, M. S., Saal, L. H., Chen, Y., George, A. M., Abbosh, C., Kanu, N., Lee, S. H., McGranahan, N., Berg, C. D., Sasieni, P., Houlston, R., Turnbull, C., Lam, S., Awadalla, P., Gronroos, E., Downward, J., Jacks, T., Carlsten, C., Malanchi, I., Hackshaw, A., Litchfield, K., Consortium, T. R., DeGregori, J., Jamal-Hanjani, M., & Swanton, C. (2023). Lung adenocarcinoma promotion by air pollutants. *Nature*, 616(7955), 159-167. <https://doi.org/10.1038/s41586-023-05874-3>
- Hoang, A. N., Pham, T. T. K., Mai, D. T. T., Nguyen, T., & Tran, P. T. M. (2022). Health risks and perceptions of residents exposed to multiple sources of air pollutions: A cross-sectional study on landfill and stone mining in Danang city, Vietnam. *Environmental Research*, 212(Pt A), 113244. <https://doi.org/10.1016/j.envres.2022.113244>

- Hoffmann, B., Boogaard, H., de Nazelle, A., Andersen, Z. J., Abramson, M., Brauer, M., Brunekreef, B., Forastiere, F., Huang, W., Kan, H., Kaufman, J. D., Katsouyanni, K., Krzyzanowski, M., Kuenzli, N., Laden, F., Nieuwenhuijsen, M., Mustapha, A., Powell, P., Rice, M., Roca-Barcelo, A., Roscoe, C. J., Soares, A., Straif, K., & Thurston, G. (2021). WHO Air Quality Guidelines 2021-Aiming for Healthier Air for all: A Joint Statement by Medical, Public Health, Scientific Societies and Patient Representative Organisations. *International Journal of Public Health*, *66*, 1604465. <https://doi.org/10.3389/ijph.2021.1604465>
- Host, S., Saunal, A., Honoré, C., Joly, F., Le Tertre, A., & Medina, S. (2018). *Bénéfices sanitaires attendus d'une zone à faibles émissions : évaluation quantitative d'impact sanitaire prospective pour l'agglomération parisienne. Observatoire régional de santé Île-de-France.* [https://www.ors-idf.org/fileadmin/DataStorageKit/ORS/Etudes/2018/Etude2018\\_8/ORS\\_benefices\\_sanitaires\\_attendus\\_ZFE\\_vd.pdf](https://www.ors-idf.org/fileadmin/DataStorageKit/ORS/Etudes/2018/Etude2018_8/ORS_benefices_sanitaires_attendus_ZFE_vd.pdf)
- INSEE. (2023). *Comparateur de territoires – Intercommunalité-Métropole de Grenoble-Alpes-Métropole (200040715).* <https://www.insee.fr/fr/statistiques/1405599?geo=EPCI-200040715>
- Institute for Advanced Biosciences. (2016). *Publication d'une étude sur l'impact sanitaire de la pollution atmosphérique à Lyon et Grenoble et lien avec la défaveur sociale.* [https://iab.univ-grenoble-alpes.fr/sites/iab/files/Mediatheque/Press/cp\\_slama\\_morelli\\_v2.pdf](https://iab.univ-grenoble-alpes.fr/sites/iab/files/Mediatheque/Press/cp_slama_morelli_v2.pdf)
- Jaffe, D. A., Miller, C., Thompson, K., Finley, B., Nelson, M., Ouimette, J., & Andrews, E. (2023). An evaluation of the U.S. EPA's correction equation for PurpleAir sensor data in smoke, dust, and wintertime urban pollution events. *Atmospheric Measurement Techniques*, *16*(5), 1311-1322. <https://doi.org/10.5194/amt-16-1311-2023>
- Jerrett, M., Burnett, R. T., Pope, C. A., 3rd, Ito, K., Thurston, G., Krewski, D., Shi, Y., Calle, E., & Thun, M. (2009). Long-term ozone exposure and mortality. *The New England Journal of Medicine*, *360*(11), 1085-1095. <https://doi.org/10.1056/NEJMoa0803894>
- Jhun, I., Coull, B. A., Zanobetti, A., & Koutrakis, P. (2015). The impact of nitrogen oxides concentration decreases on ozone trends in the USA. *Air Quality, Atmosphere & Health*, *8*(3), 283-292. <https://doi.org/10.1007/s11869-014-0279-2>
- Jia, Y., Lin, Z., He, Z., Li, C., Zhang, Y., Wang, J., Liu, F., Li, J., Huang, K., Cao, J., Gong, X., Lu, X., & Chen, S. (2023). Effect of Air Pollution on Heart Failure: Systematic Review and Meta-Analysis. *Environmental Health Perspectives*, *131*(7), 76001. <https://doi.org/10.1289/EHP11506>
- Jo, E. J., Choi, M. H., Kim, C. H., Won, K. M., Kim, Y. K., Jeong, J. H., An, H. Y., Hwang, M. K., & Park, H. K. (2021). Patterns of medical care utilization according to environmental factors in asthma and chronic obstructive pulmonary disease patients. *Korean Journal of Internal Medicine*, *36*(5), 1146-1156. <https://doi.org/10.3904/kjim.2020.168>

- Karagulian, F. (2023). New Challenges in Air Quality Measurements. In S. De Vito, K. Karatzas, A. Bartonova, & G. Fattoruso (Eds.), *Air Quality Networks* (pp. 178). Springer Cham. <https://doi.org/10.1007/978-3-031-08476-8>
- Kaur, S., Nieuwenhuijsen, M. J., & Colvile, R. N. (2007). Fine particulate matter and carbon monoxide exposure concentrations in urban street transport microenvironments. *Atmospheric Environment*, 41(23), 4781-4810. <https://doi.org/10.1016/j.atmosenv.2007.02.002>
- Kelly, K. E., Whitaker, J., Petty, A., Widmer, C., Dybwad, A., Sleeth, D., Martin, R., & Butterfield, A. (2017). Ambient and laboratory evaluation of a low-cost particulate matter sensor. *Environmental Pollution*, 221, 491-500. <https://doi.org/10.1016/j.envpol.2016.12.039>
- Keuken, M., Sanderson, E., van Aalst, R., Borcken, J., & Schneider, J. (2005). Contribution of traffic to levels of ambient air pollution in Europe. In M. Krzyzanowski, B. Kuna-Dibbert, & J. Schneider (Eds.), *Health effects of transport-related air pollution* (pp. 53). <https://iris.who.int/handle/10665/328088>
- Klepac, P., Locatelli, I., Korosec, S., Kunzli, N., & Kukec, A. (2018). Ambient air pollution and pregnancy outcomes: A comprehensive review and identification of environmental public health challenges. *Environmental Research*, 167, 144-159. <https://doi.org/10.1016/j.envres.2018.07.008>
- Koehler, K., Wilks, M., Green, T., Rule, A. M., Zamora, M. L., Buehler, C., Datta, A., Gentner, D. R., Putcha, N., Hansel, N. N., Kirk, G. D., Raju, S., & McCormack, M. (2023). Evaluation of calibration approaches for indoor deployments of PurpleAir monitors. *Atmospheric Environment*, 310. <https://doi.org/10.1016/j.atmosenv.2023.119944>
- Koenig, J. Q. (2012). *Health Effects of Ambient Air Pollution: How safe is the air we breathe?* Springer US. <https://doi.org/10.1007/978-1-4615-4569-9>
- Koritsoglou, K., Christou, V., Ntritsos, G., Tsoumanis, G., Tsipouras, M. G., Giannakeas, N., & Tzallas, A. T. (2020). Improving the Accuracy of Low-Cost Sensor Measurements for Freezer Automation. *Sensors (Basel)*, 20(21). <https://doi.org/10.3390/s20216389>
- Kosmopoulos, G., Salamalikis, V., Matrali, A., Pandis, S. N., & Kazantzidis, A. (2022). Insights about the Sources of PM<sub>2.5</sub> in an Urban Area from Measurements of a Low-Cost Sensor Network. *Atmosphere*, 13(3). <https://doi.org/10.3390/atmos13030440>

- Kosmopoulos, G., Salamalikis, V., Pandis, S. N., Yannopoulos, P., Bloutsos, A. A., & Kazantzidis, A. (2020). Low-cost sensors for measuring airborne particulate matter: Field evaluation and calibration at a South-Eastern European site. *Science of the Total Environment*, 748, 141396. <https://doi.org/10.1016/j.scitotenv.2020.141396>
- Kuula, J., Mäkelä, T., Aurela, M., Teinilä, K., Varjonen, S., González, Ó., & Timonen, H. (2020). Laboratory evaluation of particle-size selectivity of optical low-cost particulate matter sensors. *Atmospheric Measurement Techniques*, 13(5), 2413-2423. <https://doi.org/10.5194/amt-13-2413-2020>
- Largeron, Y., & Staquet, C. (2016). Persistent inversion dynamics and wintertime PM<sub>10</sub> air pollution in Alpine valleys. *Atmospheric Environment*, 135, 92-108. <https://doi.org/10.1016/j.atmosenv.2016.03.045>
- LCSQA. (2020). *Suivi de l'adéquation des analyseurs automatiques de PM à la méthode de référence : bilan réglementaire 2016-2019 et synthèse des travaux menés depuis 2013*. <https://www.lcsqa.org/fr/rapport/suivi-de-ladequation-des-analyseurs-automatiques-de-pm-la-methode-de-referance-bilan>
- Le Bouëdec, E. (2021). *Circulation atmosphérique hivernale dans le bassin Grenoblois : caractérisation et impact sur la qualité de l'air. Wintertime characteristic atmospheric circulation in the Grenoble basin and impact on air pollution*. Thèse de Doctorat [Doctoral dissertation, Université Grenoble Alpes]. <https://theses.hal.science/tel-04148049>
- Lee, J. E., Lim, H. J., & Kim, Y. Y. (2021). Publication trends in research on particulate matter and health impact over a 10-year period: 2009-2018. *Environmental Analysis, Health and Toxicology*, 36(1), e2021005-2021000. <https://doi.org/10.5620/eaht.2021005>
- Lefler, J. S., Higbee, J. D., Burnett, R. T., Ezzati, M., Coleman, N. C., Mann, D. D., Marshall, J. D., Bechle, M., Wang, Y., Robinson, A. L., & Arden Pope, C., 3rd. (2019). Air pollution and mortality in a large, representative U.S. cohort: multiple-pollutant analyses, and spatial and temporal decompositions. *Environmental Health*, 18(1), 101. <https://doi.org/10.1186/s12940-019-0544-9>
- Levy Zamora, M., Buehler, C., Datta, A., Gentner, D. R., & Koehler, K. (2023). Identifying optimal co-location calibration periods for low-cost sensors. *Atmospheric Measurement Techniques*, 16(1), 169-179. <https://doi.org/10.5194/amt-16-169-2023>
- Lewis, A. C., Lee, J. D., Edwards, P. M., Shaw, M. D., Evans, M. J., Moller, S. J., Smith, K. R., Buckley, J. W., Ellis, M., Gillot, S. R., & White, A. (2016). Evaluating the performance of low cost chemical sensors for air pollution research. *Faraday Discussions*, 189, 85-103. <https://doi.org/10.1039/c5fd00201j>

- Li, J., & Biswas, P. (2022). Calibration and applications of low-cost particle sensors: a review of recent advances. In P. Biswas & G. Yablonsky (Eds.), *Aerosols: Science and Engineering* (pp. 91-114). De Gruyter. <https://doi.org/10.1515/9783110729481-004>
- Li, J., Crooks, J., Murdock, J., de Souza, P., Hohsfield, K., Obermann, B., & Stockman, T. (2023). A nested machine learning approach to short-term PM<sub>2.5</sub> prediction in metropolitan areas using PM<sub>2.5</sub> data from different sensor networks. *Science of the Total Environment*, 873, 162336. <https://doi.org/10.1016/j.scitotenv.2023.162336>
- Li, X., Huang, S., Jiao, A., Yang, X., Yun, J., Wang, Y., Xue, X., Chu, Y., Liu, F., Liu, Y., Ren, M., Chen, X., Li, N., Lu, Y., Mao, Z., Tian, L., & Xiang, H. (2017). Association between ambient fine particulate matter and preterm birth or term low birth weight: An updated systematic review and meta-analysis. *Environmental Pollution*, 227, 596-605. <https://doi.org/10.1016/j.envpol.2017.03.055>
- Liang, L. (2021). Calibrating low-cost sensors for ambient air monitoring: Techniques, trends, and challenges. *Environmental Research*, 197, 111163. <https://doi.org/10.1016/j.envres.2021.111163>
- Lim, C. C., Kim, H., Vilcassim, M. J. R., Thurston, G. D., Gordon, T., Chen, L.-C., Lee, K., Heimbinder, M., & Kim, S.-Y. (2019). Mapping urban air quality using mobile sampling with low-cost sensors and machine learning in Seoul, South Korea. *Environment International*, 131, 105022. <https://doi.org/10.1016/j.envint.2019.105022>
- Lin, H., Tao, J., Du, Y., Liu, T., Qian, Z., Tian, L., Di, Q., Rutherford, S., Guo, L., Zeng, W., Xiao, J., Li, X., He, Z., Xu, Y., & Ma, W. (2016). Particle size and chemical constituents of ambient particulate pollution associated with cardiovascular mortality in Guangzhou, China. *Environmental Pollution*, 208, 758-766. <https://doi.org/10.1016/j.envpol.2015.10.056>
- Liu, C., Chen, R., Sera, F., Vicedo-Cabrera, A. M., Guo, Y., Tong, S., Coelho, M. S. Z. S., Saldiva, P. H. N., Lavigne, E., Matus, P., Valdes Ortega, N., Osorio Garcia, S., Pascal, M., Stafoggia, M., Scortichini, M., Hashizume, M., Honda, Y., Hurtado-Díaz, M., Cruz, J., Nunes, B., Teixeira, J. P., Kim, H., Tobias, A., Íñiguez, C., Forsberg, B., Åström, C., Ragettli, M. S., Guo, Y.-L., Chen, B.-Y., Bell, M. L., Wright, C. Y., Scovronick, N., Garland, R. M., Milojevic, A., Kyselý, J., Urban, A., Orru, H., Indermitte, E., Jaakkola, J. J. K., Ryti, N. R. I., Katsouyanni, K., Analitis, A., Zanobetti, A., Schwartz, J., Chen, J., Wu, T., Cohen, A., Gasparrini, A., & Kan, H. (2019). Ambient Particulate Air Pollution and Daily Mortality in 652 Cities. *The New England Journal of Medicine*, 381(8), 705-715. <https://doi.org/10.1056/NEJMoa1817364>
- Liu, F., Chen, G., Huo, W., Wang, C., Liu, S., Li, N., Mao, S., Hou, Y., Lu, Y., & Xiang, H. (2019). Associations between long-term exposure to ambient air pollution and risk of type 2 diabetes mellitus: A systematic review and meta-analysis. *Environmental Pollution*, 252, 1235-1245. <https://doi.org/10.1016/j.envpol.2019.06.033>



- Ma, J., Tao, Y., Kwan, M.-P., & Chai, Y. (2019). Assessing Mobility-Based Real-Time Air Pollution Exposure in Space and Time Using Smart Sensors and GPS Trajectories in Beijing. *Annals of the American Association of Geographers*, 110(2), 434-448. <https://doi.org/10.1080/24694452.2019.1653752>
- Ma, Q., Li, R., Wang, L., Yin, P., Wang, Y., Yan, C., Ren, Y., Qian, Z., Vaughn, M. G., McMillin, S. E., Hay, S. I., Naghavi, M., Cai, M., Wang, C., Zhang, Z., Zhou, M., Lin, H., & Yang, Y. (2021). Temporal trend and attributable risk factors of stroke burden in China, 1990-2019: an analysis for the Global Burden of Disease Study 2019. *The Lancet Public Health*, 6(12), e897-e906. [https://doi.org/10.1016/S2468-2667\(21\)00228-0](https://doi.org/10.1016/S2468-2667(21)00228-0)
- Ma, X., Li, X., Kwan, M. P., & Chai, Y. (2020). Who Could Not Avoid Exposure to High Levels of Residence-Based Pollution by Daily Mobility? Evidence of Air Pollution Exposure from the Perspective of the Neighborhood Effect Averaging Problem (NEAP). *International Journal of Environmental Research and Public Health*, 17(4). <https://doi.org/10.3390/ijerph17041223>
- Mallik, C. (2019). Anthropogenic Sources of Air Pollution. In P. Saxena & V. Naik (Eds.), *Air Pollution: Sources, Impacts and Controls*. CAB International eBooks. <https://doi.org/10.1079/9781786393890.0000>
- Manisalidis, I., Stavropoulou, E., Stavropoulos, A., & Bezirtzoglou, E. (2020). Environmental and Health Impacts of Air Pollution: A Review. *Frontiers in Public Health*, 8, 14. <https://doi.org/10.3389/fpubh.2020.00014>
- Mebrahtu, T. F., Santorelli, G., Yang, T. C., Wright, J., Tate, J., & McEachan, R. R. (2023). The effects of exposure to NO<sub>2</sub>, PM<sub>2.5</sub> and PM<sub>10</sub> on health service attendances with respiratory illnesses: A time-series analysis. *Environmental Pollution*, 333, 122123. <https://doi.org/10.1016/j.envpol.2023.122123>
- Mei, L., Yan, S., Li, Y., Jin, X., Sun, X., Wu, Y., Liang, Y., Wei, Q., Yi, W., Pan, R., He, Y., Tang, C., Liu, X., Cheng, J., Su, H., & Xu, Q. (2022). Association between short-term PM<sub>1</sub> exposure and cardiorespiratory diseases: Evidence from a systematic review and meta-analysis. *Atmospheric Pollution Research*, 13(1). <https://doi.org/10.1016/j.apr.2021.101254>
- Météo-France. (2021). *Les nouvelles projections climatiques de référence DRIAS 2020 pour la Métropole*. <http://www.drias-climat.fr/document/rapport-DRIAS-2020-red3-2.pdf>



- Météo-France, Institut National de l'Environnement Industriel et des Risques (Ineris), Aarhus University, Norwegian Meteorological Institute (MET Norway), Jülich Institut für Energie- und Klimaforschung (IEK), Institute of Environmental Protection – National Research Institute (IEP-NRI), Koninklijk Nederlands Meteorologisch Instituut (KNMI), Nederlandse Organisatie voor toegepast-natuurwetenschappelijk onderzoek (TNO), Swedish Meteorological and Hydrological Institute (SMHI), Finnish Meteorological Institute (FMI). (2020). *CAMS European air quality forecasts, ENSEMBLE data. Copernicus Atmosphere Monitoring Service (CAMS) Atmosphere Data Store (ADS)*. <https://ads.atmosphere.copernicus.eu/cdsapp#!/dataset/cams-europe-air-quality-forecasts?tab=overview>
- Miller, K. A., Siscovick, D. S., Sheppard, L., Shepherd, K., Sullivan, J. H., Anderson, G. L., & Kaufman, J. D. (2007). Long-Term Exposure to Air Pollution and Incidence of Cardiovascular Events in Women. *The New England Journal of Medicine*, 356(5), 447-458. <https://doi.org/10.1056/NEJMoa054409>
- Molina Rueda, E., Carter, E., L'Orange, C., Quinn, C., & Volckens, J. (2023). Size-Resolved Field Performance of Low-Cost Sensors for Particulate Matter Air Pollution. *Environmental Science & Technology Letters*. <https://doi.org/10.1021/acs.estlett.3c00030>
- Morelli, X., Gabet, S., Rieux, C., Bouscasse, H., Mathy, S., & Slama, R. (2019). Which decreases in air pollution should be targeted to bring health and economic benefits and improve environmental justice? *Environment International*, 129, 538-550. <https://doi.org/10.1016/j.envint.2019.04.077>
- Mueller, M., Meyer, J., & Hueglin, C. (2017). Design of an ozone and nitrogen dioxide sensor unit and its long-term operation within a sensor network in the city of Zurich. *Atmospheric Measurement Techniques*, 10(10), 3783-3799. <https://doi.org/10.5194/amt-10-3783-2017>
- Mui, W., Der Boghossian, B., Collier-Oxandale, A., Boddeker, S., Low, J., Papapostolou, V., & Polidori, A. (2021). Development of a Performance Evaluation Protocol for Air Sensors Deployed on a Google Street View Car. *Environmental Science & Technology*, 55(3), 1477-1486. <https://doi.org/10.1021/acs.est.0c05955>
- Mulholland, E., Miller, J., Bernard, Y., Lee, K., & Rodríguez, F. (2022). The role of NO<sub>x</sub> emission reductions in Euro 7/VII vehicle emission standards to reduce adverse health impacts in the EU27 through 2050. *Transportation Engineering*, 9. <https://doi.org/10.1016/j.treng.2022.100133>
- Munir, M. M., Adrian, M., Saputra, C., & Lestari, P. (2022). Utilizing Low-cost Mobile Monitoring to Estimate the PM<sub>2.5</sub> Inhaled Dose in Urban Environment. *Aerosol and Air Quality Research*, 22(6). <https://doi.org/10.4209/aaqr.220079>

- National Research Council. (2010). *Global Sources of Local Pollution: An Assessment of Long-Range Transport of Key Air Pollutants to and from the United States*. The National Academies Press. <https://doi.org/10.17226/12743>
- Nikolova, I., Janssen, S., Vrancken, K., Vos, P., Mishra, V., & Berghmans, P. (2011). Size resolved ultrafine particles emission model - A continuous size distribution approach. *Science of the Total Environment*, 409(18), 3492-3499. <https://doi.org/10.1016/j.scitotenv.2011.05.015>
- O'Regan, A. C., Byrne, R., Hellebust, S., & Nyhan, M. M. (2022). Associations between Google Street View-derived urban greenspace metrics and air pollution measured using a distributed sensor network. *Sustainable Cities and Society*, 87, 104221. <https://doi.org/10.1016/j.scs.2022.104221>
- Orellano, P., Quaranta, N., Reynoso, J., Balbi, B., & Vasquez, J. (2017). Effect of outdoor air pollution on asthma exacerbations in children and adults: Systematic review and multilevel meta-analysis. *PloS One*, 12(3), e0174050. <https://doi.org/10.1371/journal.pone.0174050>
- Ostro, B., & World Health Organization. (2004). *Outdoor air pollution : assessing the environmental burden of disease at national and local levels / Bart Ostro. Occupational and Environmental Health Team*. <https://apps.who.int/iris/handle/10665/42909>
- Palas GmbH. (2020). *Datasheet of the Palas Fidas® 200 S - Version: October 11, 2023* [Technical datasheet]. <https://www.palas.de/en/product/download/fidas200s/datasheet/pdf>
- Palupi, F., & Abeng, A. (2023). The Invisible Threat: Investigating the Effects of Air Pollution on Human Health and the Environment. *West Science Interdisciplinary Studies*, 1(6), 271-281. <https://doi.org/10.58812/wsis.v1i6.102>
- Papaconstantinou, R., Demosthenous, M., Bezantakos, S., Hadjigeorgiou, N., Costi, M., Stylianiou, M., Symeou, E., Savvides, C., & Biskos, G. (2023). Field evaluation of low-cost electrochemical air quality gas sensors under extreme temperature and relative humidity conditions. *Atmospheric Measurement Techniques*, 16(12), 3313-3329. <https://doi.org/10.5194/amt-16-3313-2023>
- Park, Y. M., & Kwan, M. P. (2017). Individual exposure estimates may be erroneous when spatiotemporal variability of air pollution and human mobility are ignored. *Health & Place*, 43, 85-94. <https://doi.org/10.1016/j.healthplace.2016.10.002>
- Pascal, M., Corso, M., Chanel, O., Declercq, C., Badaloni, C., Cesaroni, G., Henschel, S., Meister, K., Haluza, D., Martin-Olmedo, P., Medina, S., & Aphekom, g. (2013). Assessing the public health impacts of urban air pollution in 25 European cities: results of the Aphekom project. *Science of the Total Environment*, 449, 390-400. <https://doi.org/10.1016/j.scitotenv.2013.01.077>

- Pascal, M., de Crouy Chanel, P., Wagner, V., Corso, M., Tillier, C., Bentayeb, M., Blanchard, M., Cochet, A., Pascal, L., Host, S., Gorla, S., Le Tertre, A., Chatignoux, E., Ung, A., Beaudou, P., & Medina, S. (2016). The mortality impacts of fine particles in France. *Science of the Total Environment*, 571, 416-425. <https://doi.org/10.1016/j.scitotenv.2016.06.213>
- Pascal, M., Yvon, J.-M., Corso, M., Blanchard, M., De Crouy-Chanel, P., & Medina, S. (2020). Conditions for a Meaningful Health Impact Assessment for Local Stakeholders: The Example of the Arve Valley in France. *Atmosphere*, 11(6), 566. <https://doi.org/10.3390/atmos11060566>
- Pavon Arocas, O. (2021). *A Thesis Template in Word (Version 1.0.0)* [Computer software]. <https://doi.org/10.5281/zenodo.6418337>
- Pearson, J. K., & Derwent, R. (2022). *Air Pollution and Climate Change: The Basics (1st ed.)*. <https://doi.org/10.4324/9781003293132>
- Pedersen, M., Giorgis-Allemand, L., Bernard, C., Aguilera, I., Andersen, A. M., Ballester, F., Beelen, R. M., Chatzi, L., Cirach, M., Danileviciute, A., Dedele, A., Eijdsen, M., Estarlich, M., Fernández-Somoano, A., Fernández, M. F., Forastiere, F., Gehring, U., Grazuleviciene, R., Gruziova, O., Heude, B., Hoek, G., de Hoogh, K., van den Hooven, E. H., Håberg, S. E., Jaddoe, V. W., Klümper, C., Korek, M., Krämer, U., Lerchundi, A., Lepeule, J., Nafstad, P., Nystad, W., Patelarou, E., Porta, D., Postma, D., Raaschou-Nielsen, O., Rudnai, P., Sunyer, J., Stephanou, E., Sørensen, M., Thiering, E., Tuffnell, D., Varró, M. J., Vrijkotte, T. G., Wijga, A., Wilhelm, M., Wright, J., Nieuwenhuijsen, M. J., Pershagen, G., Brunekreef, B., Kogevinas, M., & Slama, R. (2013). Ambient air pollution and low birthweight: a European cohort study (ESCAPE). *The Lancet Respiratory medicine*, 1(9), 695-704. [https://doi.org/10.1016/s2213-2600\(13\)70192-9](https://doi.org/10.1016/s2213-2600(13)70192-9)
- Perez, L., Tobias, A., Querol, X., Kunzli, N., Pey, J., Alastuey, A., Viana, M., Valero, N., Gonzalez-Cabre, M., & Sunyer, J. (2008). Coarse particles from Saharan dust and daily mortality. *Epidemiology*, 19(6), 800-807. <https://doi.org/10.1097/ede.0b013e31818131cf>
- Perillo, H. A., Broderick, B. M., Gill, L. W., McNabola, A., Kumar, P., & Gallagher, J. (2022). Spatiotemporal representativeness of air pollution monitoring in Dublin, Ireland. *Science of the Total Environment*, 827, 154299. <https://doi.org/10.1016/j.scitotenv.2022.154299>
- Peters, J., Theunis, J., Poppel, M. V., & Berghmans, P. (2013). Monitoring PM<sub>10</sub> and Ultrafine Particles in Urban Environments Using Mobile Measurements. *Aerosol and Air Quality Research*, 13(2), 509-522. <https://doi.org/10.4209/aaqr.2012.06.0152>
- Pfleger, E., Adrian, C., Lutz, R., & Drexler, H. (2023). Science communication on the public health risks of air pollution: a computational scoping review from 1958 to 2022. *Archives of public health*, 81(1), 14. <https://doi.org/10.1186/s13690-023-01031-4>

- Philip, S., Martin, R. V., van Donkelaar, A., Lo, J. W.-H., Wang, Y., Chen, D., Zhang, L., Kasibhatla, P. S., Wang, S., Zhang, Q., Lu, Z., Streets, D. G., Bittman, S., & Macdonald, D. J. (2014). Global Chemical Composition of Ambient Fine Particulate Matter for Exposure Assessment. *Environmental Science & Technology*, 48(22), 13060-13068. <https://doi.org/10.1021/es502965b>
- Phung, J., & Wagstrom, K. (2023). Monitoring PM<sub>2.5</sub> Pollution In The North End Of Hartford, CT. *Honors Scholar Theses [University of Connecticut] UCONN Library*, 959. [https://digitalcommons.lib.uconn.edu/srhonors\\_theses/959](https://digitalcommons.lib.uconn.edu/srhonors_theses/959)
- Plantower. (2016). *PMS7003 - Digital universal particle concentration sensor - PMS7003 series 2016 data manual from Plantower* [Technical datasheet]. [https://download.kamami.pl/p564008-PMS7003%20series%20data%20manua\\_English\\_V2.5.pdf](https://download.kamami.pl/p564008-PMS7003%20series%20data%20manua_English_V2.5.pdf)
- Pond, Z. A., Saha, P. K., Coleman, C. J., Presto, A. A., Robinson, A. L., & Arden Pope Iii, C. (2022). Mortality risk and long-term exposure to ultrafine particles and primary fine particle components in a national U.S. Cohort. *Environment International*, 167, 107439. <https://doi.org/10.1016/j.envint.2022.107439>
- Pope, C. A., 3rd, Burnett, R. T., Thun, M. J., Calle, E. E., Krewski, D., Ito, K., & Thurston, G. D. (2002). Lung cancer, cardiopulmonary mortality, and long-term exposure to fine particulate air pollution. *JAMA*, 287(9), 1132-1141. <https://doi.org/10.1001/jama.287.9.1132>
- Pope, C. A., 3rd, Ezzati, M., & Dockery, D. W. (2009). Fine-particulate air pollution and life expectancy in the United States. *The New England Journal of Medicine*, 360(4), 376-386. <https://doi.org/10.1056/NEJMsa0805646>
- Pope, C. A., & Dockery, D. W. (2006). Health effects of fine particulate air pollution: lines that connect. *Journal of the Air and Waste Management Association*, 56, 709-742. <https://doi.org/10.1080/10473289.2006.10464485>
- Pope, C. A., Thun, M. J., Namboodiri, M. M., Dockery, D. W., Evans, J. S., Speizer, F. E., & Heath, C. W. (1995). Particulate Air Pollution as a Predictor of Mortality in a Prospective Study of U.S. Adults. *American Journal of Respiratory and Critical Care Medicine*, 151(3 Pt 1), 669-674. [https://doi.org/10.1164/ajrccm/151.3\\_Pt\\_1.669](https://doi.org/10.1164/ajrccm/151.3_Pt_1.669)
- Préfet de l'Isère. (2022). *Plan de Protection de l'Atmosphère de Grenoble Alpes Dauphiné 2022-2027 - Rapport PPA 3*. Direction Régionale de l'Environnement, de l'Aménagement et du Logement (DREAL) Auvergne-Rhône-Alpes. Retrieved October 12, 2023 from <https://www.isere.gouv.fr/contenu/telechargement/66125/433106/file/202212-ppa38-rapportprincipal-ppa3-bdef.pdf>

- PurpleAir. (2023). *PurpleAir: Real-Time Air Quality Map*. Retrieved October 10, 2023 from <https://map.purpleair.com>
- Qiu, X., Shi, L., Kubzansky, L. D., Wei, Y., Castro, E., Li, H., Weiskopf, M. G., & Schwartz, J. D. (2023). Association of Long-term Exposure to Air Pollution With Late-Life Depression in Older Adults in the US. *JAMA network open*, 6(2), e2253668. <https://doi.org/10.1001/jamanetworkopen.2022.53668>
- Quénel, P., Vadel, J., Garbin, C., Durand, S., Favez, O., Albinet, A., Raghoumandan, C., Guyomard, S., Alleman, L. Y., & Mercier, F. (2021). PM<sub>10</sub> Chemical Profile during North African Dust Episodes over French West Indies. *Atmosphere*, 12(2). <https://doi.org/10.3390/atmos12020277>
- Querol, X., Perez, N., Reche, C., Ealo, M., Ripoll, A., Tur, J., Pandolfi, M., Pey, J., Salvador, P., Moreno, T., & Alastuey, A. (2019). African dust and air quality over Spain: Is it only dust that matters? *Science of the Total Environment*, 686, 737-752. <https://doi.org/10.1016/j.scitotenv.2019.05.349>
- R Core Team. (2023). *R: A language and environment for statistical computing*. R Foundation for Statistical Computing, Vienna, Austria. <https://www.R-project.org/>
- Raaschou-Nielsen, O., Andersen, Z. J., Beelen, R., Samoli, E., Stafoggia, M., Weinmayr, G., Hoffmann, B., Fischer, P., Nieuwenhuijsen, M. J., Brunekreef, B., Xun, W. W., Katsouyanni, K., Dimakopoulou, K., Sommar, J., Forsberg, B., Modig, L., Oudin, A., Oftedal, B., Schwarze, P. E., Nafstad, P., De Faire, U., Pedersen, N. L., Ostenson, C. G., Fratiglioni, L., Penell, J., Korek, M., Pershagen, G., Eriksen, K. T., Sorensen, M., Tjonneland, A., Ellermann, T., Eeftens, M., Peeters, P. H., Meliefste, K., Wang, M., Bueno-de-Mesquita, B., Key, T. J., de Hoogh, K., Concin, H., Nagel, G., Vilier, A., Grioni, S., Krogh, V., Tsai, M. Y., Ricceri, F., Sacerdote, C., Galassi, C., Migliore, E., Ranzi, A., Cesaroni, G., Badaloni, C., Forastiere, F., Tamayo, I., Amiano, P., Dorransoro, M., Trichopoulou, A., Bamia, C., Vineis, P., & Hoek, G. (2013). Air pollution and lung cancer incidence in 17 European cohorts: prospective analyses from the European Study of Cohorts for Air Pollution Effects (ESCAPE). *Lancet Oncology*, 14(9), 813-822. [https://doi.org/10.1016/S1470-2045\(13\)70279-1](https://doi.org/10.1016/S1470-2045(13)70279-1)
- Raheja, G., Sabi, K., Sonla, H., Gbedjangni, E. K., McFarlane, C. M., Hodoli, C. G., & Westervelt, D. M. (2022). A Network of Field-Calibrated Low-Cost Sensor Measurements of PM<sub>2.5</sub> in Lomé, Togo, Over One to Two Years. *ACS Earth and Space Chemistry*, 6(4), 1011–1021. <https://doi.org/10.1021/acsearthspacechem.1c00391>

- Rai, M., Stafoggia, M., de'Donato, F., Scortichini, M., Zafeiratou, S., Vazquez Fernandez, L., Zhang, S., Katsouyanni, K., Samoli, E., Rao, S., Lavigne, E., Guo, Y., Kan, H., Osorio, S., Kysely, J., Urban, A., Orru, H., Maasikmets, M., Jaakkola, J. J. K., Ryti, N., Pascal, M., Hashizume, M., Fook Sheng Ng, C., Alahmad, B., Hurtado Diaz, M., De la Cruz Valencia, C., Nunes, B., Madureira, J., Scovronick, N., Garland, R. M., Kim, H., Lee, W., Tobias, A., Iniguez, C., Forsberg, B., Astrom, C., Maria Vicedo-Cabrera, A., Ragetti, M. S., Leon Guo, Y. L., Pan, S. C., Li, S., Gasparrini, A., Sera, F., Masselot, P., Schwartz, J., Zanobetti, A., Bell, M. L., Schneider, A., & Breitner, S. (2023). Heat-related cardiorespiratory mortality: Effect modification by air pollution across 482 cities from 24 countries. *Environment International*, 174, 107825. <https://doi.org/10.1016/j.envint.2023.107825>
- Ravina, M., Caramitti, G., Panepinto, D., & Zanetti, M. (2022). Air quality and photochemical reactions: analysis of NO<sub>x</sub> and NO<sub>2</sub> concentrations in the urban area of Turin, Italy. *Air Quality, Atmosphere & Health*, 15(3), 541-558. <https://doi.org/10.1007/s11869-022-01168-1>
- Raysoni, A. U., Pinakana, S. D., Mendez, E., Wladyka, D., Sepielak, K., & Temby, O. (2023). A Review of Literature on the Usage of Low-Cost Sensors to Measure Particulate Matter. *Earth*, 4(1), 168-186. <https://doi.org/10.3390/earth4010009>
- Réseau d'Observation Météo du Massif Alpin. (2022). *Données Station de Saint-Martin-d'Hères - Jeu de données réservé aux membres [Members data set]*. <https://romma.fr/>
- Reuters. (2023). *Euro 7 emissions proposals, the sequel Europe's carmakers don't want to see* <https://www.reuters.com/business/autos-transportation/euro-7-emissions-proposals-sequel-europes-carmakers-dont-want-see-2023-03-28/>
- Ritchie, H., & Roser, M. (2020). *Air Pollution*. Retrieved October 10, 2023 from <https://ourworldindata.org/air-pollution>
- Roberts, F. A., Van Valkinburgh, K., Green, A., Post, C. J., Mikhailova, E. A., Commodore, S., Pearce, J. L., & Metcalf, A. R. (2022). Evaluation of a new low-cost particle sensor as an internet-of-things device for outdoor air quality monitoring. *Journal of the Air and Waste Management Association*, 72(11), 1219-1230. <https://doi.org/10.1080/10962247.2022.2093293>
- Robinson, E. S., Gu, P., Ye, Q., Li, H. Z., Shah, R. U., Apte, J. S., Robinson, A. L., & Presto, A. A. (2018). Restaurant Impacts on Outdoor Air Quality: Elevated Organic Aerosol Mass from Restaurant Cooking with Neighborhood-Scale Plume Extents. *Environmental Science & Technology*, 52(16), 9285-9294. <https://doi.org/10.1021/acs.est.8b02654>
- Sayahi, T., Butterfield, A., & Kelly, K. E. (2019). Long-term field evaluation of the Plantower PMS low-cost particulate matter sensors. *Environmental Pollution*, 245, 932-940. <https://doi.org/10.1016/j.envpol.2018.11.065>



- Schmitz, S., Towers, S., Villena, G., Caseiro, A., Wegener, R., Klemp, D., Langer, I., Meier, F., & Von Schneidmesser, E. (2020). Unraveling a black box: An open-source methodology for the field calibration of small air quality sensors (1.0.0), Zenodo [code]. <https://doi.org/10.5281/zenodo.4317521>
- Schmitz, S., Towers, S., Villena, G., Caseiro, A., Wegener, R., Klemp, D., Langer, I., Meier, F., & Von Schneidmesser, E. (2021). Unravelling a black box: An open-source methodology for the field calibration of small air quality sensors. *Atmospheric Measurement Techniques*, 4, 7221–7241. <https://doi.org/10.5194/amt-2020-489>
- Schraufnagel, D. E., Balmes, J. R., De Matteis, S., Hoffman, B., Kim, W. J., Perez-Padilla, R., Rice, M., Sood, A., Vanker, A., & Wuebbles, D. J. (2019). Health Benefits of Air Pollution Reduction. *Annals of the American Thoracic Society*, 16(12), 1478-1487. <https://doi.org/10.1513/AnnalsATS.201907-538CME>
- Searle, N., Kaur, K., & Kelly, K. (2023). Technical note: Identifying a performance change in the Plantower PMS 5003 particulate matter sensor. *Journal of Aerosol Science*, 174. <https://doi.org/10.1016/j.jaerosci.2023.106256>
- Sensirion. (2023a). *SHT3x-DIS - Humidity and Temperature Sensor - Version 7* [Technical datasheet]. [https://sensirion.com/media/documents/213E6A3B/63A5A569/Datasheet\\_SHT3x\\_DIS.pdf](https://sensirion.com/media/documents/213E6A3B/63A5A569/Datasheet_SHT3x_DIS.pdf)
- Sensirion. (2023b). *SHT85 - Humidity and Temperature Sensor - Version 4* [Technical datasheet]. [https://sensirion.com/media/documents/4B40CEF3/640B2346/Sensirion\\_Humidity\\_Sensors\\_SHT85\\_Datasheet.pdf](https://sensirion.com/media/documents/4B40CEF3/640B2346/Sensirion_Humidity_Sensors_SHT85_Datasheet.pdf)
- Sensirion. (2023c). *SPS30 - Particulate Matter Sensor - Version 2.0 - D1* [Technical datasheet]. [https://sensirion.com/media/documents/8600FF88/64A3B8D6/Sensirion\\_PM\\_Sensors\\_Datasheet\\_SPS30.pdf](https://sensirion.com/media/documents/8600FF88/64A3B8D6/Sensirion_PM_Sensors_Datasheet_SPS30.pdf)
- Sensor.Community. (2023). *Worldwide Map of Sensor.Community*. Retrieved October 11, 2023 from <https://sensor.community/en>
- Shah, A. S., Langrish, J. P., Nair, H., McAllister, D. A., Hunter, A. L., Donaldson, K., Newby, D. E., & Mills, N. L. (2013). Global association of air pollution and heart failure: a systematic review and meta-analysis. *Lancet*, 382(9897), 1039-1048. [https://doi.org/10.1016/S0140-6736\(13\)60898-3](https://doi.org/10.1016/S0140-6736(13)60898-3)
- Shah, A. S., Lee, K. K., McAllister, D. A., Hunter, A., Nair, H., Whiteley, W., Langrish, J. P., Newby, D. E., & Mills, N. L. (2015). Short term exposure to air pollution and stroke: systematic review and meta-analysis. *BMJ*, 350, h1295. <https://doi.org/10.1136/bmj.h1295>



- Shi, L., Zhu, Q., Wang, Y., Hao, H., Zhang, H., Schwartz, J., Amini, H., van Donkelaar, A., Martin, R. V., Steenland, K., Sarnat, J. A., Caudle, W. M., Ma, T., Li, H., Chang, H. H., Liu, J. Z., Wingo, T., Mao, X., Russell, A. G., Weber, R. J., & Liu, P. (2023). Incident dementia and long-term exposure to constituents of fine particle air pollution: A national cohort study in the United States. *Proceedings of the National Academy of Sciences of the United States of America*, *120*(1), e2211282119. <https://doi.org/10.1073/pnas.2211282119>
- Singh, V., Meena, K. K., & Agarwal, A. (2021). Travellers' exposure to air pollution: A systematic review and future directions. *Urban Climate*, *38*, 100901. <https://doi.org/10.1016/j.uclim.2021.100901>
- Siouti, E., Skyllakou, K., Kioutsioukis, I., Ciarelli, G., & Pandis, S. N. (2021). Simulation of the cooking organic aerosol concentration variability in an urban area. *Atmospheric Environment*, *265*. <https://doi.org/10.1016/j.atmosenv.2021.118710>
- Sipos, A., Kim, K. J., Sioutas, C., & Crandall, E. D. (2023). Kinetics of autophagic activity in nanoparticle-exposed lung adenocarcinoma (A549) cells. *Autophagy Reports*, *2*(1). <https://doi.org/10.1080/27694127.2023.2186568>
- Slama, R., Darrow, L., Parker, J., Woodruff, T. J., Strickland, M., Nieuwenhuijsen, M., Glinianaia, S., Hoggatt, K. J., Kannan, S., Hurley, F., Kalinka, J., Sram, R., Brauer, M., Wilhelm, M., Heinrich, J., & Ritz, B. (2008). Meeting report: atmospheric pollution and human reproduction. *Environmental Health Perspectives*, *116*(6), 791-798. <https://doi.org/10.1289/ehp.11074>
- Soares, J., González Ortiz, A., Gsella, A., Horálek, J., Plass, D., & Kienzler, S. (2022). *Health risk assessment of air pollution and the impact of the new WHO guidelines (Eionet Report – ETC HE Report 2022/10)*. European Topic Centre on Human Health and the Environment. <https://www.eionet.europa.eu/etcs/etc-he/products/etc-he-products/etc-he-reports/etc-he-report-2022-10-health-risk-assessment-of-air-pollution-and-the-impact-of-the-new-who-guidelines>
- Spinelle, L., Gerboles, M., & Aleixandre, M. (2015). Performance Evaluation of Amperometric Sensors for the Monitoring of O<sub>3</sub> and NO<sub>2</sub> in Ambient Air at ppb Level. *Procedia Engineering*, *120*, 480-483. <https://doi.org/10.1016/j.proeng.2015.08.676>
- Stampfer, O., Austin, E., Ganuelas, T., Fiander, T., Seto, E., & Karr, C. (2020). Use of low-cost PM monitors and a multi-wavelength aethalometer to characterize PM<sub>2.5</sub> in the Yakama Nation Reservation. *Atmospheric Environment*, *224*. <https://doi.org/10.1016/j.atmosenv.2020.117292>

- Steinle, S., Reis, S., & Sabel, C. E. (2013). Quantifying human exposure to air pollution—Moving from static monitoring to spatio-temporally resolved personal exposure assessment. *Science of the Total Environment*, 443, 184-193. <https://doi.org/10.1016/j.scitotenv.2012.10.098>
- Strak, M., Janssen, N., Beelen, R., Schmitz, O., Vaartjes, I., Karsenberg, D., van den Brink, C., Bots, M. L., Dijst, M., Brunekreef, B., & Hoek, G. (2017). Long-term exposure to particulate matter, NO<sub>2</sub> and the oxidative potential of particulates and diabetes prevalence in a large national health survey. *Environment International*, 108, 228-236. <https://doi.org/10.1016/j.envint.2017.08.017>
- Tan, Y., Yang, R., Zhao, J., Cao, Z., Chen, Y., & Zhang, B. (2017). The Associations Between Air Pollution and Adverse Pregnancy Outcomes in China. *Advances in Experimental Medicine and Biology*, 1017, 181-214. [https://doi.org/10.1007/978-981-10-5657-4\\_8](https://doi.org/10.1007/978-981-10-5657-4_8)
- Tan, Z., Berry, A., Charalambides, M., Mijic, A., Pearse, W., Porter, A., Ryan, M. P., Shorten, R. N., Stettler, M. E. J., Tetley, T. D., Wright, S., & Masen, M. A. (2023). *Tyre wear particles are toxic for us and the environment - Imperial Zero Pollution*. Imperial College London. <https://doi.org/10.25561/101707>
- Thurston, G. D., Kipen, H., Annesi-Maesano, I., Balmes, J., Brook, R. D., Cromar, K., De Matteis, S., Forastiere, F., Forsberg, B., Frampton, M. W., Grigg, J., Heederik, D., Kelly, F. J., Kuenzli, N., Laumbach, R., Peters, A., Rajagopalan, S. T., Rich, D., Ritz, B., Samet, J. M., Sandstrom, T., Sigsgaard, T., Sunyer, J., & Brunekreef, B. (2017). A joint ERS/ATS policy statement: what constitutes an adverse health effect of air pollution? An analytical framework. *European Respiratory Journal*, 49(1). <https://doi.org/10.1183/13993003.00419-2016>
- Tiwari, S., & Mishra, N. (2019). Methods for the Measurement of Air Pollutants. In P. Saxena & V. Naik (Eds.), *Air Pollution: Sources, Impacts and Controls*. CAB International. <https://doi.org/10.1079/9781786393890.0000>
- Tiwary, A., Williams, I., & Colls, J. (2018). *Air pollution: measurement, modelling and mitigation* (4th ed., Vol. 1). CRC Press. <https://doi.org/10.1201/9780429469985>
- United Nations Department of Economic and Social Affairs. (2023). *Leaving No One Behind In An Ageing World - World Social Report 2023*. <https://www.un.org/development/desa/dspd/wp-content/uploads/sites/22/2023/01/2023wsr-references.pdf>
- United Nations Department of Economic and Social Affairs. (May 16, 2018). *68% of the world population projected to live in urban areas by 2050, says UN* [Press release]. <https://www.un.org/development/desa/en/news/population/2018-revision-of-world-urbanization-prospects.html>

- United States Environmental Protection Agency. (2009). *Integrated Science Assessment (ISA) for Particulate Matter*. <https://cfpub.epa.gov/ncea/isa/recordisplay.cfm?deid=216546>
- United States Environmental Protection Agency. (2011). *Benefits and Costs of the Clean Air Act 1990-2020, the Second Prospective Study*. <https://www.epa.gov/clean-air-act-overview/benefits-and-costs-clean-air-act-1990-2020-supporting-technical-reports>
- United States Environmental Protection Agency. (2022). *Air Quality and Climate Change Research*. <https://www.epa.gov/air-research/air-quality-and-climate-change-research>
- United States Environmental Protection Agency. (2023). *Health Effects of Ozone Pollution*. <https://www.epa.gov/ground-level-ozone-pollution/health-effects-ozone-pollution>
- van Donkelaar, A., Martin, R. V., Li, C., & Burnett, R. T. (2019). Regional Estimates of Chemical Composition of Fine Particulate Matter Using a Combined Geoscience-Statistical Method with Information from Satellites, Models, and Monitors. *Environmental Science & Technology*, 53(5), 2595-2611. <https://doi.org/10.1021/acs.est.8b06392>
- Vicedo-Cabrera, A. M., Sera, F., Liu, C., Armstrong, B., Milojevic, A., Guo, Y., Tong, S., Lavigne, E., Kyselý, J., Urban, A., Orru, H., Indermitte, E., Pascal, M., Huber, V., Schneider, A., Katsouyanni, K., Samoli, E., Stafoggia, M., Scortichini, M., Hashizume, M., Honda, Y., Ng, C. F. S., Hurtado-Diaz, M., Cruz, J., Silva, S., Madureira, J., Scovronick, N., Garland, R. M., Kim, H., Tobias, A., Íñiguez, C., Forsberg, B., Åström, C., Ragetti, M. S., Rösli, M., Guo, Y.-L. L., Chen, B.-Y., Zanobetti, A., Schwartz, J., Bell, M. L., Kan, H., & Gasparrini, A. (2020). Short term association between ozone and mortality: global two stage time series study in 406 locations in 20 countries. *BMJ*, 368, m108. <https://doi.org/10.1136/bmj.m108>
- Wang, A., Machida, Y., deSouza, P., Mora, S., Duhl, T., Hudda, N., Durant, J. L., Duarte, F., & Ratti, C. (2023). Leveraging machine learning algorithms to advance low-cost air sensor calibration in stationary and mobile settings. *Atmospheric Environment*, 301. <https://doi.org/10.1016/j.atmosenv.2023.119692>
- Wang, L., Xie, J., Hu, Y., & Tian, Y. (2022). Air pollution and risk of chronic obstructed pulmonary disease: The modifying effect of genetic susceptibility and lifestyle. *EBioMedicine*, 79, 103994. <https://doi.org/10.1016/j.ebiom.2022.103994>

- Weagle, C. L., Snider, G., Li, C., van Donkelaar, A., Philip, S., Bissonnette, P., Burke, J., Jackson, J., Latimer, R., Stone, E., Abboud, I., Akoshile, C., Anh, N. X., Brook, J. R., Cohen, A., Dong, J., Gibson, M. D., Griffith, D., He, K. B., Holben, B. N., Kahn, R., Keller, C. A., Kim, J. S., Lagrosas, N., Lestari, P., Khian, Y. L., Liu, Y., Marais, E. A., Martins, J. V., Misra, A., Muliane, U., Pratiwi, R., Quel, E. J., Salam, A., Segev, L., Tripathi, S. N., Wang, C., Zhang, Q., Brauer, M., Rudich, Y., & Martin, R. V. (2018). Global Sources of Fine Particulate Matter: Interpretation of PM<sub>2.5</sub> Chemical Composition Observed by SPARTAN using a Global Chemical Transport Model. *Environmental Science & Technology*, 52(20), 11670-11681. <https://doi.org/10.1021/acs.est.8b01658>
- Wendt, E. A., Ford, B., Cheeseman, M., Rosen, Z., Pierce, J. R., Jathar, S. H., L'Orange, C., Quinn, C., Long, M., Mehaffy, J., Miller-Lionberg, D. D., Hagan, D. H., & Volckens, J. (2023). A national crowdsourced network of low-cost fine particulate matter and aerosol optical depth monitors: results from the 2021 wildfire season in the United States. *Environmental Science: Atmospheres*. <https://doi.org/10.1039/d3ea00086a>
- Wilker, E. H., Osman, M., & Weisskopf, M. G. (2023). Ambient air pollution and clinical dementia: systematic review and meta-analysis. *BMJ*, 381, e071620. <https://doi.org/10.1136/bmj-2022-071620>
- Williams, D. E. (2019). Low Cost Sensor Networks: How Do We Know the Data Are Reliable? *ACS Sensors*, 4(10), 2558-2565. <https://doi.org/10.1021/acssensors.9b01455>
- Won, W. S., Oh, R., Lee, W., Ku, S., Su, P. C., & Yoon, Y. J. (2021). Hygroscopic properties of particulate matter and effects of their interactions with weather on visibility. *Scientific Reports*, 11(1), 16401. <https://doi.org/10.1038/s41598-021-95834-6>
- World Health Organization. (2013). *Health risks of air pollution in Europe – HRAPIE project. Recommendations for concentration–response functions for cost–benefit analysis of particulate matter, ozone and nitrogen dioxide*. WHO Regional Office for Europe. <https://apps.who.int/iris/handle/10665/153692>
- World Health Organization. (2018). Burden of disease from the joint effects of household and ambient air pollution for 2016. [https://cdn.who.int/media/docs/default-source/air-quality-database/aqd-2018/ap\\_joint\\_effect\\_bod\\_results\\_may2018.pdf](https://cdn.who.int/media/docs/default-source/air-quality-database/aqd-2018/ap_joint_effect_bod_results_may2018.pdf)
- World Health Organization. (2021a). *Review of evidence on health aspects of air pollution: REVIHAAP project: technical report*. <https://apps.who.int/iris/handle/10665/341712>
- World Health Organization. (2021b). *WHO global air quality guidelines: particulate matter (PM<sub>2.5</sub> and PM<sub>10</sub>), ozone, nitrogen dioxide, sulfur dioxide and carbon monoxide*. World Health Organization. <https://apps.who.int/iris/handle/10665/345329>

- Xing, Y., & Wong, G. W. (2022). Environmental Influences and Allergic Diseases in the Asia-Pacific Region: What Will Happen in Next 30 Years? *Allergy, Asthma & Immunology Research*, *14*(1), 21-39. <https://doi.org/10.4168/aaair.2022.14.1.21>
- Xu, R., Huang, S., Shi, C., Wang, R., Liu, T., Li, Y., Zheng, Y., Lv, Z., Wei, J., Sun, H., & Liu, Y. (2023). Extreme Temperature Events, Fine Particulate Matter, and Myocardial Infarction Mortality. *Circulation*, *148*(4), 312-323. <https://doi.org/10.1161/circulationaha.122.063504>
- Xu, R., Ye, T., Yue, X., Yang, Z., Yu, W., Zhang, Y., Bell, M. L., Morawska, L., Yu, P., Zhang, Y., Wu, Y., Liu, Y., Johnston, F., Lei, Y., Abramson, M. J., Guo, Y., & Li, S. (2023). Global population exposure to landscape fire air pollution from 2000 to 2019. *Nature*, *621*(7979), 521-529. <https://doi.org/10.1038/s41586-023-06398-6>
- Yacong, B., Yongjian, Z., Xiaolan, Z., Hui, C., Junxi, Z., Xiang Qian, L., & Zengli, Y. (2023). Spatiotemporal Trends of Stroke Burden Attributable to Ambient PM<sub>2.5</sub> in 204 Countries and Territories, 1990–2019: A Global Analysis. *Neurology*, *101*(7), e764-e776. <https://doi.org/10.1212/WNL.0000000000207503>
- Yang, B. Y., Qian, Z., Howard, S. W., Vaughn, M. G., Fan, S. J., Liu, K. K., & Dong, G. H. (2018). Global association between ambient air pollution and blood pressure: A systematic review and meta-analysis. *Environmental Pollution*, *235*, 576-588. <https://doi.org/10.1016/j.envpol.2018.01.001>
- Yang, M., Wu, Q.-Z., Zhang, Y.-T., Leskinen, A., Komppula, M., Hakkarainen, H., Roponen, M., Xu, S.-L., Lin, L.-Z., Liu, R.-Q., Hu, L.-W., Yang, B.-Y., Zeng, X.-W., Dong, G.-H., & Jalava, P. (2022). Concentration, chemical composition and toxicological responses of the ultrafine fraction of urban air particles in PM<sub>1</sub>. *Environment International*, *170*. <https://doi.org/10.1016/j.envint.2022.107661>
- Yang, T., Wang, J., Huang, J., Kelly, F. J., & Li, G. (2023). Long-term Exposure to Multiple Ambient Air Pollutants and Association With Incident Depression and Anxiety. *JAMA Psychiatry*, *80*(4), 305-313. <https://doi.org/10.1001/jamapsychiatry.2022.4812>
- Yu, W., & Thurston, G. D. (2023). An interrupted time series analysis of the cardiovascular health benefits of a coal coking operation closure. *Environmental Research Health*, *1*(4). <https://doi.org/10.1088/2752-5309/ace4ea>
- Yu, W., Ye, T., Zhang, Y., Xu, R., Lei, Y., Chen, Z., Yang, Z., Zhang, Y., Song, J., Yue, X., Li, S., & Guo, Y. (2023). Global estimates of daily ambient fine particulate matter concentrations and unequal spatiotemporal distribution of population exposure: a machine learning modelling study. *The Lancet Planetary Health*, *7*(3), e209-e218. [https://doi.org/10.1016/S2542-5196\(23\)00008-6](https://doi.org/10.1016/S2542-5196(23)00008-6)

- Zauli-Sajani, S., Marchesi, S., Boselli, G., Broglia, E., Angella, A., Maestri, E., Marmiroli, N., & Colacci, A. (2022). Effectiveness of a Protocol to Reduce Children's Exposure to Particulate Matter and NO<sub>2</sub> in Schools during Alert Days. *International Journal of Environmental Research and Public Health*, 19(17). <https://doi.org/10.3390/ijerph191711019>
- Zhang, J., Jiang, H., Zhang, W., Ma, G., Wang, Y., Lu, Y., Hu, X., Zhou, J., Peng, F., Bi, J., & Wang, J. (2019). Cost-benefit analysis of China's Action Plan for Air Pollution Prevention and Control. *Frontiers of Engineering Management*, 6(4), 524-537. <https://doi.org/10.1007/s42524-019-0074-8>
- Zhang, Y., Ni, H., Bai, L., Cheng, Q., Zhang, H., Wang, S., Xie, M., Zhao, D., & Su, H. (2019). The short-term association between air pollution and childhood asthma hospital admissions in urban areas of Hefei City in China: A time-series study. *Environmental Research*, 169, 510-516. <https://doi.org/10.1016/j.envres.2018.11.043>
- Zheng, B., Ciais, P., Chevallier, F., Yang, H., Canadell, J. G., Chen, Y., van der Velde, I. R., Aben, I., Chuvieco, E., Davis, S. J., Deeter, M., Hong, C., Kong, Y., Li, H., Li, H., Lin, X., He, K., & Zhang, Q. (2023). Record-high CO<sub>2</sub> emissions from boreal fires in 2021. *Science*, 379(6635), 912-917. <https://doi.org/10.1126/science.ade0805>
- Zhou, Z., Shuai, X., Lin, Z., Yu, X., Ba, X., Holmes, M. A., Xiao, Y., Gu, B., & Chen, H. (2023). Association between particulate matter (PM<sub>2.5</sub>) air pollution and clinical antibiotic resistance: a global analysis. *The Lancet Planetary Health*, 7(8), e649-e659. [https://doi.org/10.1016/S2542-5196\(23\)00135-3](https://doi.org/10.1016/S2542-5196(23)00135-3)
- Zuurbier, M., Hoek, G., Oldenwening, M., Lenters, V., Meliefste, K., van den Hazel, P., & Brunekreef, B. (2010). Commuters' exposure to particulate matter air pollution is affected by mode of transport, fuel type, and route. *Environmental Health Perspectives*, 118(6), 783-789. <https://doi.org/10.1289/ehp.0901622>

# 8 APPENDIX

## APPENDIX A- PUBLICATIONS AND COMMUNICATIONS

### Publications in international peer-reviewed journals

Aix, M. L., Schmitz, S., & Bicout, D. J. (2023). Calibration methodology of low-cost sensors for high-quality monitoring of fine particulate matter. *Science of the Total Environment*, 889, 164063. <https://doi.org/10.1016/j.scitotenv.2023.164063>

Aix, M. L., Petit, P., & Bicout, D. J. (2022). Air pollution and health impacts during the COVID-19 lockdowns in Grenoble, France. *Environmental Pollution*, 303, 119134. <https://doi.org/10.1016/j.envpol.2022.119134>

### Publications in conferences

Aix, M. L., Claitte, M., & Bicout, D. J. (2023). A Low-Cost Sensors Study Measuring Exposure to Particulate Matter in Mobility Situations. *Proceedings of the 12th International Conference on Sensor Networks*, 1, 32-41. <https://doi.org/10.5220/0011747600003399><sup>1</sup>

Aix, M. L., & Bicout, D. J. (2023). *Protocole d'évaluation et d'utilisation d'une station low-cost de mesure des particules fines [Protocole for evaluation and use of a low-cost particulate matter monitoring station]*. Congrès Français des Aérosols, Paris, France. <https://doi.org/10.25576/ASFERA-CFA2023-32891><sup>2</sup>

---

<sup>1</sup> In Appendix B below

<sup>2</sup> Under embargo until March 19, 2024. Included in this manuscript (Article n°2, Section 3.2)



## Communication in conferences

Aix, M. L., & Donsez, D. (2023, May 23). *Low-cost sensors for particulate matter measurement* [Conference session]. Workshop IoT platforms for indoor air quality, Paris, France.

Aix, M. L., & Bicout, D. J. (2023, March 16). *Protocole d'évaluation et d'utilisation d'une station low-cost de mesure des particules fines*. [Paper presentation]. Congrès Français des Aérosols, Paris, France.

Aix, M. L., Claitte, M., & Bicout, D. J. (2023, February 23). *A low-cost sensors study measuring exposure to particulate matter in mobility situations*. [Paper presentation]. 12th International Conference on Sensor Networks (SENSORNETS 2023).

Aix, M. L., & Bicout, D. J. (2022, April 12). *Calibration methodology of low-cost sensors for high-quality monitoring of fine particulate matter* [Conference session]. TIMC PhD students' day, Grenoble, France.

## Poster presentations

Aix, M. L., & Donsez, D. (2023, May 22). *Low-cost sensors for particulate matter measurement* [Poster presentation]. Workshop IoT platforms for indoor air quality, Paris, France. [https://github.com/airqualitystation/airqualitystation.github.io/blob/master/presentations/poster\\_uspn\\_mlaix.pdf](https://github.com/airqualitystation/airqualitystation.github.io/blob/master/presentations/poster_uspn_mlaix.pdf) (1<sup>st</sup> prize)<sup>3</sup>

Aix, M. L., & Bicout, D. J. (2022, June 2). *Designing low-cost sensors for high-quality air pollution monitoring* [Poster presentation]. EDISCE 20th PhD students' day, Grenoble, France (2<sup>nd</sup> jury prize)<sup>4</sup>

---

<sup>3</sup> In Appendix C

<sup>4</sup> In Appendix D

## Mediation work

Aix, M.L., Bicout, D. J., Zoppis, C. (2023, April 25) *Pollution atmosphérique, mobilités et santé dans l'agglomération grenobloise* [Video]. YouTube. <https://www.youtube.com/watch?v=vJPfUDi-qo0>. TIMC PhD students' day, Grenoble, France (1<sup>st</sup> prize)<sup>5</sup>

Aix, M.L., Alfieri, R., Hartmann, P., Heredia Guzmán, M.B., Uleda, C., Veillas, C., Piolat, G. (2023, March 10-12). *Particule Fun* [Video game]. <https://pholothe1.itch.io/particule-fun>. Scientific Game Jam 2023, Grenoble, France<sup>6</sup>



---

<sup>5</sup> See Appendix E

<sup>6</sup> See Appendix F

## APPENDIX B

## A Low-cost Sensors Study Measuring Exposure to Particulate Matter in Mobility Situations

Marie-Laure Aix<sup>1</sup><sup>a</sup>, Méline Claitte<sup>1</sup> and Dominique J Bicot<sup>1</sup><sup>b</sup>

<sup>1</sup>Univ. Grenoble Alpes, CNRS, UMR 5525, VetAgro Sup, Grenoble INP, TIMC, 38000 Grenoble, France  
[marie-laure.aix@univ-grenoble-alpes.fr](mailto:marie-laure.aix@univ-grenoble-alpes.fr), [dominique.bicot@univ-grenoble-alpes.fr](mailto:dominique.bicot@univ-grenoble-alpes.fr)


Keywords: Low-cost Sensor, PM<sub>2.5</sub>, Calibration, Mobility, Exposure Assessment.


**Abstract:** In 2013, the International Agency for Research on Cancer classified particulate matter (PM) as carcinogenic to humans. It is therefore essential to measure PM concentrations to minimize the exposure of individuals. Our objective was to investigate personal exposure to PM<sub>2.5</sub> (PM with diameter  $\leq 2.5 \mu\text{m}$ ) in Grenoble (France) during commuting in different transportation modes: bike, walk, bus and tramway. PM<sub>2.5</sub> measurements were found to be the highest for bikes, followed by walk, bus, and tramway. In this study, conducted in spring during low pollution levels of PM, exposure levels are greatly influenced by the time of day. Pedestrian and cyclists' exposure generally stayed under background reference values. Exposure in public transportation was usually below reference values, but when background PM<sub>2.5</sub> levels went lower (evening), levels registered in the tramway or bus reached those of the reference. Therefore, public transport users could be less exposed than active commuters, except when ambient pollutant levels are low. Environmental parameters like wind might be important in Grenoble, and it would be worthwhile to reproduce this study at a time when wind speed is lower.

### 1 INTRODUCTION

Every year, it is estimated that outdoor air pollution causes 7 million deaths around the world (Fuller et al., 2022). Particulate matter (PM) is made of solid compounds suspended in the air that are small enough to be inhaled. Considered as the most dangerous form of air pollution, PM can enter blood circulation, and accumulate in numerous organs (Pryor, Cowley, & Simonds, 2022). Therefore, it is important to assess populations' exposure to PM, which is generally done by official reference monitoring stations. However, more and more scientists state that stationary monitoring stations are not always representative of people's exposure (Van den Bossche et al., 2015; F. Yang et al., 2019). This might be related to the time that people spend indoor and outdoor, in places where the pollutant levels do not always equal to reference values. Time spent in transportation could represent up to 30% of the inhaled dose (Dons, Int Panis, Van Poppel, Theunis, & Wets, 2012). According to Han et al. (2021), personal exposure to PM<sub>2.5</sub> (PM with diameter  $\leq 2.5 \mu\text{m}$ ) measured by portable sensors, is significantly associated with an increase in

respiratory and systemic inflammatory biomarkers. However, the associations are weaker when ambient PM<sub>2.5</sub> concentrations, measured by fixed reference stations, are used as an exposure proxy. Low-cost sensors demonstrate good accuracy to measure individual exposure to PM (Motlagh et al., 2021) and can therefore be used for exposure studies, especially during commuting. Few mobility studies involving low-cost sensors have been performed, especially in low-concentration situations. Many surveys take place in Asia where pollution levels are usually higher than in Europe. During 10 working days, we conducted a field experiment to collect PM measurements using four transportation modes around Grenoble (France): bike, walk, bus, and tramway. Our objective was to estimate personal exposures to PM<sub>2.5</sub> with a low-cost sensor during commuting in different modes. Another purpose was to compare the so measured concentrations with reference values. We wanted to know whether the low-cost sensors could be used to assess differences between transport modes and the time of day. In doing this, we hope to contribute to the exposure literature using low-cost sensors.

<sup>a</sup> <https://orcid.org/0000-0001-5366-2372>

<sup>b</sup> <https://orcid.org/0000-0003-0750-997X>

## 2 MATERIALS AND METHODS

### 2.1 Particulate matter sensor

#### 2.1.1 Monitoring devices

PM concentrations were measured using two AirBeam2 (HabitatMap), which entail an optical sensor (Plantower PMS7003). AirBeam2 are inexpensive (\$249) and measure concentrations of PM<sub>1</sub>, PM<sub>2.5</sub>, PM<sub>10</sub>, temperature and relative humidity (RH). They are connected to a smartphone via Bluetooth and provide real time values to users. With the growth of the Internet of Things (IoT) sector (Das, Ghosh, Chatterjee, & De, 2022; Y. Yang et al., 2022), cheaper PM sensors are currently available on the market. However, they often have to be assembled with other components like microcontrollers or GPS modules, and an IoT platform has to be set-up for data visualisation. Designing a monitoring station, assembling components and developing a data visualisation tool are different steps which can be time-consuming. HabitatMap already provides an online platform (<http://aircasting.org>) for viewing and downloading AirBeam2 data. Furthermore, AirBeam2 are ready-to-use devices. South Coast Air Quality Management District (2018) compared the AirBeam2 PM<sub>2.5</sub> measurements to values given by three Federal Equivalent Method instruments. They observed very strong correlations in the laboratory studies ( $R^2 > 0.99$ ) and moderate to strong correlations with different reference instruments from the field ( $0.68 < R^2 < 0.79$ ). More recently, Tong, Shi, Shi, and Zhang (2022) found that Airbeam2 measurements correlated well with roadside official monitoring stations. They also reported a good agreement ( $R^2 = 0.67-0.89$ ) between Airbeam2 local measurements and the predictions from a model involving satellite observations. AirBeam2 is already calibrated by the manufacturer, but the calibration equations do not account for RH (HabitatMap, 2022). Huang et al. (2022) found that the accuracy and bias of the PM data reported by AirBeam2 sensors were affected by rainy weather and high humidity environments. Moreover, Zou, Clark, and May (2021) suggested that there was a significant linear relationship between RH and the relative response of the low-cost PM sensors to the research-grade instruments. Therefore, we calibrated the devices by accounting for RH.

#### 2.1.2 Calibration

The calibration process involved two steps (Figure 1).

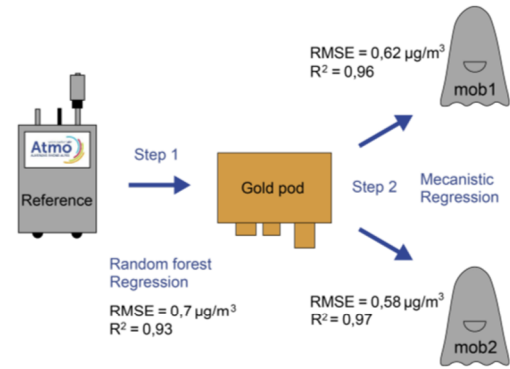


Figure 1. Two steps calibration process.

- **Step 1: calibration of a fixed low-cost sensor (“gold pod”) with a reference device**

Before this study, we had already calibrated a low-cost fixed station by collocating it with a Palas GmbH 200 (Reference) from Atmo Auvergne-Rhône-Alpes (Atmo AuRA) in Grenoble “Les Frênes” (Refer Figure 4). This calibration was performed using a random forest regression technique developed by Schmitz et al. (2021) comparing this individual fixed sensor with the reference station. This low-cost fixed station, called “gold pod” used the same optical sensor (PMS7003) than the mobile devices.

- **Step 2: AirBeam2 sensors calibration with a fixed low-cost sensor (“gold pod”)**

Next, 44 days of calibration were performed from September 20, 2022 to November 3, 2022 where the two AirBeam2 were collocated close to the “gold pod”. The two mobile devices were calibrated independently: first, the AirBeam2 used by experimenter 1 (“mob1”) and then the device used by experimenter 2 (“mob2”). This was motivated by the observation that mob2 was delivering concentrations a bit higher than mob1. By using the nls() function from RStudio 2022.07.1 (R Core Team, 2022) on 75% of the dataset, we applied the mechanistic equation (Equation 1) involving relative humidity and temperature for calibration:

$$PM_{2.5\ gp} = a + b \frac{PM_{2.5\ mob}}{\left(1 + d \frac{RH_{mob}}{100 - RH_{mob}}\right)^{\frac{1}{3}}} + c T_{mob} \quad (1)$$

where  $PM_{2.5\ gp} = PM_{2.5}$  concentrations in  $\mu\text{g}/\text{m}^3$  given by the “gold pod”,  $PM_{2.5\ mob} = PM_{2.5}$  concentrations ( $\mu\text{g}/\text{m}^3$ ) measured with the AirBeam2,  $RH_{mob} =$  relative humidity in % determined by the AirBeam2,



$T_{\text{mob}}$  = temperature in °C given by the AirBeam2. For mob1, we found  $a = 0.49$ ,  $b = 0.91$ ,  $c = 0.07$  and  $d = 0.43$ . For mob2, we had  $a = -0.1$ ,  $b = 0.86$ ,  $c = 0.08$  and  $d = 0.31$ . We then tested these two calibration formulas on the remaining 25% dataset, and we found the following performance indicators. For mob1, we had  $\text{RMSE} = 0.62 \mu\text{g}/\text{m}^3$  and  $R^2 = 0.96$  and for mob2, we found  $\text{RMSE} = 0.58 \mu\text{g}/\text{m}^3$  and  $R^2 = 0.97$ . RMSE (root mean square error) reflects the accuracy of the model to predict actual  $\text{PM}_{2.5}$  values, and  $R^2$  (coefficient of determination) refers to the correlation between the AirBeam2 values and the reference concentrations. Based on this, we decided to continue with these models as the indicators were good compared to what is found in the literature (Blanco et al., 2022; Haghbayan & Tashayo, 2021).

## 2.2 Sampling design

### 2.2.1 Monitoring routes

The study took place in Grenoble, the largest city in the Alps, hosting around 450,000 inhabitants. Five different monitoring sites were selected (Figure 2): two wide streets (“Jaurès” and “Pain”) and two narrow (also called “canyon”) streets surrounded by higher buildings (“Grégoire” and “Blanchard”). We also monitored PM when we commuted between Blanchard and Grégoire (“Cross” route).

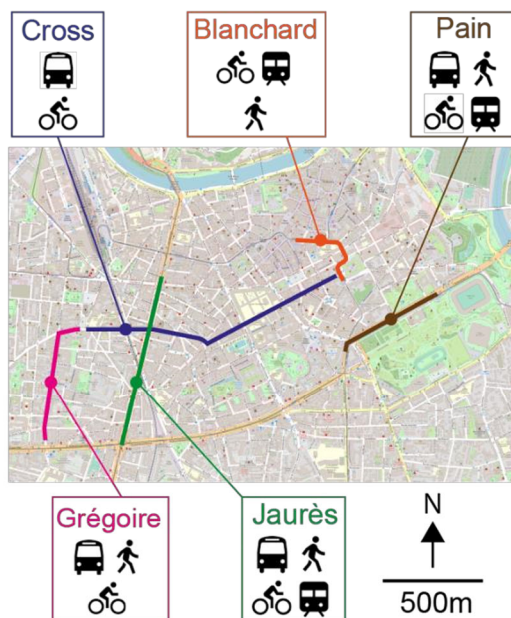


Figure 2. Monitoring routes used in the experiment. Credits: © OpenStreetMap contributors

### 2.2.2 Experimental timings

Ground measurements were conducted from April 25, 2022 to May 12, 2022 during 10 working days (Figure 3). Three different measurement sessions were performed daily: a first session (S1, morning) between 8:00 and 9:00, a second session (S2, noontime) between 12:00 and 13:00 and a third session (S3, afternoon) between 16:00 and 17:00. Sometimes, for reasons related to the public transport timetables, the sessions went slightly beyond the time slots. Nine sessions were postponed because of rainy conditions.

Two experimenters were involved in the study. For each session, they had to travel the same routes in parallel using different modes of transport: bike, walk, bus or tramway (Appendix). Each site was sampled for at least three days (Figure 3). On the days when we studied Blanchard and Grégoire, we also monitored PM while travelling in between the two sites (“Cross” route). Jaurès was sampled four times because this street, longer than the others, had many potential biases (intersections, stores, idling cars) and we thought it might be interesting to replicate the measurements further.

		S1 8-9h	S2 12-13h	S3 16-17h	Site
2022-04-25	Mon				Blanchard
2022-04-26	Tue				Jaurès
2022-04-27	Wed				Pain
2022-04-28	Thu				Grégoire
2022-04-29	Fri				Jaurès
2022-05-02	Mon				Grégoire
2022-05-03	Tue				Jaurès
2022-05-04	Wed	Canceled (rain)			
2022-05-05	Thu	Canceled (rain)			
2022-05-06	Fri				Pain
2022-05-11	Wed				Jaurès
2022-05-12	Thu				Blanchard

Figure 3. Measurement campaign schedule.

Next, we analysed carefully the public transportation schedules. A session example is reported in the Appendix. The same document was used as a roadmap by the experimenters for each session. Reproducing measurements on the same street is important to be representative (Van den Bossche et al., 2015). Every day, each experimenter performed at least 12 repetitions of the route.

## 2.3 Data cleaning

In this paper, we decided to focus only on  $PM_{2.5}$  analysis and on commuting times. We left  $PM_{10}$ ,  $PM_{1}$ , and results related to waiting times for further work. Data were extracted via AirCasting application and analysed with RStudio. We retrieved 214 comparison trips where the two experimenters were travelling along the same routes (428 trips in total, considering both experimenters). PM sensors can be vulnerable to inaccuracies resulting from drift, temperature, humidity and other factors (Motlagh et al., 2021). As both AirBeam2 were quite new, drift was not an issue, but we blew compressed air through the intake of the gold pod used for calibration as recommended by Bathory, Dobo, Garami, Palotas, and Toth (2021). As explained above, both AirBeam2 devices were calibrated using formulas accounting for RH and temperature. We also checked the presence of dust with CAMS (Copernicus Atmosphere Monitoring Service) satellite data (retrieved  $0.1^\circ \times 0.1^\circ$  resolution dust values from ENSEMBLE dataset (METEO FRANCE, 2020) ('analysis' type)). Fortunately, no dust event happened during the experiment period. We removed outliers in the dataset because we had peak events on trips, even inside public transports, mainly because of smokers or idling cars. In public transports, those peaks were often caused by door openings. All outliers with more than 1.5 times the interquartile range above the third quartile (Q3) or less than 1.5 times the interquartile range below the first quartile (Q1) were removed. Hourly background reference  $PM_{2.5}$  concentrations from Atmo AuRA were collected through their Application Programming Interface (<https://api.atmo-aura.fr/>). For this study, we used the average from two background reference stations (Les Frênes and Saint-Martin d'Hères). Both references, placed at approximately 3 km from the experimental sites, were located in relatively open areas (Figure 4). For each measurement made every second with our mobile devices, we affected the corresponding hourly value given by the reference stations. We also used meteorological data from the Réseau d'Observation Météo du Massif Alpin (ROMMA, 2022). Their nearest weather station (GPS coordinates: latitude =  $45.169^\circ$ , longitude =  $5.768^\circ$ ) was located around 3 km from the collocation site (Figure 4). A Davis Vantage Pro2 instrument registered all weather parameters. Wind speed (km/h) corresponded to a 10-mn average, with a measurement frequency of 2.5-3 s. We checked that all data sources used the same time zone (Europe/Paris).

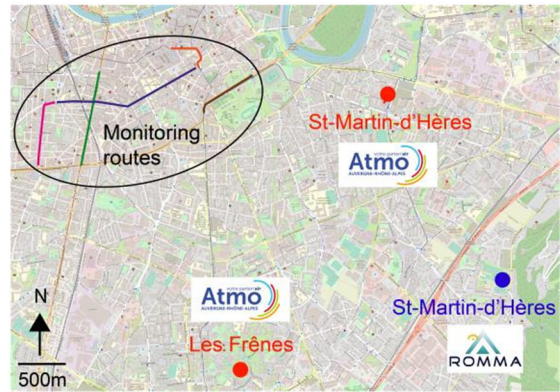


Figure 4. Location of the Atmo AuRA reference stations (in red) and ROMMA meteorological station (in blue). Credits: © OpenStreetMap contributors

## 3 RESULTS

### 3.1 Descriptive statistics

Collected  $PM_{2.5}$  data are summarized in Table 1. More measurements were performed on walking mode because, in order to replicate the experiment and use public transportation again, we had to walk back to the starting point. This was especially true on routes where public transport was only running in one direction. The number of measurements made on foot were also higher because walking the road segment took longer than cycling, taking the bus or tramway.

Table 1. Descriptive statistics on  $PM_{2.5}$  concentrations and number of measurements (count) performed in different commuting modes.

Dataset with outliers					
		$PM_{2.5}$ ( $\mu\text{g}/\text{m}^3$ )			
mode	count	median	SD	min	max
Bike	21448	8.21	2.33	3.04	35.46
Walk	73438	8.03	3.10	2.34	79.99
Bus	23374	7.44	2.05	2.30	26.44
Tram	14592	7.16	1.71	2.69	18.03
Dataset without outliers					
		$PM_{2.5}$ ( $\mu\text{g}/\text{m}^3$ )			
mode	count	median	SD	min	max
Bike	20451	8.08	1.94	3.04	17.50
Walk	69570	7.88	1.81	2.34	16.91
Bus	22638	7.37	1.97	2.30	18.97
Tram	13990	7.08	1.65	2.69	12.98



More outliers were identified for walking (5.3%) than for cycling (4.6%), tramway (4.1%) or bus (3.1%). Walkers are generally more exposed to PM coming from smokers, restaurants or bakeries. In addition, they are close to idling cars. When leaving outliers in the dataset, cyclists were more exposed (median:  $8.2 \mu\text{g}/\text{m}^3$ ) than walkers (median:  $8 \mu\text{g}/\text{m}^3$ ), followed by buses (median:  $7.4 \mu\text{g}/\text{m}^3$ ) and tramway (median:  $7.2 \mu\text{g}/\text{m}^3$ ). Compared with cyclists, pedestrians were 2.2% less exposed, bus users 9.4% less and tramway commuters 12.8% less. When removing outliers, the exposure ranking proved to be the same. Cyclists were more exposed (median value of  $8.1 \mu\text{g}/\text{m}^3$ ) than walkers (median:  $7.9 \mu\text{g}/\text{m}^3$ ), followed by bus users (median:  $7.4 \mu\text{g}/\text{m}^3$ ) and tramway (median:  $7.1 \mu\text{g}/\text{m}^3$ ). Compared to cyclists, walkers were 2.4% less exposed, bus commuters 8.6% less and tramway users 12.2% less. Qiu and Cao (2020) also found that walkers were more exposed than bus commuters. Peng et al. (2021) and Wang et al. (2021) found the same exposure ranking (bike>walk>bus). They used a PMS3003 device, similar to PMS7003. According to Shen and Gao (2019), cyclists and pedestrians can be directly exposed to other local particle emissions along the road, which probably results in elevated PM concentrations in specific areas and times. In a study taking place in Nantes (France), Muresan and François (2018) stated that public transport users would accumulate 4–11 times less PM in their lungs than nearby pedestrians walking the same route. We decided to pursue all further analyses after having removed outliers in our dataset.

### 3.2 Comparison between travel modes

Exposure levels are greatly influenced by the time of day (Figure 5). The morning session (S1) showed higher  $\text{PM}_{2.5}$  concentrations, followed by the noontime (S2) and the afternoon session (S3).

Of all transport modes combined, S1  $\text{PM}_{2.5}$  median was 12.9% higher than S2, while S2 median was 15.3% higher than S3. In the tramway, diurnal variations seem to be reduced compared to other modes. deSouza, Lu, Kinney, and Zheng (2021) also found that time of day (evening/morning) had an influence. In their ANOVA analysis, travel mode explained 9% of the variability in  $\text{PM}_{2.5}$  concentrations whereas time of day explained 8% variability.

All sessions considered, cyclists are the most exposed commuters. Abbass, Kumar, and El-Gendy (2021) studied morning and evening  $\text{PM}_{2.5}$  peaks. In their work, daily exposure patterns when walking or

cycling looked similar, whereas microbus concentrations behaved differently, and cycling resulted in exposure to the highest average  $\text{PM}_{2.5}$  concentrations.

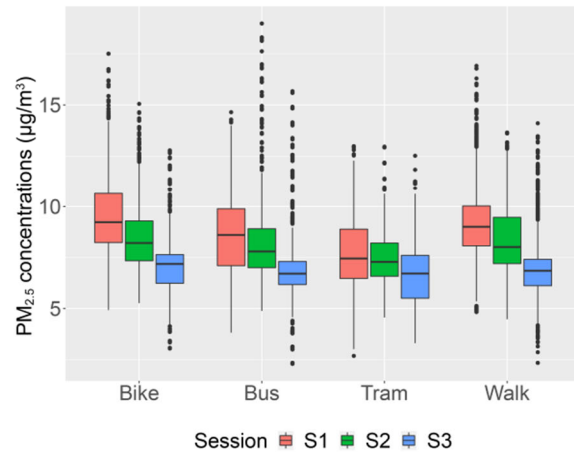


Figure 5. Boxplots of  $\text{PM}_{2.5}$  concentrations by transport mode. Upper and lower whiskers show the ranges of 5% to 95%, the central dark lines indicate the median. The bars outside the box represent 1.5 times the interquartile range, and circles are outliers.

Per session, we observe the same  $\text{PM}_{2.5}$  exposure ranking (bike > walk > bus > tramway) but, during S3, the levels measured in the bus get close to those measured in the tramway. When  $\text{PM}_{2.5}$  levels are high (S1), the differences between the transport modes are important, but when the levels are low, during the afternoon (S3), the differences become less pronounced. This suggests that when PM levels are low, public transports no longer play a “protective” role against  $\text{PM}_{2.5}$ . In addition, relative differences between sessions are lower in the tramway than in the other transportation modes. This could mean that levels in the tramway are less influenced by background concentrations, which are higher in the morning.

### 3.3 Comparison with reference value

One of the objectives of this study was to compare the  $\text{PM}_{2.5}$  values measured by the mobile sensors with those returned by the reference stations. The graph below (Figure 6) shows  $\text{PM}_{2.5}$  levels measured by the mobile devices and the corresponding background reference levels. The hours marked in bold are the times when we carried out the most  $\text{PM}_{2.5}$  measurements. As an example, the 10 am measurements were those that we were unable to perform as planned between 8 and 9 am. As this rarely



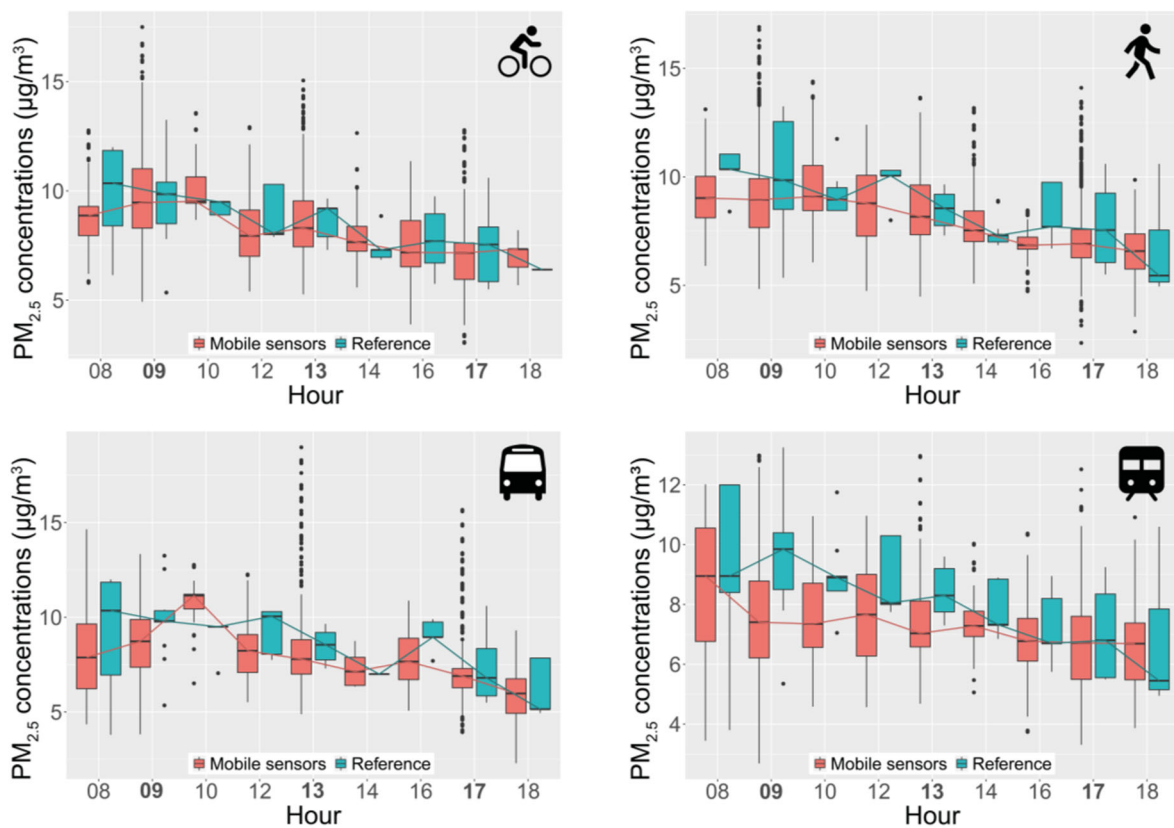


Figure 6. Comparison between values measured by mobile devices and reference values. The 9 o'clock boxplot corresponds to the values measured by mobile sensors between 8 and 9 am. The hours in bold are the ones where we had the more measurements taken by mobile devices.

happened, we got fewer observations for those extra hours.

In general,  $PM_{2.5}$  levels given by the mobile sensors were lower than values given by background stations, especially when considering hours when the counts were the highest (9, 13, and 17). This could come from microscale  $PM_{2.5}$  variations, as  $PM_{2.5}$  at the local scale could be affected by different factors. This was surprising that measured  $PM_{2.5}$  values were lower than reference values, because we were in a traffic situation and the reference stations are located in a background environment. Both reference stations, situated in opened areas, could be exposed to more  $PM_{2.5}$  which would be covered by the dense and high buildings of the city centre where experiments took place. The AirBeam2 calibration could also be an explanation. The ideal way to perform a calibration would have been to collocate our mobile devices directly with the reference station, without using a gold pod as an intermediary. It is also important to note that the calibration with the reference was performed at an hourly scale, and we had to apply it

to values given at a fine scale (seconds). Knowing the RMSE related to step 1 calibration (Refer Figure 1), we could expect a maximal error of  $0.7 \mu\text{g}/\text{m}^3$ . The average difference between reference and mobile values during S1 and S2 (considering 9, 13 and 17 o'clock timings) was about  $1.1 \mu\text{g}/\text{m}^3$ . Therefore, the calibration error alone could most probably not explain the observed difference. Motlagh et al. (2021) used low-cost sensors to measure  $PM_{2.5}$  in Helsinki and saw that roadside measurements were higher than reference values. But during spring or summer, the pollution levels in the train, bus or tramway were well below the ambient reference pollution levels. They attributed this to the fact that the transport fleet in Helsinki was quite modern and the indoor air heavily filtered. This should be the case for tramways in Grenoble. However, older buses might remain in operation, and the practice of using conditioned air depends on the weather and the driver. It would have been interesting to know if the air was filtered in the different buses and trams we used. Han et al (2021) also used low-cost sensors and observed that personal

PM<sub>2.5</sub> levels were consistently lower than ambient concentrations. The Center for Advancing Research in Transportation Emissions, Energy, and Health (2019) measured exposure of urban cyclists in Atlanta (United States) with a PMS5003. They concluded that few segments recorded air quality worse than the background concentration. During most of the routes, riders experienced a better air quality than the one registered at the monitoring location.

In our study, wind could be an important factor determining PM<sub>2.5</sub> levels. We observed that wind speed values were increasing starting from 10 am (Figures 7 and 8). The relief around Grenoble could contribute to this phenomenon.

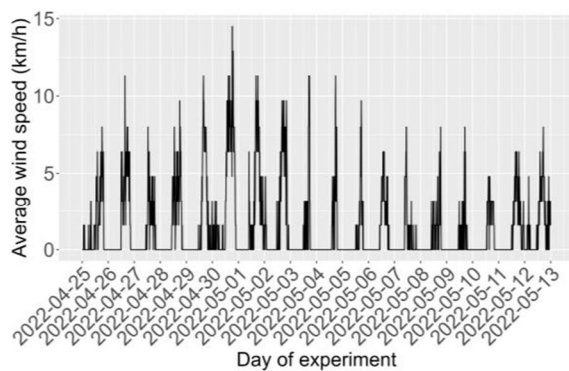


Figure 7. Wind speed values during the experiment.

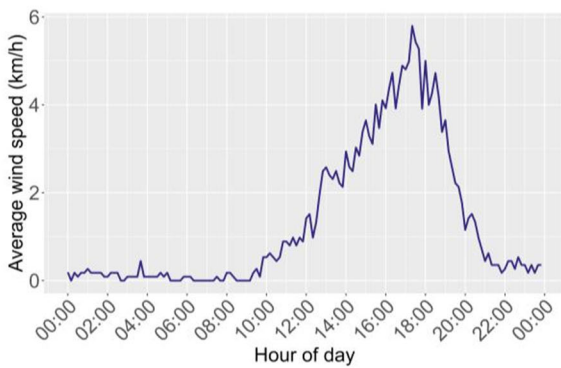


Figure 8. Average wind speed values between April 25, 2022 and May 12, 2022.

Interestingly, we observed that bus and tramway had levels close to the reference during S3 (Refer Figure 6). When PM levels in Grenoble were high, public transports provided an important advantage, but when PM levels were lower, close to their minimum, public transportation systems did not seem to offer this benefit any longer. Wang et al. (2021) also performed three daily measurement sessions

(morning/noon/afternoon). Their GRIMM instrument showed that at lower pollutant levels, the concentrations registered in the bus were higher than the background levels. When pollutants levels were higher (noontime), the difference between inside and outside got larger, as in our study. They also observed lower levels of PM<sub>2.5</sub> compared to the reference when the pollutant levels were higher. Furthermore, by using a similar low-cost sensor (PMS3003), they found as well that when PM<sub>2.5</sub> levels were lower, the difference between reference levels and bus carriage levels was lower.

## 4 CONCLUSIONS

During this spring experiment, performed in 2022 at low pollutant levels, cyclists were more exposed than pedestrians, bus users and tramway commuters. This ranking was the same whether we removed outliers or not. We counted more outliers for walking than for cycling, tramway or bus.

When comparing exposure values to reference stations measurements: (1) pedestrian and cyclists' exposure generally stayed under background values, (2) public transportation systems were under reference values at 9 or 13 o'clock but when PM levels went lower, levels reached those of the reference value. Public transport users could be less exposed than commuters using active modes, except when ambient PM levels are low.

The time of day seems to influence exposure more than mode of transport, with a gradual concentration decrease throughout the day. Environmental parameters like wind might play a role in Grenoble. It would be interesting to reproduce this work during another season when wind speed is lower.

In the future, we will perform an inhalation dose calculation on the same dataset in order to consider breathing rate differences among commuting modes. In Grenoble, about 15% of the working population cycles to work (Agence de la Transition Écologique, 2015), which makes the problem of PM exposure more acute. However, we must emphasize that cycling helps prevent many chronic diseases and brings environmental benefits.

## REFERENCES

- Abbass, R. A., Kumar, P., & El-Gendy, A. (2021). Fine particulate matter exposure in four transport modes of Greater Cairo. *Science of*

- The Total Environment*, 791, 148104. doi:10.1016/j.scitotenv.2021.148104
- Agence de la Transition Écologique. (2015). La mobilité durable de Grenoble Alpes Métropole. Retrieved from <https://territoireengagetransitionecologique.ademe.fr/metropole-de-grenoble-met-en-place-un-systeme-de-mobilite-durable-1-2-2/>
- Bathory, C., Dobo, Z., Garami, A., Palotas, A., & Toth, P. (2021). Low-cost monitoring of atmospheric PM-development and testing. *Journal of Environmental Management*, 304, 114158. doi:<https://doi.org/10.1016/j.jenvman.2021.114158>
- Blanco, M. N., Gassett, A., Gould, T., Doubleday, A., Slager, D. L., Austin, E., . . . Sheppard, L. (2022). Characterization of Annual Average Traffic-Related Air Pollution Concentrations in the Greater Seattle Area from a Year-Long Mobile Monitoring Campaign. *Environmental Science & Technology*, 56(16), 11460-11472. doi:10.1021/acs.est.2c01077
- Center for Advancing Research in Transportation Emissions, Energy, and Health. (2019). *Measuring Temporal and Spatial Exposure of Urban Cyclists to Air Pollutants Using an Instrumented Bike* (Report No. GT-01-09). Retrieved from <https://rosap.nrl.bts.gov/view/dot/56809>
- Das, P., Ghosh, S., Chatterjee, S., & De, S. (2022). A Low Cost Outdoor Air Pollution Monitoring Device With Power Controlled Built-In PM Sensor. *IEEE Sensors Journal*, 22(13), 13682-13695. doi:10.1109/jsen.2022.3175821
- deSouza, P., Lu, R., Kinney, P., & Zheng, S. (2021). Exposures to multiple air pollutants while commuting: Evidence from Zhengzhou, China. *Atmospheric Environment*, 247, 118168. doi:10.1016/j.atmosenv.2020.118168
- Dons, E., Int Panis, L., Van Poppel, M., Theunis, J., & Wets, G. (2012). Personal exposure to Black Carbon in transport microenvironments. *Atmospheric Environment*, 55, 392-398. doi:10.1016/j.atmosenv.2012.03.020
- Fuller, R., Landrigan, P. J., Balakrishnan, K., Bathan, G., Bose-O'Reilly, S., Brauer, M., . . . Yan, C. (2022). Pollution and health: a progress update. *The Lancet Planetary Health*, 6(6), e535–e547. doi:[https://doi.org/10.1016/S2542-5196\(22\)00090-0](https://doi.org/10.1016/S2542-5196(22)00090-0)
- HabitatMap. (2022). AirBeam3 Technical Specifications, Operation & Performance. Retrieved from <https://www.habitatmap.org/blog/airbeam3-technical-specifications-operation-performance>
- Haghighbayan, S., & Tashayo, B. (2021). Integrating ground-based air quality monitoring stations with mobile sensor units to improve the accuracy of PM<sub>2.5</sub> concentration modeling. *Scientific - Research Quarterly of Geographical Data (SEPEHR)*, 29(116), 45-58. doi:10.22131/sepehr.2021.242859
- Han, Y., Chatzidiakou, L., Yan, L., Chen, W., Zhang, H., Krause, A., . . . Kelly, F. J. (2021). Difference in ambient-personal exposure to PM<sub>2.5</sub> and its inflammatory effect in local residents in urban and peri-urban Beijing, China: results of the AIRLESS project. *Faraday Discussions*, 226, 569-583. doi:10.1039/d0fd000097c
- Huang, J., Kwan, M. P., Cai, J., Song, W., Yu, C., Kan, Z., & Yim, S. H. (2022). Field Evaluation and Calibration of Low-Cost Air Pollution Sensors for Environmental Exposure Research. *Sensors (Basel)*, 22(6), 2381. doi:<https://doi.org/10.3390/s22062381>
- METEO FRANCE, Institut National de l'Environnement Industriel et des Risques (Ineris), Aarhus University, Norwegian Meteorological Institute (MET Norway), Jülich Institut für Energie- und Klimaforschung (IEK), Institute of Environmental Protection – National Research Institute (IEP-NRI), Koninklijk Nederlands Meteorologisch Instituut (KNMI), Nederlandse Organisatie voor toegepast-natuurwetenschappelijk onderzoek (TNO), Swedish Meteorological and Hydrological Institute (SMHI), Finnish Meteorological Institute (FMI). (2020). *CAMS European air quality forecasts, ENSEMBLE data. Copernicus Atmosphere Monitoring Service (CAMS) Atmosphere Data Store (ADS)*. [dataset]. Retrieved from: <https://ads.atmosphere.copernicus.eu/cdsap>

- p#!/dataset/cams-europe-air-quality-forecasts?tab=overview
- Motlagh, N. H., Zaidan, M. A., Fung, P. L., Lagerspetz, E., Aula, K., Varjonen, S., . . . Tarkoma, S. (2021). Transit pollution exposure monitoring using low-cost wearable sensors. *Transportation Research Part D: Transport and Environment*, *98*. doi:10.1016/j.trd.2021.102981
- Muresan, B., & François, D. (2018). Air quality in tramway and high-level service buses: A mixed experimental/modeling approach to estimating users' exposure. *Transportation Research Part D: Transport and Environment*, *65*, 244-263. doi:10.1016/j.trd.2018.09.005
- Peng, L., Shen, Y., Gao, W., Zhou, J., Pan, L., Kan, H., & Cai, J. (2021). Personal exposure to PM<sub>2.5</sub> in five commuting modes under hazy and non-hazy conditions. *Environmental Pollution*, *289*, 117823. doi:10.1016/j.envpol.2021.117823
- Pryor, J. T., Cowley, L. O., & Simonds, S. E. (2022). The Physiological Effects of Air Pollution: Particulate Matter, Physiology and Disease. *Frontiers in Public Health*, *10*, 882569. doi:10.3389/fpubh.2022.882569
- Qiu, Z., & Cao, H. (2020). Commuter exposure to particulate matter in urban public transportation of Xi'an, China. *Journal of Environmental Health Science and Engineering*, *18*(2), 451-462. doi:10.1007/s40201-020-00473-0
- R Core Team. (2022). *R: A language and environment for statistical computing*. R Foundation for Statistical Computing, Vienna, Austria. Retrieved from: <https://www.R-project.org/>
- Réseau d'Observation Météo du Massif Alpin. (2022). *Données Station de Saint-Martin-d'Hères [Members dataset]*. Retrieved from: <https://romma.fr/>
- Schmitz, S., Towers, S., Villena, G., Caseiro, A., Wegener, R., Klemp, D., . . . Von Schneidmesser, E. (2021). Unravelling a black box: An open-source methodology for the field calibration of small air quality sensors. *Atmospheric Measurement Techniques*, *4*, 7221-7241. doi:<https://doi.org/10.5194/amt-2020-489>
- Shen, J., & Gao, Z. (2019). Commuter exposure to particulate matters in four common transportation modes in Nanjing. *Building and Environment*, *156*, 156-170. doi:10.1016/j.buildenv.2019.04.018
- South Coast Air Quality Management District. (2018). *Field Evaluation - AirBeam2 PM Sensor, AQ-SPEC*. Retrieved from <http://www.aqmd.gov/docs/default-source/aq-spec/summary/habitatmap-airbeam2---summary-report.pdf?sfvrsn=16>
- Tong, C., Shi, Z., Shi, W., & Zhang, A. (2022). Estimation of On-Road PM<sub>2.5</sub> Distributions by Combining Satellite Top-of-Atmosphere With Microscale Geographic Predictors for Healthy Route Planning. *Geohealth*, *6*(9), e2022GH000669. doi:10.1029/2022GH000669
- Van den Bossche, J., Peters, J., Verwaeren, J., Botteldooren, D., Theunis, J., & De Baets, B. (2015). Mobile monitoring for mapping spatial variation in urban air quality: Development and validation of a methodology based on an extensive dataset. *Atmospheric Environment*, *105*, 148-161. doi:10.1016/j.atmosenv.2015.01.017
- Wang, W.-C. V., Lung, S.-C. C., Liu, C.-H., Wen, T.-Y. J., Hu, S.-C., & Chen, L.-J. (2021). Evaluation and Application of a Novel Low-Cost Wearable Sensing Device in Assessing Real-Time PM<sub>2.5</sub> Exposure in Major Asian Transportation Modes. *Atmosphere*, *12*(2). doi:10.3390/atmos12020270
- Yang, F., Lau, C. F., Tong, V. W. T., Zhang, K. K., Westerdahl, D., Ng, S., & Ning, Z. (2019). Assessment of personal integrated exposure to fine particulate matter of urban residents in Hong Kong. *Journal of the Air & Waste Management Association*, *69*(1), 47-57. doi:10.1080/10962247.2018.1507953
- Yang, Y., Wang, H., Jiang, R., Guo, X., Cheng, J., & Chen, Y. (2022). A Review of IoT-Enabled Mobile Healthcare: Technologies, Challenges, and Future Trends. *IEEE Internet of Things Journal*, *9*(12), 9478-9502. doi:10.1109/jiot.2022.3144400
- Zou, Y., Clark, J. D., & May, A. A. (2021). A systematic investigation on the effects of temperature and relative humidity on the performance of eight low-cost particle sensors and devices. *Journal of Aerosol Science*, *152*. doi:10.1016/j.jaerosci.2020.105715

**ABBREVIATIONS**

Acronym	Definition
ANOVA	Analysis of variance
Atmo AuRA	Atmo Auvergne-Rhône-Alpes
CAMS	Copernicus Atmosphere Monitoring Service
IoT	Internet of Things
mob1	AirBeam2 used by experimenter 1
mob2	AirBeam2 used by experimenter 2
PM	Particulate matter
PM <sub>1</sub>	Particulate matter with aerodynamic diameter $\leq 1 \mu\text{m}$
PM <sub>2.5</sub>	Particulate matter with aerodynamic diameter $\leq 2.5 \mu\text{m}$
PM <sub>10</sub>	Particulate matter with aerodynamic diameter $\leq 10 \mu\text{m}$
R <sup>2</sup>	Coefficient of determination
RH	Relative humidity
RMSE	Root mean square error
ROMMA	Réseau d'Observation Météo du Massif Alpin

## APPENDIX

### Example of a measurement session

Date : 4/25/2022

Weather	humid, light rain, clouds
Wind	low
Traffic intensity	low

J1_S1 session	Experimenter	Code	Transport mode	Start "Chavant"	Arrival "Hôtel de Ville"	Start "Hôtel de Ville"	Arrival "Chavant"	Observations			
								Smokers	Idling vehicles	Crosses	Others
Wait 1	mob2	A_VM_CH	Wait at "Chavant"	7:50:18	7:54:08						
	mob2	A_T_CH	Wait at "Chavant"	7:54:09	7:59:12			7:57 smokers			
	mob1	A_VM_CH	Tram wait	7:50:07	7:54:46						
	mob1	A_B_CH	Bus wait	7:54:46	7:57:50						
Trip 1	mob2	T_CH_HV	Tram C	7:59:13	8:01:28						
	mob1	B_CH_HV	Bus C1	7:57:51	7:59:20				7:59 - 8:00 bus		
Waiting 2	mob2	A_B_HV	Bus wait			8:03:44	8:10:32				
	mob1	A_VM_HV	Walk wait			8:03:10	8:06:10				
Trip 2	mob2	B_HV_CH	Bus C1			8:10:33	8:12:00				
	mob1	M_HV_CH	Walk			8:06:11	8:14:25		8:09 garbage truck	8:13 stop	
Wait 3	mob2	A_T_CH	Tram wait	8:15:12	8:20:58						
	mob1	A_VM_CH	Bike wait	8:14:26	8:19:44						
Trip 3	mob2	T_CH_HV	Tram C	8:21:00	8:22:31						
	mob1	VD_CH_HV	Dedicated bike	8:19:45	8:21:51						
Wait 4	mob2	A_VM_HV	Walk wait			8:22:32	8:23:36				
	mob1	A_VM_HV	Walk wait			8:21:52	8:23:36				
Trip 4	mob2	M_HV_CH	Walk			8:23:37	8:30:40				
	mob1	M_HV_CH	Walk			8:23:36	8:30:40				
Wait 5	mob2	A_B_CH	Bus wait	8:31:52	8:34:00						
	mob1	A_VM_CH	Bike wait	8:30:41	8:33:12						
Trip 5	mob2	B_CH_HV	Bus C1	8:34:01	8:35:20						
	mob1	VD_CH_HV	Dedicated bike	8:33:13	8:35:37						
Wait 6	mob2	A_T_HV_RO	Tram wait			8:35:36	8:43:12				
	mob1	A_VM_HV	Walk wait			8:35:38	8:40:37				
Trip 6	mob2	T_HV_CH	Tram C			8:43:13	8:45:28				
	mob1	M_HV_CH	Walk			8:40:38	8:47:50				
Wait 7	mob2	A_VM_CH	Walk wait	8:45:29	8:48:30						
	mob1	A_VM_CH	Bike wait	8:47:51	8:51:45						
Trip 7	mob2	M_CH_HV	Walk	8:48:31	8:55:00			8:53 smoker			
	mob1	VD_CH_HV	Dedicated bike	8:51:46	8:54:10						
Wait 8	mob2	A_B_HV	Bus wait			8:55:20	8:57:49				
	mob1	A_T_HV_RO	Tram wait			8:56:22	8:59:17				
Trip 8	mob2	B_HV_CH	Bus C1			8:57:59	9:00:08				
	mob1	T_HV_CH	Tram C			8:59:18	9:01:02				



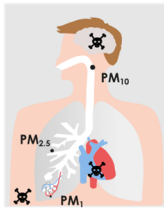
# APPENDIX C

## Low-cost sensors for particulate matter measurement

Marie-Laure Aix<sup>1</sup>, Bertrand Baudour<sup>2</sup>, Gilles Mertens<sup>2</sup>, Dominique J. Bicoût<sup>1</sup>, Didier Donsez<sup>3</sup>  
<sup>1</sup> Univ. Grenoble Alpes, CNRS, UMR 5525, VetAgro Sup, Grenoble INP, TIMC, 38000, Grenoble, France  
<sup>2</sup> École Polytechnique (Polytech Grenoble), Univ. Grenoble Alpes, 38000, Grenoble, France  
<sup>3</sup> Univ. Grenoble Alpes, Laboratoire Informatique de Grenoble, 38000, Grenoble, France

### INTRODUCTION

Particulate matter (PM) is a global threat to human health, associated with respiratory, cardiovascular, and neurological diseases, as well as premature mortality. PM toxicity depends on several factors, size being a crucial determinant. PM<sub>10</sub> (< 10µm), typically remains in the upper tract and is less hazardous than PM<sub>2.5</sub>, which can penetrate deeper into the lungs and PM<sub>1</sub>, which can enter the bloodstream. Accurate measurement of fine PM is critical, and low-cost sensors (LCS) represent a cost-effective complement to official monitoring networks. This feasibility study aims to compare the performance of a Wi-Fi and two LoRaWAN air quality stations (AQ stations) using LCS to measure PM, with the goal of determining whether the LoRa AQ stations can deliver accurate measurements.



### MATERIAL & METHODS

#### 1. Prototyping

A first Wi-Fi AQ station was designed and calibrated with a reference monitor (REF) from Atmo Auvergne Rhône-Alpes. This Wi-Fi AQ station performed well in measuring fine PM [1]. Then a LoRaWAN AQ station was developed to eliminate the dependence on Wi-Fi and allow broader deployment. Both stations were equipped with different temperature (T) and relative humidity (RH) sensors. BME280 should perform better than DHT 22 in high-humidity situations. The firmware used for the Wi-Fi AQ station was developed by sensor community (<https://firmware.sensor.community/airrohr/flashing-tool/>) and enabled reporting of PM<sub>1</sub>, PM<sub>2.5</sub>, PM<sub>10</sub>, T, and RH. For the LoRaWAN AQ stations, a novel firmware using RIOT OS (<https://github.com/RIOT-OS/RIOT>) was developed ([https://github.com/airqualitystation/firmware\\_for\\_bmx280\\_pms7003](https://github.com/airqualitystation/firmware_for_bmx280_pms7003)), allowing the extraction of additional parameters, particularly PM counts within different size ranges.

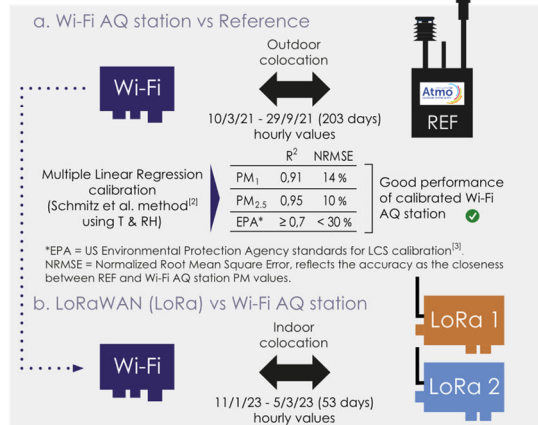
Wi-Fi AQ station		
<b>Variables :</b>	<b>Component</b>	<b>Price (€)</b>
PM <sub>10</sub> , PM <sub>2.5</sub> , PM <sub>1</sub> , RH, T	PMS7003 (PM sensor)	23.8
	DHT22 (RH & T sensor)	10.9
<b>Frequency :</b>	NodeMCU ESP8266 microcontroller	12.3
Every 150 s	Polycarbonate IP66 outer case	15.9
	Euromas II wall brackets	3.2
	USB / USB-A 2m flat cable	11.9
	5V USB power supply	6.9
		<b>84.9</b>

LoRaWAN AQ station		
<b>Variables :</b>	<b>Component</b>	<b>Price (€)</b>
PM <sub>10</sub> , PM <sub>2.5</sub> , PM <sub>1</sub> ,	PMS7003 (PM sensor)	23.8
RH, T, pressure,	BME280 (RH & T sensor)	19.9
particles count	LoRa-ES mini board	27.9
>0.3µm, >0.5µm,	Polycarbonate IP66 outer case	15.9
>1µm, >2.5µm, >10µm	Euromas II wall brackets	3.2
<b>Frequency :</b>	USB-C / USB-A 3m flat cable	14.9
8 s median (99.4 % of	5V USB power supply	6.9
time intervals < 150 s) *		<b>112.5</b>

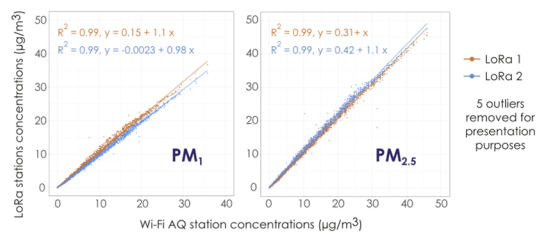
\* According to ESI regulation, the measurement period is adapted to the datarate depending on the range between the LoRaWAN AQ station & the gateways (5 to 160 s).

#### 2. Calibration



### RESULTS

#### 1. LoRaWAN performance vs. Wi-Fi AQ station



➤ R<sup>2</sup> slope & intercept conform to EPA standards ✓

➤ Additional metrics :

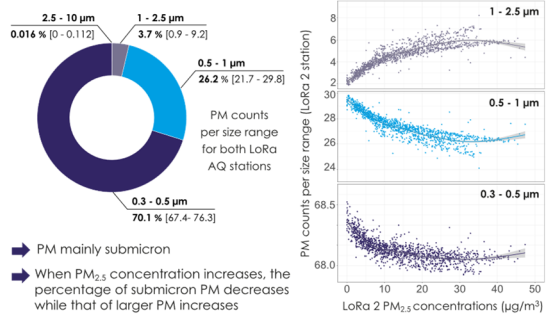
	NRMSE (%)	SD (µg/m <sup>3</sup> )	CV (%)
PM <sub>1</sub>	9	0.7	6.6
PM <sub>2.5</sub>	11	0.6	4.2
EPA	< 30	< 5	≤ 30

LoRaWAN AQ stations : sensor - sensor precision ✓  
 SD: standard deviation  
 CV: coefficient of variation

+ NRMSE Wi-Fi / REF (refer part 2.a)  
 PM<sub>1</sub>: NRMSE = 23 %  
 PM<sub>2.5</sub>: NRMSE = 21 %

LoRaWAN AQ stations : sensors accuracy vs REF ✓

#### 2. Particle counts



### CONCLUSION

- LoRaWAN AQ stations performance metrics conform to EPA standards.
- LoRaWAN AQ stations deliver precise & reliable particulate matter measurements.
- The firmware allows particles counts extraction, which will be useful for further research.

### REFERENCES

1. Aix ML, et al. (2023). Calibration Methodology of Low-Cost Sensors for High-Quality Monitoring of Fine Particulate Matter [Manuscript under revision]. 2023.
2. Schmitz S, et al. (2021). Unravelling a black box: An open-source methodology for the field calibration of small air quality sensors. Atmos. Meas. Tech. 4:7221-41.
3. Duvall R, et al. (2021). Performance Testing Protocols, Metrics, and Target Values for Fine Particulate Matter Air Sensors: Use in Ambient, Outdoor, Fixed Site, Non-Regulatory Supplemental and Informational Monitoring Applications. EPA/600/R-20/280. US Environmental Protection Agency, Office of Research and Development.





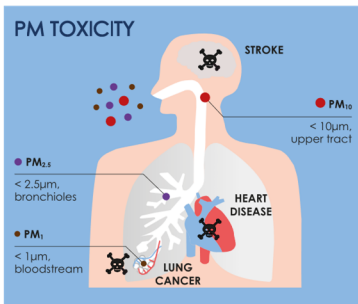
# APPENDIX D

## Designing low-cost sensors for high-quality air pollution monitoring

Marie-Laure Aix, Dominique J. Bicot  
 Univ. Grenoble Alpes, CNRS, UMR 5525, VetAgro Sup, Grenoble INP, TIMC, 38000, Grenoble, France

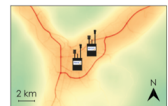
### PARTICULATE MATTER

is highly toxic, especially small size particles reaching vital organs through blood. In Grenoble, the spatial distribution of particulate matter (PM) is heterogeneous but only two official background stations monitor small size PM. Therefore, public exposure to PM is poorly estimated. A solution is to build easy to move low-cost measurement stations which can be deployed at various locations in the city. But the data quality of such stations must be characterized beforehand. We have developed a low-cost station (LCS) solution and compared data from LCS with that from an official reference station (Atmo Auvergne Rhône-Alpes) used by authorities.



### HETEROGENEITY

The local landscape in Grenoble plays a role in the heterogeneous distribution of particles.

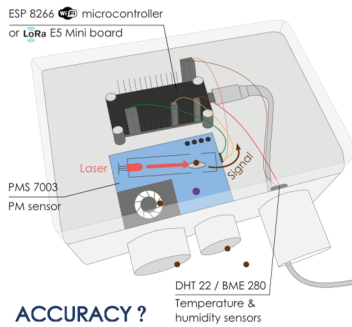


Only two official stations measure PM<sub>2.5</sub>. They are highly accurate but they are expensive (10 - 100k€) and cannot be moved.

### MATERIAL & METHODS

#### 1. Prototyping

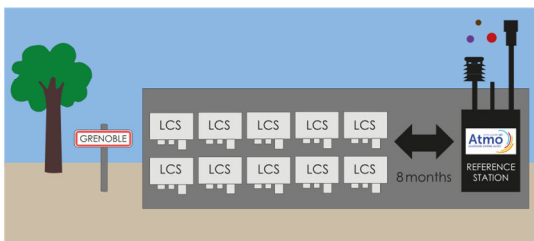
The solution was to build a cheap (65€) and easy to move low-cost station. We used an optical PM sensor in which a laser gets scattered by PM. An electric signal is then sent to a microcontroller where it is converted to a particle size and a number of particles in different size groups. The LCS also gives PM concentrations in µg/m<sup>3</sup>. We also assembled a humidity sensor because we knew humidity could influence particles growth.



ACCURACY ?

#### LOW-COST STATION

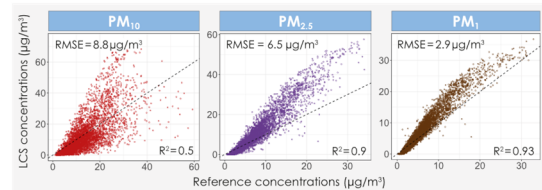
#### 2. Colocation with reference



To evaluate the performance of low-cost stations, ten LCS were installed for 8 months next to the Atmo reference station in Grenoble for the comparison of PM concentrations.

### RESULTS

#### 1. Comparison with reference



R<sup>2</sup> refers to the correlation between the LCS and the reference PM concentrations, while the Root Mean Square Error (RMSE) reflects the accuracy as the closeness between LCS and reference values. An R<sup>2</sup> as close to 1 as possible and a RMSE as small as possible are both indicators of good sensor performance.

#### CALIBRATION IS NEEDED

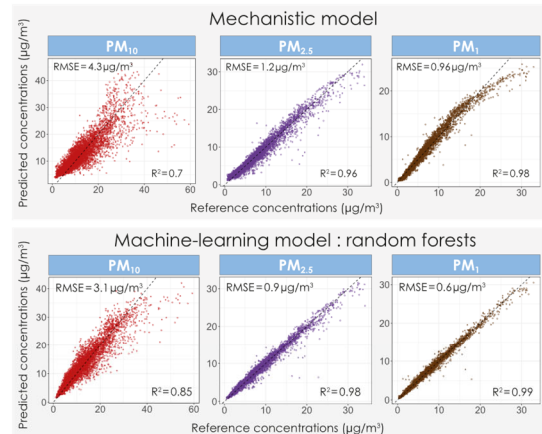
#### 2. Calibration models

Two models involving both Temperature and Relative Humidity are used for calibration : a mechanistic model and the random forests from the machine-learning approach.

Model	Formula	Dataset
Mechanic	$PM_{ref} = a + b \frac{PM_{LCS}}{\left(1 + c \frac{RH_{LCS}}{100 - RH_{LCS}}\right)^{\frac{1}{3}}} + d T_{LCS}$	100%
Random forests	$PM_{ref} = a PM_{LCS} + b RH_{LCS} + c T_{LCS}$	75% TRAIN, 25% TEST

\*100% means all 8 months dataset while 75-25% reflects a 6 months training + 2 months testing set

#### 3. Models performance

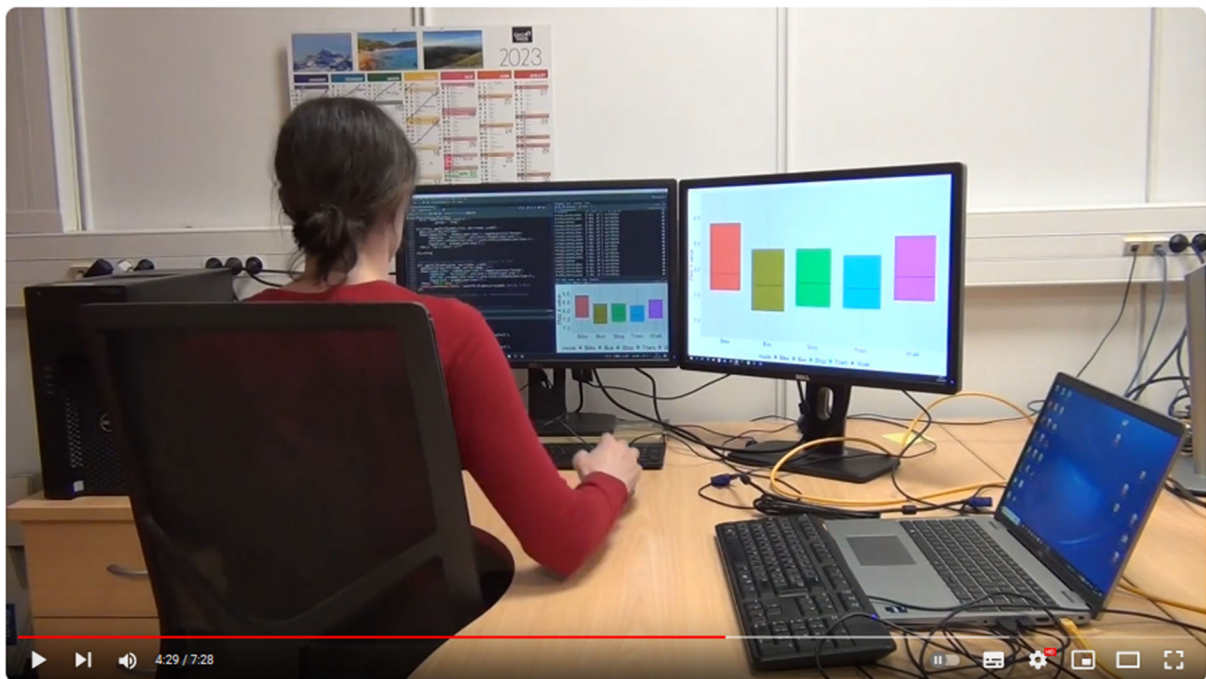


### CONCLUSION

- The performance of the models is higher for more toxic PM<sub>1</sub> and PM<sub>2.5</sub>, than for PM<sub>10</sub>.
- The best calibration method is achieved using machine-learning (random forests).
- Such calibrated low-cost stations can be deployed in Grenoble to monitor PM.

## APPENDIX E

Aix, M.L., Bicout, D. J., Zoppis, C. (2023, April 25) *Pollution atmosphérique, mobilités et santé dans l'agglomération grenobloise* [Video]. YouTube. <https://www.youtube.com/watch?v=vJJPfUDi-qq0>.



Marie-Laure AIX - 1er prix - Journée Doctorants TIMC 2023 - « Pollution atmosphérique, mobilités...»

TIMC TIMC lab  
4,17 k abonnés

Abonné

J'aime Comment Partager Extrait Enregistrer

25 vues 4 oct. 2023

Marie-Laure AIX - 1er prix des vidéos de la Journée des Doctorants-tes TIMC 2023 - « Pollution atmosphérique, mobilités et santé dans l'agglomération grenobloise ...».

« Pollution atmosphérique, mobilités et santé dans l'agglomération grenobloise. », thèse préparée par Marie-Laure AIX au laboratoire TIMC sous la direction de Dominique J. BICOUT (Laboratoire TIMC - Équipe EPSP), dans le cadre de l'EDISCE, École Doctorale Ingénierie pour la santé la Cognition et l'Environnement (Grenoble).

Capsule vidéo réalisée dans le cadre de la Journée des doctorants 2023 du laboratoire TIMC, 1er prix des vidéos 2023.

\* TIMC (CNRS / UGA / G INP / VetAgroSup) <https://www.timc.fr> et <https://www.timc.fr/EPSP>

\* partenaire du CHU Grenoble Alpes <https://www.chu-grenoble.fr>

\* CNRS <https://www.cnrs.fr>

\* UGA <https://www.univ-grenoble-alpes.fr>

\* G INP <https://www.grenoble-inp.fr>

\* VetAgro Sup <https://www.vetagro-sup.fr>

## APPENDIX F

Aix, M.L., Alfieri, R., Hartmann, P., Heredia Guzmán, M.B., Uleda, C., Veillas, C., Piolat, G. (2023, March 10-12). *Particule Fun* [Video game]. <https://pholothe1.itch.io/particule-fun>. Scientific Game Jam 2023, Grenoble, France



### **Particule Fun est un runner immersif ou le joueur est une particule fine !**

Cette particule rencontre des éléments favorables à sa survie (pots d'échappements) qui vont lui permettre de cheminer jusqu'au bout de chaque rue en survolant ses victimes.

As a fine particle you encounter elements favorable to your survival (exhausts pipes) which will allow you to travel to the end of each street by flying over your victims.

**Condition de victoire :** Dépasser le meilleur score en parcourant de la distance.

**Fin de partie :** Tomber dans la foule.

**Controls:**

Button	Action
Left Arrow / Left Joystick	Fly to the left
Right Arrow	Fly to the right
Top Arrow	Fly forward
Down Arrow	Fly backward
Mouse / Right Joystick	Turn view

TITRE: Pollution atmosphérique, mobilités et santé dans l'agglomération grenobloise

RÉSUMÉ: La pollution atmosphérique est un problème de santé publique mondial responsable d'une partie de la mortalité et de diverses maladies chroniques. Il est donc important de la mesurer la plus finement possible. Les objectifs de ce travail étaient d'identifier les risques sanitaires liés aux polluants de l'air à Grenoble (France) et de mesurer le plus finement possible les particules fines (PM), responsables d'une part importante de la mortalité. Ce travail débute par une analyse des risques pendant la pandémie de COVID-19, montrant des variations de niveaux de polluants : NO<sub>2</sub> (- 32%), PM<sub>2.5</sub> (- 22%), PM<sub>10</sub> (- 15%), et O<sub>3</sub> (+ 11%). Ces variations ont favorisé des baisses de risques sanitaires à court-terme liés aux PM<sub>2.5</sub> (- 3% de visites aux urgences pour asthme infantile) et au NO<sub>2</sub> (- 2% d'hospitalisations pour maladies respiratoires). À long terme, les PM<sub>2.5</sub> jouaient aussi un rôle prédominant, réduisant la mortalité toutes causes (- 3%), les cancers du poumon (- 2%), et les petits poids de naissance (- 8%), suivis du NO<sub>2</sub> (- 1% de mortalité non-accidentelle). En raison de leur impact sanitaire majeur, la thèse s'est ensuite focalisée sur les PM<sub>2.5</sub>, ainsi que sur les PM<sub>1</sub> (PM < 1 µm). Afin d'estimer le plus finement possible les niveaux de PM dans Grenoble, ainsi que leur hétérogénéité, nous avons assemblé des capteurs low-cost (LCS) pour compléter les stations de référence d'Atmo Auvergne-Rhône-Alpes. Les LCS ont été calibrés avec des méthodes incluant le machine-learning, en ôtant les jours de dusts sahariens perturbant les mesures de PM<sub>2.5</sub>. Les LCS utilisés étant peu performants pour mesurer les PM<sub>10</sub>, l'étude a été poursuivie sans les inclure. Un réseau fixe de 8 LCS a ensuite été déployé dans Grenoble, montrant des disparités temporelles et spatiales, avec en particulier un hotspot dans le centre-ville présentant des ratios à la référence ( $PM_{1 \text{ ratio}} = PM_1 / PM_{1 \text{ Ref}}$ ) plus élevés. Une expérience avec les LCS en mobilité a par ailleurs mis en évidence l'importance du mode de transport, de l'heure de déplacement et du site, influencé par le trafic et/ou la configuration de la rue. Le vélo montrait les PM<sub>1</sub> ratios les plus élevés, suivi de la marche (- 2%), du bus (- 9%), et du tramway (- 14%). Pour les doses inhalées, l'ordre était différent, avec d'abord la marche, suivie du vélo (- 2%), du bus (- 26%), et du tramway (- 32%). Cette thèse souligne l'importance de considérer les variations temporelles et spatiales des polluants pour le calcul des risques sanitaires, et montre l'utilité des LCS pour estimer ces variations. En conclusion, des recommandations sont données pour monter, calibrer et déployer des LCS.

Mots-clés: pollution de l'air, mobilité, risques sanitaires, capteurs low-cost, particules fines, Grenoble

TITLE: Air pollution, mobility and health in the Grenoble area

ABSTRACT: Air pollution is a global public health issue responsible for an important part of mortality and various chronic diseases. It is therefore crucial to measure it as precisely as possible. The objectives of this thesis were to identify health risks associated with air pollutants in Grenoble (France), and to measure particulate matter (PM), recognized as a major contributor to mortality, as accurately as possible. This work starts with a health risks analysis during the COVID-19 period, showing significant changes in pollutants levels: NO<sub>2</sub> (- 32%), PM<sub>2.5</sub> (- 22%), PM<sub>10</sub> (- 15%), and O<sub>3</sub> (+ 11%). These variations led to short-term reductions in health risks related to PM<sub>2.5</sub> (- 3% decrease in child asthma emergency room visits) and NO<sub>2</sub> (- 2% decrease in respiratory disease hospitalizations). In the long term, PM<sub>2.5</sub> also played a major role, reducing all-cause mortality (- 3%), lung cancer (- 2%), and low birth weights (- 8%), followed by NO<sub>2</sub> (- 1% non-accidental mortality). Due to their significant impact on health risks, the thesis then focused on PM<sub>2.5</sub> and PM<sub>1</sub> (PM < 1 µm). In order to estimate PM levels and their heterogeneity in Grenoble, we assembled low-cost sensors (LCS) with the goal to deploy them in the city, in addition to the reference stations of Atmo Auvergne-Rhône-Alpes. The LCS were first calibrated using methods including machine-learning, while excluding days with Saharan dust events that impacted LCS' ability to properly measure PM<sub>2.5</sub>. Given the poor performance of the LCS to measure PM<sub>10</sub>, we proceeded without including them. A fixed network of 8 LCS was subsequently deployed in Grenoble, highlighting temporal and spatial disparities, notably a hotspot in the city center with higher PM<sub>1</sub> ratios to the reference ( $PM_{1 \text{ ratio}} = PM_1 / PM_{1 \text{ Ref}}$ ). An experiment using mobile LCS also indicated the importance of transport mode, travel time, and site, the latter being influenced by traffic and/or street layout. Cycling exhibited the highest PM<sub>1</sub> ratios, followed by walking (- 2%), bus (- 9%), and tramway (- 14%). For inhaled doses, the order was different, with walking first, followed by cycling (- 2%), bus (- 26%), and tram (- 32%). This thesis underscores the importance of considering temporal and spatial variations in pollutants when calculating health risks and demonstrates the utility of LCS in estimating this variability. In conclusion, practical recommendations are given for assembling, calibrating, and deploying LCS that can benefit both scientists and citizen scientists.

Keywords: air pollution, mobility, health risks, low-cost sensors, particulate matter, Grenoble